// RENDICONTI
DEL SEMINARIO
MATEMATICO

Università e Politecnico di Torino

Geometry, Continua and Microstuctures, I

CONTENTS

Volume 58, N. 1 **2000**

Preface

In 1997 Gerard Maugin organized the first International Seminar on “Geometry, Continua and Microstructures” at the P. and M. Curie University in Paris. The success of the Seminar induced the organizers to repeat it in Madrid (1998) and in Bad Herrenalb (1999). Hence, when Gerard Maugin asked me to organize the fourth edition of the Seminar in Turin, I accepted with pleasure and I am now honoured to present the proceedings of the 4$^{\text{th}}$ International Seminar , which was held at the Department of Mathematics of the University of Turin from October 26th -28th, 2000.
The proceedings of the meeting appear as a special issue of the Rendiconti del Seminario Matematico (Università e Politecnico di Torino) and I am indebted to the Editor, Andrea Bacciotti, who gave me the opportunity to publish the papers in this journal.
The meeting, as the previous ones, was successful and dense with scientific results, as demonstrated by the contents, the number of lectures, the 23 papers which fill two volumes of the proceedings as well as the high scientific level of participants (about 50 scientists and young researchers from many different countries of Europe, Israel, Canada, U.S.A, and Russia).
The focus of the Seminar was the modelling of new phenomena in continuum mechanics which require the introduction of non-standard descriptors. The framework is Rational Continuum Mechanics which encompasses all descriptions of new phenomena from the macroscopic point of view. Processes occurring at microscopic scales are then taken into account by suitable generalized parameters. The introduction of these new descriptors has enriched the classical framework, since they often take values in manifolds with non trivial topological and differential structure (i.e. liquid crystals) and the purpose of the Seminar was just to discuss and point out the various problems related to these topics.
The lectures appearing in this volume provide an up-to-date insight of the state of the art and of the more recent evolution of research, with many new relevant results. Such evolution emerged clearly from the proceedings of the previous meetings and this volume represents a step along the way. In fact, a 5$^{\text{th}}$ International Seminar bearing the same title and focusing on the same topics has been organized by Sanda Cleja-Tigoiu in Sinaia (Rumania) from Seprember 25th - 28th, 2001 and will surely constitute a new milestone for future developments in this field of research.

Acknowledgements.
I am grateful to the members of the organizing committee (Manuelita Bonadies, Luca Bortoloni, Paolo Cermelli, Gianluca Gemelli, Maria Luisa Tonon) who made this meeting possible and successful and allowed this volume to be finished, notwithstanding some hindrances and difficulties.
I would also like to thank:
the Department of Mathematics of the University of Turin for providing the meeting room, the facilities and the necessary assistance;
the University of Turin for the financial support;
the M.U.R.S.T. for the funding provided through the research project COFIN 2000 “Modelli Matematici in Scienza dei Materiali”;
the co-ordinator of this research project, Paolo Podio Guidugli, for his generosity.

Franco Pastrone

4th International Seminar on
"Geometry, Continua & Microstructures"
Torino, 26-28 October 2000

List of partecipants

Gianluca Allemandi
Dipartimento di Matematica, Università di Torino
Via Carlo Alberto 10
10123, Torino, Italy
Phone: +39 0349 2694243
e-mail: `allemandi@dm.unito.it`

Albrecht Bertram
Institut für Mechanik Otto-von-Guericke, Universität Magdeburg
Universitätsplatz 2
D-39106 Magdeburg, Germany
Phone: +391 67 18062
Fax: +391 67 12863
e-mail: `bertram@mb.uni-magdeburg.de`

Ernst Binz
Fakultät für Mathematik und Informatik, Universität Mannheim
Lehrstuhl für Mathematik 1, D7, 27, Raum 404
D-68131 Mannheim, Germany
Phone: +391 621 2925389
Fax: +391 621 2925335
e-mail: `binz@math.uni-mannheim.de`

Luca Bortoloni
Dipartimento di Matematica, Università di Bologna
Piazza di Porta San Donato 5
40127 Bologna, Italy
e-mail: `bortolon@dm.unibo.it`

Manfred Braun
Department of Mechanics, University of Duisburg
47048 Duisburg, Germany
Phone: +49 203 3793342
Fax: +49 203 3792494
e-mail: `braun@mechanik.uni-duisburg.de`

Gianfranco Capriz
Dipartimento di Matematica, Università di Pisa
Via F. Buonarroti 5

56126 Pisa, Italy
e-mail: `capriz@gauss.dm.unipi.it`

Alberto Carpinteri
Dipartimento Ingegneria Strutturale e Geotecnica, Politecnico di Torino
Corso Duca degli Abruzzi 24
10129 Torino, Italy
Phone: +39 011 5644850
e-mail: `carpinteri@polito.it`

Paolo Cermelli
Dipartimento di Matematica, Università di Torino
Via Carlo Alberto 10
10123 Torino, Italy
e-mail: `cermelli@dm.unito.it`

Bernardino Chiaia
Dipartimento Ingegneria Strutturale e Geotecnica, Politecnico di Torino
Corso Duca degli Abruzzi 24
10129 Torino, Italy
Phone: +39 011 5644866
Fax: +39 011 5644899
e-mail: `chiaia@polito.it`

Vincenzo Ciancio
Dipartimento di Matematica, Università di Messina
Contrada Papardo, Salita Sperone 31
98166 Messina, Italy
Phone: +39 090 6765061
Fax: +39 090 393502
e-mail: `ciancio@dipmat.unime.it`

Sanda Cleja-Tigoiu
Department of Mechanics, Faculty of Mathematics, University of Bucharest
Str. Accademiei, 14
70109 Bucharest, Romania
Phone: 6755118
e-mail: `tigoiu@math.math.unibuc.ro`

Fiammetta Conforto
Dipartimento di Matematica, Università di Messina
Contrada Papardo, Salita Sperone 31
98166 Messina, Italy
Phone: +39 090 6765063
Fax: +39 090 393502
e-mail: `fiamma@dipmat.unime.it`

Piero Cornetti
Dipartimento Ingegneria Strutturale e Geotecnica, Politecnico di Torino
Corso Duca degli Abruzzi 24
10129 Torino, Italy
Phone: +39 011 5644901
e-mail: cornetti@polito.it

Antonio Di Carlo
Dipartimento di Scienze dell'Ingegneria Civile, Facoltà di Ingegneria, Università di Roma 3
Via Corrado Segre 60
00146 Roma, Italy
Phone: +39 06 55175002/3/4/5
e-mail: adc@uniroma3.it

Juri Engelbrecht
Department of Mechanics and Applied Mathematics, Tallinn Technical University
Akadeemia tee, 21
12618 Tallinn, Estonia
Phone: +37 26 442129
Fax: +37 26 451805
e-mail: je@ioc.ee

Marcelo Epstein
Department of Mechanical and Manufacturing Engineering, University of Calgary
Calgary, Alberta T2N1 N4, Canada
Phone: 1-403-220-5791,
Fax: 1-403-282-8406
e-mail: epstein@enme.ucalgary.ca and mepstein@agt.net

Samuel Forest
Ecole Nationale Superieure des Mines de Paris
Centre des Materiaux / UMR 7633, B.P. 8791003
91003 Evry, France
Phone: +33 1 60763051
Fax: +33 1 60763150
e-mail: samuel.forest@mat.ensmp.fr

Jean-Francois Ganghoffer
Lemta- Ensem
2, Avenue de la Foret de Haye, B.P. 160- 54504
Vandoeuvre Cedex, France
Phone : +33 0383595530
Fax : +33 0383595551
e-mail: Jean-francois.Ganghoffer@ensem.inpl-nancy.fr

Sebastian Gümbel
Institut für theoretische Physik, Technische Universitaet Berlin
Sekretariat PN7-1, Hardenbergstrasse 36,

D-10623 Berlin, Germany
Phone: +49 030 31423000
Fax: +49 030 31421130
e-mail: guembel@physik.tu-berlin.de

Klaus Hackl
Lehrstuhl für Allgemeine Mechanik
Ruhr-Universität Bochum
D-44780 Bochum, Germany
Phone: +49 234 3226025
Fax: +49 234 3214154
e-mail: hackl@am.bi.ruhr-uni-bochum.de

Heiko Herrmann
Institut für Theoretische Physik, Technische Universität Berlin
Sekretariat PN7-1, Hardenbergstrasse 36
D-10623 Berlin, Germany
Phone: +49 030 31424443
Fax: +49 030 31421130
e-mail: hh@physik.tu-berlin.de

Yordanka Ivanova
Institute of Mechanics and Biomechanics, B.A.S.
Sofia, Bulgaria
Phone: +359 27131769
e-mail: ivanova@imbm.bas.bg

Akiko Kato
Institut für theoretische Physik, Technische Universitaet Berlin
Sekretariat PN7-1, Hardenbergstrasse 36
D-10623 Berlin, Germany,
Phone: +49 030 31424443
Fax: +49 030 31421130
e-mail: akiko@itp4.physik.tu-berlin.de

Massimo Magno
Groupe Securite et Ecologie Chimiques, Ecole Nationale Superieure de Chimie de Mulhouse
3, Rue Alfred Werner
F-68093 Mulhouse Cedex, France
e-mail: massimo.magno@mageos.com

Chi-Sing Man
Department of Mathematics, University of Kentucky
715 Patterson Office Tower
Lexington, KY 40506-0027, U.S.A.
e-mail: mclxyh@ms.uky .edu

Gerard A. Maugin
Laboratoire de Modalisation en Mecanique, Universite Pierre et Marie Curie
Case 162, 8 rue du Capitaine Scott
75015 Paris, France
Phone: +33 144 275312, Fax: +33 144 275259
e-mail: gam@ccr.jussieu.fr

Marco Mosconi
Istituto di Scienza e Tecnica delle Costruzioni, Università di Ancona
Via Brecce Bianche, Monte d'Ago
60131 Ancona, Italy
Phone: +39 0171 2204553
Fax: +39 0171 2204576
e-mail: mmosconi@popcsi.unian.it

Wolfgang Muschik
Institut für Theoretyche Physik, Technische Universität Berlin
Sekretariat PN7-1 , Hardenbergstrasse 36
D-10623 Berlin, Germany
Phone: +49 030 31423765, Fax: +49 030 31421130
e-mail: muschik@physik.tu-berlin.de

Rodolphe Parisot
Ecole Nationale Superieure des Mines de Paris
Centre des Materiaux / UMR 7633, B.P. 8791003
91003 Evry, France
Phone: +33 01 60763061
Fax: +33 01 60763150
e-mail: rparisot@mat.ensmp.fr

Alexey V. Porubov
loffe Physico-Technical Institute of the Russian Academy of Sciences
Polytechnicheskaya st., 26
194021 Saint Petersburg, Russia
Phone: +7 812 2479352
Fax: +7 812 2471017
e-mail: porubov@soliton.ioffe.rssi.ru

Guy Rodnay
Department of Mechanical Engineering, Ben-Gurion University
84105 Beer-Sheva, Israel
Phone: +972 54 665330
Fax: +972 151 54 665330
e-mail: rodnay@bgumail.bgu.ac.il

Patrizia Rogolino
Dipartimento di Matematica, Università di Messina
Contrada Papardo, Salita Sperone 31

98166 Messina, Italy
e-mail: `patrizia@dipmat.unime.it`

Gunnar Rueckner
Institut für Theoretische Physik, Technische Universität Berlin
Sekretariat PN7-1, Hardenbergstrasse 36
D-10623 Berlin, Germany
Phone: +49 030 31424443
Fax: +49 030 31421130
e-mail: `guembel@physik.tu-berlin.de`

Giuseppe Saccomandi
Dipartimento di Ingegneria dell'Innovazione, Università di Lecce
Via Arnesano
73100 Lecce, Italy
e-mail: `giuseppe@ibm.isten.ing.unipg.it`

Reuven Segev
Department of Mechanical Engineering, Ben-Gurion University
P.O. Box 653,
84105 Beer-Sheva, Israel
Phone: +972 7 6477108
Fax: +972 7 6472813
e-mail: `rsegev@bgumail.bgu.ac.il`

Dan Socolescu
Fachbereich Mathematik, Universität Kaiserslautern
67663 Kaiserslautern, Germany
Phone: +49 631 2054032
Fax: +49 631 2053052
e-mail: `socolescu@mathematik.uni-kl.de`

Bob Svendsen
Department of Mechanical Engineering, University of Dormtund
D-44221 Dormtund, Germany,
Phone: +49 231 7552686
Fax: +49 231 7552688
e-mail: `bob.svendsen@mech.mb.uni-dortmund.de`

Carmine Trimarco
Dipartimento Matematica Applicata "U. Dini", Università di Pisa
Via Bonanno 25/B
I-56126 Pisa, Italy
Tel. +39 050 500065/56
Fax: +39 050 49344
e-mail: `trimarco@dma.unipi.it`

Robin Tucker
Department of Physics, Lancaster University
Lancaster LA1 4Y, UK
Phone: +44 0152 4593610
Fax: +44 0152 4844037
e-mail: robin.tucker@lancaster.ac.uk

Varbinca Valeva
Institute of Mechanics and Biomechanics, B.A.S.
ul Ac. Bonchev bl 4
1113 Sofia, Bulgaria

Rend. Sem. Mat. Univ. Pol. Torino
Vol. 58, 1 (2000)
Geom., Cont. and Micros., I

E. Binz - S. Pods - W. Schempp

NATURAL MICROSTRUCTURES ASSOCIATED WITH SINGULARITY FREE GRADIENT FIELDS IN THREE-SPACE AND QUANTIZATION

Abstract.

Any singularity free vector field X defined on an open set in a three-dimensional Euclidean space with curl $X = 0$ admits a complex line bundle F^a with a fibre-wise defined symplectic structure, a principal bundle $\mathcal{P}^a$ and a Heisenberg group bundle G^a. For the non-vanishing constant vector field X the geometry of $\mathcal{P}^a$ defines for each frequency a Schrödinger representation of any fibre of the Heisenberg group bundle and in turn a quantization procedure for homogeneous quadratic polynomials on the real line.

1. Introduction

In [2] we described microstructures on a deformable medium by a principal bundle on the body manifold. The microstructure at a point of the body manifold is encoded by the fibre over it, i.e. the collection of all internal variables at the point. The structure group expresses the internal symmetries.

In these notes we will show that each singularity free gradient field defined on an open set of the Euclidean space hides a natural microstructure. The structure group is $U(1)$.

If the vector field X is a gradient field with a nowhere vanishing principal part a, say, then there are natural bundles over O such as a complex line bundle F^a with a fibre-wise defined symplectic form ω^a, a Heisenberg group bundle G^a and a four-dimensional principal bundle $\mathcal{P}^a$ with structure group $U(1)$. (Fibres over O are indicated by a lower index x.) For any $x \in O$ the fibre F^a_x is the orthogonal complement of $a(x)$ formed in E and encodes internal variables at x. It is, moreover, identified as a coadjoint orbit of G^a_x. The principal bundle $\mathcal{P}^a$, a subbundle of the fibre bundle F^a, is equipped with a natural connection form α^a, encoding the vector field in terms of the geometry of the local level surfaces: The field X can be reconstructed from α^a. The collection of all internal variables provides all tangent vectors to all locally given level surfaces. The curvature Ω^a of α^a describes the geometry of the level surfaces of the gradient field in terms of ω^a and the Gaussian curvature.

There is a natural link between this sort of microstructure and quantum mechanics. To demonstrate the mechanism we have in mind, the principal part a of the vector field X is assumed to be constant (for simplicity only). Thus the integral curves, i.e. the field lines, are straight lines. Fixing some $x \in O$ and a solution curve β passing through $x \in O$, we consider the collection of all geodesics on the restriction of the principal bundle $\mathcal{P}^a$ to β. Each of these geodesics with the same speed is called a periodic lift of β and passes through a common initial point $v_x \in \mathcal{P}^a_x$, say. If the periodic lifts rotate in time, circular polarized waves are established. Hence the integral curve β is accompanied by circular polarized waves on $\mathcal{P}^a$ of arbitrarily given frequencies. This collection of periodic lifts of β defines unitary representations ρ_ν of the Heisenberg group G_x^a, the Schrödinger representations (cf. [11] and [13]). The frequencies of the polarized waves correspond to the equivalence classes of ρ_ν due to the theorem of Stone-von Neumann.

The automorphism group of G_x^a is the symplectic group $Sp(F_x^a)$ of the symplectic complex line F_x^a. Therefore, the representation ρ_1 of G_x^a yields a projective representation of $Sp(F_x^a)$, due to the theorem of Stone-von Neumann again. This projective representation is resolved to a unitary representation W of the metaplectic group $Mp(F_x^a)$ in the usual way. Its infinitesimal representation dW of the Lie algebra $mp(F_x^a)$ of $Mp(F_x^a)$ yields the quantization procedure for all homogeneous quadratic polynomials defined on the real line. Of course, this is in analogy to the quantization procedure emanating from the quadratic approximation in optics.

2. The complex line bundle associated with a singularity free gradient field in Euclidean space

Let O be an open subset not containing the zero vector 0 in a three-dimensional oriented $\mathbb{R}$-vector space E with scalar product $< \, , \, >$. The orientation on the Euclidean space E shall be represented by the Euclidean volume form μ_E.

Our setting relies on a smooth, singularity free vector field $X : O \longrightarrow O \times E$ with principal part $a : O \longrightarrow E$, say. We shall frequently identify X with its principal part.

Moreover, let $\mathbb{H} := \mathbb{R} \cdot e \oplus E$ be the skew field of quaternions where e is the multiplicative unit element. The scalar product $< \, , \, >$ and the orientation on E extend to all of $\mathbb{H}$ such that $e \in \mathbb{H}$ is a unit vector and the above splitting of $\mathbb{H}$ is orthogonal. The unit sphere S^3, i.e. $Spin(E)$, is naturally isomorphic to $SU(2)$ and covers $SO(E)$ twice (cf. [8] and [9]).

Given any $x \in O$, the orthogonal complement F_x^a of $a(x) \in E$ is a complex line as can be seen from the following: Let $\mathbb{C}_x^a \subset \mathbb{H}$ be the orthogonal complement of F_x^a. Hence the field of quaternions $\mathbb{H}$ splits orthogonally into

$$\mathbb{H} = \mathbb{C}_x^a \oplus F_x^a. \tag{1}$$

As it is easily observed,

$$\mathbb{C}_x^a = \mathbb{R} \cdot e \oplus \mathbb{R} \cdot \frac{a(x)}{|a(x)|}$$

is a commutative subfield of $\mathbb{H}$ naturally isomorphic to $\mathbb{C}$ due to

$$\left(\frac{a(x)}{|a(x)|} \right)^2 = -e \qquad \forall \, x \in O,$$

where $| \cdot |$ denotes the norm defined by $< \, , \, >$. This isomorphism shall be called

$$j_x^a : \mathbb{C} \longrightarrow \mathbb{C}_x^a \, ;$$

it maps 1 to e and i to $\frac{a(x)}{|a(x)|}$. The multiplicative group on the unit circle of $\mathbb{C}_x^a$ is denoted by $U_x^a(1)$. It is a subgroup of $SU(2) \subset \mathbb{H}$ and hence a group of spins. Obviously $a(x)$ generates the Lie algebra of $U_x^a(1)$.

F_x^a is a $\mathbb{C}_x^a$-linear space under the (right) multiplication of $\mathbb{H}$ and hence a $\mathbb{C}$-linear space, a complex line. Moreover, $\mathbb{H}$ is the Clifford algebra of F_x^a equipped with $- < \, , \, >$ (cf. [9]).

The topological subspace $F^a := \bigcup_{x \in O} \{x\} \times F_x^a$ of $O \times E$ is a $\mathbb{C}$-vector subbundle of $O \times E$, if curl $X = 0$, as can easily be seen. In this case F^a is a complex line bundle (cf. [15]), the complex line bundle associated with X. Let $\mathrm{pr}^a : F^a \longrightarrow O$ be its projection. Accordingly there is a bundle of fields $\mathbb{C}^a \longrightarrow O$ with fibre $\mathbb{C}^a_x$ at each $x \in O$. Clearly,

$$O \times \mathbb{H} = \mathbb{C}^a \times F^a$$

as vector bundles over O. Of course, the bundle $F^a \longrightarrow O$ can be regarded as the pull-back of TS^2 via the Gauss map assigning $\frac{a(x)}{|a(x)|}$ to any $x \in O$.

We, therefore, assume that curl $X = 0$ from now on. Due to this assumption there is a locally given real-valued function V, a potential of a, such that $a = \text{grad } V$. Each (locally given) level surface S of V obviously satisfies $TS = F^a|_S$. Here $F^a|_S = \bigcup_{x\in S}\{x\} \times F^a_x$. Each fibre F^a_x of F^a is oriented by its Euclidean volume form $i_{\frac{a(x)}{|a(x)|}}\mu_E := \mu_E\left(\frac{a(x)}{|a(x)|}, \ldots, \ldots\right)$. For any level surface the scalar product yields a Riemannian metric g_S on S given by

$$g_S(x; v_x, w_x) := < v_x, w_x > \qquad \forall\, x \in O \quad \text{and} \quad \forall\, v_x, w_x \in T_xS.$$

For any vector field Y on S, any $x \in O$ and any $v_x \in T_xS$, the covariant derivative ∇^S of Levi-Cività determined by g_S satisfies

$$\nabla^S_{v_x} Y(x) \quad = \quad dY(x; v_x) + < Y(x), W^a_x(v_x) > .$$

Here $W^a_x : T_xS \longrightarrow T_xS$ is the Weingarten map of S assigning to each $w_x \in T_xS$ the vector $d\frac{a}{|a|}(x; w_x)$, the differential of $\frac{a}{|a|}$ at x evaluated at w_x. The Riemannian curvature R of ∇^S at any x is expressed by the well-known equation of Gauss as

$$\begin{aligned} R(x; v_x, w_x.u_x, y_x) \quad &= \quad < W^a_x(w_x), u_x > \cdot < W^a_x(v_x), y_x > \\ &\quad - < W^a_x(v_x), u_x > \cdot < W^a_x(w_x), y_x > \end{aligned} \tag{2}$$

for any choice of the vectors $v_x, w_x, u_x, y_x \in T_xS$.

A simple but fundamental observation in our setting is that each fibre $F^a_x \subset F^a$ carries a natural symplectic structure ω^a defined by

$$\omega^a(x; h, k) := < h \times a(x), k > = < h \cdot a(x), k > \qquad \forall\, h, k \in F^a_x,$$

where $\times$ is the cross product, here being identical with the product in $\mathbb{H}$. In the context of F^a_x as a complex line we may write

$$\omega^a(x; h_0, h_1) = |a(x)| \cdot < h_0 \cdot i, h_1 > .$$

This is due to the fact that h and $a(x)$ are perpendicular elements in E. The bundle F^a is fibre-wise oriented by $-\omega^a$. In fact ω^a extends on all of E by setting

$$\omega^a(x; y, z) :=< y \times a(x), z >$$

for all $y, z \in E$; it is not a symplectic structure on O, of course. Let $\kappa(x) := \det W^a_x$ for all $x \in S$, the Gaussian curvature of S. Provided v_x, w_x is an orthonormal basis of T_xS, the relation between the Riemannian curvature R and ω is given by

$$R(x; v_x, w_x.u_x, y_x) = \frac{\kappa(x)}{|a(x)|} \cdot \omega^a(x; u_x, y_x)$$

for every $x \in S$ and $u_x, y_x \in T_xS = F^a_x$.

3. The natural principal bundle $\mathcal{P}^a$ associated with X

We recall that the singularity free vector field X on O has the form $X = (\mathrm{id}\,, a)$. Let $\mathcal{P}^a_x \subset F^a_x$ be the circle centred at zero with radius $|a(x)|^{-\frac{1}{2}}$ for any $x \in O$. Then

$$\mathcal{P}^a := \bigcup_{x\in O} \{x\} \times \mathcal{P}^a_x$$

equipped with the topology induced by F^a is a four-dimensional fibre-wise oriented submanifold of F^a. It inherits its smooth fibre-wise orientation from F^a. Moreover, $\mathcal{P}^a$ is a $U(1)$-principal bundle. $U(1)$ acts from the right on the fibre $\mathcal{P}^a_x$ of $\mathcal{P}^a$ via $j^a_x|_{U(1)} : U(1) \longrightarrow U^a_x(1)$ for any $x \in O$. This operation is fibre-wise orientation preserving. The reason for choosing the radius of $\mathcal{P}^a_x$ to be $|a(x)|^{-\frac{1}{2}}$ will be made apparent below.

Both F^a and $\mathcal{P}^a$ encode collections of internal variables over O and both are constructed out of X, of course. Clearly, the vector bundle F^a is associated with $\mathcal{P}^a$.

The vector field X can be reconstructed out of the smooth, fibre-wise oriented principal bundle $\mathcal{P}^a$ as follows: For each $x \in O$ the fibre $\mathcal{P}^a_x$ is a circle in F^a_x centred at zero. The orientation of this circle yields an orientation of the orthogonal complement of F^a_x formed in E, the direction of the field at x. Hence $|a(x)|$ is determined by the radius of the circle $\mathcal{P}^a_x$. Therefore, the vector field X admits a characteristic geometric object, namely the smooth, fibre-wise oriented principal bundle $\mathcal{P}^a$ on which all properties of X can be reformulated in geometric terms. Vice versa, all geometric properties of $\mathcal{P}^a$ reflect characteristics of a. The fibre-wise orientation can be implemented in a more elegant way by introducing a connection form, α^a, say, which is in fact much more powerful. This will be our next task. Since $\mathcal{P}^a \subset O \times E$, any tangent vector $\xi \in T_{v_x}\mathcal{P}^a$ can be represented as a quadruple

$$\xi = (x, v_x, h, \zeta_{v_x}) \in O \times E \times E \times E$$

for $x \in O$, $v_x \in \mathcal{P}^a_x$ and $h, \zeta_{v_x} \in E \subset \mathbb{H}$ with the following restrictions, expressing the fact that ξ is tangent to $\mathcal{P}^a$:
Given a curve $\sigma = (\sigma_1, \sigma_2)$ on $\mathcal{P}^a$ with $\sigma_1(s) \in O$ and $\sigma_2(s) \in \mathcal{P}^a_{\sigma_1(s)}$ for all s, then

$$< \sigma_2(s), a(\sigma_1(s)) > = 0 \quad \text{and} \quad |\sigma_2(s)|^2 = \frac{1}{|a(\sigma_1(s))|} \qquad \forall\, s.$$

Each $\zeta \in T_{v_x}\mathcal{P}^a$ given by $\zeta = \dot{\sigma}_2\,(0)$ is expressed as

$$\zeta = r_1 \cdot \frac{a(x)}{|a(x)|} + r_2 \cdot \frac{v_x}{|v_x|} + r \cdot \frac{v_x \times a(x)}{|v_x| \cdot |a(x)|}$$

with

$$r_1 = - < W^a_x(v_x), h > \quad , \quad r_2 = -\frac{|v_x|}{2} \cdot d \ln |a|(x; h)$$

and a free parameter $r \in \mathbb{R}$. The Weingarten map W^a_x is of the form

$$da(x; k) = |a(x)| \cdot W^a_x(k) + a(x) \cdot d \ln |a|(x; k) \qquad \forall\, x \in O \;,\; \forall\, k \in E,$$

where we set $W^a_x(a(x)) = 0$ for all $x \in O$. With these preparations we define the one-form

$$\alpha^a : T\mathcal{P}^a \longrightarrow \mathbb{R}$$

for each $\xi \in T\mathcal{P}^a$ with $\xi = (x, v_x, h, \zeta)$ to be

$$\alpha^a(v_x, \xi) := < v_x \times a(x), \zeta > . \tag{3}$$

One easily shows that α^a is a connection form (cf. [10] and for the field theoretic aspect [1]). To match the requirement of a connection form in this metric setting, the size of the radius of $\mathcal{P}^a_x$ is crucial for any $x \in O$. The negative of the connection form on $\mathcal{P}^a$ is in accordance with the smooth fibre-wise orientation, of course.

Thus the principal bundle $\mathcal{P}^a$ together with the connection form α^a characterizes the vector field X, and vice versa. To determine the curvature Ω^a which is defined to be the exterior covariant derivative of α^a, the horizontal bundles in $T\mathcal{P}^a$ will be characterized. Given $v_x \in \mathcal{P}^a$, the horizontal subspace $Hor_{v_x} \subset T\mathcal{P}^a$ is defined by

$$Hor_{v_x} := ker\ \alpha^a(v_x; \ldots).$$

A vector $\xi_{v_x} \in Hor_{v_x}$, being orthogonal to $v_x \times a(x)$, has the form $(x, v_x, h, \zeta^{hor}) \in O \times E \times E \times E$ where h varies in O and ζ^{hor} satisfies

$$\zeta^{hor} = - < W^a_x(v_x), h > \cdot \frac{a(x)}{|a(x)|} - \frac{|v_x|}{2} \cdot d \ln |a|(x; h) \cdot \frac{v_x}{|v_x|}.$$

Since $T\mathrm{pr}^a : Hor_{v_x} \longrightarrow T_x O$ is an isomorphism for any $v_x \in \mathcal{P}^a$, dim $Hor_{v_x} = 3$ for all $v_x \in \mathcal{P}^a$ and for all $x \in O$. The collection $Hor \subset T\mathcal{P}^a$ of all horizontal subspaces in the tangent bundle $T\mathcal{P}^a$ inherits a vector bundle structure $T\mathcal{P}^a$.
The exterior covariant derivative $d^{hor}\alpha^a$ is defined by

$$d^{hor}\alpha^a(v_x, \xi_0, \xi_1) := d\alpha^a(v_x; \xi_0^{hor}, \xi_1^{hor})$$

for every $\xi_0, \xi_1 \in T_{v_x}\mathcal{P}^a$, $v_x \in \mathcal{P}^a_x$ and $x \in O$.
The curvature $\Omega^a := d^{hor}\alpha^a$ of α^a is sensitive in particular to the geometry of the (locally given) level surfaces, as is easily verified by using equation (2):

PROPOSITION 1. *Let X be a smooth, singularity free vector field on O with principal part a. The curvature Ω^a of the connection form α^a is*

$$\Omega^a = \frac{\kappa}{|a|} \cdot \omega^a$$

where $\kappa : O \longrightarrow \mathbb{R}$ is the leaf-wise defined Gaussian curvature on the foliation of O given by the collection of all level surfaces of the locally determined potential V. The curvature Ω^a vanishes along field lines of X.

The fact that the curvature Ω^a vanishes along field lines plays a crucial role in our set-up. It will allow us to establish (on a simple model) the relation between the transmission of internal variables along field lines of X and the quantization of homogeneous quadratic polynomials on the real line.

4. Two examples

If we consider specific vector fields in these notes, we will concentrate on the two types presented in more detail in this section. At first let us regard a constant vector field X on $O \subset E\backslash\{0\}$ with a principal part having the non-zero value $a \in E$ for all $x \in O$. Obviously the principal bundle $\mathcal{P}^a$ is trivial, i.e.

$$\mathcal{P}^a \cong O \times U^a(1).$$

Since an integral curve β of X is a straight line segment parametrized by

$$\beta(t) = t \cdot a + x_0 \quad \text{with} \quad \beta(t_0) = x_0,$$

the restriction $\mathcal{P}^a|_{im\ \beta}$ of $\mathcal{P}^a$ to the image $im\ \beta$ is a cylinder with radius $|a|^{-\frac{1}{2}}$.

As the second type of example of a principal bundle $\mathcal{P}^a$ associated with a singularity free vector field let us consider a central symmetric field $X = \text{grad}\ V_{sol}$ on $E\backslash\{0\}$ with the only singularity at the origin. The potential V_{sol} is given by

$$V_{sol}(x) := -\frac{\bar{m}}{|x|} \qquad \forall\, x \in O$$

where $\bar{m}$ is a positive real. This potential governs planetary motions and hence grad V_{sol} is called the solar field here. The principal part a of the gradient field is

$$\text{grad}\ \ V_{sol}(x) = -\frac{\bar{m}}{|x|^2} \cdot \frac{x}{|x|} \qquad \forall\, x \in E\backslash\{0\}. \tag{4}$$

For reasons of simplicity we illustrate from a longitudinal point of view the principal bundle $\mathcal{P}^a$ associated with the gradient field. An integral curve β passing through x at the time $t_0 = 1$ is of the form

$$\beta(t) = -\bar{m} \cdot (3 \cdot t - 2)^{\frac{1}{3}} \cdot x \qquad \text{for} \quad \frac{2}{3} < t < \infty. \tag{5}$$

Hence the (trivial) principal bundle $\mathcal{P}^a|_{im\ \beta}$ is a cone. The radius r of a circle $\mathcal{P}^a_x$ with $x \in im\ \beta$ is $r = \frac{|x|}{\sqrt{\bar{m}}}$ for all $x \in O$ (cf. [12]).

5. Heisenberg group bundles associated with the singularity free vector field and curves and the solar field

Associated with the $(2+1)$-splitting of the Euclidean space E caused by the vector field X there is a natural Heisenberg group bundle G^a with ω^a as symplectic form. The bundle G^a allows us to reconstruct X as well. Heisenberg groups play a central role in signal theory (cf. [13], [14]). We essentially restrict us to the two types of examples presented in the previous section.

Given $x \in O$, the vector $a(x) \neq 0$ determines F^a_x with the symplectic structure $\omega^{a(x)}$ and $\mathbb{C}^a_x$ which decompose $\mathbb{H}$ according to (1).

The submanifold $G^a_x := |a(x)|^{-\frac{1}{2}} \cdot e \cdot U^a_x(1) \oplus F^a_x$ of $\mathbb{H}$ carries the Heisenberg group structure the (non-commutative) multiplication of which is defined by

$$(z_1 + h_1) \cdot (z_2 + h_2) := |a(x)|^{-\frac{1}{2}} \cdot z_1 \cdot z_2 \cdot e^{\frac{1}{2} \cdot \omega^a(x;h_1,h_2) \cdot \frac{a}{|a|}} + h_1 + h_2 \tag{6}$$

for any two $z_1, z_2 \in |a(x)|^{-\frac{1}{2}} \cdot e \cdot U^a_x(1)$ and any pair $h_1, h_2 \in F^a_x$ (cf. [12]). The (commutative) multiplication in the centre $|a(x)|^{\frac{1}{2}} \cdot e \cdot U^a_x(1)$ of G^a_x is given by adding angles. The reason the centre has radius $|a(x)|^{-\frac{1}{2}}$ is the length scale on $\mathcal{P}^a_x$ for any $x \in O$. The group bundle

$\cup_{x \in O}\{x\} \times |a(x)|^{-\frac{1}{2}} \cdot e \cdot U_x^a(1)$, which is the collection of all centres, is associated with $\mathcal{P}^a$ and forms a natural torus bundle together with $\mathcal{P}^a$. The collection

$$G^a := \bigcup_{x \in O} \{x\} \times G_x^a$$

can be made into a group bundle which is associated with the principal bundle $\mathcal{P}^a$, too. Clearly $F^a \subset G^a$ as fibre bundles. In the cases of a constant vector field and the solar field the Heisenberg group bundle along field lines is trivial.

In particular, a in (6) takes the values $|a(x)|^{-\frac{1}{2}} = |a|^{-\frac{1}{2}}$ and $|a(x)|^{-\frac{1}{2}} = \frac{|x|}{m}$ for all $x \in O$ in the cases of the constant vector field respectively the solar field.

The Lie algebra $\mathcal{G}_x^a$ of G_x^a is

$$\mathcal{G}_x^a := \mathbb{R} \cdot \frac{a}{|a|} \oplus F_x^a$$

together with the operation

$$\left[\vartheta_1 \cdot \frac{a}{|a|} + h_1, \vartheta_2 \cdot \frac{a}{|a|} + h_2\right] := \omega^a(x; h_1, h_2) \cdot \frac{a}{|a|}$$

for any $\vartheta_1, \vartheta_2 \in \mathbb{R}$ and any $h_1, h_2 \in F_x^a$. The exponential map $\exp_{G_x^a} : \mathcal{G}_x^a \longrightarrow G_x^a$ is surjective. Obviously, X can be reconstructed from both G^a and $\mathcal{G}^a$. The coadjoint orbit of Ad^{a^*} passing through $< \vartheta \cdot \frac{a}{|a|} + h_1, .. > \in \mathcal{G}_x^{a*}$ with $\vartheta \neq 0$ is $\vartheta \cdot \frac{a}{|a|} \oplus F_x^a$.

In this context we will study the solar field next (cf. [12]). At first let us see how it emanates from Keppler's laws of circular planetary motion. Suppose σ is a closed planetary orbit in $E \backslash \{0\}$ defined on all of $\mathbb{R}$; it lies in a plane $F^{b'}$, say, with $b' \in E \backslash \{0\}$, due to Keppler's second law. Let σ be a circle of radius r. It is generated by a one-parameter group φ in $SO(F^b)$ with generator b, say, yielding

$$\varphi(t) = e^{t \cdot b} \qquad \forall t \in \mathbb{R}.$$

Hence

$$\ddot{\varphi} = b^2 \cdot \varphi = -|b|^2 \cdot \varphi.$$

This generator, a skew linear map in $so(F^b)$, is identified with a vector in E in the obvious way. The invariant norms on $so(F^b)$ are positive real multiples of the trace norm, and hence on $so(F^b)$ the generator has a norm

$$||b||^2 = -G'^2 \cdot \operatorname{tr} b^2 = G'^2 \cdot |b|^2$$

for some positive real number G' and a fixed constant $||b||$.

The time of revolution $T := \frac{2\pi}{|b|}$ is determined by Keppler's third law which states

$$T^2 = r^3 \cdot \text{ const.} \tag{7}$$

Therefore $\ddot{\varsigma}$ of $\varsigma := \varphi \cdot x_0$ with $|x_0| = r$ has the form

$$\ddot{\varsigma} = -\frac{||b||^2}{G'^2} \cdot \varsigma = -\frac{G \cdot m}{|\varsigma|^2} \cdot \frac{\varsigma}{|\varsigma|}$$

with $G'^2 = G^{-1} \cdot r^3$ and $m := ||b||^2$ as solar mass. This is the reason why X with principal part grad V_{sol} here is called the solar field. Newton's field of gravitation includes the mass of the planet, which is not involved here.

Next let us point out a consequence of the comparison of the cone $\mathcal{P}^a|_\beta$ embedded into $\mathcal{G}_x^a$ for a fixed $x \in im\ \beta$, but shifted forward such that its vertex is in $0 \in E$, with the cone C_M of a Minkowski metric g_M^a on $\mathcal{G}_x^a$. The metric g_M^a relies on the following observation: Up to the choice of a positive constant c, there is a natural Minkowski metric on $\mathbb{H}$ inherited from squaring any quaternion $k = \lambda \cdot e + u$ with $\lambda \in \mathbb{R}$ and $u \in E$ since the e-component $(k^2)_e$ of k^2 is

$$-(k^2)_e = (|u|^2 - \lambda^2) \cdot e = (b^2 \cdot k^2)_e$$

with $b \in S^2$. Introducing the positive constant c, the Minkowski metric g_M^a on $\mathcal{G}_x^a$ mentioned above is pulled back to $\mathcal{G}_x^a$ by the right multiplication with $\frac{a}{|a|}$ and reads

$$g_M^a(h_1, h_2) :=< u_1, u_2 > -c \cdot \lambda_1 \cdot \lambda_2$$

for any $h_r \in F^{\frac{a}{|a|}}$ represented by $h_r = \lambda_r \cdot \frac{a}{|a|} + u_r$ for $r = 1, 2$. The respective interior angles φ^a and φ_{C_M} which the meridians on $\mathcal{P}|_{im\ \beta}$ and C_M form with the axis $\mathbb{R} \cdot \frac{x}{|x|}$ satisfy

$$\tan \varphi^a = \bar{m}^{-\frac{1}{2}} \quad \text{and} \quad \tan \varphi_{C_M} = \frac{1}{c},$$

and

$$m \cdot c^2 = G^{-1} \cdot \cot^2 \varphi^a \cdot \cot^2 \varphi_{C_M},$$

provided $m := \frac{\bar{m}}{G}$. This is a geometric basis to derive within our setting $E = m \cdot c^2$ from special relativity (cf. [12]).

Now we will study planetary motions in terms of Heisenberg algebras. In particular we will deduce Keppler's laws from the solar field by means of a holographic principle (we will make this terminology precise below). To this end we first describe natural Heisenberg algebras associated with each time derivative of a smooth injective curve σ in O defined on an interval $I \subset \mathbb{R}$. For any $t \in I$ the n-th derivative $\sigma^{(n)}(t)$, assumed to be different from zero, defines a Heisenberg algebra bundle $\mathcal{G}^{(n)}$ for $n = 0, 1 \ldots$ with fibre

$$\mathcal{G}_{\sigma(t)}^{(n)} := \mathbb{R} \cdot \sigma^{(n)}(t) \oplus F_{\sigma(t)}^{(n)}$$

where $F_{\sigma(t)}^{(n)} := \sigma^{(n)}(t)^\perp$ (formed in E) with the symplectic structure $\omega^{(n)}$ defined by

$$\omega^{(n)}(\sigma(t); h_1, h_2) \quad = \quad < h_1 \times \sigma^{(n)}(t), h_2 > \qquad \forall h_1, h_2 \in F_{\sigma(t)}^{(n)}.$$

Here $F^{(n)}$ is the complex line bundle along $im\ \sigma$ for which $F_{\sigma(t)}^{(n)} := \sigma^{(n)}(t)^\perp$ for each t. The two-forms $\omega^{(n)}$ are extended to all of O by letting h_1 and h_2 vary also in $\mathbb{R} \cdot \frac{\sigma^{(n)}(t)}{|\sigma^{(n)}(t)|}$ for all $t \in I$. The Heisenberg algebra $\mathcal{G}_{\sigma(t)}^{(n)}$ is naturally isomorphic to $\mathcal{G}_{\sigma(t_0)}^{(n)}$ for a given $t_0 \in I$, any t and any n for which $\sigma^{(n)}(t) \neq 0$.

As a subbundle of $F^{(n)}$ we construct $\mathcal{P}^{(n)} \subset F^{(n)}$ which constitutes of the circles $\mathcal{P}_{\sigma(t)}^{(n)} \subset F_{\sigma(t)}^{(n)}$ with radius $|\sigma^{(n)}(t)|^{-\frac{1}{2}}$. On $F^{(n)}$ the curve σ admits an analogue $\alpha^{(n)}$ of the one-form α^a described in (3), determined by

$$\alpha^{(n)}(\sigma(t); h) \ =< \sigma(t) \times \sigma^{(n)}(t), h > \qquad \forall\, h \in F_{\sigma(t)}^{(n)}$$

for any t. Since the Heisenberg algebra bundle evolves from $\mathcal{G}_0^{(n)}$ we may ask how $\alpha^{(n)}$ evolves along σ, in particular for $\alpha^{(1)}$. The evolution of $\alpha^{(n)}$ can be expressed in terms of $\dot{\alpha}^{(n)}$ defined by

$$\begin{aligned}\dot{\alpha}^{(n)}(\sigma(t);h) &:= \frac{d}{dt}\alpha^{(n)}(\sigma(t);h) - \alpha^{(n)}(\dot{\sigma}(t),h)\\ &= <\sigma(t)\times\sigma^{(n+1)}(t),h> \qquad \forall\, h\in F^{(n)}_{\sigma(t)}.\end{aligned}$$

A slightly more informative form for $\dot{\alpha}^{(1)}$ is

$$\dot{\alpha}^{(1)}(\sigma(t);h) = \omega^{(2)}(\sigma(t);\sigma(t),h) \qquad \forall\, h\in F^{(1)}_{\sigma(t)}.$$

Thus the evolution of $\alpha^{(1)}$ along σ is governed by the Heisenberg algebras $\mathcal{G}^{(2)}$, yielding in particular

$$\alpha^{(1)} = \text{ const.} \quad \text{iff} \quad \sigma\times\ddot{\sigma}=0, \quad \text{meaning} \quad i_\sigma\omega^{(2)}=0.$$

Hence $\alpha^{(1)}$ = const. is the analogue of Keppler's second law. In this case the quaternion $b := \sigma\times\dot{\sigma}$ is constant and hence σ is in the plane $F\subset E$ perpendicular to b. Thus $\mathbb{R}\cdot b\times F^b$ is a Heisenberg algebra with

$$\omega^b(h_1,h_2) :=< h_1\times b, h_2 > \qquad \forall\, h_1,h_2\in F^b$$

as symplectic form on F^a. Hence the planetary motion can be described in only one Heisenberg algebra, namely in $\mathcal{G}^b$, which is caused by the angular momentum b, of course. We have $\ddot{\sigma} = f\cdot\sigma$ for some smooth real-valued function f defined along a planetary motion σ, implying $\omega^{(2)} = f\cdot\frac{|\sigma|^2}{\bar{m}}\cdot\omega^a$. In case σ is a circle, f is identical with the constant map with value $\frac{\bar{m}}{|\sigma|^2}$, due to the third Kepplerian law (cf. equation (7)). This motivates us to set

$$\mathcal{G}^{(2)}_{\sigma(t)} = \mathcal{G}^a_{\sigma(t)} \qquad \forall t \tag{8}$$

along any closed planetary motion σ which hence implies $\omega^{(2)} = \omega^a$ along σ. In turn one obtains

$$\ddot{\sigma}(t) = \text{grad } V_{sol}(\sigma(t)) \qquad \forall\, t, \tag{9}$$

a well-known equation from Newton implying Keppler's laws. Equation (9) is derived from a holographic principle in the sense that equation (8) states that the oriented circle of $\mathcal{P}^2_{\sigma(t)}$ matches the oriented circle of $\mathcal{P}^a_{\sigma(t)}$ at any t.

6. Horizontal and periodic lifts of β

Since, in general, $\Omega^a\neq 0$, the horizontal distribution in $T\mathcal{P}^a$ does not need to be integrable along level surfaces. However, Ω^a vanishes along field lines and thus the horizontal distribution is integrable along these curves. Let us look at $\mathcal{P}^a|_\beta$ where β is a field line of the singularity free vector field X.

A horizontal lift of $\dot{\beta}$ is a curve $\dot{\beta}^{hor}$ in $Hor_\beta = \ker\alpha^a$ which satisfies $T\text{pr}^a\dot{\beta}^{hor} = \dot{\beta}$ and obeys an initial condition in $T\mathcal{P}^a|_\beta$. Hence there is a unique curve β^{hor} passing through $v_{\beta(t_0)}\in\mathcal{P}^a_{\beta(t_0)}$, say, called horizontal lift of β. In the case of a constant vector field or in the case of the solar field this is nothing else but a meridian of the cylinder respectively the cone $\mathcal{P}^a|_\beta$ containing $v_{\beta(t_0)}$. Let $\beta(t_0) = x$ for a fixed $x \in O$.

Obviously, a horizontal lift is a geodesic on $\mathcal{P}^a|_\beta$ equipped with the metric g_{Hor_β}, say, induced by the scalar product $<\, ,\, >$ on E.

At first let a be a non-vanishing constant. A curve γ on $\mathcal{P}^a|_\beta$ here is called a periodic lift of β through v_x iff it is of the form

$$\gamma(s) = \beta^{hor}(s) \cdot e^{p \cdot s \cdot \frac{a}{|a|}} \in \mathcal{P}^a_{\beta(s)} \qquad \forall\, s$$

where p is a fixed real.

Clearly, γ is a horizontal lift through v_x iff $\gamma = \beta^{hor}$, i.e. iff $p = 0$. In fact any periodic lift γ of β is a geodesic on $\mathcal{P}^a|_\beta$. Hence $\ddot{\gamma}$ is perpendicular to $\mathcal{P}^a|_\beta$. Due to the $U(1)$-symmetry of $\mathcal{P}^a|_\beta$, a geodesic σ on $\mathcal{P}^a|_\beta$ is of the form

$$\sigma(s) = \beta^{hor}(\theta \cdot s) \cdot e^{p \cdot \theta \cdot s \cdot \frac{a}{|a|}} \qquad \forall\, s$$

as it is easily verified. Here p and θ denote reals. θ determines the speed of the geodesic. Thus σ and β have accordant speeds if $\theta = 1$ (which will be assumed from now on), as can be easily seen from

$$\dot{\gamma}(0) = p \cdot v_x \cdot \frac{a}{|a|} + \dot{\beta}^{hor}(0)$$

for $t_0 = 0$. The real number p determines the spatial frequency of the periodic lift γ due to $\frac{2 \cdot \pi}{T} = \frac{p}{|v_x|}$. The spatial frequency of γ counts the number of revolutions around $\mathcal{P}^a|_\beta$ per unit time and is determined by the F^a_x-component p of the initial velocity due to the $U(1)$-symmetry of the cylinder $\mathcal{P}^a|_\beta$. We refer to p as a momentum.

For the solar field $X(x) = \left(x, -\frac{x}{|x|^3}\right)$ with $x \in O$, let $|x_0| = 1$ and let a parametrization of the body of revolution $\mathcal{P}^a|_\beta$ be given in Clairaut coordinates via the map $\mathbf{x} : \mathcal{U} \to E$ defined by

$$\mathbf{x}(u, v) := -\bar{m} \cdot (3v - 2)^{\frac{1}{3}} \cdot r\left(e^{u \cdot \frac{a}{|a|}}\right) \cdot \left(v_x + \frac{a}{|a|}\right)$$

on an open set $\mathcal{U} \subset \mathbb{R}^2$. Here r is the representation of $U^{\frac{a}{|a|}}(1)$ onto $SO\left(F^{\frac{a}{|a|}}\right)$ for any $x \in O$. Then a geodesic γ on $\mathcal{P}^a|_\beta$ takes the form

$$\gamma(s) = \mathbf{x}(u(s), v(s)) \quad = \quad -\bar{m} \cdot (3v(s) - 2)^{\frac{1}{3}} \cdot r\left(e^{u(s) \cdot \frac{a}{|a|}}\right) \cdot \left(v_x + \frac{a}{|a|}\right)$$

where the functions u and v are determined by

$$\text{(10)} \qquad u(s) \quad = \quad \sqrt{2} \cdot \arctan\left(\frac{s}{\sqrt{2}\, d} + \frac{c_1}{2\, d}\right) + c_2$$

$$\text{(11)} \qquad \text{and} \quad v(s) \quad = \quad \pm\frac{1}{3}\left(\left(\frac{1}{\sqrt{2}} s + c_1\right)^2 + d^2\right)^{\frac{3}{2}} + \frac{2}{3}$$

(cf. [12]) with s in an open interval $I \subset \mathbb{R}$ containing 1. Here c_1 and c_2 are integration constants determining the initial conditions. Since we are concerned with a forward movement along the channel $\mathbb{R} \cdot \frac{a}{|a|}$, only the positive sign in (11) is of interest. The constant d fixes the slope of the geodesic via

$$\cos\vartheta = \frac{d}{\sqrt{\left(\frac{1}{\sqrt{2}}s + c_1\right)^2 + d^2}}$$

where ϑ is the constant angle between the geodesic γ, called periodic lift, again, and the parallels given in Clairaut coordinates. This means that d vanishes precisely for a meridian. A periodic lift γ is a horizontal lift of β iff γ is a meridian. Thus the parametrization of a meridian as a horizontal lift β^{hor} of an integral curve β parametrized as in (5) has the form

$$\beta^{hor}(t) = -\bar{m} \cdot (3t-2)^{\frac{1}{3}} \cdot v_x$$

with $\beta^{hor}(1) = -\bar{m} \cdot v_x$ as well as $\beta(1) = -\bar{m} \cdot x$ for $\frac{2}{3} \leq t < 1$ and any initial $v_x \in \mathcal{P}^a_{\beta(1)}$.

For the constant vector field from above, any periodic lift γ of β through v_x is uniquely determined by the $U^a(1)$-valued map

$$s \mapsto e^{p \cdot s \cdot \frac{a}{|a|}},$$

while for the solar field a periodic lift is characterized by

$$s \mapsto e^{u(s) \cdot \frac{a}{|a|}}$$

with $u(s)$ as in (10). These two maps here are called an elementary periodic function respectively an elementary Clairaut map. Therefore, we can state:

PROPOSITION 2. *Let $x = \beta(0)$. Under the hypothesis that a is a non-zero constant, there is a one-to-one correspondence between all elementary periodic $U^a(1)$-valued functions and all periodic lifts of β passing through a given $v_x \in \mathcal{P}^a_x$. In case X is the solar field there is a one-to-one correspondence between all periodic lifts passing through a given $v_x \in \mathcal{P}^a_x$ and all elementary Clairaut maps.*

An internal variable can be interpreted as a piece of information. Thus the fibres F^a_x and $\mathcal{P}^a_x$ can be regarded as a collection of pieces of information at x. The periodic lifts of β on $\mathcal{P}^a|_\beta$ describe the evolution of information of $\mathcal{P}^a|_\beta$ along β. This evolution can be further realized by a circular polarized wave: Let the lift rotate with frequency $\nu \neq 0$. Then a point $w(s;t)$, say, on this rotating lift is described by

$$w(s;t) = |v_x| \cdot \frac{\beta^{hor}_{v_x}(s)}{|\beta^{hor}_{v_x}(s)|} \cdot e^{2\pi\nu(t-p\cdot s)\cdot\frac{a}{|a|}} \qquad \forall s,t \in \mathbb{R}, \quad s \neq 0 \tag{12}$$

a circular polarized wave on the cylinder with $\frac{1}{|p|}$ as speed of the phase and $|v_x|$ as amplitude. w travels along $\mathbb{R} \cdot \frac{a}{|a|}$, the channel of information. Clearly, $\mathcal{P}^a|_{im\ \beta}$ is in $O \times E$ and not in E. However, w could be coupled to the space E and could be a wave in E traveling along β, e.g. as an electric or magnetic field. More types of waves can be obtained by using the complex line bundle F^a instead of the principal bundle $\mathcal{P}^a$, of course.

7. Representation of the Heisenberg group associated with periodic lifts of β on $\mathcal{P}^a|_\beta$ of a constant vector field

Let $a \neq 0$ be constant on O and $x \in im\ \beta$ a fixed vector. There is a unique periodic lift γ of β passing through $v_x = \gamma(0)$ with prescribed velocity $\dot{\gamma}(0)$. At first we will associate with $\dot{\gamma}(0)$ a well-defined unitary linear operator on a Hilbert space as follows.

The specification of $v_x \in \mathcal{P}^a_x$ turns F^a_x into a field $\hat{F}^a_x$ isomorphic to $\mathbb{C}$, since $\frac{v_x}{|v_x|} \cdot \mathbb{C} = F^a_x$. The real axis is $\mathbb{R} \cdot \frac{v_x}{|v_x|}$ and the imaginary one is $\mathbb{R} \cdot \frac{v_x}{|v_x|} \times \frac{a}{|a|}$. We rename these axes by q-axis carried by the unit vector $\bar{q}_x$ and by p-axis carried by the unit vector $\bar{p}_x$, respectively. Clearly, $\bar{p}_x = \bar{q}_x \cdot j^a_x(i)$. Any $h \in F^a_x$ is thus of the form $h = (q, p)$. The Schwartz space of the real axis and its L^2- completion are denoted by $\mathcal{S}(\mathbb{R}, \mathbb{C})$ and $L^2(\mathbb{R}, \mathbb{C})$, respectively. The Schrödinger representation ρ_x of G^a_x acts on each complex-valued $\psi \in \mathcal{S}(\mathbb{R}, \mathbb{C}) \subset L^2(\mathbb{R}, \mathbb{C})$ by

$$\rho_x(z + h)(\psi)(\tau) := z \cdot e^{p\cdot\tau\cdot i} \cdot e^{-\frac{1}{2}\cdot p\cdot q\cdot i} \cdot \psi(\tau - q) \qquad \forall\, \tau \in \mathbb{R} \tag{13}$$

for all $z + h \in G^a_x$ with $h = (q, p)$ (cf. [11], [13] and [7]). Clearly,

$$-p \cdot q \cdot i = \omega^a_x((0, p), (q, 0)) \cdot i \quad \text{and} \quad z = e^{\vartheta \cdot \frac{a}{|a|}}$$

for some $\vartheta \in \mathbb{R}$. By the Stone-von Neumann theorem ρ_x is irreducible (cf. [13] and [7]). Setting $q = |v_x|$, for any $p \in \mathbb{R}$, equation (13) turns into

$$\rho_x(z + (|v_x|, p))(\psi)\left(\tau + \frac{|v_x|}{2}\right) = z \cdot e^{p\cdot\tau\cdot i} \cdot \psi\left(\tau - \frac{|v_x|}{2}\right) \qquad \forall\, \tau \in \mathbb{R}.$$

Operators of this form generate $\rho_x(G^a_x)$, of course. In case $2\pi\nu$ with the frequency ν (justified by (12)) is different from one, for each $p \in \mathbb{R}$ equation (13) turns into

$$\rho_\nu\left(e^{t\cdot\frac{a}{|a|}} + (|v_x|, p)\right)(\psi)\left(\tau + \frac{|v_x|}{2}\right) = e^{2\pi\nu\cdot(t - p\cdot\tau)\cdot i} \cdot \psi\left(\tau - \frac{|v_x|}{2}\right) \tag{14}$$

for every $\tau, t \in \mathbb{R}$.

This shows that $2\pi\nu(t - p \cdot s)$ in the exponent of the factor $e^{2\pi\nu(t-p\cdot s)\cdot i}$ for $s = \tau$ is characteristic for the circular polarized wave described in (14) and determines the Schrödinger representation. Thus the geometry on the collection $\mathcal{P}^a|_\beta$ of all internal variables along β is directly transfered to the Hilbert space $L^2(\mathbb{R}, \mathbb{C})$ via the Schrödinger representation. Differently formulated, the Schrödinger representation has a geometric counterpart, namely $\mathcal{P}^a$ together with its geometry, which is, for example, used for holography. The counterpart of i in quantum mechanics is the imaginary unit $\frac{a}{|a|} \in \mathbb{H}$.

On the other hand the $U^a_x(1)$-valued function $\tau \longrightarrow e^{2\pi\nu(t-p\cdot\tau)\cdot\frac{a}{|a|}}$ entirely describes the periodic lift γ, rotating with frequency ν and passing through v_x, as expressed in (13). Thus the circular polarized wave w is characterized by the unitary linear transformation $\rho_\nu(e^{t\cdot\frac{a}{|a|}} + (|v_x|, p))$ on $L^2(\mathbb{R}, \mathbb{C})$. Due to the Stone-von Neumann theorem, the equivalence class of ρ_ν is uniquely determined by ν and vice versa. Therefore, we state:

THEOREM 1. *Let a be a non-vanishing constant. Any periodic lift γ of β on $\mathcal{P}^a|_\beta$ with initial conditions $\gamma(0) = v_x$ and momentum p is uniquely characterized by the unitary linear* *transformation* $\rho_x(1 + (|v_x|, p))$ *of* $L^2(\mathbb{R}, \mathbb{C})$ *with* $(1 + (|v_x|, p)) \in G^a_x$ *and vice versa. Thus* $v_x \in \mathcal{P}^a_x$ *determines a unitary representation* ρ *on* $L^2(\mathbb{R}, \mathbb{C})$ *characterizing the collection* $C^a_{v_x}$ *of all periodic lifts of* β *passing through* v_x*. The unitary linear transformation* $\rho_\nu(e^{t\cdot\frac{a}{|a|}} + (|v_x|, p))$ *of* $L^2(\mathbb{R}, \mathbb{C})$ *characterizes the circular polarized wave* w *on* $\mathcal{P}^a|_{im\ \beta}$ *with frequency* $\nu \neq 0$ *generated by* γ *and vice versa. The frequency determines the equivalence class of* ρ_ν*.*

As a consequence we have

COROLLARY 1. *The Schrödinger representation* ρ_ν *of* G^a_x *describes the transport of any piece of information* $(|v_x|, p) \in T_{(v_x,0)}\mathcal{P}^a|_\beta$ *along the field line* β*, with* $\mathbb{R} \cdot \frac{a}{|a|}$ *as information transmission channel.*

The mechanism by which each geodesic is associated with a Schrödinger representation as expressed in theorem 1 is generalized for the solar field as follows (cf. [12]): Let $O = E\backslash\{0\}$. Given $im\ \beta$ of an integral curve β, we consider the Heisenberg algebra $\mathbb{R} \cdot \frac{a}{|a|} \oplus F^{\frac{a}{|a|}}$ equipped with the symplectic structure determined by $\frac{a}{|a|}$. Now let γ be a geodesic on $\mathcal{P}^a|_{im\ \beta}$ and $\psi \in \mathcal{S}(\mathbb{R}, \mathbb{C})$. Then the Schrödinger representation ρ_{sol} of the solar field on the Heisenberg group G^a_x is given by

$$\rho_{sol}(z, \mathbf{x}(s))(\psi)(\tau)(s) := z \cdot e^{u(s)\cdot\tau\cdot i} \cdot e^{-\frac{1}{2}\cdot u(s)\cdot v(s)\cdot i} \cdot \psi(\tau - v(s))$$

for all s in the domain of γ and any $\tau \in \mathbb{R}$.

8. Periodic lifts of β on $\mathcal{P}^a|_\beta$, the metaplectic group $Mp(F^a_x)$ and quantization

Let ρ_x be given as in (13), meaning that Planck's constant is set to one. For $v_x \in \mathcal{P}^a_x$ and $\dot\gamma_{v_x}(0)$ of a periodic lift γ_{v_x} of β,

$$\dot\gamma_{v_x}(0) = \dot\gamma_{v_x}(0)^{F^a_x} + \dot\beta^{hor}_{v_x}(0)$$

is an orthogonal splitting of the velocity of γ_{v_x} at 0. Clearly, the F^a_x-component of $\dot\gamma_{v_x}(0)$ is $\dot\gamma_{v_x}(0)^{F^a_x} = p \cdot \bar p_x$, where p is the momentum. Thus the momenta of periodic lifts of β passing through v_x are in a one-to-one correspondence with elements in $T_{v_x}\mathcal{P}^a_x$.

Therefore, the collection $\bar C^a_x$ of all periodic lifts of β on $\mathcal{P}^a|_\beta$ is in a one-to-one correspondence with $T\mathcal{P}^a_x$ (being diffeomorphic to a cylinder) via a map $f : \bar C^a_x \longrightarrow T\mathcal{P}^a_x$, say. Let

$$j : T\mathcal{P}^a_x|_\beta \longrightarrow F^a_x$$

be given by $j := T\tilde j$ where $\tilde j : \mathcal{P}^a_x \longrightarrow \mathcal{P}^a_x$ is the antipodal map. Thus

$$j(w_x, \lambda) = j(w_{-x}, \lambda) = \lambda$$

for every $(w_x, \lambda) \in T_{w_x}\mathcal{P}^a_x$ with $w_x \in \mathcal{P}^a_x$ and $\lambda \in \mathbb{R}$. Clearly, j is two-to-one. Setting $\dot F^a_x = F^a_x\backslash\{0\}$, the map

$$j \circ f : \bar C^a_x \longrightarrow \dot F^a_x$$

is two-to-one, turning $\bar C^a_x$ into a two-fold covering of $\dot F^a_x$. $j \circ f$ describes the correspondence between periodic lifts in $\bar C^a_x$ and their momenta. The symplectic group $Sp(F^a_x)$ acts transitively on F^a_x equipped with ω^a as symplectic structure. Therefore, the metaplectic group $Mp(F^a_x)$, which is the two-fold covering of $Sp(F^a_x)$, acts transitively on $T\mathcal{P}^a_x$.

Thus given $u \in F_x^a$, there is a smooth map

$$\Phi : Sp(F_x^a) \longrightarrow F_x^a$$

given by $\Phi(A) := A(u)$ for all $A \in Sp(F_x^a)$. Since $j \circ f(u_{w_x}) = j \circ f(u_{-w_x})$ for all $u_{w_x} \in T\mathcal{P}^a|_{\beta(0)}$, the map Φ lifts smoothly to

$$\tilde{\Phi} : Mp(F_x^a) \longrightarrow \bar{C}_x^a$$

such that

$$(j \circ f) \circ \tilde{\Phi} = \tilde{\mathrm{pr}} \circ \Phi$$

where $\tilde{\mathrm{pr}} : Mp(F_x^a) \longrightarrow Sp(F_x^a)$ is the covering map. Clearly, the orbit of $Mp(F_x^a)$ on $\bar{C}_x^a$ is all of $\bar{C}_x^a$, and $Mp(F_x^a)$ acts on F_x^a with a one-dimensional stabilizing group (cf. [14]). Now let us sketch the link between this observation and the quantization on $\mathbb{R}$. $Sp(F_x^a)$ operates as an automorphism group on the Heisenberg group G_x^a (leaving the centre fixed) via

$$A(z + h) = z + A(h) \qquad \forall\, z + h \in G_x^a.$$

Any $A \in Sp(F_x^a)$ determines the irreducible unitary representation ρ_A defined by

$$\rho_A(z + h) := \rho_x(z + A(h)) \qquad \forall\, (z + h) \in G_x^a.$$

Due to the Stone-von Neumann theorem it must be equivalent to ρ_x itself, meaning that there is an intertwining unitary operator U_A on $L^2(\mathbb{R}, \mathbb{C})$, determined up to a complex number of absolute value one in $\mathbb{C}_x^a$, such that $\rho_A = U_A \circ \rho \circ U_A^{-1}$ and $U_{A_1} \circ U_{A_2} = coc(A_1, A_2) \cdot U_{A_1 \circ A_2}$ for all $A_1, A_2 \in Sp(F_x^a)$. Here *coc* is a cocycle with value $coc(A_1, A_2) \in \mathbb{C}\backslash\{0\}$. Thus U is a projective representation of $Sp(F_x^a)$ and hence lifts to a representation W of $M_p(F_x^a)$. Since the Lie algebra of $M_p(F_x^a)$ is isomorphic to the Poisson algebra of homogenous quadratic polynomials, dW provides the quantization procedure of quadratic homogeneous polynomials on $\mathbb{R}$ and moreover describes the transport of information in $\mathcal{P}^a$ along the field line β, as described in [4].

References

[1] BINZ E., SNIATYCKI J. AND FISCHER H., *The geometry of classical fields*, Mathematical Studies **154**, North Holland 1988.

[2] BINZ E., DE LEÓN M. AND SOCOLESCU D., *On a smooth geometric approach to the dynamics of media with microstructures*, C.R. Acad. Sci. Paris **326** Série II b (1998), 227–232.

[3] BINZ E. AND SCHEMPP W., *Quantum teleportation and spin echo: a unitary symplectic spinor approach*, in: "Aspects of complex analysis, differential geometry, mathematical physics and applications" (Eds. S. Dimiev and K. Sekigawa), World Scientific 1999, 314–365.

[4] BINZ E. AND SCHEMPP W., *Vector fields in three-space, natural internal degrees of freedom, signal transmission and quantization*, Result. Math. **37** (2000), 226–245.

[5] BINZ E. AND SCHEMPP W., *Entanglement parataxy and cosmology*, Proc. Leray Conference, Kluwer Publishers, to appear.

[6] BINZ E. AND SCHEMPP W., *Quantum systems: from macro systems to micro systems, the holographic technique*, to appear.

[7] FOLLAND G. B., *Harmonic analysis in phase space*, Princeton University Press 1989.

[8] GREUB W., *Linear algebra*, Springer Verlag 1975.

[9] GREUB W. *Multilinear algebra*, Springer Verlag 1978.

[10] GREUB W., HALPERIN S. AND VANSTONE R., *Connections, curvature and cohomology*, Vol. II, Academic Press 1973.

[11] GUILLEMIN V. AND STERNBERG S., *Symplectic techniques in physics*, Cambridge University Press 1991.

[12] PODS S., *Bildgebung durch klinische Magnetresonanztomographie*, Diss. Universität Mannheim, in preparation.

[13] SCHEMPP W. J., *Harmonic analysis on the heisenberg nilpotent lie group with applications to signal theory*, Pitman Research Notes in Mathematics **147**, Longman Scientific & Technical 1986.

[14] SCHEMPP W. J., *Magnetic resonance imaging, mathematical foundations and applications*, Wiley-Liss 1998.

[15] SNIATYCKI J., *Geometric quantization and quantum mechanics*, Applied Math. Series **30**, Springer-Verlag 1980.

AMS Subject Classification: 53D25, 43A65.

Ernst BINZ, Sonja PODS
Lehrstuhl für Mathematik I
Universität Mannheim
D-68131 Mannheim, GERMANY
e-mail: `binz@math.uni-mannheim.de`
e-mail: `pods@math.uni-mannheim.de`

Walter SCHEMPP
Lehrstuhl für Mathematik I
Universität Siegen
D-57068 Siegen, GERMANY
e-mail: `schempp@mathematik.uni-siegen.de`

Rend. Sem. Mat. Univ. Pol. Torino
Vol. 58, 1 (2000)
Geom., Cont. and Micros., I

E. Binz - D. Socolescu

MEDIA WITH MICROSTRUCTURES AND THERMODYNAMICS FROM A MATHEMATICAL POINT OF VIEW

Abstract. Based on the notion of continua with microstructures we introduce the notion of microstructures on discrete bodies. Using the analogy with of differential forms on discrete media we develop the discrete virtual work and the thermodynamics in the sense of Caratheodory.

1. Continua with microstructures

Let B be a medium, i.e. a three dimensional compact, differentiable manifold with boundary. In the case of classical continuum mechanics this medium is thought to be moving and deforming in $\mathbb{R}^3$. A configuration is then a smooth embedding $\Phi : B \to \mathbb{R}^3$. The configuration space is then either $\mathcal{E}(B, \mathbb{R}^3)$, the collection of all smooth embeddings from B into $\mathbb{R}^3$, a Fréchet manifold, or, for physical reasons, a subset of $\mathcal{E}(B, \mathbb{R}^3)$ which we denote by $conf\ (B, \mathbb{R}^3)$. This classical setting can be generalized to media with microstructures.

A medium B with microstructure is thought as a medium whose points have internal degrees of freedom. Such a medium was recently modelled by a specified principal bundle $P \xrightarrow{\pi} B$ with structure group H, a compact Lie group ([3])

Accordingly the medium B with microstructure is thought to be moving and deforming in the ambient space $\mathbb{R}^3$ with microstructure, which is modelled by another specified principal bundle $Q \xrightarrow{\omega} \mathbb{R}^3$, with structure group G, a Lie group containing H. A configuration is then a smooth, H-equivariant, fibre preserving embedding $\tilde{\Phi} : P \to Q$, i.e.

$$\tilde{\Phi}(p, h) = \tilde{\Phi}(p) \cdot h, \qquad \forall\ p \in P, \ \ \forall\ h \in H.$$

The configuration space is then either $\mathcal{E}(P, Q)$, i.e. the collection of all these configurations, or again for physical reasons $Conf(P, Q)$, a subset of $\mathcal{E}(P, Q)$. Clearly any $\tilde{\Phi} \in \mathcal{E}(P, Q)$ determines some $\Phi \in \mathcal{E}(B, \mathbb{R}^3)$ by

$$\Phi\,(\pi(p)) = \omega\left(\tilde{\Phi}(p)\right), \ \forall\ p \in P.$$

The map $\pi_{\mathcal{E}} : \mathcal{E}(P, Q) \to \mathcal{E}(B, \mathbb{R}^3)$ given by

$$\pi_{\mathcal{E}}(\tilde{\Phi})(\pi(p)) = \omega(\tilde{\Phi}(p)), \ \forall\ p \in P, \ \forall\ \tilde{\Phi} \in \mathcal{E}(P, Q),$$

is not surjective in general. For the sake of simplicity we assume in the following that $\pi_{\mathcal{E}}$ is surjective. Given two configurations $\tilde{\Phi}_1, \tilde{\Phi}_2$ in $\pi_{\mathcal{E}}^{-1}(\Phi) \subset \mathcal{E}(P, Q)$ for $\Phi \in \mathcal{E}(B, \mathbb{R}^3)$, there exists a smooth map $\tilde{g} : P \to G$, called gauge transformation, such that

$$\tilde{\Phi}_1(p) = \tilde{\Phi}_2(p) \cdot \tilde{g}(p), \ \forall\ p \in P.$$

Moreover, $\tilde{g}$ satisfies

$$\tilde{g}(p \cdot h) = h^{-1} \cdot \tilde{g}(p) \cdot h, \ \forall \ p \in P, \ \forall \ h \in H.$$

The collection G_P^H of all gauge transformations $\tilde{g}$ form a group, the so-called gauge group.

The gauge group G_P^H is a smooth Fréchet manifold. In fact $\mathcal{E}(P, Q)$ is a principal bundle over $\mathcal{E}(B, \mathbb{R}^3)$ with G_P^H as structure group.

2. Discrete systems with microstructures

In the following we show how the notion of media with microstructure dealed with above in the continuum case can be introduced in the discrete case. To this end we replace the body manifold, i.e. the medium B, by a connected, two-dimensional polyhedron $\mathbb{P}$. We denote the collection of all vertices q of $\mathbb{P}$ by $S^0\mathbb{P}$, the collection of all bounded edges e of $\mathbb{P}$ by $S^1\mathbb{P}$, and the collection of all bounded faces f of $\mathbb{P}$ by $S^2\mathbb{P}$. We assume that:

i) every edge $e \in S^1\mathbb{P}$ is directed, having e^- as initial and e^+ as final vertex, and therefore oriented,

ii) every face $f \in S^2\mathbb{P}$ is plane starshaped with respect to a given barycenter B_f and oriented. Morever, f is regarded as the plane cone over its boundary ∂f, formed with respect to B_f. This cone inherits from $\mathbb{R}^2$ a smooth linear parametrization along each ray joining B_f with the vertices of f and with distinguished points of the edges belonging to ∂f and joining these vertices, as well as a picewise smooth, linear parametrization along the boundary ∂f of f, i.e. along the edges.

A configuration of $\mathbb{P}$ is a map $\Phi : \mathbb{P} \to \mathbb{R}^3$ with the following defining properties:

i) $j : S^0\mathbb{P} \to \mathbb{R}^3$ is an embedding;

ii) if any two vertices q_1 and q_2 in $S^0\mathbb{P}$ are joined by some edge e in $S^1\mathbb{P}$, then the image $\Phi(e)$ is the edge joining $\Phi(q_1)$ and $\Phi(q_2)$;

iii) the image $\Phi(f)$ of every face f in $S^2\mathbb{P}$, regarded as the plane cone over its boundary ∂f formed with respect to B_f, is a cone in $\mathbb{R}^3$ over the corresponding boundary $\Phi(\partial f)$ formed with respect to $\Phi(B_f)$;

iv) Φ preserves the orientation of every face $f \in S^2\mathbb{P}$ and of every edge $e \in S^1\mathbb{P}$.

We denote by $\mathcal{E}(\mathbb{P}, \mathbb{R}^3)$ the collection of all configurations Φ of $\mathbb{P}$, and by $conf\left(\mathbb{P},\mathbb{R}^3\right)$ the configuration space, which is either $\mathcal{E}(\mathbb{P}, \mathbb{R}^3)$ or eventually a subset of it.

As in the continuum case we model the plyhedron $\mathbb{P}$ with microstructure by a principal bundle $P \xrightarrow{\pi} \mathbb{P}$ with structure group H, a compact Lie group, while the ambient space $\mathbb{R}^3$ with microstructure is modelled by another principal bundle $Q \xrightarrow{\omega} \mathbb{R}^3$ with structure group G, a Lie group containing H.

We note that we implement the interaction of internal variables by fixing a connection on $P \xrightarrow{\pi} \mathbb{P}$, and this can be done by using an argument similar to that one in [4]. Clearly not every closed, piecewise linear curve in $\mathbb{P}$ can be lifted to a closed, piecewise linear curve in P.

The configuration space $Conf(P, Q)$ is a subset of the collection $\mathcal{E}(P, Q)$ of smooth, H-equivariant, fibre preserving embeddings $\tilde{\Phi} : P \to Q$.

Again $Conf(P, Q)$ is a principal bundle over $conf(\mathbb{P}, \mathbb{R}^3)$ or over some open subset of it with G_P^H as structure group.

3. The interaction form and its virtual work

Let us denote by $F(S^0\mathbb{P}, \mathbb{R}^3)$ the collection of all $\mathbb{R}^3$-valued functions on $S^0\mathbb{P}$, by $A(S^1\mathbb{P}, \mathbb{R}^3)$ the collection of all $\mathbb{R}^3$-valued one-forms on $\mathbb{P}$, i.e. of all maps $\gamma : S^1\mathbb{P} \to \mathbb{R}^3$, and by $A^2\left(S^2\mathbb{P}, \mathbb{R}^3\right)$ the collection of all $\mathbb{R}^3$-valued two-forms on $\mathbb{P}$, i.e. of all maps $\omega : S^2\mathbb{P} \to \mathbb{R}^3$. We note that $F(S^0\mathbb{P}, \mathbb{R}^3)$, $A^1 S^1\mathbb{P}, \mathbb{R}^3)$ and $A^2(S^2\mathbb{P}, \mathbb{R}^3)$ are finite dimensional $\mathbb{R}$-vector spaces due to the fact that $\mathbb{P}$ has finitely many vertices, edges and faces. In all these vector spaces we can present natural bases. Indeed, given any $z \in \mathbb{R}^3$ and a fixed vertex $q \in S^0\mathbb{P}$, we define $h_q^z \in F(S^0\mathbb{P}, \mathbb{R}^3)$ as follows:

$$h_q^z(q') = \begin{cases} z \ , & \text{if } q = q' \\ 0 \ , & \text{otherwise} \ . \end{cases}$$

On the other hand, for a fixed edge $e \in S^1\mathbb{P}$ respectively a fixed face $f \in S^2\mathbb{P}$, $\gamma_e^z \in A^1(S^1\mathbb{P}, \mathbb{R}^3)$ and $\omega_f^z \in A^2(S^2\mathbb{P}, \mathbb{R}^3)$ are given in the following way:

$$\gamma_e^z(e') = \begin{cases} z \ , & \text{if } e = e' \ , \\ 0 \ , & \text{otherwise} \ , \end{cases} \qquad \omega_f^z(f') = \begin{cases} z \ , & \text{if } f = f' \ , \\ 0 \ , & \text{otherwise} \ . \end{cases}$$

If now $\{z_1, z_2, z_3\}$ is a base in $\mathbb{R}^3$, then

$$\{h_q^{z_i} \mid q \in S^0\mathbb{P}, i = 1, 2, 3\} \subset F(S^0\mathbb{P}, \mathbb{R}^3)$$

$$\{\gamma_e^{z_i} \mid e \in S^1\mathbb{P}, i = 1, 2, 3\} \subset A^1(S^1\mathbb{P}, \mathbb{R}^3)$$

and

$$\{\omega_q^{z_i} \mid f \in S^2\mathbb{P}, i = 1, 2, 3\} \subset A^2(S^2\mathbb{P}, \mathbb{R}^3)$$

are the natural bases mentioned above.

Given now a scalar product $\langle\cdot,\cdot\rangle$ on $\mathbb{R}^3$, we define the scalar product G^0, G^1 and G^2 on $F(S^0\mathbb{P}, \mathbb{R}^3)$, $A^1(S^1\mathbb{P}, \mathbb{R}^3)$ and respectively $A^2(S^2\mathbb{P}, \mathbb{R}^3)$ by

$$G^0(h_1, h_2) := \sum_{q \in S^0 P} \langle h_1(q), h_2(q)\rangle \ , \ \forall\, h_1, h_2 \in F(S^0\mathbb{P}, \mathbb{R}^3) \ ,$$

$$G^1(\gamma_1, \gamma_2) := \sum_{e \in S^1 P} \langle \gamma_1(e), \gamma_2(e)\rangle \ , \ \forall\, \gamma_1, \gamma_2 \in A^1(S^1\mathbb{P}, \mathbb{R}^3) \ ,$$

and

$$G^2(\omega_1, \omega_2) := \sum_{f \in S^2 P} \langle \omega_1(f), \omega_2(f)\rangle \ , \ \forall\, \omega_1, \omega_2 \in A^2(S^2\mathbb{P}, \mathbb{R}^3).$$

The differential dh of any $h \in F(S^0\mathbb{P}, \mathbb{R}^3)$ is a one-form on $\mathbb{P}$ given by

$$dh(e) = h(e^+) - h(e^-) \ , \ \forall\, e \in S^1\mathbb{P} \ ,$$

where e^- and e^+ are the initial and the final vertex of e.

The exterior differential $d : A^1(S^1\mathbb{P}, \mathbb{R}^3) \to A^2(S^2\mathbb{P}, \mathbb{R}^3)$ applied to any $\gamma \in A^1(S^1\mathbb{P}, \mathbb{R}^3)$ is given by

$$d\gamma(f) := \sum_{e \in \partial f} \gamma\,(e) \ \ , \ \forall\, f \in S^2\mathbb{P} \ .$$

The exterior differential $d\omega$ for any two-form ω on $\mathbb{P}$ vanishes. Associated with d and the above scalar products are the divergence operators

$$\delta : A^2(S^2\mathbb{P}, \mathbb{R}^3) \to A^1(S^1\mathbb{P}, \mathbb{R}^3)$$

and

$$\delta : A^1(S^1\mathbb{P}, \mathbb{R}^3) \to F(S^0\mathbb{P}, \mathbb{R}^3) ,$$

respectively defined by the following equations

$$G^1(\delta\omega, \alpha) = G^2(\omega, d\alpha) \quad , \quad \forall\, \omega \in A^2(S^2\mathbb{P}, \mathbb{R}^3) \text{ and } \forall\, \alpha \in A^1(S^1\mathbb{P}, \mathbb{R}^3) ,$$

and

$$G^0(\delta\alpha, h) = G^1(\alpha, dh) \quad , \quad \forall\, \alpha \in A^1(S^1\mathbb{P}, \mathbb{R}^3) \text{ and } \forall\, h \in F(S^0\mathbb{P}, \mathbb{R}^3) .$$

$d \circ d = 0$ implies $\delta \circ \delta = 0$. Elements of the form dh in $A^1(S^1\mathbb{P}, \mathbb{R}^3)$ for any $h \in F(S^0\mathbb{P}, \mathbb{R}^3)$ are called exact, while elements of the form $\delta\omega$ in $A^1(S^1\mathbb{P}, \mathbb{R}^3)$ for any $\omega \in A^2(S^2\mathbb{P}, \mathbb{R}^3)$ are called coexact.
The Laplacians $\Delta_0,\ \Delta_1$ and Δ_2 on $F(S^0\mathbb{P}, \mathbb{R}^3),\ A^1(S^1\mathbb{P}, \mathbb{R}^3)$ and $A^2(S^2\mathbb{P}, \mathbb{R}^3)$ are respectively defined by

$$\Delta_i := \delta \circ d + d \circ \delta\ ,\ i = 0, 1, 2\ .$$

Due to dim $\mathbb{P} = 2$ these Laplacians, selfadjoint with respect to $G^i,\ i = 0, 1, 2$, simplify to $\Delta_0 = \delta \circ d$ on functions, $\Delta_1 = \delta \circ d + d \circ \delta$ on one-forms and $\Delta_2 = d \circ \delta$ on two-forms. Hence there are the following G^0, G^1- and respectively G^2-orthogonal splittings, the so called Hodge splittings [1]:

$$\begin{array}{rcl} A^0(S^0\mathbb{P}, \mathbb{R}^3) & = & \delta A^1(S^1\mathbb{P}, \mathbb{R}^3) \oplus Harm^0(S^0\mathbb{P}, \mathbb{R}^3)\ , \\ A^1(S^1\mathbb{P}, \mathbb{R}^3) & = & dF(S^0\mathbb{P}, \mathbb{R}^3) \oplus \delta A^2(S^2\mathbb{P}, \mathbb{R}^3) \oplus Harm^1(S^1\mathbb{P}, \mathbb{R}^3)\ , \\ A^2(S^2\mathbb{P}, \mathbb{R}^3) & = & dA^1(S^1\mathbb{P}, \mathbb{R}^3) \oplus Harm^2(S^2\mathbb{P}, \mathbb{R}^3)\ . \end{array}$$

Here $Harm^i(S^i\mathbb{P}, \mathbb{R}^3) := Ker\ d \cap Ker\ \delta\ ,\ i = 0, 1, 2$. Reformulated, this says that $\beta \in Harm^i(S^i\mathbb{P}, \mathbb{R}^3)$ if $\Delta_i\beta = 0,\ i = 0, 1, 2$; we note that $\beta \in Harm^0(S^0\mathbb{P}, \mathbb{R}^3)$ is a constant function.

Letting $H^i(\mathbb{P}, \mathbb{R}^3)$ be the i-th cohomology group of $\mathbb{P}$ with coefficients in $\mathbb{R}^3$, we hence have:

$$H^i(\mathbb{P}, \mathbb{R}^3) \cong Harm^i(S^i\mathbb{P}, \mathbb{R}^3)\ ,\ i = 1, 2\ .$$

Next we introduce the stress or interaction forms, which are constitutive ingredients of the polyhedron $\mathbb{P}$. To this end we consider the interaction forces, i.e. vectors in $\mathbb{R}^3$,which act up on any vertex q, along any edge e and any face f of $\mathbb{P}$.

The collection of all these forces acting up on the vertices defines a configuration dependent function $\alpha^0(\Phi) \in F(S^0\mathbb{P}, \mathbb{R}^3)$, where $\Phi \in conf\left(\mathbb{P}, \mathbb{R}^3\right)$. Analogously the collection of all the interaction forces acting up along the edges or along the faces defines a one form $\alpha^1(\Phi) \in A^1(S^1\mathbb{P}, \mathbb{R}^3)$ or a two-form $\alpha^2(\Phi) \in A^2(S^2\mathbb{P}, \mathbb{R}^3)$ respectively. The virtual work $\mathcal{A}^i(\Phi)$ caused respectively by any distortion $\gamma^i \in A^i(S^i\mathbb{P}, \mathbb{R}^3)$, $i = 0, 1, 2$, is given by

$$\mathcal{A}^i(\Phi)(\gamma^i) = \mathcal{G}^i(\alpha^i(\Phi), \gamma^i),\ i = 0, 1, 2\ .$$

However, it is important to point out that the total virtual work $\mathcal{A}(\Phi)$ caused by a deformation of the polyhedron $\mathbb{P}$ is given only by $\mathcal{A}^1(\Phi)(\gamma^1) + \mathcal{A}^2(\Phi)\left(\rho^2\right)$, where ρ^2 is the harmonic part of $\gamma^2 \in A^2(S^2\mathbb{P}, \mathbb{R}^3)$. In order to justify it we give the virtual works $\mathcal{A}^i(\Phi)(\gamma^i),\ i = 1, 2,$ in accordance with the Hodge splitting for $\alpha^i(\Phi)$ and $\gamma^i,\ i = 0, 1, 2,$ and with the definition of the divergence operators δ, the equivalent forms

$$\begin{array}{rcl} \mathcal{G}^0(\alpha^0(\Phi), \delta\gamma^1) & = & \mathcal{G}^1(d\alpha^0(\Phi), \gamma^1), \\ \mathcal{G}^1(\alpha^1(\Phi), \gamma^1) & = & \mathcal{G}^1(d\beta^0 + \delta\omega^2 + \varkappa^1, \gamma^1) \\ & = & \mathcal{G}^0(\beta^0, \delta\gamma^1) + \mathcal{G}^2(\omega^2, d\gamma^1) + \mathcal{G}^1(\varkappa^1, \rho^1) \\ \mathcal{G}^2(\alpha^0(\Phi), \delta\gamma^1) & = & \mathcal{G}^2(d\beta^1 + \varkappa^2, \gamma^2) = \mathcal{G}^1(\beta^1, \delta\gamma^2) + \mathcal{G}^2(\varkappa^2, \rho^2), \end{array}$$

Here the two terms

$$\mathcal{G}^1(\varkappa^1, \gamma^1) = \mathcal{G}^1(\varkappa^1, dh^0 + dh^2 + \rho^1) = \mathcal{G}^1(\varkappa^1, \rho^1),$$

and

$$\mathcal{G}^2(\varkappa^2, \gamma^2) = \mathcal{G}^2(\varkappa^2, dh^1 + \rho^2) = \mathcal{G}^2(\varkappa^2, \rho^2)$$

depend only on the topology of the polyhedron $\mathbb{P}$.

Comparing now the different expressions for the virtual works we get

$$\begin{array}{rcl} \mathcal{A}^1(\Phi)\left(\gamma^1\right) + \mathcal{G}^2(\varkappa^2, \rho^2) & = & \mathcal{G}^0(\alpha^0(\Phi), \delta\gamma^1) + \mathcal{G}^2(\alpha^2(\Phi), d\gamma^1) + \\ & + & \mathcal{G}^1(\varkappa^1, \rho^1) + \mathcal{G}^2(\varkappa^2, \rho^2), \end{array}$$

$$\begin{array}{rcl} \alpha^0(\Phi) & = & \delta\alpha^1(\Phi), \\ \alpha^1(\Phi) & = & d\alpha^0(\Phi) + \delta\alpha^2(\Phi) + \rho^1, \\ \alpha^2(\Phi) & = & d\alpha^1(\Phi) + \rho^2. \end{array}$$

Moreover

$$\begin{array}{rcl} \Delta_0\alpha^0(\Phi) & = & \alpha^0(\Phi)\ , \\ \Delta_2\alpha^2(\Phi) + \varkappa^2 & = & \alpha^2(\Phi)\ . \end{array}$$

Accordingly, the total virtual work on $\mathbb{P}$ associated, as discussed above, with α^0, α^1 and α^2 is given by

$$\begin{array}{rcl} \mathcal{A}(\Phi)(\gamma^1, \gamma^2) & := & \mathcal{A}^1(\Phi)(\gamma^1) + \mathcal{A}^2(\Phi)(\rho^2) \\ & = & \mathcal{G}^1(\alpha^1(\Phi), \Delta_1\gamma^1) + \mathcal{G}^1(\varkappa^1, \rho^1) + \mathcal{G}^2(\varkappa^2, \rho^2) \end{array}$$

However, due to translational invariance

$$\alpha^i(\Phi) = \alpha^i(d\Phi),\ i = 0, 1, 2\ .$$

For this reason we let $d\Phi$ vary in a smooth, compact and bounded manifold $K \subset dconf(\mathbb{P}, \mathbb{R}^3)$ with non-empty interior. The virtual work on $\mathbb{P}$ has then the form

$$\mathcal{A}(\Phi)(\gamma^1, \gamma^2) = \mathcal{A}(d\Phi)(\gamma^1, \gamma^2)$$

for any $d\Phi \in K$ and any $\gamma^i \in A^i(S^i\mathbb{P}, \mathbb{R}^3)$. Since $dconf\left(\mathbb{P}, \mathbb{R}^3\right) \subset A^1\left(S^1\mathbb{P}, \mathbb{R}^3\right)$ according to the Hodge splitting is not open, not all elements in $A^1\left(S^1\mathbb{P}, \mathbb{R}^3\right)$ are tangent to

$dconf\left(\mathbb{P}, \mathbb{R}^3\right)$. Therefore, $\mathcal{A}$ is not a one-form on $\mathcal{K} \subset dconf\left(\mathbb{P}, \mathbb{R}^3\right)$, in general. To use the formalism of differential forms, we need to extend the virtual work $\mathcal{A}$ to some compact bounded submanifold $\mathcal{K}^1 \subset A^1\left(S^1\mathbb{P}, \mathbb{R}^3\right)$ with $\mathcal{K} \subset \mathcal{K}^1$- See [2] for details -

The one-form $\mathcal{A}(d\Phi)$ needs not to be exact, in general. We decompose accordingly $\mathcal{A}$ into

$$\mathcal{A}(d\Phi) = \ dI\,F + \Psi.$$

This decomposition is the so called Neumann one, given by

$$div\mathcal{A} = \Delta F,\ \ \mathcal{A}(\xi)\,(\nu(\xi)) = \mathbb{D}(\xi)(\nu(\xi))$$

for all ξ in the boundary $\partial\mathcal{K}^1$ of $\mathcal{K}^1$. $\mathbb{D}$ is the Fréchet derivative on $A^1\left(S^1\mathbb{P}, \mathbb{R}^3\right)$, while ν is the outward directed unit normal field on ∂K^1. The differential opeators div and Δ are the divergence and respectively the Laplacian on $A^1\left(S^1\mathbb{P}, \mathbb{R}^3\right)$.

4. Thermodynamical setting

This Neumann decomposition, combined with the idea of integrating factor of the heat, as presented in [1], [6] and [7], yields a thermodynamical setting.

In order to do this let us remember first that $A^1\left(S^1\mathbb{P}, \mathbb{R}^3\right)$ has according to the Hodge splitting the decomposition

$$A^1\left(S^1\mathbb{P}, \mathbb{R}^3\right) = dF\left(S^0\mathbb{P}, \mathbb{R}^3\right) \oplus \delta A^2\left(S^2\mathbb{P}, \mathbb{R}^3\right) \oplus Harm^1\left(S^1\mathbb{P}, \mathbb{R}^3\right).$$

This fact implies the necessity of one additional coordinate function for the construction of the therodynamical setting. Accordingly we extend $\mathcal{K}^1$ to $\mathcal{K}_{\mathbb{R}} := \mathcal{K}^1 \times \mathbb{R}$ and pull $\mathcal{A}$ back to $\mathcal{K}_{\mathbb{R}}$. The pull back is again denoted by $\mathcal{A}$.

We follow now the argument in [2] and denote by U the additional coordinate function on $\mathcal{K}_{\mathbb{R}}$: we set for the heat

$$H := \ dIU - \mathcal{A}$$

where by dI we denote here the differential on $\mathcal{K}_{\mathbb{R}}$.

Let now $\frac{1}{T}$ be an integrating factor of H; i.e.

$$H = T\ dIS \quad \text{on} \quad \mathcal{K}_{\mathbb{R}},$$

where $S : \mathcal{K}_{\mathbb{R}} \to \mathbb{R}$ is a smooth function ([2]). Next we introduce the free energy $F_{\mathcal{K}_{\mathbb{R}}}$ by setting

$$F_{\mathcal{K}_{\mathbb{R}}} := U - T \cdot S\ ,$$

yielding

$$\mathcal{A} = \ dI\,F_{\mathcal{K}_{\mathbb{R}}} - S\ dIT\ .$$

Both $F_{\mathcal{K}_{\mathbb{R}}}$ and T depend on the tuple $(\xi, U) \in \mathcal{K}_{\mathbb{R}}$. The one-form $\mathcal{A}$ on $\mathcal{K}_{\mathbb{R}}$ depends trivially on U. We think of some dependence of U on ξ, i.e. we think of a map $s : \mathcal{K}^1 \to \mathbb{R}$ and restrict the above decomposition of $\mathcal{A}$ to the graph of s. s is determined by the equation

$$F_{\mathcal{K}_{\mathbb{R}}}\,(\xi, s(\xi)) = F(\xi) + F^0,$$

$\forall \xi$ in some submanifolds V of $\mathcal{K}^1$. We call F the free energy, too. Then

$$\mathcal{A} = \; dI\,F + \Psi \quad \text{on} \quad \mathcal{K}^1,$$

where Ψ on V has the form

$$\Psi(\xi)(\gamma) = S(s(\xi)) \cdot \; dI\,T(s(\xi)) \;\; \forall \xi \in V \subset \mathcal{K}^1 \text{ and } \forall \gamma \in A^1\left(S^1\mathbb{P}, \mathbb{R}^3\right)$$

dI is here the differential on $\mathcal{K}^1$.

We have considered here the thermodynamical setting only in the case of the virtual work done on $\mathbb{P}$. This can be easily generalized to the virtual work on the microstructure. To do this we define first the virtual work on the microstructure [4] and then we repeat the above argument.

References

[1] BAMBERG P. AND STERNBERG S., *A course in mathematics for students of phisic, II*, Cambridge University Press, Cambridge 1988.

[2] BINZ E., *On discrete media, their interaction forms and the origin of non-exactness of the virtual work*, in: "Symmetries in Science", (Eds. B. Gruber and M. Ramek), Plenum Press, New York 1997, 47–61.

[3] BINZ E., DE LEÓN M. AND SOCOLESCU D., *On a smooth geometric approach to the dynamics of media with microstructure*, C.R. Acad. Sci. Paris **326** IIb (1998), 227–232.

[4] BINZ E., DE LEÓN M. AND SOCOLESCU D., *Global dynamics of media with microstructure*, Extracta Math. **14** 2 (1999), 99–125.

[5] ECKMANN B., *Harmonische Funktionen und Randwertaufgaben in einem Komplex*, Comment. Math. Helv. **17** 2 (1944-45), 240–255.

[6] MAUGIN G.A., *The thermomechanics of nonlinear irreversible behaviours, An introduction*, World Scientific, New Jersey 1998.

[7] STRAUMANN E., *Thermodynamik*, Lecture Notes in Physics **265**, Springer, Berlin 1986.

AMS Subject Classification: 58F05, 73C50, 73Bxx, 80A10.

Ernst BINZ
Fakultät für Mathematik und Informatik
Universität Mannheim
68131 Mannheim, GERMANY
e-mail: `binz@math.uni-mannheim.de`

Dan SOCOLESCU
Fachbereich Mathematik
Universität Kaiserslautern
67663 Kaiserslautern, GERMANY
e-mail: `socolescu@mathematik.uni-kl.de`

Rend. Sem. Mat. Univ. Pol. Torino
Vol. 58, 1 (2000)
Geom., Cont. and Micros., I

L. Bortoloni - P. Cermelli*

STATISTICALLY STORED DISLOCATIONS IN RATE-INDEPENDENT PLASTICITY

Abstract. Work hardening in crystalline materials is related to the accumulation of statistically stored dislocations in low-energy structures. We present here a model which includes dislocation dynamics in the rate-independent setting for plasticity. Three basic physical features are taken into account: (i) the role of dislocation densities in hardening; (ii) the relations between the slip velocities and the mobility of gliding dislocations; (iii)the energetics of self and mutual interactions between dislocations. The model unifies a number of different approaches to the problem presented in literature. Reaction-diffusion equation with mobility depending on the slip velocities are obtained for the evolution of the dislocations responsible of hardening.

1. Introduction

Slip lines and slip bands on the surface of a plastically deformed crystal are due to complicated phenomena which occur inside the crystal. When plastic deformation occurs, dislocations are generated : some of them move towards the crystal surface forming slip lines, others may be stored to harden the material and form more or less regular patterns ([1]-[16]). As reported in Fleck *et al.* [1], "dislocations become stored for two reasons : they accumulate by trapping each other in a random way or they are required for compatible deformation of various parts of the crystal. The dislocation which trap each other randomly are referred to as *statistically stored dislocations*...gradients of plastic shear result in the storage of *geometrically necessary dislocations*".

Taking into account both statistically stored dislocation (SSD) and geometrically necessary dislocations (GND), our purpose in this paper is to construct a model which is able, at least in the simple case of single slip, to describe dislocations patterns. The basic idea here is to introduce dislocation densities as independent variables in the framework of Gurtin's theory of gradient plasticity [17].

Total dislocation densities have been introduced frequently in the literature, both to describe hardening and the formation of patterns during plastic deformations ([18]-[26]).

In fact, materials scientists often describe hardening due to dislocation accumulation by means of the so-called Kocks' model (see [22]): the resistance to slip ζ is assumed to depend on the total dislocation density ϱ through a relation of the form

$$\zeta = \zeta(\varrho),$$

*This paper has been completed with the support of the Italian M.U.R.S.T. 1998-2000 research project "Modelli matematici per la scienza dei materiali". We also wish to thank M.E. Gurtin, for his stimulating comments and suggestions.

and the accumulation of dislocations during plastic slip evolves according to an ordinary differential equation which can be rewritten in the form

$$\frac{d\varrho}{dt} = |\nu|(k_s\sqrt{\varrho} - k_r\varrho), \tag{1}$$

where ν is the resolved (plastic) shear strain rate and k_r, k_s are positive constants. In the right hand side of equation (1), the term $k_s\sqrt{\varrho}$ represents dislocation storage and the terms $k_r\varrho$ represents dynamic recovery. An important consequence of this approach is immediately recognizable by equation (1): the dislocation rate $\dot{\varrho}$ depends on the strain rate. Roughly, this means that dislocations are less mobile when the material hardens.

The above approach does not take into account dislocation density gradients and thus, while very efficient for small strain rates, it does not allow to study spatial variations of the density. One of the first approaches to *non-local* models, which should take into account both spatial and temporal variations of the dislocation density, is due to Holt [18], which obtains a Cahn-Hilliard equation for the total dislocation densities to describe patterning in a manner analogous to spinoidal decomposition in alloys. His model is based on a free energy density which takes into account dislocation interactions through higher gradients of the dislocation density, in conjunction with a gradient-flow derivation of a balance equation for such densities.

Other authors, for instance Aifantis (see for example [23]) and co-workers, model the complex phenomena due to dislocation interaction and annihilation by means of a reaction-diffusion system: in this approach two or more dislocation species are involved (e.g., mobile and immobile dislocations) and an evolution equation for each specie, say $\varrho(\mathbf{X}, t)$, is postulated

$$\frac{d\varrho}{dt} = D\Delta\varrho + g(\varrho) \tag{2}$$

where $g(\varrho)$ is a source term describing creation and annihilation of dislocations (e.g., $g(\varrho) = a\varrho - b\varrho^2$, with a and b phenomenological coefficients), D is a diffusive-like coefficient and Δ is the laplacian. Models like (2) may be used to describe various phenomena related to pattern formation, but they do not include (plastic) strain rate effects of the type described by (1).

The main goal of our work is a unified model which includes all the basic features of the models described above, i.e., the dependence of (plastic) shear rate on dislocation density rate, the non-locality, and finally a term describing work and soft-hardening.

Using consistently the assumption of rate-independence (see Gurtin [17]), we obtain an equation for the total edge dislocation density of the form

$$\frac{d\varrho}{dt} = |\nu|\left(\epsilon\Delta\varrho - \frac{\partial\varphi}{\partial\varrho}\right) \tag{3}$$

where ϵ may be interpreted as a diffusive coefficient and $\varphi(\varrho)$ is a dislocation energy including work and soft-hardening behavior. Notice that equilibrium solutions satisfy

$$\epsilon\Delta\varrho - \frac{\partial\varphi}{\partial\varrho} = 0. \tag{4}$$

Those solutions may correspond to low energy dislocations structures (LEDS, see Kuhlmann-Wilsdorf [2]), or patterns forming during fatigue, where dislocations arrange themselves in such a way that their self and interaction energy are minimized, and their average density does not change with time, even if plastic flow does occur and $\nu \neq 0$.

If τ and $\zeta(\varrho)$ denote the resolved shear stress and the slip resistance respectively, then by regularization of the classical yield equation $\tau = (\mathtt{sgn}\,\nu)\zeta(\varrho)$, by letting $\tau = (\mathtt{sgn}\,\nu)|\nu|^{1/n}\zeta(\varrho)$ for a large positive integer n, we obtain

(5) $$|\nu| = \left(\frac{|\tau|}{\zeta(\varrho)}\right)^n.$$

By substitution of ν, as given by (5), into (3), we obtain the non linear parabolic differential equation

(6) $$\frac{d\varrho}{dt} = \left(\frac{|\tau|}{\zeta(\varrho)}\right)^n \left(\epsilon\Delta\varrho - \frac{\partial\varphi}{\partial\varrho}\right),$$

which can be solved if the resolved shear stress $\tau = \tau(\mathbf{X}, t)$ is known as a function of position and time.

2. Kinematics

Consider a body identified with its reference configuration $\mathcal{B}_R$, a regular region in $\mathbb{R}^3$, and let $\mathbf{X} \in \mathcal{B}_R$ denote an arbitrary material point of the body. A motion of the body is a time-dependent one-to-one smooth mapping $\mathbf{x} = \mathbf{y}(\mathbf{X}, t)$. At each fixed time t, the deformation gradient is a tensor field defined by

(7) $$\mathbf{F} = \mathtt{Grad}\,\mathbf{y}$$

and consistent with $\mathtt{det}\;\mathbf{F}(\mathbf{X}, t) > 0$ for any $\mathbf{X}$ in $\mathcal{B}_R$. A superposed dot denotes material time derivative so that, for instance, $\dot{\mathbf{y}}$ is the velocity of the motion.

We assume that the classic elastic-plastic decomposition holds, i.e.,

(8) $$\mathbf{F} = \mathbf{F}_e\mathbf{F}_p,$$

with $\mathbf{F}_e$ and $\mathbf{F}_p$ the elastic and plastic gradients, consistent with $J_e = \mathtt{det}\;\mathbf{F}_e > 0$ and $J_p = \mathtt{det}\;\mathbf{F}_p > 0$. The usual interpretation of these tensors is that $\mathbf{F}_e$ represents stretching and rotation of the atomic lattice embedded in the body, while $\mathbf{F}_p$ represents disarrangements due to slip of atomic planes.

We restrict attention to *plastic slip shear deformation*, i.e., deformations such that the decomposition (8) holds, with $\mathbf{F}_e$ arbitrary and with $\mathbf{F}_p$ of the form

(9) $$\mathbf{F}_p = \mathbf{I} + \alpha\mathbf{s}\otimes\mathbf{m}, \qquad \mathbf{s}\cdot\mathbf{m} = 0,$$

with $\mathbf{I}$ the identity in $\mathbb{R}^3$, $\mathbf{s}$ and $\mathbf{m}$ constant unit vectors and $\alpha = \alpha(\mathbf{X}, t)$. In (9), $\dot{\alpha}$ may be interpreted as slip rate on the slip plane, defined by the glide direction $\mathbf{s}$ and the slip-plane normal $\mathbf{m}$. This plane is understood to be the only one active among all the available slip systems.

2.1. The geometrically necessary dislocation tensor

The presence of geometrically necessary dislocations in a crystal is usually described in terms of Burgers vector, a notion strictly related to the incompatibility of the elastic deformation.

DEFINITION 1. *Let S be a surface in the deformed configuration, whose boundary ∂S is a smooth closed curve. The Burgers vector of ∂S is defined as*

$$\mathbf{b}(\partial S) = \int_{\partial S} \mathbf{F}_e^{-1} d\mathbf{x}$$

where $d\mathbf{x}$ is the line element of the circuit ∂S. Stokes' theorem implies that

$$\mathbf{b}(\partial S) = \int_S \left(\mathtt{curl}\ \mathbf{F}_e^{-1}\right)^{\mathrm{T}} \mathbf{n} da,$$

where $\mathbf{n}$ is the unit normal to the surface S and $\mathtt{curl}$ and da are, respectively, the curl operator with respect to the point $\mathbf{x}$ and the area element in the deformed configuration.

Since $\mathtt{curl}\ \mathbf{F}_e^{-1} \neq 0$ is necessary to have non null Burgers vectors, the tensor $\mathtt{curl}\ \mathbf{F}_e^{-1}$ seems to be a candidate to measure geometrically necessary dislocations. As such, however, it suffers some drawbacks: for example, $\mathtt{curl}\ \mathbf{F}_e^{-1}$ is not invariant under superposed compatible elastic deformations; moreover, in view of applications to gradient theories of plasticity, it should be desirable to work in terms of a dislocation measure which can be expressed in terms of the plastic strain gradient also. In [27], Cermelli and Gurtin prove the existence of a dislocation tensor which satisfies both requirements above. We can rephrase their result as follows:

DEFINITION 2. *Let $\mathbf{y}$ be a deformation and $\mathbf{F} = \nabla\mathbf{y}$ its deformation gradient. If $\mathbf{F}_e$ and $\mathbf{F}_p$ are smooth fields satisfying (8), then the identity $\frac{1}{J_p}\mathbf{F}_p\mathtt{Curl}\ \mathbf{F}_p = J_e\mathbf{F}_e^{-1}\mathtt{curl}\ \mathbf{F}_e^{-1}$ holds: we define therefore the geometrically necessary dislocation tensor (GND tensor) as*

$$\mathbf{D}_G := \frac{1}{J_p}\mathbf{F}_p\mathtt{Curl}\ \mathbf{F}_p = J_e\mathbf{F}_e^{-1}\mathtt{curl}\ \mathbf{F}_e^{-1}. \tag{10}$$

By (10), we have an alternative plastic and elastic representation of $\mathbf{D}_G$. As pointed out in [27], in developing a constitutive theory "it would seem advantageous to use the representation of $\mathbf{D}_G$ in terms of $\mathbf{F}_p$, which characterizes defects, leaving $\mathbf{F}_e$ to describe stretching and rotation of the lattice". See [27] for an exhaustive discussion of the geometrical dislocation tensor defined by (10).

For single slip plastic deformations (9), the GND tensor has the form

$$\mathbf{D}_G = (\nabla\alpha \times \mathbf{m}) \otimes \mathbf{s} = s_g\mathbf{s} \otimes \mathbf{s} + e_g\mathbf{t} \otimes \mathbf{s} \tag{11}$$

where $\mathbf{t} = \mathbf{s} \times \mathbf{m}$ and

$$e_g = \nabla\alpha \cdot \mathbf{s}, \qquad s_g = -\nabla\alpha \cdot \mathbf{t}. \tag{12}$$

The quantities e_g and s_g can be interpreted as densities associated to geometrically necessary *edge* and *screw* dislocations, respectively, with Burgers vector parallel to $\mathbf{s}$.

2.2. The total dislocation tensor

Individual dislocations can be visualized by electron microscopy and their direction and Burgers vector can be determined experimentally. We thus assume that the microscopic arrangement of dislocations at each point is characterized by scalar densities of edge end screw dislocations, for any given Burgers vector. More precisely, assuming that only dislocations with Burgers vector $\mathbf{s}$

are present, and their line direction is contained in the slip plane $\mathbf{m}^{\perp}$, we introduce nonnegative functions

$$e_{+} = e_{+}(\mathbf{X}, t), \quad e_{-} = e_{-}(\mathbf{X}, t), \quad s_{+} = s_{+}(\mathbf{X}, t), \quad s_{-} = s_{-}(\mathbf{X}, t), \tag{13}$$

with the following interpretation : e_{+} and e_{-} are the densities of dislocations with Burgers vector $\mathbf{s}$ and line direction $\mathbf{t}$ and $-\mathbf{t}$ respectively (edge dislocations); s_{+} and s_{-} are the densities of dislocations with Burgers vector $\mathbf{s}$ and line direction $\mathbf{s}$ and $-\mathbf{s}$ respectively (screw dislocations).

Noting that all the information on a given system of dislocations may be summarized in one of the tensorial quantities (recall that $e\pm$, $s\pm \geq 0$)

$$e_{+}\mathbf{t} \otimes \mathbf{s}, \quad -e_{-}\mathbf{t} \otimes \mathbf{s}, \quad s_{+}\mathbf{s} \otimes \mathbf{s}, \quad -s_{-}\mathbf{s} \otimes \mathbf{s},$$

we assume that the edge and screw densities above are related to the geometrically necessary dislocation tensor by a compatibility relation of the form

$$\mathbf{D}_{G} = (e_{+} - e_{-})\mathbf{t} \otimes \mathbf{s} + (s_{+} - s_{-})\mathbf{s} \otimes \mathbf{s} \tag{14}$$

from which it follows that

$$e_{+} - e_{-} = e_{g}, \qquad s_{+} - s_{-} = s_{g}.$$

DEFINITION 3. *Introducing the total edge and screw dislocation densities*

$$e := e_{+} + e_{-}, \qquad s := s_{+} + s_{-},$$

we define the total dislocation tensor by

$$\mathbf{D}_{S} := e\, \mathbf{t} \otimes \mathbf{s} + s\, \mathbf{s} \otimes \mathbf{s}. \tag{15}$$

3. Dynamics

3.1. Standard forces and microforces

To describe the force systems associated to the motion of the body, plastic deformation and the evolution of the total dislocation densities, we introduce a tensor field $\mathbf{S}$, vector fields $\mathbf{b}^{ext}$, ξ, κ_e and κ_s, and scalar fields Π, Π^{ext}, M_e, M_e^{ext}, M_s and M_e^{ext}, all functions of $(\mathbf{X}, t)$.

These fields correspond to three physically distinct sets of forces acting on the body.

The first force system is standard, and is given by the usual Piola-Kirchhoff stress tensor $\mathbf{S}$ and the body force $\mathbf{b}^{ext}$.

The second force system has been introduced by Gurtin in his theory of gradient plasticity of single crystals (see [17]), to describe forces that perform work associated to plastic slip. This system consists in a vector microstress ξ, a scalar internal microforce Π, and a scalar external microforce Π^{ext}.

The last set of forces is introduced to account for the dynamics of the total screw and edge dislocation densities. It consists of a vector force κ_e, a scalar internal microforce M_e, and a scalar external microforce M_e^{ext} for edge dislocations, and corresponding quantities κ_s, M_s and M_s^{ext} for screw dislocations.

A balance law is associated to each force system. We consider first the standard system $(\mathbf{S}, \mathbf{b}^{ext})$, which is governed by the classical force balances, in local form given by

$$\mathtt{Div}\, \mathbf{S} + \mathbf{b}^{ext} = 0, \qquad \mathbf{S}\mathbf{F}^{\mathrm{T}} = \mathbf{F}\mathbf{S}^{\mathrm{T}}, \tag{16}$$

where we have omitted the inertial terms. To the second force system (ξ, Π, Π^{ext}), governing plastic slip, a corresponding microforce balance is associated (Gurtin, [17])

$$\mathtt{Div}\ \xi + \Pi + \Pi^{ext} = 0. \tag{17}$$

Following Gurtin, [17] we shall see later that this relation replaces the usual yield condition for the single slip system under consideration.

In our theory two more balances must be introduced, in order to obtain a complete integrable set of equations once an adequate constitutive theory is developed. These new balances are associated to the force systems $(\kappa_e, \Pi_e, \Pi_e^{ext})$ and $(\kappa_s, \Pi_s, \Pi_s^{ext})$, and are given in local form by

$$\begin{aligned} \mathtt{Div}\ \kappa_e + M_e + M_e^{ext} &= 0, \\ \mathtt{Div}\ \kappa_s + M_s + M_s^{ext} &= 0. \end{aligned} \tag{18}$$

Each of the above force system is characterized by the way it expends power on the rate of change of the corresponding microstructural field : precisely, we assume that the working of the forces on an arbitrary portion $\mathcal{P}$ of the body is

$$\begin{aligned} W(\mathcal{P}) \quad = \quad & \int_{\partial\mathcal{P}} (\mathbf{Sn}\cdot\dot{\mathbf{y}} + \xi\cdot\mathbf{n}\dot{\alpha} + \kappa_e\cdot\mathbf{n}\dot{e} + \kappa_s\cdot\mathbf{n}\dot{s})da \\ & + \int_{\mathcal{P}} (\mathbf{b}^{ext}\cdot\dot{\mathbf{y}} + \dot{\alpha}\Pi^{ext} + \dot{e}M_e^{ext} + \dot{s}M_s^{ext})dv. \end{aligned} \tag{19}$$

Notice that the microstress ξ and the corresponding external force, expend power on the slip velocity $\dot{\alpha}$, while the total dislocation forces κ_e and κ_s expand power on the rate of change of the corresponding dislocation densities.

We take the second law in the form of a dissipation inequality, stating that the time-derivative of the free energy relative to an arbitrary subregion $\mathcal{P}$ of the body may not exceed the working of the external forces acting on $\mathcal{P}$, i.e.,

$$\frac{d}{dt}\int_{\mathcal{P}} \psi dv \leq W(\mathcal{P}) \tag{20}$$

where ψ is the free energy, density per unit volume in the reference configuration. Using the balance equations, this inequality becomes, in local form,

$$\dot{\psi} \leq \mathbf{T}_e\cdot\dot{\mathbf{F}}_e + \xi\cdot\nabla\dot{\alpha} + \kappa_e\cdot\nabla\dot{e} + \kappa_s\cdot\nabla\dot{s} + \pi\dot{\alpha} - M_e\dot{e} - M_s\dot{s} \tag{21}$$

where

$$\mathbf{T}_e = \mathbf{S}\mathbf{F}_p^T \qquad \pi = \tau - \Pi, \qquad \tau = \mathbf{S}\cdot(\mathbf{F}_e\mathbf{s}\otimes\mathbf{m}). \tag{22}$$

Notice that τ is the *resolved shear stress* on the slip system under consideration.

3.2. Constitutive equations

Letting $\sigma = (\mathbf{F}_e, e_+, e_-, s_+, s_-, \nabla e_+, \nabla e_-, \nabla s_+, \nabla s_-)$ and $\upsilon = (\dot{\alpha}, \dot{e}, \dot{s})$ we consider constitutive equations of the form

$$\psi = \hat{\psi}(\sigma), \qquad \mathbf{T}_e = \hat{\mathbf{T}}_e(\sigma), \qquad \xi = \hat{\xi}(\sigma), \qquad \kappa_e = \hat{\kappa}_e(\sigma), \qquad \kappa_s = \hat{\kappa}_s(\sigma) \tag{23}$$

and

$$\pi = \hat{\pi}(\sigma, v), \qquad M_e = \hat{M}_e(\sigma, v), \qquad M_s = \hat{M}_s(\sigma, v). \tag{24}$$

Requiring the consistency of the constitutive equations with the dissipation inequality for any process, we obtain by the classical Coleman-Noll procedure the result that the constitutive functions above cannot depend on $\nabla e_+,\ \nabla e_-,\ \nabla s_+$ and ∇s_-, but only on ∇e and ∇s, i.e., we can rewrite the constitutive relations (23) in terms of the list

$$\sigma' = (\mathbf{F}_e, e_+, e_-, s_+, s_-, \nabla e, \nabla s)$$

or, equivalently,

$$\sigma'' = (\mathbf{F}_e, e_g, s_g, e, s, \nabla e, \nabla s).$$

Furthermore, the constitutive relations in (23) must satisy the requirements

$$\begin{aligned} \mathbf{T}_e &= \frac{\partial \hat{\psi}}{\partial \mathbf{F}_e}, & \xi &= \frac{\partial \hat{\psi}}{\partial e_g}\mathbf{s} + \frac{\partial \hat{\psi}}{\partial s_g}\mathbf{m} \times \mathbf{s}, \\ \kappa_e &= \frac{\partial \hat{\psi}}{\partial \nabla e}, & \kappa_s &= \frac{\partial \hat{\psi}}{\partial \nabla s}, \end{aligned} \tag{25}$$

while the internal microforces M_e and M_s decompose as

$$M_e = -M_e^{dis} - \frac{\partial \hat{\psi}}{\partial e}, \qquad M_s = -M_s^{dis} - \frac{\partial \hat{\psi}}{\partial s} \tag{26}$$

where $M_e^{dis},\ M_s^{dis}$ and π must satisfy the residual dissipation inequality

$$\delta = \pi \dot{\alpha} + M_e^{dis} \dot{e} + M_s^{dis} \dot{s} \geq 0 \tag{27}$$

for all processes (σ, v).

3.3. Rate independence

Notice that, under a time scale transformation defined by $t \to t/\theta$, $\theta > 0$, the fields $\dot{\alpha},\ \dot{e}$ and $\dot{s}$ transform according to $\dot{\alpha} \to \theta\dot{\alpha},\ \dot{e} \to \theta\dot{e}$ and $\dot{s} \to \theta\dot{s}$. Following Gurtin, we assume that the constitutive equations for $M_e^{dis},\ M_s^{dis}$ and π are rate-independent, in the sense that they satisfy

$$M_e^{dis}(\sigma, v) = M_e^{dis}(\sigma, \theta v), \quad M_s^{dis}(\sigma, v) = M_s^{dis}(\sigma, \theta v), \quad \pi(\sigma, v) = \pi(\sigma, \theta v),$$

for any (σ, v) and for all $\theta > 0$.

4. A nonlinear model

For the applications presented in this paper, we choose a particular form of the free energy function ψ, namely

$$\psi = \psi_e(\mathbf{F}_e) + \varphi(e_g, s_g, e, s) + \frac{1}{2}\epsilon_1 |\nabla e|^2 + \frac{1}{2}\epsilon_2 |\nabla s|^2 \tag{28}$$

where ψ_e and φ are non-negative functions and ϵ_1 and ϵ_2 are positive constants.

Moreover, we shall assume that the dissipative fields M_e^{dis}, M_s^{dis} and π are given by

$$
\begin{aligned}
M_e^{dis}(\sigma, v) &= a(e,s)\frac{\dot{e}}{|\dot{\alpha}|},\\
M_s^{dis}(\sigma, v) &= b(e,s)\frac{\dot{s}}{|\dot{\alpha}|},\\
\pi(\sigma, v) &= \zeta(e,s)\,\mathtt{sgn}\,\dot{\alpha},
\end{aligned}
\tag{29}
$$

where $a(e,s)$, $b(e,s)$ and $\zeta(e,s)$ are positive functions. This choice guarantees rate-independence, and yields a dissipation density Δ quadratic in the rates of change of the total dislocation densities. Moreover, as we shall see, when $\dot{\alpha} = 0$, equations $(29)_1$ and $(29)_2$ are well-defined.

Following Gurtin [17], the function ζ may be interpreted as the *slip resistance*. In [17], ζ is introduced as internal variable, whose evolution is given by an ordinary differential equation, called the *hardening equation*, of the form

$$\dot{\zeta} = f(\lambda, \dot{\alpha}),$$

where λ is a list possibly containing the fields $\mathbf{F}_e$, $\mathbf{F}_p$, $\nabla\mathbf{F}_p$ and ζ. As shown in [17], when restricted by rate independence, the hardening equation becomes

$$\dot{\zeta} = K(\lambda)|\dot{\alpha}|. \tag{30}$$

Our approach to hardening is substantially different from that based on internal variables: we assume in fact that ζ is given by a constitutive relation compatible with the dissipation inequality and the hypothesis of rate independence. Therefore it is not necessary to introduce the hardening equation *a priori*, since, as shown below, it is a consequence of the constitutive choices $(29)_1$ and $(29)_2$ for M_e^{dis} and M_s^{dis}.

To write explicitly the evolution equations for our model, we assume that no external forces are present, and choose a cartesian coordinate system (X, Y, Z) in the reference configuration such that

$$(1,0,0) = \mathbf{s}\times\mathbf{m} \qquad (0,1,0) = \mathbf{s} \qquad (0,0,1) = \mathbf{m}.$$

The balance equations are then

1) the balances of linear and angular momentum

$$\mathtt{Div}\left(\frac{\partial\psi_e}{\partial\mathbf{F}_e}\mathbf{F}_p^{-T}\right) = 0, \qquad \text{and} \qquad \frac{\partial\psi_e}{\partial\mathbf{F}_e}\mathbf{F}_e^T = \mathbf{F}_e\left(\frac{\partial\psi_e}{\partial\mathbf{F}_e}\right)^T. \tag{31}$$

2) the yield equation

$$\tau = (\mathtt{sgn}\,\dot{\alpha})\zeta - \frac{\partial^2\varphi}{\partial e_g^2}\frac{\partial^2\alpha}{\partial Y^2} + 2\frac{\partial^2\varphi}{\partial e_g\partial s_g}\frac{\partial^2\alpha}{\partial X\partial Y} - \frac{\partial^2\varphi}{\partial s_g^2}\frac{\partial^2\alpha}{\partial X^2}, \tag{32}$$

Notice that the yield condition is modified by the presence of geometrically necessary dislocations (we have used (12) to express the geometrically necessary dislocation densities in terms of the derivatives of the plastic slip α), which can be thought as inducing isotropic hardening-softening.

3) a reaction-diffusion system for the total dislocation densities

$$\dot{e} = \frac{|\dot{\alpha}|}{a}\left(\epsilon_1\Delta e - \frac{\partial\varphi}{\partial e}\right), \qquad \dot{s} = \frac{|\dot{\alpha}|}{b}\left(\epsilon_2\Delta s - \frac{\partial\varphi}{\partial s}\right). \tag{33}$$

Notice that the dislocation mobility is proportional to the modulus of the slip velocity $\dot{\alpha}$. Henceforth, two characteristic features of dislocation dynamics are immediately recognizable from (33):

(i) one can have equilibrium configurations for edge dislocations, i.e.,

$$\epsilon_1 \Delta e - \frac{\partial \varphi}{\partial e} = 0$$

such that $\dot{e} = 0$ and dislocations are "locked" in low energy structures, but plastic flow does occur, and the slip velocity does not vanish: $\dot{\alpha} \neq 0$. A similar discussion applies to screw densities.

(ii) if the material behaves elastically, so that $\dot{\alpha} = 0$, then dislocations cannot move.

Besides, by derivations with respect the time of the constitutive relation $\zeta(e, s)$ for the slip resistance, and using equations $(33)_1$ and $(33)_2$, we obtain a hardening equation

$$\dot{\zeta} = \left[\frac{1}{a} \frac{\partial \zeta}{\partial e} \left(\epsilon_1 \Delta e - \frac{\partial \varphi}{\partial e} \right) + \frac{1}{b} \frac{\partial \zeta}{\partial s} \left(\epsilon_2 \Delta s - \frac{\partial \varphi}{\partial s} \right) \right] |\dot{\alpha}| \tag{34}$$

which is a generalization of the classical equation (30).

5. One dimensional model

In this section we describe some simplifying assumptions which allow to reduce the reaction-diffusion system for the total dislocation densities, to a single one-dimensional equation for the total edge density.

ASSUMPTIONS

(i) We assume that the geometrically necessary dislocation densities vanish, i.e.,

$$e_g = s_g = 0,$$

which implies that $e_+ = e_-$, $s_+ = s_-$ and thus, by (12), α only depends on (Z, t) .

(ii) Screw dislocations densities are assumed to vanish identically, and the total edge dislocation density e is constant on each slip plane, so that e depends only on (Z, t). Thus e is the only non-vanishing dislocation density.

(iii) The resolved shear stress τ is assumed to be constant with respect to $(\mathbf{X}, t)$.

(iv) The constitutive relation for the slip resistance has the form

$$\zeta(e) = \zeta_0 + c\sqrt{e}$$

where ζ_0 and c are positive constants. This relation is well known in the materials science literature (cf. Livingston [4], Van Drunen and Saimoto [5], Staker and Holt [6]).

(v) We approximate $\mathtt{sgn}\,\dot{\alpha}$ for $\dot{\alpha} \neq 0$ by

$$|\dot{\alpha}|^{\frac{1}{n}} \mathtt{sgn}\,\dot{\alpha}$$

with n large (viscoplastic regularization).

(vi) Assuming that the body $\mathcal{B}$ is an infinite layer between the planes $Z = 0$ and $Z = L$, we take natural boundary conditions for the microstress associated to the total edge dislocation density,

$$\left.\frac{\partial e}{\partial Z}\right|_{Z=0} = \left.\frac{\partial e}{\partial Z}\right|_{Z=L} = 0.$$

5.1. A particular energy dislocation function

We further choose $\varphi(e)$ in the form

$$\varphi(e) = \frac{1}{4}[e(e - e_m)]^2, \tag{35}$$

with $e_m > 0$ a constant. The function $\varphi(e)$ is non-convex and non-negative with a local minimum at $e = 0$ and $e = e_m$ and a local maximum at $e = e_m/2$.

5.2. The model

Assuming that the standard balance of momentum (31) is identically satisfied, the previous assumptions reduce the general model to the following two equations

$$\tau = (\mathtt{sgn}\,\dot{\alpha})|\dot{\alpha}|^{1/n}(\zeta_0 + c\sqrt{e}), \tag{36}$$

and

$$\dot{e} = \frac{1}{a}|\dot{\alpha}|\left(\epsilon_1 \frac{\partial^2 e}{\partial Z^2} - e(e - e_m/2)(e - e_m)\right). \tag{37}$$

Using (36), equation (37) becomes

$$\dot{e} = \frac{1}{a}\left(\frac{|\tau|}{\zeta_0 + c\sqrt{e}}\right)^n \left(\epsilon_1 \frac{\partial^2 e}{\partial Z^2} - e(e - e_m/2)(e - e_m)\right), \tag{38}$$

supplemented by the natural boundary conditions discussed above. Equation (38), which is the basic result of this work, is a non-linear partial differential equation which may be solved numerically: a complete discussion of the behavior of the solutions to (38) will be published elsewhere.

References

[1] FLECK N. A., MULLER G. M., ASHBY M. F. AND HUTCHINSON J. W., *Strain gradient plasticity: theory and experiment*, Acta metall. mater. **42** (1994), 475–487.

[2] KUHLMANN-WILSDORF D., *Modelling of plastic deformation via segmented voce curves, linked to characteristic LEDS's which are generated by LEDS transformation between workhardening stages*, Phys. Stat. Sol. **149** (1995), 131–153.

[3] ASARO R. J., *Micromechanics of crystals and polycrystals*, Advances in Applied Mechanics **23**, Academic Press, 1983.

[4] LIVINGSTON J. D., *The density and distribution of dislocation in deformed copper crystals*, Acta Met. **10** (1962), 229–239.

[5] VAN DRUNEN G. AND SAIMOTO S., *Deformation and recovery of* [001] *oriented copper crystals*, Acta Met. **19** (1971), 213–221.

[6] STAKER M. R. AND HOLT D. L., *The dislocation cell size and dislocation density in copper deformed at temperatures between 25 and 700° C*, Acta Met. **20** (1972), 567–579.

[7] HAASEN P., *Physical metallurgy*, Cambridge University Press, 1996.

[8] FERNANDES J. V. AND SCHMITT J. H., *Dislocation microstructures in steel during deep drawing*, Phil. Magazine **48** A (1983), 841–870.

[9] KUHLMANN-WILSDORF D., *Theory of plastic deformation:-properties of low energy dislocation structures*, Mater. Sci. Eng. **113** A (1989), 1–41.

[10] SWANN P. R., *Dislocation arrangements in face-centred cubic metals and alloys*, in: "The impact of the transmission electron microscopy on theories of the strength of crystals" Proceeding of the First Berkeley International Materials Conference, University of California, July 5-8, Berkeley 1961.

[11] NEUMANN P., *Low energy dislocation configurations: a possible key to the understanding of fatigue*, Mat. Sci. Eng. **81** (1986), 465-475.

[12] NABARRO F. R. N., *Theory of crystal dislocations*, Clarendon Press, Oxford 1967.

[13] GLAZOV M., LLANES L. M. AND LAIRD C., *Self-organized dislocation structures (SODS) in fatigue metals*, Phys. Stat. Sol. **149** b (1995), 297–321.

[14] N. HANSEN AND HUGHES D. A., *Analysis of large dislocation populations in deformed metals*, Phys. Stat. Sol. **149** b (1995), 155–171.

[15] ZAISER M. AND AIFANTIS E. C., *Material instabilities and deformation patterning in plasticity*, Recent Res. Devel. Metallurg. and Material Sci. **3** (1999), 79–103.

[16] ORTIZ M. AND REPETTO E. A., *Nonconvex energy minimization and dislocation structures in ductile single crystals*, J. Mech. Phys. Sol. **47** (1999), 397–462.

[17] GURTIN M., *On the plasticity of single crystal: free energy, microforces, plastic-strain gradients*, J. Mech. and Phys. Sol. **48** (2000), 989–1036.

[18] HOLT L., *Dislocation cell formation in metals*, J. Appl. Phys. **41** 8 (1970), 3197–3201.

[19] KRATOCHVIL J., *Plastic properties and internal stability of deformed metals*, Czech. J. Phys. **38** B (1988), 421–424.

[20] KRATOCHVIL J., *Dislocation pattern formation in metals*, Revue Phys. Appl. **23** (1988), 419–429.

[21] SUN S., ADAMS B. L., SHET C., SAIGAL S. AND KING W., *Mesoscale investigation of the deformation field of an aluminium bicrystal*, Scripta Materialia **39** (1998), 501–508.

[22] KOCKS U. F., *Laws for work-hardening and low-temperature creep*, J. Eng. Mate. Tech. (1976), 76–85.

[23] AIFANTIS E. C., *Pattern formation in plasticity*, Int. J. Engng Sci. **33** (1995), 2161–2178.

[24] AIFANTIS E. C., *Gradient deformation models at Nano, Micro, and macro scales*, J. Eng. Mater. Tech. **121** (1999), 189–202.

[25] AIFANTIS E. C., *The physics of plastic deformation*, Inter. J. Plasticity **3** (1987), 211–247.

[26] SALAZAR J. M., FOURNET R. AND BANAI N., *Dislocation patterns from reaction-diffusion*, Acta Metall. Mater. **43** (1995), 1127–1134.

[27] CERMELLI P. AND GURTIN M., *On the characterisation of geometrically necessary dislocations in finite plasticity*, J. Mech. Phys. Solids **49** (2001), 1539–1568.

AMS Subject Classification: 74C05, 74C15.

Luca BORTOLONI
Dipartimento di Matematica
Università di Bologna
Piazza di Porta San Donato 5
40127 Bologna, ITALY
e-mail: `bortolon@dm.unibo.it`

Paolo CERMELLI
Dipartimento di Matematica
Università di Torino
Via Carlo Alberto 10
10123 Torino, ITALY
e-mail: `cermelli@dm.unito.it`

Rend. Sem. Mat. Univ. Pol. Torino
Vol. 58, 1 (2000)
Geom., Cont. and Micros., I

M. Braun

COMPATIBILITY CONDITIONS FOR DISCRETE ELASTIC STRUCTURES

Abstract. The theory of plane, elastic trusses is reconsidered from the viewpoint of the continuum theory of elastic media. A main difference between continuum and discrete theories is the following: In the continuous case all quantities are declared throughout the whole body, whereas in the discrete case each quantity has its own "carrier". In a truss, for instance, displacements and applied forces are declared in the nodes while strain and stress live in the members of the truss.

The paper deals with the proper formulation of compatibility conditions for a truss. They are derived along the same lines as St.-Venant's compatibility conditions of plane elasticity, i. e. by stipulating that Cesàro's integrals are path independent. Compatibility conditions can be formulated at each *inner* node of a truss, and they relate the strains of all members which constitute the rosette surrounding the inner node.

1. Continuous and discrete elastic systems

Continuum theories are usually developed from physical models that are discrete in nature. A continuous distribution of dislocations, for instance, would hardly be conceivable, if we had not a clear idea of an *isolated* dislocation. Even the notion of stress as a distributed force follows the example of a single force. Within the framework of a continuum theory, however, discrete quantities appear as singularities and are formally less convenient to handle than their continuous counterparts.

By the process of *homogenization* the underlying discrete ideas are transformed into a continuum theory. The resulting partial differential equations do not admit closed-form solutions, in general. To solve them numerically a *discretization* process is invoked, which approximates the continuum by a discrete system. In this sense a continuum theory is squeezed between the underlying discrete *physical* model and the discrete *numerical* approximation.

The general structure of a physical theory should be perceptible independently of the discrete or continuum formulation. A balance equation, for instance, has a genuine physical meaning whether the model is continuous or discrete. The theory of a discrete elastic structure, be it a crystal lattice, a finite-element system or an elastic truss, should exhibit the same fundamental laws as continuum elasticity theory. The general form of the fundamental equations can be represented most suggestively by a so-called TONTI diagram [6, 7]. Figure 1 shows the TONTI diagram of plane, linear elasticity theory. If we consider a plane, *discrete* elastic system, we should encounter the same physical laws, although in a rather different formal garment.

This paper deals with the governing equations of plane, elastic trusses with special emphasize of the compatibility conditions, which are derived along the same lines as ST.-VENANT's compatibility conditions of plane elasticity, i. e. by stipulating that CESÀRO's integrals are path independent.

The theory of plane, elastic trusses is reconsidered from the viewpoint of the continuum theory of elastic media. Mathematically a truss is considered as an oriented 2-complex, on which displacement, strain, etc. are defined. In contrast to the continuous body the mechanical quantities in a truss are not available everywhere in the body, each quantity resides on its own "carrier": Displacements and applied forces are declared in the nodes while strain and stress live in the members of the truss. It will be shown that the compatibility conditions are attached to "rosettes", i. e. inner nodes that are completely surrounded by triangles of truss members.

To consider trusses from the point of view of elasticity theory is not at all new. KLEIN and WIEGHARDT [4] have presented such an exposition even in 1905, and they rely on earlier works of MAXWELL and CREMONA. Meanwhile, however, trusses have become more a subject of structural mechanics and the more theoretical aspects have been banned from textbooks. As an exception a manuscript by RIEDER [5] should be mentioned, in which the cross-relations between electrical and mechanical frameworks are studied in great detail.

2. Trusses

Mechanically a truss is a system of elastic *members* joint to each other in hinges or *nodes* without friction. The truss is loaded by forces acting on the nodes only.

The appropriate mathematical model of a truss is a 1-complex consisting of 0-simplexes (nodes) and 1-simplexes (members), which are "properly joined" [3]. The subsequent analysis gives rise to two extensions of this model, namely (i) each member is given an orientation, which

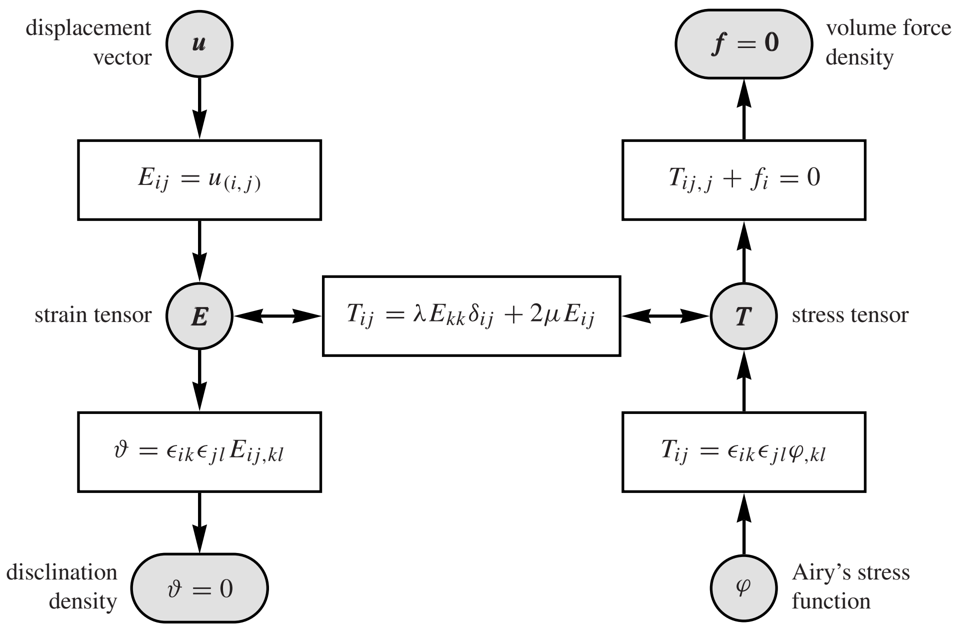

Figure 1: Tonti diagram of plane linear elasticity

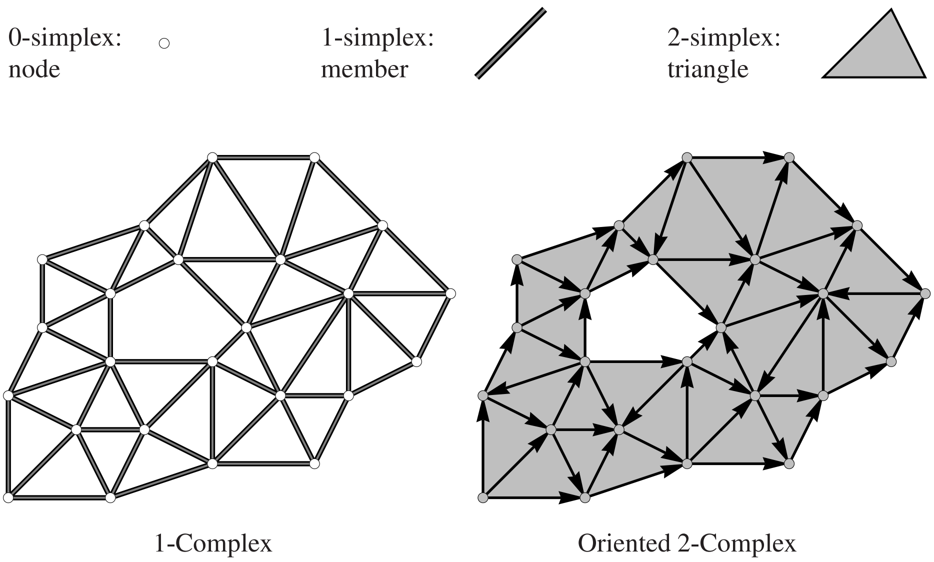

Figure 2: Plane truss as a geometric complex

may be prescribed arbitrarily, and (ii) the triangles or 2-simplexes formed by the members are taken into account. Thus the mathematical model of a truss is extended to an *oriented 2-complex* (Figure 2). Only the non-oriented 1-complex is reproduced in hardware while the imposed orientation and the appended triangular patches are mere mathematical constructs which facilitate the formulation of the theory.

Subsequently nodes will be designated by Latin letters $i, j, \ldots$ while Greek letters $\alpha, \beta, \ldots$ denote the members. The connectivity of the truss is described by *incidence numbers* $[\alpha, k]$, which are defined as

$$[\alpha, k] = \begin{cases} -1 & \text{if member } \alpha \text{ starts at node } k, \\ +1 & \text{if member } \alpha \text{ ends at node } k, \\ 0 & \text{else.} \end{cases}$$

The distinction between start and end point of a member provides its orientation. The matrix of all incidence numbers describes the topological structure of the truss.

The geometry may be specified by prescribing the position vectors $\boldsymbol{x}_k$ of all nodes in the unloaded, stress-free state of the truss. The edge vector of a member α can then be represented by

$$\boldsymbol{a}_\alpha = \sum_k [\alpha, k] \boldsymbol{x}_k, \tag{1}$$

where the summation index may run over all nodes, since the incidence numbers single out the proper starting and terminating points, thus reducing the sum to a simple difference. The decomposition

$$\boldsymbol{a}_\alpha = \ell_\alpha \boldsymbol{e}_\alpha$$

yields the length ℓ_α and the direction vector $\boldsymbol{e}_\alpha$ of a member.

It has been tacitly assumed that there exists an unloaded, stress-free state of the truss. In continuum elasticity theory this corresponds to the assumption that the unloaded elastic body is free of initial stresses. In a more general setting one has to start from the lengths ℓ_α of the undeformed members rather than from a given initial placement $k \mapsto \boldsymbol{x}_k$ of the nodes. This approach within a nonlinear theory is indicated in [2].

3. Displacement and strain

When loads are applied to the truss, each node k is displaced by a certain vector $\boldsymbol{u}_k$ from its original position. The *strain* or relative elongation ε of a member due to displacements $\boldsymbol{u}_1$ and $\boldsymbol{u}_2$ of its endpoints is

$$\varepsilon = \frac{1}{\ell}\boldsymbol{e} \cdot (\boldsymbol{u}_2 - \boldsymbol{u}_1),$$

if only linear terms are retained. Using again the incidence numbers $[\alpha, k]$ the strain ε_α of an arbitrary member α can be represented by

$$\varepsilon_\alpha = \frac{1}{\ell_\alpha}\boldsymbol{e}_\alpha \cdot \sum_k [\alpha, k]\boldsymbol{u}_k \,. \tag{2}$$

As in (1) above, the incidence numbers single out the end nodes of the member and the sum reduces to a simple difference.

Due to the nodal displacements each member α undergoes also a rotation ω_α. Restriction to linear approximation yields

$$\omega_\alpha = \frac{1}{\ell_\alpha}\boldsymbol{e}_\alpha \wedge \sum_k [\alpha, k]\boldsymbol{u}_k \,,$$

where $\wedge$ denotes the outer product of two plane vectors. An approach starting from displacements does not need these rotations explicitly, since they do not enter the stress-strain relation. However, if the displacements have to be reconstructed from given strains, the rotations are needed as well.

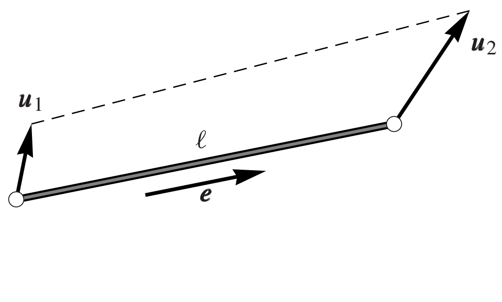

Figure 3: Elongation of a member

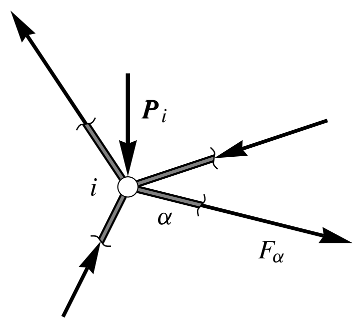

Figure 4: Equilibrium

4. Equilibrium condition

Once the strain of a member α is known, one obtains the transmitted force by HOOKE's law

(3) $$F_\alpha = (EA)_\alpha \varepsilon_\alpha \ ,$$

where EA denotes the axial rigidity of the member, i. e. the product of YOUNG's modulus and cross-sectional area.

At any node i of the truss the applied external force $\boldsymbol{P}_i$ and the member forces acting on that node must be in equilibrium (Figure 4). The force acted upon the node by the member α is $-[\alpha, i] F_\alpha \boldsymbol{e}_\alpha$. Thus the equilibrium condition can be formulated as

(4) $$\sum_\alpha [\alpha, i] F_\alpha \boldsymbol{e}_\alpha = \boldsymbol{P}_i \ .$$

The sum may be taken over all members of the truss, since the incidence numbers single out only those which start or end at node i.

Combining the equilibrium condition (4), the constitutive equation (3), and the definition of strain (2) yields the linear system of equations

$$\sum_k \sum_\alpha [\alpha, i]\,[\alpha, k] \left(\frac{EA}{\ell} \boldsymbol{e} \otimes \boldsymbol{e} \right)_\alpha \boldsymbol{u}_k = \boldsymbol{P}_i \ ,$$

which is the discrete analogue of NAVIER's equations. In structural analysis the matrix of this system of equations would be called the global stiffness matrix of the truss. The three constituents of NAVIER's equations can be arranged in a TONTI diagram (Figure 5), which is still incomplete, since the lower part with the compatibility condition and AIRY's stress function is missing.

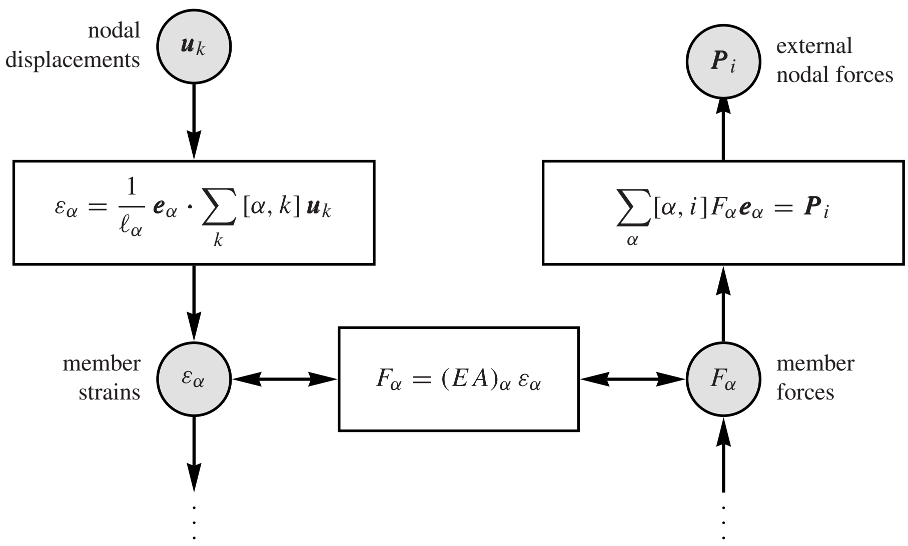

Figure 5: Tonti diagram (upper part) for an elastic truss

5. Compatibility in plane elasticity

Before developing the compatibility conditions for a truss we shall first review the ST.-VENANT compatibility condition of plane elasticity, which may be used as paradigm. Starting from a position $\boldsymbol{x}_0$ with given displacement vector the whole displacement field has to be reconstructed from the strain field $E_{ij} = u_{(i,j)}$. Integration along a curve $\mathcal{C}$ connecting $\boldsymbol{x}_0$ with an arbitrary position $\boldsymbol{x}$ yields the displacement components in terms of CESÀRO's integral,

$$u_i(\boldsymbol{x}) = u_i(\boldsymbol{x}_0) + \int_{\mathcal{C}} (E_{ij} + \omega\epsilon_{ij})\,\mathrm{d}x_j\ , \tag{5}$$

where ϵ_{ij} denotes the two-dimensional permutation symbol. The rotation $\omega = \frac{1}{2}(u_{2,1} - u_{1,2})$, however, is still unknown and has to be reconstructed from the strain field too.

For the integral in (5) to be path independent the integrand has to satisfy the integrability condition

$$a_i \equiv E_{ij,k}\epsilon_{kj} - k_i = 0, \tag{6}$$

where $k_i = \omega_{,i}$ denotes the rotation gradient or *structural curvature* [1]. Geometrically this means that the body is free of dislocations. On the other hand the rotation field itself can be reconstructed by another integral,

$$\omega(\boldsymbol{x}) = \omega(\boldsymbol{x}_0) + \int_{\mathcal{C}} k_i\,\mathrm{d}x_i\ . \tag{7}$$

For this integral to be path-independent the integrability condition

$$\vartheta \equiv k_{i,j}\epsilon_{ji} = 0 \tag{8}$$

has to be satisfied, which means that the body is free of disclinations. Combining the two conditions (6) and (8) yields the ST.-VENANT compatibility condition

$$\epsilon_{ik}\epsilon_{jl}E_{ij,kl} = 0, \tag{9}$$

which stipulates that both the dislocation and the disclination densities vanish.

The compatibility condition emerges from a two-stage process and combines two independent conditions. To unwrap this combination the geometric part of the TONTI diagram, Figure 1, has to be extended to show all the details, see Figure 6.

6. Compatibility condition for a plane truss

The displacement difference $\Delta\boldsymbol{u}$ between the terminating nodes of a single member can be reconstructed from the strain ε and the rotation ω of that member. According to Figure 7 one obtains

$$\Delta\boldsymbol{u} = \varepsilon\boldsymbol{a} + \omega\boldsymbol{a}^{\wedge}, \tag{10}$$

where the vector $\boldsymbol{a}$ is aligned with the member and $\boldsymbol{a}^{\wedge}$ denotes the vector obtained by rotation through $+\pi/2$.

The role of the path $\mathcal{C}$ in CESÀRO's integrals is adopted by an oriented 1-chain of truss members (Figure 9). A 1-chain $\mathcal{C}$ can be specified by incidence numbers

$$[\mathcal{C}, \alpha] = \begin{cases} +1 & \text{if } \mathcal{C} \text{ contains } \alpha \text{ and has the same orientation,} \\ -1 & \text{if } \mathcal{C} \text{ contains } \alpha \text{ and has opposite orientation,} \\ 0 & \text{if } \mathcal{C} \text{ does not contain } \alpha. \end{cases}$$

Extending (10) to an oriented 1-chain $\mathcal{C}$ yields the rotation difference

$$\Delta \boldsymbol{u}_{\mathcal{C}} = \sum_{\alpha} [\mathcal{C}, \alpha](\varepsilon_\alpha \boldsymbol{a}_\alpha + \omega_\alpha \boldsymbol{a}_\alpha^{\wedge}). \tag{11}$$

This is the discrete analogue to CESÀRO's first integral (5).

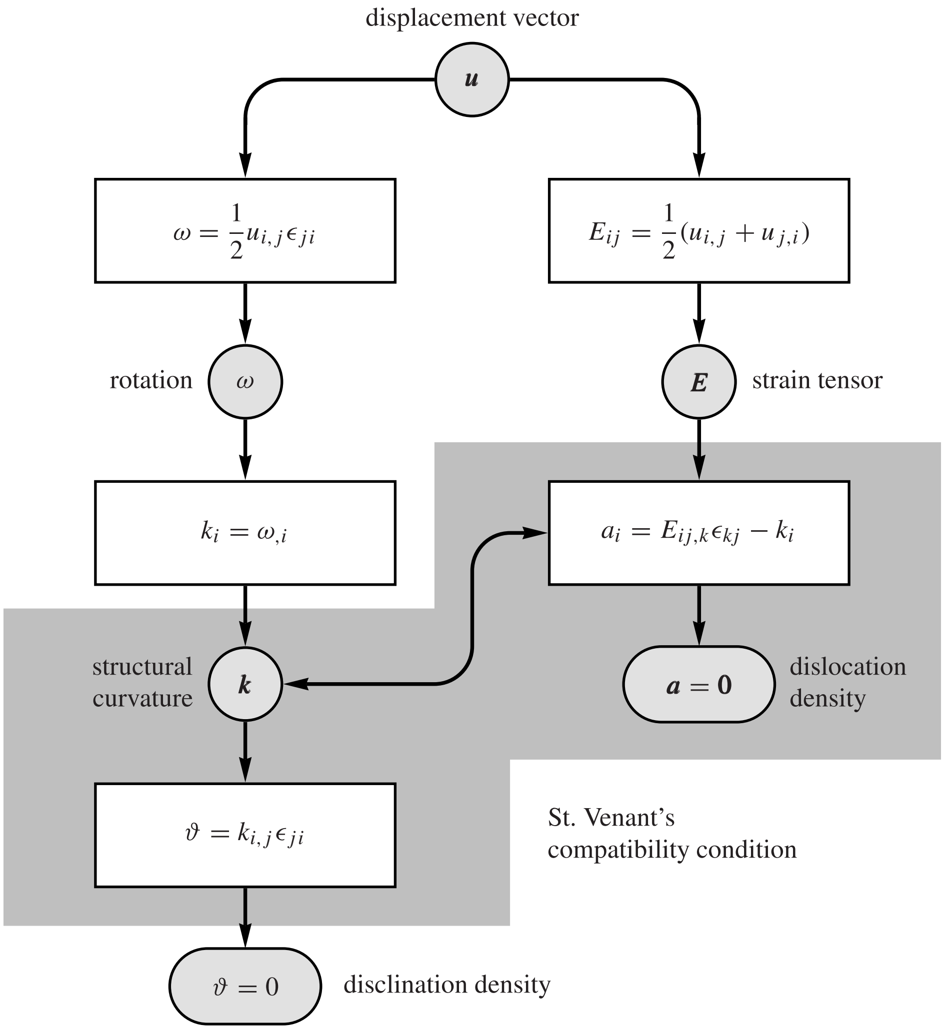

Figure 6: Geometry of continuous deformation

The displacement difference (11) has to vanish for any *closed* 1-chain, or 1-cycle, $\mathcal{C}$. The simplest nontrivial 1-cycle is a triangle formed by three members. With the numbering and orientation as provided in Figure 10 the closing condition for this triangular 1-cycle reads

$$\varepsilon_1 \boldsymbol{a}_1 + \omega_1 \boldsymbol{a}_1^{\wedge} + \varepsilon_2 \boldsymbol{a}_2 + \omega_2 \boldsymbol{a}_2^{\wedge} + \varepsilon_3 \boldsymbol{a}_3 + \omega_3 \boldsymbol{a}_3^{\wedge} = 0.$$

Scalar multiplication by one of the edge vectors, $\boldsymbol{a}_1$ say, yields

$$\omega_2 - \omega_3 = \frac{1}{2A}\,(\varepsilon_1 \boldsymbol{a}_1 + \varepsilon_2 \boldsymbol{a}_2 + \varepsilon_3 \boldsymbol{a}_3) \cdot \boldsymbol{a}_1\,,$$

where $2A = \boldsymbol{a}_1 \wedge \boldsymbol{a}_2 = -\boldsymbol{a}_1 \wedge \boldsymbol{a}_3$ is twice the area of the triangle. From elementary geometric considerations this can also be written as

$$\omega_2 - \omega_3 = (\varepsilon_1 - \varepsilon_2)\cot\alpha_3 + (\varepsilon_1 - \varepsilon_3)\cot\alpha_2\,, \tag{12}$$

where the angles of the undeformed triangle are denoted as in Figure 10. Within each triangle the rotation difference of two adjacent members can be computed from the strains in the members of that triangle. This corresponds to the local integrability condition (6) of the continuum theory, which expresses the rotation gradient in terms of derivatives of the local strain field.

The simplest 1-chain, for which a rotation difference can be defined, has length 2, it is formed by two adjacent members (Figure 8). An extended 1-chain may be decomposed into a sequence of such elementary 1-chains c. Thus the rotation difference of an arbitrary 1-chain is

$$\Delta\omega_{\mathcal{C}} = \sum_c [\mathcal{C}, c]\Delta\omega_c$$

with appropriately defined incidence numbers $[\mathcal{C}, c]$. Whereas the rotation difference $\Delta\omega_c$ is defined for all pairs c of adjacent members, an explicit formula is available only, if these adjacent members are complemented by a third member to a closed triangle. Therefore, in order to actually compute the rotation difference $\Delta\omega_{\mathcal{C}}$ between the first and the last member of a connected 1-chain $\mathcal{C}$, it has to be accompanied by an appropriate sequence of triangles, i. e. a 2-chain. Also the original 1-chain $\mathcal{C}$ must be extended by certain detours along the edges of the triangles (Figure 11).

For any 1-cycle $\mathcal{C}$ the rotation difference $\Delta\omega_{\mathcal{C}}$ has to vanish,

$$\sum_c [\mathcal{C}, c]\Delta\omega_c = 0 \quad \text{if } \partial\mathcal{C} = \emptyset. \tag{13}$$

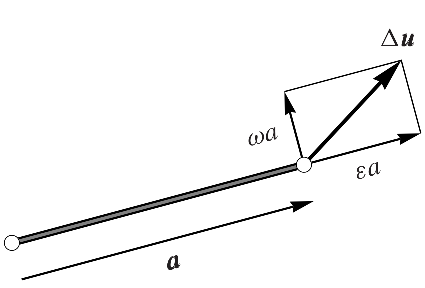

Figure 7: Single member

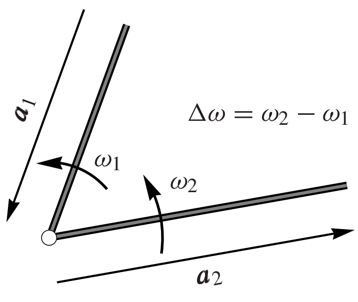

Figure 8: Two members

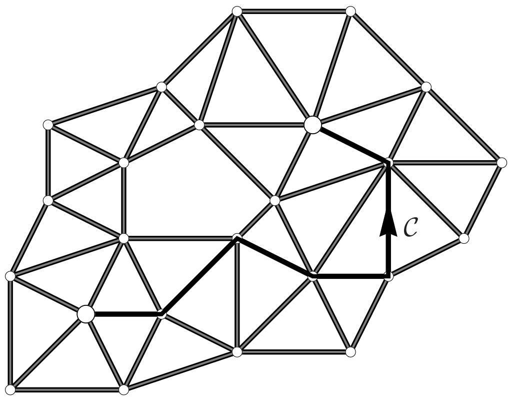

Figure 9: Oriented 1-chain

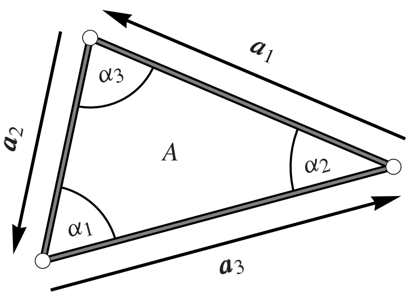

Figure 10: Triangle

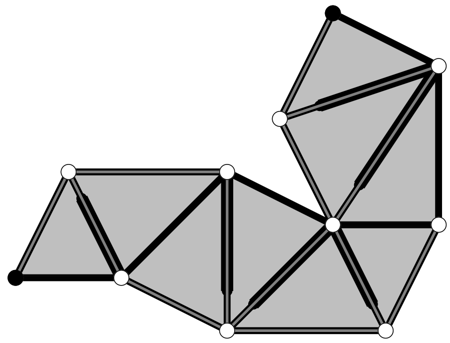

Figure 11: Chain of triangles

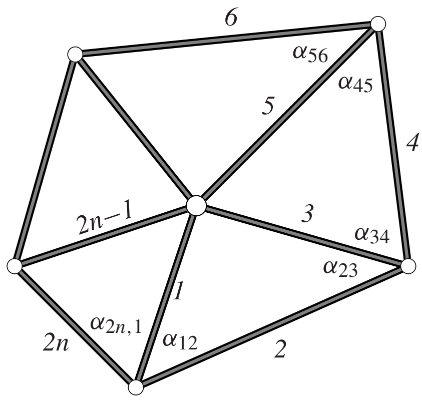

Figure 12: Rosette

The shortest nontrivial 1-cycles are those surrounding an inner node of the truss (Figure 12). For each of these rosette-like substructures we can formulate an appropriate condition, which corresponds to the integrability condition (8) in the continuum case.

The closing condition for a rosette contains the differences $\Delta\omega_c$ of successive members. By use of (12) these can be expressed in the strains of the members of the corresponding triangles. Using the numbering of members and angles indicated in Figure 12 one arrives at a single condition of the form

$$\sum_{i=1}^{n}\big(\cot\underset{\mathrm{mod}\,2n}{\alpha_{2i-2,2i-1}} + \cot\alpha_{2i-1,2i}\big)\varepsilon_{2i-1} = \sum_{i=1}^{n}\big(\cot\alpha_{2i-1,2i} + \cot\underset{\mathrm{mod}\,2n}{\alpha_{2i,2i+1}}\big)\varepsilon_{2i}\,. \tag{14}$$

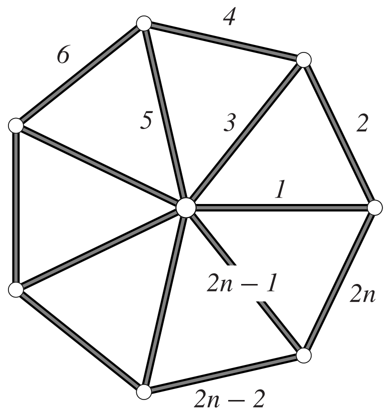

Figure 13: Regular rosette

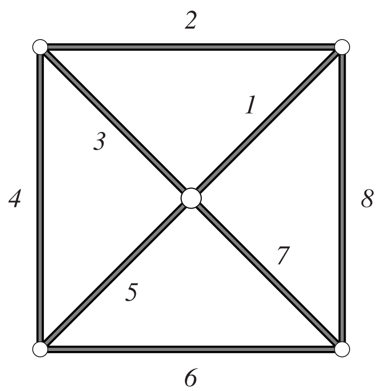

Figure 14: Quadratic rosette

This is the analogue of ST.-VENANT's compatibility condition for a truss. It is obtained by combining the closing condition (13) for the rotations around a rosette with the closing condition (12) for the displacements around a triangle. For the truss to be stress-free in its unloaded state the condition (14) is necessary but not sufficient, in general. If the 2-complex does not contain any holes, the condition is also sufficient. The compatibility conditions are closely connected with the extended model of the truss as an oriented 2-complex, although the 2-simplexes are not material parts of the truss.

In the special case of a regular rosette (Figure 13) all the angles $\alpha_{i,i+1}$ are equal and cancel out. Thus the compatibility condition reduces to

$$\sum_{i=1}^{n} \varepsilon_{2i-1} = \sum_{i=1}^{n} \varepsilon_{2i} \,.$$

The sum of the circumferential strains must be equal to the sum of the radial strains. The general compatibility condition (14) has a similar structure, with the strains being affected by certain geometrical weight factors. For a quadratic rosette the compatibility condition reads

$$\varepsilon_1 + \varepsilon_3 + \varepsilon_5 + \varepsilon_7 = \varepsilon_2 + \varepsilon_4 + \varepsilon_6 + \varepsilon_8 \,.$$

This equation can be interpreted as a discretization of ST.-VENANT's compatibility condition (9).

7. Conclusion

The general structure of elasticity theory is not confined to the continuum version, but holds also for discrete elastic systems such as trusses or finite-element models. A remarkable difference between the theories of plane trusses and of elastic continua is the fact that in the continuous case all quantities are declared throughout the whole body, whereas in the discrete case of the truss each quantity has its own "carrier": Displacements are declared in the nodes, strain and rotation are available in the members, rotation differences need pairs of members, and compatibility conditions can be formulated for "rosettes", i. e. inner nodes that are completely surrounded by triangles of truss members. In this sense the continuum theory could be regarded as "easier", since all quantities are defined in each material point. A closer look shows, however, that the continuum theory can also provide different carriers for different quantities. This becomes manifest, if the mechanical quantities are described in terms of differential forms rather than ordinary field functions.*

The compatibility condition for a truss have been developed using the same ideas as in the continuum. It rests upon the postulation that displacement and rotation can be represented by *path-independent* integrals or, in the discrete case, by path-independet finite sums. To generate *localized* integrability conditions in a continuum the integral around a closed path is transformed via STOKES's theorem into a surface integral, which must vanish identically. In the truss case the local conditions are obtained by choosing the smallest nontrivial closed paths or 1-cycles, namely triangles for the displacements and rosettes for the rotations.

The theory of trusses can be developed further and extended along these lines. The compatibility condition should be complemented by its dual, the representation of member forces by AIRY's stress function. This quantity has the same carrier as the compatibility condition, i. e., it resides in the rosettes surrounding inner nodes of the truss. The generalization to three dimensions is more intricate, especially with respect to the closing condition for the rotation vector.

Quite interesting is the appropriate treatment of frame trusses, with members rigidly clamped to each other. A frame truss allows forces *and couples* to be applied to the nodes, and its members deform under extension, *bending*, and *torsion*. In this case the corresponding continuum theory has to include couple stresses. It might be interesting to compare the common features of continuous and discrete couple-stress theories.

Also a nonlinear theory of trusses can be formulated from the paradigm of nonlinear elasticity theory. The concept of different *placements* is easily transferred to a truss, and also the ESHELBY stress tensor has its counterpart in the discrete case. A first attempt in this direction has been made by the author in [2].

References

[1] ANTHONY K. H., *Die Theorie der Disklinationen* Archive for Rational Mechanics and Analysis **39** (1970), 43–88.

[2] BRAUN M., *Continuous and discrete elastic structures*, Proceedings of the Estonian Academy of Sciences, Physics–Mathematics **48** (1999), 174–188.

[3] CROOM F. H. *Basic concepts of algebraic topology*, Springer Verlag, New York Heidelberg Berlin 1978.

[4] KLEIN F. AND WIEGHARDT K. *Über Spannungsflächen und reziproke Diagramme, mit besonderer Berücksichtigung der Maxwellschen Arbeiten*, Archiv der Mathematik und Physik III Reihe **8** (1905), 1–10, 95–119.

[5] RIEDER G. *Mechanik* (Festigkeitslehre), Vorlesung an der RWTH Aachen 1978.

[6] TONTI E. *On the mathematical structure of a large class of physical theories*, Atti della Academia Nazionale dei Lincei **52** (1972), 48–56.

[7] TONTI E. *The reason for analogies between physical theories*, Applied Mathematics Modelling **1** (1976), 37–53 .

*This aspect has been pointed out by Professor ANTONIO DI CARLO in the discussion of the paper at the Torino seminar.

AMS Subject Classification: 74B99, 55U10.

Manfred BRAUN
Gerhard-Mercator-Universität Duisburg,
Institute of Mechatronics and System Dynamics
47048 Duisburg, GERMANY
e-mail: braun@mechanik.uni-duisburg.de

Rend. Sem. Mat. Univ. Pol. Torino
Vol. 58, 1 (2000)
Geom., Cont. and Micros., I

M. Brocato - G. Capriz*

POLYCRYSTALLINE MICROSTRUCTURE

Abstract. Polycrystals are often modelled as Cosserat continua, the crystallographic directions within single crystals being represented through elements of $SO(3)$. To address the problem of an overall representation of a polycrystalline aggregate, following the example of nematics, one may choose an appropriate embedding of $SO(3)$ in a linear space. Some possibilities are explored and a suggestion is made for such a choice.

1. Introduction

1.1. Orientation distribution in polycrystals

A polycrystal is a material body the elements of which comprise each a population of 'specks' having the structure of a single perfect crystal. In the simplest instance all such crystallites are of the same kind, i.e., any two of them can be superposed through a rigid displacement. Thus a reference crystallite can be chosen and a lattice orientation function can be assigned to describe the polycrystal's substructure. This approach is standard in metallurgical analyses and the problem of determining the orientation function is of industrial import.

The sketch above pertains to a particular range of observation scales. Actually no lattice at all can be defined within dislocations cores, while, observing metals at low temperature and at a scale significantly larger than the average dislocation spacing, a grain pattern appears. The lattice orientation function is constant on regions of finite volume (the bulk of grains) and jumps across their boundaries.

When observations at a scale much larger than the largest grain size are involved no account is taken of grain shapes and the polycrystal is described simply through an orientation distribution function on the basis of probabilistic assumptions. The need arises for a global description through a distribution of lattice orientations.

Thus when computations at a scale much larger than the largest grain size are involved, one may wish to consider body elements which include many hundreds of grains and are characterised by a whole distribution of lattice orientations. The question arises as to the constitutive nature of the interactions between neighbouring body elements; it seems reasonable to start by assuming that these interactions depend on the first moment of the distribution and thus on some 'average' orientation of the crystals within the material elements, and that these averages evolve according to general rules described by multifield theories, whereas evolutions of the orientation distribution function deep within the element be described on the basis of a multivariable theory (cf. [4, 5, 7, 8, 18]).

*We thank our friend Fulvio Lazzeri for useful suggestions. This research is part of the programme "Modelli Matematici per la Scienza dei Materiali" of the Italian Ministero dell'Università e della Ricerca Scientifica e Tecnologica.

In the case of polycrystals the manifold $\mathcal{M}$ of 'deep' states, *l'éspace profond* of [7], is a subset of $SO(3)$ (symmetry arguments may make $\mathcal{M}$ a proper subgroup of $SO(3)$) and, at each point $x \in \mathcal{E}$, $\mathcal{M}$ is endowed with the structure of a probability space, so that each $\mu \in \mathcal{M}$ is a random variable with probability density, say, γ (the orientation distribution function). Assuming that self-effects be weakly non-local in $\mathcal{M}$, in the sense of [14], evolution equations of general type can be found for γ, whereas interactions among neighbours in $\mathcal{E}$ occur through some kind of average over $\mathcal{M}$ based on γ.

To achieve that average a device, simple to use, could be invoked. Whitney's theorem affirms that a linear space $\mathcal{S}$, of dimension $2m + 1$, exists within which the manifold $\mathcal{M}$, of dimension m, can be embedded. The embedding is not unique and there are even cases where the embedding is feasible in a linear space of dimension lower than $2m + 1$ (e.g., $SO(3)$, of dimension 3, can be embedded in a 5-dimensional linear space). However the essential point is that $\mathcal{S}$ exists and, in it, averages can be evaluated in a straightforward manner; they fall, generally, outside the image $\widehat{\mathcal{M}}$ of $\mathcal{M}$ in $\mathcal{S}$, and fill altogether the convex hull $\mathcal{H}$ of that image. Within $\mathcal{H}$ complete disorder is represented by the average of a uniform distribution on $\mathcal{M}$.

1.2. General remarks on continuum models

The possible teaming up, for certain tasks, of a multifield and a multivariable theory has led one of us to advance the remarks which follow [16]; we recall them here because they are strictly relevant and give to our present proposal a very general setting.

Multifield theories are based on the classical space-time $\mathcal{E}\times\mathcal{T}$. Fields $\nu : \mathcal{E}\times\mathcal{T} \to \mathcal{N}$ ($\mathcal{N}$ a manifold of 'substructures') enrich the 'natural' classic description which invokes only bijections $\mathcal{E} \to \mathcal{E}$ at each instant. Interactions between elements are supposed to have short range in $\mathcal{E}$ *à la Cauchy*, though the nature of these interactions depends now, by duality arguments, on the greater kinematic richness of the model.

Multivariable theories start from a wider representation of physical space, obtained by adding to standard placements in $\mathcal{E}$ a set $\mathcal{M}$ of 'deep' placements μ. Interactions range now between neighbours in $\mathcal{E} \times \mathcal{M}$, but the duality is usually narrow. These theories take the components μ^α of μ as extra independent variables beside the place variable x (and time if the case requires). They introduce a distribution function $\gamma(\mu, x)$ such that $\gamma(\mu, x)\, d\mu$ measures the fraction of fragments of the element at x having a value of the substructure falling within the interval $(\mu, \mu + d\mu)$.

In some current research contributions it is assumed that the evolution of γ is totally dictated by the internal state of each element and related to gradients in the variable μ in a sort of weakly nonlocal (on $\mathcal{M}$) mode. Within the element spatial distances do not count, whereas it is easy to believe that two fragments with slightly different values of μ influence one another more than two fragments whose values are, in some measure, distant, irrespective of the exact location of the two fragments within the element. The assumption of an exclusively internal dependence may be sometimes a limiting factor, but this is not so critical in some problems for polycrystalline solids where interelement effects due to spatial gradients are modest, or occur mainly through the agency of macrostress; contrariwise, when studying nematics and hyperfluids [10], one perceives easily the depth of influence of certain constraining boundary conditions.

One way to fix the loophole: find somehow an average value of μ over each element and imagine such average influenced by the averages in neighbouring elements in the same way as happens in less deep theories where all fragments in an element lead to the same value of the substructural variable. Perhaps extract some 'frame' or background from the averages and, if objectivity commands, describe the internal distributions γ and their internal evolution against that background. Judicious steps are always required to arrive at a proper and significant definition of average. Previous embedding of the manifold $\mathcal{M}$ in a linear space $\mathcal{S}$ of higher dimension is always possible (in dimension $2m+1$, by the already quoted theorem of Whitney); then calculation of averages is straightforward.

Actually reference to $\widehat{\mathcal{M}}$, as a hypersurface in $\mathcal{S}$, rather then to the intrinsic manifold $\mathcal{M}$, if managed with care, makes many developments easier; correspondingly $\mathcal{S}$ may take the place of $\mathcal{N}$, again if prudence is exercised to avoid breaches of objectivity. Known concepts and relations may be imported with advantage from available multifield theories.

Thus, for our present task, the matter of embedding $SO(3)$ in a linear space is an essential prerequisite and becomes the core of our developments. To pave the way and make it even more evident, we pause to consider first the simpler, and in part already well established, case of nematic liquid crystals.

2. The example of nematics

In the theory of nematic liquid crystals $\mathcal{M}$ is the manifold of directions, hence of dimension 2. Whitney's embedding can be realised in a linear space of dimension 5. Each direction is put first into one-to-one correspondence with the tensor $n \otimes n - \frac{1}{3}I$, where n is any one of the two unit vectors having the required direction and I is the identity. All those tensors belong to the linear space (with dimension 5) of the symmetric traceless tensors; one of them, say N, will be the average when the element contains molecules with varying degree of orientation. The principal axes of N provide the frame upon which details regarding the distribution of orientations can be assigned. Still, already the eigenvalues of $N + \frac{1}{3}I$, call them λ_i determine two parameters which describe essential traits of the distribution: the degree of prolation s (called also, by Ericksen, degree of orientation) in $\left[-\frac{1}{2}, 1\right]$:

$$s = 3\left(\frac{1}{2}\prod_{i=1}^{3}\lambda_i\right)^{1/3}$$

and the degree of triaxiality in [0, 1]

$$\beta = 3^{1/2}2^{1/3}\left|\prod_{i=1}^{3}\left(\lambda_i - \lambda_{i+1}\right)\right|^{1/3}.$$

Perfect ordering corresponds to the values $s = 1$, $\beta = 0$; 'melting' of the liquid crystal occurs when both parameters vanish.

Many problems have been solved satisfactorily using N as a substructural variable and writing for it an appropriate evolution equation which involves the gradient of N in physical space (for a partial analysis in this direction see [2] and [12]; a fuller study is in a forthcoming paper by Biscari and Capriz).

However, if the details of the distribution of directions $\gamma(n)$ become relevant for specific problems, then the following further steps must be taken. An evolution equation for γ must be proposed, expressing its 'conservation' (the total of γ over $\mathcal{N}$ must always equal to 1); here a suggestion of Muschik [3, 17] may be accepted though modified so as to admit also an influence on γ of N and of the gross displacement gradient F.

Ultimately one comes to the equation

$$\frac{\partial \gamma}{\partial \tau} + \operatorname{div}_N(\gamma \dot{n}) + (\operatorname{grad}_N \gamma) \cdot \dot{N} + (\operatorname{grad}_F \gamma) \cdot \dot{F} = 0\,,$$

where gradients enter along the manifolds $\mathcal{M}$ and $\mathcal{N}$. Actually if $n \otimes n$, rather than n, had been chosen as a variable, then div_n would have been substituted by the appropriate surface divergence along $\widehat{\mathcal{M}}$ in $\mathcal{S}$.

The balance equation above, exhaustive though it be in very special cases, must be supplemented in general by a 'deep' balance equation, which, in statics, may express a minimality condition for the energy connected with a certain choice of $\gamma(N)$ and of its gradient on $\widehat{\mathcal{M}}$. Alternatively, there may be steady states of deformation (e.g. of shearing) dominated by some sort of viscous action which must be itself balanced (for matching developments in the theory of polycrystals see [4, 6, 7, 9]).

3. Embedding of $SO(3)$ in $\mathbb{R}^5$

The so called 'easy Whitney embedding theorem' (cfr. [19]) proves that $SO(3)$ can, as any compact (Hausdorff C^r, $2 \leq r \leq \infty$) three dimensional manifold, be embedded in $\mathbb{R}^7$, though embeddings into linear spaces of smaller dimension may be possible.

It has been proved that $SO(3)$ cannot be embedded into $\mathbb{R}^4$ (cfr. [11]), while an embedding into $\mathbb{R}^5$ is known. The latter result can be shown through a chain of differentiable inclusions: $SO(3)$ can be included into $S^2 \times S^2$ associating with each element of the orthogonal matrix any two column vectors of it:

$$\begin{bmatrix} c_1^{(1)} & c_1^{(2)} & c_1^{(3)} \\ c_2^{(1)} & c_2^{(2)} & c_2^{(3)} \\ c_3^{(1)} & c_3^{(2)} & c_3^{(3)} \end{bmatrix} \in SO(3) \to (c^{(1)}, c^{(2)}) \in S^2 \times S^2$$

One of the two unit 2-spheres S^2 can be included into $]0, +\infty[\times\mathbb{R}^2$:

$$c^{(2)} \in S^2 \to (\xi c_1^{(2)} + \zeta, \xi c_2^{(2)}, \xi c_3^{(2)}) \in]0, +\infty[\times\mathbb{R}^2\,,$$

with $0 < \xi < \zeta$; then

$$S^2 \times (]0, +\infty[\times\mathbb{R}^2) = (S^2\times]0, +\infty[) \times \mathbb{R}^2 \approx (\mathbb{R}^3 - \{0\}) \times \mathbb{R}^2 \subset \mathbb{R}^5\,.$$

Notice that $S^2\times]0, +\infty[$ is diffeomorphic to $\mathbb{R}^3 - \{0\}$ as it can be shown, e.g., choosing coordinates (ϑ, ϕ) on S^2 and taking the corresponding polar coordinates $c^{(1)} = (\sin\phi\cos\vartheta, \sin\phi\sin\vartheta, \cos\phi)$ on $\mathbb{R}^3 - \{0\}$:

$$(\vartheta, \phi, \rho) \in S^2\times]0, +\infty[\to (\rho\sin\phi\cos\vartheta, \rho\sin\phi\sin\vartheta, \rho\cos\phi) \in \mathbb{R}^3 - \{0\}\,.$$

We thus have the embedding:

$$\left[c_j^{(i)}\right] \in SO(3) \to$$

$$(c_1^{(1)}(\xi c_1^{(2)} + \zeta), c_2^{(1)}(\xi c_1^{(2)} + \zeta), c_3^{(1)}(\xi c_1^{(2)} + \zeta), \xi c_2^{(2)}, \xi c_3^{(2)}) \in \mathbb{R}^5\,.$$

It can be shown that the conditions $\|c^{(1)}\| = 1$ and $\|c^{(2)}\| = 1$, and the condition $c^{(1)} \cdot c^{(2)} = 0$ correspond respectively to the equations ($x \in \mathbb{R}^5$):

$$(1) \qquad \begin{aligned} &(\|x\|^2 - \xi^2 - \zeta^2)^2 + 4\zeta^2(x_4^2 + x_5^2) = 4\xi^2\zeta^2 \,, \\ &x_1(\|x\|^2 - \xi^2 - \zeta^2) + 2\zeta(x_2x_4 + x_3x_5) = 0 \,. \end{aligned}$$

4. Embedding a subgroup of $SO(3)$ into Sym_0

The embedding recalled in Sect. 3 from texts in differential geometry does not appear to have intrinsic character required on principle for its use in a physical theory; the appropriate alternative is the introduction of a symmetric tensor of a special class to denote a particular lattice orientation.

We must emphasise, however, at the outset that application of the theorem to our physical context will be legitimate only when a set of three mutually orthogonal directions (no arrow!), each endowed with a different characteristic length, exist having an immediate physical significance in the description of crystallites (e.g. the edges of the elementary cell if the crystalline system is orthorombic). Call $\{m^{(i)} \mid i \in \{1, 2, 3\}\}$, $\|m^{(1)}\| < \|m^{(2)}\| < \|m^{(3)}\|$, the vectors representing a crystallite, their sign being immaterial to the physical description of the crystallite, normalized to make

$$\sum_{i=1}^{3} (m^{(i)})^2 = 1 \,.$$

A polycrystal is a cluster of such crystallites, each uniquely identified through the proper orthogonal tensor Q giving the rotation from a set of reference unit vectors $\{c^{(i)}\}$ to the crystallite's unit vectors $\{m^{(i)}/\|m^{(i)}\|\}$ modulus rotations of π about any $c^{(i)}$; call $\mathcal{M} \subset SO(3)$ the subgroup of such rotations.

Now let us define the following map from the same set of crystallites to the linear space of symmetric tensors

$$S(\{m^{(i)}\}) = \sum_{i=1}^{3} m^{(i)} \otimes m^{(i)} \,;$$

for all $\{m^{(i)}\}$ it is $\mathrm{tr}S = 1$, $\mathrm{tr}S^2 = \sum_{i=1}^{3} (m^{(i)})^4$, and $\det S = \prod_{i=1}^{3} (m^{(i)})^2$.

There is a one to one differentiable map between the set of crystallites and the elements of Sym which verify the conditions listed above; in particular any tensor S verifying these conditions has three distinct eigenvalues $(m^{(i)})^2$, with the corresponding eigenvectors parallel to the vectors $m^{(i)}$. The spectral decomposition of such a tensor S is thus

$$S(\{m^{(i)}\}) = QD^2Q^T \,,$$

where D is the diagonal matrix

$$D := \begin{bmatrix} \|m^{(1)}\| & 0 & 0 \\ 0 & \|m^{(2)}\| & 0 \\ 0 & 0 & \|m^{(3)}\| \end{bmatrix} .$$

Therefore

$$\mathcal{M} \approx \left\{ S \in Sym \;\middle|\; \mathrm{tr}S = 1,\ \mathrm{tr}S^2 = \sum_{i=1}^{3} (m^{(i)})^4,\ \det S = \prod_{i=1}^{3} (m^{(i)})^2 \right\} ,$$

and one can suggest the embedding in the affine space:

$$\mathcal{M} \hookrightarrow \mathcal{S} \equiv \{S \in Sym \mid \operatorname{tr} S = 1\} \ .$$

REMARK 1. Chosen any reference the general element of $\mathcal{S}$ is represented by

$$S = \left[\begin{array}{ccc} x_1 & x_5 & x_4 \\ x_5 & x_2 & x_3 \\ x_4 & x_3 & 1 - x_1 - x_2 \end{array} \right] ,$$

i.e., by a mapping $\mathcal{S} \to \mathbb{R}^5$. The conditions $\operatorname{tr} S^2 = \sum_{i=1}^{3} (m^{(i)})^4$ and $\det S = \prod_{i=1}^{3} (m^{(i)})^2$, can be written in coordinates (cfr. equations (1)):

$$\begin{gathered} \|x\|^2 + x_1 x_2 - x_1 - x_2 + 1 = \textstyle\sum_{i=1}^{3} (m^{(i)})^4 \, , \\ (x_1 x_2 - x_5^2)(1 - x_1 - x_2) - x_1 x_3^2 - x_2 x_4^2 + 2 x_3 x_4 x_5 = \textstyle\prod_{i=1}^{3} (m^{(i)})^2 \, , \end{gathered}$$

representing the image $\widehat{\mathcal{M}}$ of $\mathcal{M}$ in $\mathcal{S}$.

5. Conclusion

A distribution of orthorhombic crystals can be represented through the mean orientation defined as:

$$\tilde{S} := \int_{SO(3)} \gamma(Q) S(Q) \, d(SO(3)) \, .$$

If the distribution is one of perfect order, with all crystals oriented as some $\widehat{Q}$, then $\tilde{S} = S(\widehat{Q})$ has three distinct eigenvalues and the corresponding eigenvectors represent the axes of the crystallite. Contrariwise, if the disorder is complete, then $\tilde{S}$ is spherical and no preferred axis can be assigned to the average representation of the distribution of crystals. Intermediate conditions are clearly possible, with the axial optical properties of the aggregate corresponding to the number of distinct eigenvalues of $\tilde{S}$.

We have thus taken the first essential step for a convenient portrait of a polycrystal, a step which opens the way for a rigourous connection between the theory of continua with microstructure as displayed in [13] and the theory of ‘deep’ space proposed in [4] with direct metallurgical applications in mind.

References

[1] BISCARI P., CAPRIZ G. AND VIRGA E., *Biaxial nematic liquid crystal*, in: “Boundary-value problems for partial differential equations and applications”, (Eds. C. Baiocchi and J.L. Lions), Masson, Paris 1993.

[2] BISCARI P. AND CAPRIZ G., *Optical and statistical anisotropy in nematics*, Rend. Acc. Lincei Matematica **4** (1993), 307–313.

[3] BLENK S., EHRENTRAUT H. AND MUSCHIK W., *A continuum theory for liquid crystals describing different degrees of orientational order*, Liquid Crystals **14** 4 (1993), 1221–1226.

[4] BROCATO M., *Un modèle thermo-mécanique de polycristal pour l’étude des bandes de cisaillement*, Ph. D. Dissertation, ENPC, Paris 1994.

[5] BROCATO M., EHRLACHER A. AND TAMAGNY P., *Cinematica dei continui eterogenei*, Atti XII Convegno Nazionale AIMETA, Napoli 1995, 105–110.

[6] BROCATO M., EHRLACHER A. AND TAMAGNY P., *A two dimensional polycrystal model in a 'deep' space representation*, Meccanica **30** (1995), 641–663.

[7] BROCATO M., *Un modèle mécanique de polycristal*, Presses de l'Ecole Nationale des Ponts et Chaussées, Paris 1996.

[8] BROCATO M., EHRLACHER A. AND TAMAGNY P., *Focal-shift and polycristal models—from the continuum with microstructure to a deep continuum*, Applied Sciences-Especially Mathematics, ZAMM - Z. Angew. Math. Mech. **76** S4 (1996), 117–120.

[9] BROCATO M. AND AIFANTIS E. C., *A theory of plasticity based on globalization of microscopic constitutive assumptions*, in: "Constitutive and damage modeling of inelastic deformation and phase transformation" (Ed. A.S. Khan) Proc. of Plasticity'99, Cancun (Mexico), Neat Press, Fulton, Mariland USA 1999, 701–704.

[10] BROCATO M. AND CAPRIZ G., *Spin fluids and hyperfluids*, Rend. Dip. Mat. Univ. Pisa 2000 and Atti XIV Convegno Nazionale AIMETA, Como (Italy), Oct. 1999, CD-ROM.

[11] BROGLIA F. AND LUMINATI D., *Connected sum of compact analytic hypersurfaces*, Ann. di Mat. Pura ed Appl. **173** 4 (1997), 203–211.

[12] CALDERER M. C. AND LIU C., *Poiseuille flow of nematic liquid crystals*, The Eringen Symposium dedicated to Pierre-Gilles de Gennes, Pullman, WA, 1998, Int. J. Engrg. Sci. **38** 9-10 (2000), 1007–1022.

[13] CAPRIZ G., *Continua with microstructure*, Springer-Verlag, New York 1989.

[14] CAPRIZ G. AND GIOVINE P., *Weakly non local effects in mechanics*, Rend. Dip. Mat. Univ. Pisa 1999.

[15] CAPRIZ G., *Continua with substructure. Part I*, Physical Mesomechanics **3** 4 (2000), 5–13.

[16] CAPRIZ G., *Continua with substructure. Part II*, Physical Mesomechanics **3** 6 (2000), 37–48.

[17] EHRENTRAUT H., MUSCHIK W. AND PAPENFUSS C., *Mesoscopically derived orientation dynamics of liquid crystals*, J. Non-Equilib. Thermodyn. **22** (1997), 285–298.

[18] EHRLACHER A., TAMAGNY P. AND BROCATO M., *Change of scale in media with microstructure*, in: "Geometry, Continua and Microstructure"', (Ed. G. A. Maugin), Hermann, Paris 1999, 131–143.

[19] MORRIS W. HIRSCH, *Differential topology*, Springer-Verlag, New York 1976.

[20] TAMAGNY P., *Les milieux à microstructure; approches par la méthode des puissances virtuelles*, Ph. D. Dissertation, ENPC, Paris 1996.

AMS Subject Classification: 74A30, 74A40, 74A60.

Maurizio BROCATO
IEI-CNR, Area della Ricerca di Pisa
via G. Moruzzi 1
56124 Pisa, ITALIA
e-mail: brocato@iei.pi.cnr.it

Gianfranco CAPRIZ
Dipartimento di Matematica
Università di Pisa
via F. Buonarroti 5
56126 Pisa, ITALIA
e-mail: `capriz@gauss.dm.unipi.it`

Rend. Sem. Mat. Univ. Pol. Torino
Vol. 58, 1 (2000)
Geom., Cont. and Micros., I

A. Carpinteri - B. Chiaia - P. Cornetti*

A FRACTIONAL CALCULUS APPROACH TO THE MECHANICS OF FRACTAL MEDIA

Abstract. Based on the experimental observation of the size effects on the structural behavior of heterogeneous material specimens, the fractal features of the microstructure of such materials is rationally described. Once the fractal geometry of the microstructure is set, we can define the quantities characterizing the failure process of a disordered material (i.e. a fractal medium). These quantities show anomalous (non integer) physical dimensions. Our analysis allows a global explanation of the size effects affecting the cohesive law, i.e. the constitutive law describing the tensile failure of heterogeneous materials. Moreover, a fractal cohesive law which is a material property is put forward and its validity is checked by some experimental data. Then we propose new mathematical operators from fractional calculus to handle the fractal quantities previously introduced. In this way, the static and kinematic (fractional) differential equations of the model are pointed out. These equations form the basis of the mechanics of fractal media. In this framework, the principle of virtual work is also obtained.

1. Introduction

In solid mechanics, with the term *size effect* we mean the dependence of one or more material parameters on the size of the structure made by that material. In other words, we speak of size effect when geometrically similar structures show a different structural behavior. The first observations about size effect in solid mechanics date back to Galileo. For instance, in his "Discorsi e dimostrazioni matematiche intorno a due nuove scienze attenenti alla meccanica e i movimenti locali" (1638), he observed that the bones of small animals are more slender than the bones of big animals. In fact, increasing the size, the growth of the load prevails on the growth of the strength, since the first increases with the bulk, the latter with the area of the fracture surface. In the last century, fracture mechanics allowed a deeper insight in the size effect phenomenon. Nowadays, the most used model to describe damage localization in materials with disordered microstructure (also called quasi-brittle materials) is the *cohesive crack model*, introduced by Hillerborg et al. [1].

According to Hillerborg's model, the material is characterized by a stress-strain relationship (σ-ε), valid for the undamaged zones, and by a stress-crack opening displacement relationship (σ-w, the cohesive law), describing how the stress decreases from its maximum value σ_u to zero as the distance between the crack lips increases from zero to the critical displacement w_c. The area below the cohesive law represents the energy $\mathcal{G}_F$ spent to create the unit crack surface. The cohesive crack model is able to simulate tests where high stress gradients are present, e.g. tests

*Support by the EC-TMR contract N° ERBFMRXCT 960062 is gratefully acknowledged by the authors. Thanks are also due to the Italian Ministry of University and Research (MURST).

on pre-notched specimens; in particular, it captures the ductile-brittle transition occurring by increasing the structural size. On the other hand, relevant scale effects are encountered also in uniaxial tensile tests on dog-bone shaped specimens [2, 3], where smaller stress gradients are present. In this case size effects, which should be ascribed to the material rather than to the stress-intensification, can not be predicted by the cohesive crack model. In the following section, a scale-independent damage model is proposed which overcomes the drawbacks of the original cohesive model, assuming that damage occurs within a band where it is spread in a fractal way. The fractal nature of the damage process allows us to explain the size effects on tensile strength, fracture energy and critical displacement and, particularly, the rising of the cohesive law tail observed in [3].

2. Damage mechanics of materials with heterogeneous microstructure

Let us start our investigation about materials with disordered microstructures analyzing the size effect on their tensile strength. Recent experimental results about porous concrete microstructure [4] led us to believe that a consistent modelling of damage in concrete can be achieved by assuming that the rarefied resisting sections in correspondence of the critical load can be represented by stochastic lacunar fractal sets with dimension $2 - d_\sigma$ ($d_\sigma \geq 0$). From fractal geometry, we know that the area of lacunar sets is scale-dependent and tends to zero as the resolution increases. Finite measures can be obtained only with non-integer (fractal) dimensions. For the sake of simplicity, let us represent the specimen cross-section as a Sierpinski carpet built on the square of side b (fig. 1a). The fractal dimension of this planar domain is 1.893 ($d_\sigma = 0.107$). The assumption of Euclidean domain characterizing the classical continuum theory states that the maximum load F is given by the product of the strength σ_u times the nominal area $A_0 = b^2$, whereas, in our model, F equals the product of the Hausdorff measure $A^* = b^{2-d_\sigma}$ of the Sierpinski carpet times the *fractal tensile strength* σ_u^* [5]:

$$F = \sigma_u A_0 = \sigma_u^* A^* \tag{1}$$

where σ_u^* presents the anomalous physical dimensions $[F][L]^{-(2-d_\sigma)}$.
The fractal tensile strength is the true material constant, i.e., it is scale-invariant. From eqn (1) we obtain the scaling law for tensile strength:

$$\sigma_u = \sigma_u^* b^{-d_\sigma} \tag{2}$$

i.e. a power law with negative exponent $-d_\sigma$. Eqn (2) represents the negative size effect on tensile strength, experimentally revealed by several authors. Experimental and theoretical results allow us to affirm that d_σ can vary between the lower limit 0 - canonical dimensions for σ_u^* and absence of size effect on tensile strength - and the upper limit 1/2 - σ_u^* with the dimensions of a stress-intensity factor and maximum size effect on tensile strength (as in the case of LEFM).

Turning now our attention from a single cross-section to the whole damage zone, it can be noticed that damage is not localized onto a single section but is spread over a finite band where the damage distribution often presents fractal patterns. This is quite common in material science. For instance, in some metals, the so-called slip-lines develop with typical fractal patterns. Also fractal crack networks develop in dry clay or in old paintings under tensile stresses due to shrinkage. Thus, as representative of the damaged band, consider now the simplest structure, a bar subjected to tension, where, at the maximum load, dilation strain tends to concentrate into different softening regions, while the rest of the body undergoes elastic unloading. If, for the sake of simplicity, we assume that strain is localized onto cross-sections whose projections on

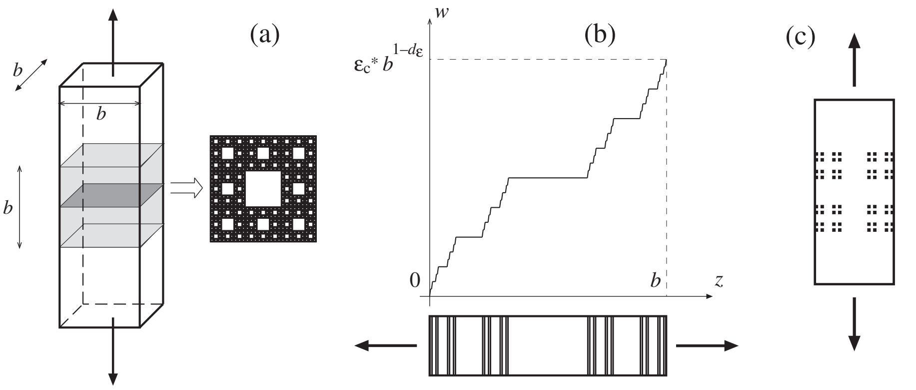

Figure 1: Fractal localization: of the stress (a), of the strain (b), of the energy dissipation (c).

the longitudinal axis are provided by a Cantor set, the displacement function at rupture can be represented (fig. 1b) by a Cantor staircase graph (sometimes called devil's staircase). The strain defined in the classical manner is meaningless in the singular points, as it tends to diverge. This drawback can be overcome introducing a fractal strain. Let $1 - d_\varepsilon = 0.6391$ be, for instance, the fractal dimension of the lacunar projection of the damaged sections ($d_\varepsilon \geq 0$). According to the fractal measure of the damage line projection, the total elongation of the band at rupture must be given by the product of the Hausdorff measure $b^{(1-d_\varepsilon)}$ of the Cantor set times the *fractal critical strain* ε_c^*, while in the classical continuum theory it equals the product of the length b times the critical strain ε_c:

(3) $$w_c = \varepsilon_c b = \varepsilon_c^* b^{(1-d_\varepsilon)}$$

where ε_c^* has the anomalous physical dimension $[L]^{d_\varepsilon}$. The fractal critical strain is the true material constant, i.e., it is the only scale-invariant parameter governing the kinematics of the fractal band. On the other hand, equation (3) states that the scaling of the critical displacement is described by a power law with positive exponent $1 - d_\varepsilon$. The fractional exponent d_ε is intimately related to the degree of disorder in the mesoscopic damage process. When d_ε varies from 0 to 1, the kinematical control parameter ε_c^* moves from the canonical critical strain ε_c – $[L]^0$ – to the critical crack opening displacement w_c – $[L]^1$. Therefore, when $d_\varepsilon = 0$ (diffused damage, ductile behavior), one obtains the classical response, i.e. collapse governed by the strain ε_c, independently of the bar length. In this case, continuum damage mechanics holds, and the critical displacement w_c is subjected to the maximum size effect ($w_c \sim b$). On the other hand, when $d_\varepsilon = 1$ (localization of damage onto a single section, brittle behavior) fracture mechanics holds and the collapse is governed by the critical displacement w_c, which is size-independent as in the cohesive model.

For what concerns the size effect upon the third parameter characterizing the cohesive law, i.e. the fracture energy $\mathcal{G}_F$, several experimental investigations have shown that $\mathcal{G}_F$ increases with the size of the specimen. This behavior can be explained by assuming that, after the peak load, the energy is dissipated inside the damage band, i.e. over the infinite lacunar sections where softening takes place (fig. 1a,b). Generalizing equations (2) and (3) to the whole softening regime, we get $\sigma = \sigma^* b^{-d_\sigma}$ and $w = \varepsilon^* b^{(1-d_\varepsilon)}$. These relationships can be considered as changes of variables and applied to the integral definition of the fracture energy:

$$\mathcal{G}_F = \int_0^{w_c} \sigma \mathrm{d}w = b^{1-d_\varepsilon - d_\sigma} \int_0^{\varepsilon_c^*} \sigma^* \mathrm{d}\varepsilon^* = \mathcal{G}_F^* b^{1-d_\varepsilon-d_\sigma} \tag{4}$$

Equation (4) highlights the effect of the structural size on the fracture energy. On the other hand, since (fig. 1c) the damage process takes place over an invasive fractal domain A^* (different from the lacunar one of equation (1)) with a dimension $(2 + d_\mathcal{G})$ larger than 2 ($d_\mathcal{G} \geq 0$), we can also affirm that the total energy expenditure W is equal to [4]:

$$W = \mathcal{G}_F A_0 = \mathcal{G}_F^* A^*$$

where $\mathcal{G}_F^*$ is called the *fractal fracture energy* and presents the anomalous physical dimensions $[FL][L]^{-(2+d_\mathcal{G})}$ and, as well as σ_u^* and ε_c^*, it is scale-independent. Since $A_0 = b^2$ and $A^* = b^{2+d_\mathcal{G}}$, the value of $d_\mathcal{G}$ is linked to the values of d_σ and d_ε:

$$d_\sigma + d_\varepsilon + d_\mathcal{G} = 1 \tag{5}$$

where all the exponents are positive. While d_ε can get all the values inside the interval [0, 1], d_σ and $d_\mathcal{G}$ tend to be comprised between 0 and 1/2 (brownian disorder). Equation (5) states a strict restriction to the maximum degree of disorder, confirming that the sum of d_σ and $d_\mathcal{G}$ is always lower than 1, as previously asserted by Carpinteri through dimensional analysis arguments [5].

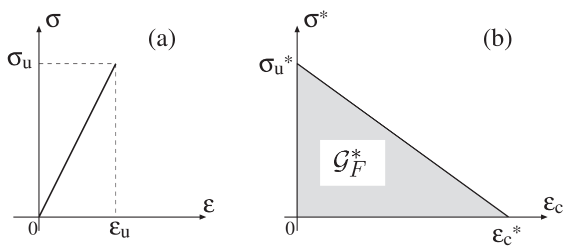

Figure 2: Fractal cohesive model.

It is interesting to note how, from equation (4), the fractal fracture energy $\mathcal{G}_F^*$ can be obtained as the area below the softening fractal stress-strain diagram (fig. 2b). During the softening regime, i.e. when dissipation occurs, σ^* decreases from the maximum value σ_u^* to 0, while ε^* grows from 0 to ε_c^*. In the meantime, the non-damaged parts of the bar undergo elastic unloading (fig. 2a). We call the σ^*-ε^* diagram the scale-independent or *fractal cohesive law*. Contrarily to the classical cohesive law, which is experimentally sensitive to the structural size, this curve should be an exclusive property of the material since it is able to capture the fractal nature of the damage process.

Recently, van Mier et al. [3] accurately performed tensile tests on dog-bone shaped concrete specimens over a wide scale range (1:32). They plotted the cohesive law for specimens of different sizes and found that, increasing the specimen size, the peak of the curve decreases whereas the tail rises. More in detail, w_c increases more rapidly than σ_u decreases, since, in the meantime, an increase of the area below the cohesive law, i.e. of the fracture energy, is observed. Thus, the fractal model consistently confirms the experimental trends of σ_u, $\mathcal{G}_F$, w_c.

The model has been applied to the data obtained by Carpinteri & Ferro [2, 6] for tensile tests on dog-bone shaped concrete specimens (fig. 3a) of various sizes under fixed boundary conditions. They interpreted the size effects on the tensile strength and the fracture energy by fractal geometry. Fitting the experimental results, they found the values $d_\sigma = 0.14$ and $d_{\mathcal{G}} = 0.38$. Some of the σ-ε and the σ-w diagrams are reported in fig. 3b,c, where w is the displacement localized in the damage band, obtained by subtracting, from the total one, the displacement due to elastic and anelastic pre-peak deformation. Equation (5) yields $d_\varepsilon = 0.48$, so that the fractal cohesive laws can be represented in fig. 3d. As expected, all the curves related to the single sizes tend to merge in a unique, scale-independent cohesive law. The overlapping of the cohesive laws for the different sizes proves the soundness of the fractal approach in the interpretation of the size effects in concrete.

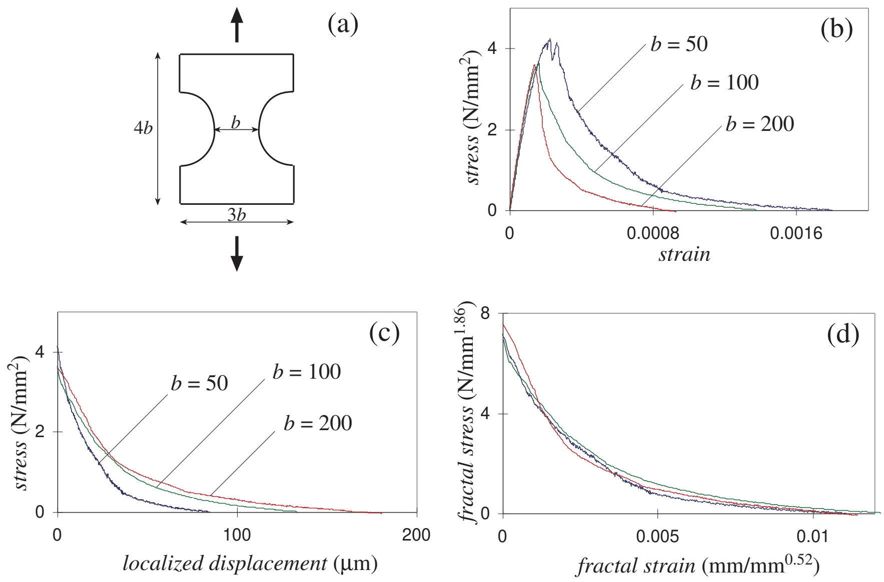

Figure 3: Tensile tests over dog-bone shaped concrete specimens (a): stress versus strain plots (b), cohesive laws (c), fractal cohesive law (d).

3. Fractional calculus, local fractional calculus and fractal functions

The main characteristic of fractals is their irregularity over all the length scales. This irregularity is the reason of the non-integer dimensions of fractal sets and, unfortunately, it makes them very difficult to handle analytically since the usual calculus is inadequate to describe such structures and processes. Fractals are too irregular to have any smooth differentiable function defined on them. Fractal functions do not possess first order derivative at any point. Therefore it is argued that a new calculus should be developed which includes intrinsically a fractal structure [7]. Recently, Kolwankar [8], based on fractional calculus, defined new mathematical operators - the local fractional derivative and the fractal integral - that appear to be useful in the description of fractal processes. It is important to emphasize that, what seems to be really interesting in studying fractals via fractional calculus, are the non-integer physical dimensions that arise dealing with both fractional operators and fractal sets. Physically, this means to find the same scaling laws both from an analytic and a geometric point of view.

Let's start our analysis from the classical fractional calculus. While classical calculus treats integrals and derivatives of integer order, fractional calculus is the branch of mathematics that deals with the generalization of integrals and derivatives to all real (and even complex) orders. There are various definitions of fractional differintegral operators not necessarily equivalent to each other. A complete list of these definitions can be found in the fractional calculus treatises [9, 10, 11, 12]. These definitions have different origin. The most frequently used definition of a fractional integral of order q ($q > 0$) is the Riemann-Liouville definition, which is a straightforward generalization to non-integer values of Cauchy formula for repeated integration:

$$\frac{\mathrm{d}^{-q} f(x)}{[\mathrm{d}(x-a)]^{-q}} = \frac{1}{\Gamma(q)} \int_a^x \frac{f(y)}{(x-y)^{1-q}} \mathrm{d}y \tag{6}$$

From this formula, it appears logical to define the fractional derivative of order $n-1 < q < n$ (n integer) as the n-th integer derivative of the $(n-q)$-th fractional integral:

$$\frac{\mathrm{d}^{q} f(x)}{[\mathrm{d}(x-a)]^{q}} = \frac{1}{\Gamma(n-q)} \frac{\mathrm{d}^n}{\mathrm{d}x^n} \int_a^x \frac{f(y)}{(x-y)^{q+1-n}} \mathrm{d}y \tag{7}$$

Once these definitions are given, it is natural to write differential equations in terms of such quantities. In the last decade, many fractional differential equations have been proposed. They include relaxation equations, wave equations, diffusion equations, etc [13]. In these generalizations, one replaces the usual integer order time derivatives by fractional ones. In such way, by varying the order of derivation, it is possible to obtain a continuous transition between completely different models of the mathematical physics. Of course, when q is not a positive integer, the fractional derivative (7) is a non-local operator since it depends on the lower integration limit a. The chain rule, Leibniz rule, composition law and other properties have been studied for the fractional derivatives [9]. Looking for a link between fractional calculus and fractals, it is worthwhile to cite the following scaling property (for $a = 0$):

$$\frac{\mathrm{d}^{q} f(bx)}{[\mathrm{d}x]^{q}} = b^q \frac{\mathrm{d}^{q} f(bx)}{[\mathrm{d}(bx)]^{q}}$$

It means that the fractional differintegral operators are subjected to the same scaling power laws the quantities defined on fractal domains are subjected to (q being the fractal dimension). For the scaling property in the case $a \neq 0$, see [9].

More recently, another important result has been achieved concerning the maximum order of fractional differentiability for non-classical differentiable functions. Let us explain this property for two kinds of functions: the Weierstrass function and the Cantor staircase. The first one is continuous but nowhere differentiable. The singularities are locally characterized by the Hölder exponent, which is everywhere constant and equal to a certain value $0 < s < 1$. It is possible to prove that the graph of this function is fractal with a box-counting dimension equal to $2 - s$ and hence greater than 1. Although fractal, the Weierstrass function admits continuous fractional derivatives of order lower than s. Hence, there is a direct relationship between the fractal dimension of the graph and the maximum order of differentiability: the greater the fractal dimension, the lower the differentiability. We have already encountered a Cantor staircase in Section 2. This kind of functions (fig. 1b) can be obtained [14] as the integral of a constant mass density upon a lacunar fractal set belonging to the interval [0, 1]. The result is a monotonic function that grows on a fractal support; elsewhere it is constant. The devil's staircases are not fractal since they present a finite length; on the other hand, they have an infinite number of singular points characterized by a Hölder exponent equal to the fractal dimension of the support. Schellnhuber & Seyler [15] proved that the Cantor staircases admit continuous fractional derivatives of order lower than the fractal dimension of the set where they grow.

From a physical point of view, some efforts have been spent to apply space fractional differential equations to the study of phenomena involving fractal distributions in space. Here we can quote Giona & Roman [16], who proposed a fractional equation to describe diffusion on fractals, and Nonnenmacher [17], who showed that a class of Lévy type processes satisfies an integral equation of fractional order. This order is also the fractal dimension of the set visited by a random walker whose jump size distribution follows the given Lévy distribution.

Recently, a new notion called *local fractional derivative* (LFD) has been introduced with the motivation of studying the local properties of fractal structures and processes [18]. The LFD definition is obtained from (7) introducing two "corrections" in order to avoid some physically undesirable features of the classical definition. In fact, if one wishes to analyze the local behavior of a function, both the dependence on the lower limit a and the fact that adding a constant to a function yields to a different fractional derivative should be avoided. This can be obtained subtracting from the function the value of the function at the point where we want to study the local scaling property and choosing as the lower limit that point itself. Therefore, restricting our discussion to an order q comprised between 0 and 1, the LFD is defined as the following limit (if it exists and is finite):

$$D^q f(y) = \lim_{x\to y} \frac{\mathrm{d}^q[f(x) - f(y)]}{[\mathrm{d}(x-y)]^q}, \qquad 0 < q \le 1$$

In [18] it has been shown that the Weierstrass function is locally fractionally differentiable up to a critical order α between 0 and 1. More precisely, the LFD is zero if the order is lower than α, does not exist if greater, while exists and is finite only if equal to α. Thus the LFD shows a behavior analogous to the Hausdorff measure of a fractal set. Furthermore, the critical order is strictly linked to the fractal properties of the function itself. In fact, Kolwankar & Gangal [18] showed that the critical order is equivalent to the local Hölder exponent (which depends, as we have seen, on the fractal dimension), by proving the following local fractional Taylor expansion of the function $f(x)$ of order $q < 1$ (for $q > 1$, see [19, 20]) for $x \to y$:

$$f(x) = f(y) + \frac{D^q f(y)}{\Gamma(q+1)}(x-y)^q + R_q(x-y) \tag{8}$$

where $R_q(x-y)$ is a remainder, negligible if compared with the other terms. Let us observe that the terms in the right hand side of equations (8) are nontrivial and finite only if q is equal to the critical order α. Moreover, for $q = \alpha$, the fractional Taylor expansion (8) gives us the geometrical interpretation of the LFD. When q is set equal to unity, one obtains from (8) the equation of a tangent. All the curves passing through the same point y with the same first derivative have the same tangent. Analogously, all the curves with the same critical order α and the same D^α form an equivalence class modeled by x^α. This is how it is possible to generalize the geometric interpretation of derivatives in terms of "tangents".

The solution of the simple differential equation $\mathrm{d}f/\mathrm{d}x = 1_{[0,x]}$ gives the length of the interval $[0, x]$. The solution is nothing but the integral of the unit function. Wishing to extend this idea to the computation of the measure of fractal sets, it can be seen immediately that the fractional integral (6) does not work as it fails to be additive because of its non-trivial kernel. On the other hand, Kolwankar [21] proved that a fractional measure of a fractal set can be obtained through the inverse of the LFD defined as:

$$
{}_aD_b^{-\alpha} f(x) = \lim_{N\to\infty} \sum_{i=0}^{N-1} f(x_i^*) \frac{\mathrm{d}^{-\alpha} 1_{\mathrm{d}x_i}(x)}{\left[\mathrm{d}(x_{i+1} - x_i)\right]^{-\alpha}} \tag{9}
$$

where $[x_i, x_{i+1}]$, $i = 0, \ldots, N-1$, $x_0 = a$ and $x_N = b$, provide a partition of the interval $[a, b]$ and x_i^* is some suitable point chosen in the subinterval $[x_i, x_{i+1}]$, while $1_{\mathrm{d}x_i}$ is the unit function defined on the same subinterval. Kolwankar called ${}_aD_b^{-\alpha} f(x)$ the *fractal integral* of order α of $f(x)$ over the interval $[a, b]$. The simple local fractional differential equation $D^\alpha f(x) = g(x)$ has not a finite solution when $g(x)$ is constant and $0 < \alpha < 1$. Interestingly, the solution exists if $g(x)$ has a fractal support whose Hausdorff dimension d is equal to the fractional order of derivation α. Consider, for instance, the triadic Cantor set C, built on the interval [0, 1], whose dimension is $d = \ln 2/\ln 3$. Let $1_C(x)$ be the function whose value is one in the points belonging to the Cantor set upon [0, 1], zero elsewhere. Therefore, the solution of $D^\alpha f(x) = 1_C(x)$ when $\alpha = d$ is $f(x) = {}_aD_b^{-\alpha} 1_C(x)$. Applying (9) with $x_0 = 0$ and $x_N = x$ and choosing x_i^* to be such that $1_C(x_i^*)$ is maximum in the interval $[x_i, x_{i+1}]$, one gets [17]:

$$
f(x) = {}_0D_x^{-\alpha} 1_C(x) = \lim_{N\to\infty} \sum_{i=0}^{N-1} F_C^i \frac{(x_{i+1} - x_i)^\alpha}{\Gamma(1+\alpha)} = \frac{S(x)}{\Gamma(1+\alpha)} \tag{10}
$$

where F_C^i is a flag function that takes value 1 if the interval $[x_i, x_{i+1}]$ contains a point of the set C and 0 otherwise; hence $S(x)$ is the Cantor (devil's) staircase (fig. 1b). Moreover, equation (10) introduces the fractional measure of a fractal set we were looking for: for the Cantor set C it is defined as $\mathcal{F}^\alpha(C) = {}_0D_1^{-\alpha} 1_C(x)$. In fact $\mathcal{F}^\alpha(C)$ is infinite if $\alpha < d$, and 0 if $\alpha > d$. For $\alpha = d$, we find $\mathcal{F}^\alpha(C) = \frac{1}{\Gamma(1+\alpha)}$. This measure definition yields the same value of the dimension predicted by the Hausdorff one, the difference being represented only by a different value of the normalization constant.

Eventually, consider two continuous functions $f(x)$ and $g(x)$ defined upon $[a, b]$ with a zero first derivative except at the points belonging to the same lacunar fractal set C where they present an Hölder exponent α equal to the dimension of the fractal support (i.e. $f(x)$ and $g(x)$ are Cantor staircase type functions). Based on equation (8), it can be proved that, in the singular points $x \in C$, (i) the product function $h(x) = f(x)g(x)$ has the same Hölder exponent α unless both the factor functions have zero value; (ii) the LFD of order α of $h(x)$ can be computed using the classical rule for the differentiation of the product:

$$
D^\alpha h(x) = f(x) D^\alpha g(x) + g(x) D^\alpha f(x) \tag{11}
$$

Performing now, for both the sides of equation (11), a fractal integration of order α upon $[a, b]$ yields to the following *fractal integration by parts*:

$$
{}_aD_b^{-\alpha}[f(x) D^\alpha g(x)] = [h(b) - h(a)] - {}_aD_b^{-\alpha}[g(x) D^\alpha f(x)] \tag{12}
$$

which will be useful in the next section.

4. Kinematic and static equations for fractal media

As shown in the Sections 1 and 2, fractality plays a very important role in the mechanics of materials with an heterogeneous microstructure. The aim of this Section is to develop a model that, by the local fractional operators introduced in Section 3, is able to capture intrinsically the fractality of the material and, consequently, the size effects upon the related physical quantities. Thus, let us start with a uniaxial model [22], hereafter called *fractal Cantor bar* according to Feder's terminology [14]. Hence, consider a specimen of disordered material of length b. Suppose now to apply a tensile load in the z (axial) direction. As pointed out in Section 2, because of the fractal localization of strain, the plot of the axial displacement w versus z is a Cantor staircase (fig. 1b). This plot corresponds to a strain field which is zero almost everywhere (corresponding to the integer portions) except in an infinite number of points where it is singular (corresponding to the localized cracks). The displacement singularities can be characterized by the LFD of order equal to the fractal dimension $\alpha = 1 - d_\varepsilon$ of the domain of the singularities, the unique value for which the LFD is finite and different from zero (the critical value). This computation is equivalent to equation (3), passing from the global level to the local one. Therefore, we can define analytically the fractal strain ε^* as the LFD of the displacement:

$$\varepsilon^*(z) = D^\alpha w(z) \tag{13}$$

Let us observe that, in equation (13), the non-integer physical dimensions $[L]^{d_\varepsilon}$ of ε^* are introduced by the LFD, whilst in equation (3) they are a geometrical consequence of the fractal dimension of the localization domain.

Now let's turn our attention to the differential equilibrium equation, when the fractal bar is subjected to an axial load. Consider again a fiber of the specimen and suppose that the body is in equilibrium, $z = 0$ and $z = b$ being its extreme cross sections. We indicate with $p^*(z)$ the axial load per unit of fractal length acting upon the fractal bar and with $N(z)$ the axial force acting on the generic cross section orthogonal to the z-axis. Take therefore into consideration a kinematical field (w, ε^*) satisfying equation (13) and a static field (N, p^*). The fractal integration by parts (12) can be interpreted as the principle of virtual work for the fractal bar. In fact, according to the fractal nature of the material microstructure, the internal virtual work can be computed as the fractal α-integral of the product of the axial force N times the fractal strain ε^* performed over the interval [0, b], which, according to equations (13) and (12), is in its turn equal to:

$${}_0D_b^{-\alpha}[N(z)\varepsilon^*(z)] = {}_0D_b^{-\alpha}[N(z)D^\alpha w(z)] = [N(z)w(z)]_{z=0}^{z=b} - {}_0D_b^{-\alpha}[w(z)D^\alpha N(z)] \tag{14}$$

Since the body is in equilibrium, the virtual work principle holds. Hence the right hand side of equation (14) must be equal to the external virtual work. This is true if and only if:

$$D^\alpha N(z) + p^*(z) = 0 \tag{15}$$

which is the (fractional) static axial equation of the fractal bar. Observe the anomalous dimension of the load p^*, $[F][L]^{-(1-d_\varepsilon)}$, since it considers forces acting on a fractal medium.

What has been done in the one-dimensional case can be formally extended in the three-dimensional case for a generic fractal medium [23]. As in the classical continuum mechanics, one needs the introduction of the fractal stress $\{\sigma^*\}$ and fractal strain $\{\varepsilon^*\}$ vectors to replace the corresponding scalar quantities in equations (13) and (15). Denoting with $\{\eta\}$ the displacement vector, the kinematic equations for a fractal medium can be expressed as:

$$\{\varepsilon^*\} = [\partial^\alpha]\{\eta\} \tag{16}$$

where $[\partial^\alpha]$ is the kinematic fractional differential operator containing local fractional derivatives of order $\alpha = 1 - d_\varepsilon$. Equation (16) is the three-dimensional extension of equation (13). Analogously, equation (15) becomes:

$$[\partial^\alpha]^T\{\sigma^*\} = -\{\mathcal{F}^*\} \tag{17}$$

where $[\partial^\alpha]^T$ is the static fractional differential operator, transposed of the kinematic one and $\{\mathcal{F}^*\}$ is the vector of the forces per unit of fractal volume. From the physical dimension of the matrices at the first hand side of equation (17) and from the fundamental relationship (5) among the fractal exponents, it can be easily shown that $\{\mathcal{F}^*\}$ owns the following physical dimension: $[F][L]^{-(2+d_{\mathcal{G}})}$, where $(2 + d_{\mathcal{G}})$, comprised between 2 and 3, should now be seen as the fractal dimension of the fractal medium.

In order to get the expression of the principle of the virtual work for a fractal medium, we need the extension to fractal domain of the Green theorem. This extension can be obtained performing a fractal integration of order $\beta - \alpha$ of both sides of equation(12):

$$D^{-\beta}_{\Omega^*}[f D^\alpha g] = D^{-(\beta-\alpha)}_{\Gamma^*}[f g n_x] - D^{-\beta}_{\Omega^*}[g D^\alpha f] \tag{18}$$

where now D^α is the LFD in the x-direction, n_x is the x-component of the outward normal vector to the fractal boundary Γ^* of the fractal body Ω^*. Other two scalar expressions can be obtained analogously to equation (18), just considering the LFDs in the y and z-directions. Thus we are now able to derive the expression of the principle of virtual work for fractal media. It is sufficient to apply the extension of the Green theorem – equation (18) – substituting appropriately to the functions f, g the components of the fractal stress $\{\sigma^*\}$ and displacement $\{\eta\}$ vectors. Furthermore, α and β are equal respectively to $(1-d_\varepsilon)$ and $(2+d_{\mathcal{G}})$. Thus for vector fields $\{\sigma^*\}$, $\{\mathcal{F}^*\}$ satisfying equation (17) (i.e. statically admissible) and vectors fields $\{\varepsilon^*\}$, $\{\eta\}$ satisfying equation (16) (i.e. kinematically admissible), it is possible to prove the validity of the following equation:

$$\int_{\Omega^*}\{\mathcal{F}^*\}^T\{\eta\}\mathrm{d}\Omega^* + \int_{\Gamma^*}\{p^*\}^T\{\eta\}\mathrm{d}\Gamma^* = \int_{\Omega^*}\{\sigma^*\}^T\{\varepsilon^*\}\mathrm{d}\Omega^* \tag{19}$$

which represents the principle of virtual work for a generic fractal medium and is the natural extension of the classical continuum mechanics formulation of the principle. For the sake of clarity, in equation (19) we used the classical symbol for the integrals; anyway they are fractal integrals over fractal domains. $\{p^*\}$ is the vector of the contact forces acting upon the (fractal) boundary of the fractal medium; it has the same physical dimension of the fractal stress, to which it is related by the relation:

$$[\mathcal{N}]^T\{\sigma^*\} = \{p^*\}$$

as naturally comes out in the proof of equation (19). $[\mathcal{N}]^T$ is defined at any dense point of the boundary as the cosine matrix of the outward normal vector to the boundary of the initiator (see [14]) of the fractal set occupied by the body.

5. Conclusions

In this paper, the topologic framework for the mechanics of deformable fractal media has been outlined. Based on the experimental observations of the size effects on the parameters characterizing the cohesive law of materials with a disordered microstructure, the fractal quantities characterizing the process of deformation have been pointed out. In the second part of the paper, new mathematical operators from fractional calculus have been applied to write the field equations for solids with a fractal microstructure. It has been shown that the classical fractional calculus cannot be used to describe properly the deformations of fractal media. Instead, the local fractional operators, recently introduced by Kolwankar [8], can be successfully applied for our purposes. The static and kinematic equations for fractal media have been obtained. Moreover, the extension of the Green Theorem to fractal quantities and domains has been proposed, naturally yielding the Principle of Virtual Work for fractal media. The next step should be the definition of proper constitutive laws (e.g. elasticity) for fractal media. At this stage, only the formal structure of the static and kinematic equations has been outlined. Moreover, further analytical research about local fractional operators has to be carried out. Thus, engineering calculations may only be at an early stage. However, once these goals were achieved, boundary value problems on fractal sets could be solved, not only in principle, by means of the Local Fractional Calculus.

References

[1] Hillerborg A., Modéer M. and Petersson P. E., *Analysis of crack formation and crack growth in concrete by means of fracture mechanics and finite elements*, Cement and Concrete Research **6** (1976), 773–782.

[2] Carpinteri A. and Ferro G., *Size effects on tensile fracture properties: a unified explanation based on disorder and fractality of concrete microstructure*, Materials and Structures **28** (1994), 563–571.

[3] Van Mier J. G. M. and Van Vliet M. R. A., *Effect of strain gradients on the size effect of concrete in uniaxial tension*, International Journal of Fracture **94** (1999), 195–219.

[4] Carpinteri A., Chiaia B. and Invernizzi S., *Three-dimensional fractal analysis of concrete fracture at the meso-level*, Theoretical and Applied Fracture Mechanics, **31** (1999), 163–172.

[5] Carpinteri A., *Fractal nature of material microstructure and size effects on apparent mechanical properties*, Mechanics of Materials **18** (1994), 89–101.

[6] Carpinteri A. and Ferro G., *Scaling behaviour and dual renormalization of experimental tensile softening responses*, Materials and Structures **31** (19998), 303–309.

[7] Carpinteri A. and Mainardi F., *Fractals and fractional calculus*, in: "Continuum mechanics", Springer Verlag, Wien 1997.

[8] Kolwankar K. M., *Studies of fractal structures and processes using methods of fractional calculus*, Ph. D. Thesis, University of Pune 1998.

[9] Oldham K. B. and Spanier J., *The fractional calculus*, Academic Press, New York 1974.

[10] Miller K. S. and Ross B., *An introduction to the fractional calculus and fractional differential equations*, Wiley, New York 1993.

[11] Samko S. G., Kilbas A. A. and Marichev O. I., *Fractional integrals and derivatives: theory and applications*, Gordon & Breach, Amsterdam 1993.

[12] Podlubny I., *Fractional differential equations*, Academic Press, San Diego 1999.

[13] Mainardi F., *Fractional relaxation-oscillation and fractional diffusion-wave phenomena*, Chaos, Solitons and Fractals **7** (1996), 1461–1477.

[14] Feder J., *Fractals*, Plenum Press, New York 1988.

[15] SCHELLNHUBER H. J. AND SEYLER A., *Fractional differentiation of devil's staircases*, Physica **191** A (1992), 491–500.

[16] GIONA M. AND ROMAN H. E., *Fractional diffusion equation on fractals: one-dimensional case and asymptotic behavior*, Journal of Physics **25** A (1992), 2093–2105.

[17] NONNENMACHER T. F., *Fractional integral and differential equations for a class of Lévy-type probability densities*, Journal of Physics **23** A (1990), L697–L700.

[18] KOLWANKAR K. M. AND GANGAL A. D., *Fractional differentiability of nowhere differentiable functions and dimensions*, Chaos **6** (1996), 505–523.

[19] KOLWANKAR K. M. AND GANGAL A. D., *Hölder exponents of irregular signals and local fractional derivatives*, Pramana Journal of Physics **48** (1997), 49–68.

[20] KOLWANKAR K. M. AND GANGAL A. D., *Local fractional Fokker-Plank equation*, Physical Review Letters **80** (1998), 214–217.

[21] KOLWANKAR K. M. AND GANGAL A. D., *Local fractional calculus: a calculus for fractal space-time*, in: "Proceedings of Fractals: theory and Applications in Engineering", Springer, Delft 1999, 171–181.

[22] CARPINTERI A. AND CORNETTI P., *A fractional calculus approach to the description of stress and strain localization in fractal media*, Chaos Solitons and Fractals **13** 1 (2002), 85–94.

[23] CARPINTERI A., CHIAIA B. AND CORNETTI P., *Static-kinematic duality and the principle of virtual work in the mechanics of fractal media*, Computer Methods in Applied Mechanics and Engineering **191** 1-2 (2001), 3–19.

AMS Subject Classification: 26A33, 28A84, 74A30, 74R10.

Alberto CARPINTERI, Bernardino CHIAIA and Piero CORNETTI
Dipartimento di Ingegneria Strutturale
Politecnico di Torino
corso Duca degli Abruzzi 24
10129 Torino, ITALIA
e-mail: `carpinteri@polito.it`
e-mail: `chiaia@polito.it`
e-mail: `cornetti@polito.it`

Rend. Sem. Mat. Univ. Pol. Torino
Vol. 58, 1 (2000)
Geom., Cont. and Micros., I

S. Cleja-Ţigoiu*

ANISOTROPIC AND DISSIPATIVE FINITE ELASTO-PLASTIC COMPOSITE

Abstract. Here we propose a macroscopic model for elasto-plastic composite, characterized by an initial anisotropy, that can evolve during the large plastic deformation. Application to transversely isotropic and orthotropic composites will be also developed. The paper deals with anisotropic finite elasto-plastic Σ-models, which accounts for the dissipative nature of the plastic flow, within the constructive framework of materials with relaxed configurations in internal variables. Here Σ stands for Mandel's non-symmetric stress tensor,or the quasi-static Eshelby stress-tensor. The appropriate variational inequalities are derived, related rate quasi-static boundary value problem, in our approach to composite materials.

1. Introduction

The continuum approach treats the composites as a single material with different properties in different directions. The macroscopic response will be transversely isotropic about the fiber direction if there exists just one family of reinforced fibres and orthotropic if there are two families. Spencer in [23] formulated yield conditions, flow rules and hardening rules for material reinforced by one and two families of fibres, in small deformations plasticity theory. The yield function is assumed to be not affected by a superposed tension in fibre direction. Spencer in [22] proposed the term of proportional hardening for the corresponding theory of isotropic hardening, for anisotropic plasticity. Rogers in [21] generalized Spencer's results concerning fibre reinforced materials, assuming that the yield condition is unaffected by the superposition of an arbitrary hydrostatic pressure.

Experimental results performed on axially reinforced tubular specimens of boron aluminium composite, under complex loading, reveal the large kinematic hardening effects, see [20]. In [26] the effect of shear on the compressive response and failure was investigated experimentally for an unidirectional composite. Here both axes of loading could be operated in either load or displacement control.

Here we propose a macroscopic model for elasto-plastic composite, characterized by an initial anisotropy, that can evolve during the large plastic deformation. Applications to transversely isotropic and orthotropic composites will be developed, based on the papers [5, 6], which generalized Spencer and Roger's results.

The paper deals with anisotropic finite elasto-plastic $\Sigma-$models, which account for the dissipative nature of the plastic flow, within the constitutive framework of materials with relaxed configurations and internal variables, [1, 2]. Here Σ stands for Mandel's non-symmetric stress tensor, see [15], or the quasi-static Eshelby stress tensor, see [17, 18]. We shown in [9], that

*This work was supported by ANSTI, Grant 5229, B1/1999.

there exist classes of $\Sigma-$models with hyperelastic properties, for which the dissipation postulate [7] can be equivalently imposed through the normality and convexity properties, despite of the non-injectivity of the function which describes Σ as dependent on elastic strain. Our dissipation postulate extend to anisotropic materials the results obtained by [13, 14, 16, 24].

During the elasto-plastic deformation process, see experimental evidences in [26], the changes in geometry and rotations of material elements cannot be disregarded. Consequently, the field equation and the boundary conditions at time t are properly formulated (see [11]) in terms of the rate of the *nominal* stress. The second objective of the paper is to derive an appropriate variational inequality, related to the rate quasi-static boundary value problem and associated with a generic stage of the process in our approach to composite materials. Only when the dissipative nature of the plastic flow is considered, the variational inequality is caracterized by a bilinear form which becomes symmetric. In a forcomming paper a complete analysis of the bifurcation of the homogeneous deformation will be performed, as in Cleja-Ţigoiu [4], based on the variational inequality, under axial compressive stress. In our analyse it is not necessary to make the assumptions either the fibres are uniformly inclined to the line of the loading by a small angle, or the existence of a sinusoidal imperfection, which is uniformly distributed, as we remark here that the stability can be lost, during plastic deformation.

Further we shall use the following notations:

$Lin, Lin^{+}-$ the second order tensors and the elements with positive determinant;

$\mathcal{V}-$ the three dimensional vector space;

$Sym, Skew, Sym^{+}-$ symmetric, skew-symmetric and symmetric and positive definite tensors;

$Ort^{+}-$ all proper rotation of the orthogonal group Ort;

$\mathbf{A}\cdot\mathbf{B} := \mathrm{tr}\,\mathbf{A}\mathbf{B}^T-$ the scalar product of $\mathbf{A}, \mathbf{B} \in Lin$;

$\mathbf{A}^s = \dfrac{1}{2}(\mathbf{A}+\mathbf{A}^T)$ and $\mathbf{A}^a = \dfrac{1}{2}(\mathbf{A}-\mathbf{A}^T)-$ the symmetrical and respectively skew- symmetrical parts of $\mathbf{A} \in Lin$; $\mathbf{I}$ is the identity tensor;

$\mathcal{E}^T-$ the transpose of $\mathcal{E}-$ fourth order tensor, defined for all $\mathbf{A}, \mathbf{B} \in Lin$ by

$\mathcal{E}^T\mathbf{A}\cdot\mathbf{B} := \mathbf{A}\cdot\mathcal{E}\mathbf{B}$;

$\dot{\mathbf{u}}-$ represents the derivative with respect to time; $\partial_{\mathbf{G}}\,\varphi(\mathbf{G},\alpha)-$ the partial derivative of the function $\varphi(\mathbf{G},\alpha)$ with respect to $\mathbf{G}$;

$d\,\hat{\Sigma}(\mathbf{G})-$ the differential of the map $\hat{\Sigma}$ at $\mathbf{G}$;

$\mathbf{A}\cdot\mathbf{B} := \mathrm{tr}\,\mathbf{A}\mathbf{B}^T-$ the scalar product of $\mathbf{A}, \mathbf{B} \in Lin$; $\mid \mathbf{A} \mid = \sqrt{\mathbf{A}\cdot\mathbf{A}} \equiv \sqrt{A_{ij}A_{ij}}$ the modulus of the second order tensor and A_{ij} denote its Cartesian components; $|\mathcal{E}|_4 = \sqrt{\sum_{ijkl}\mathcal{E}^2_{ijkl}}$ denotes the modulus of fourth order tensor and $\mathcal{E}_{ijkl}$ are Cartesian components of $\mathcal{E}$;

$< z >= 1/2\,(z+\mid z\mid),\ \forall z \in \mathbf{R}-$ the set of all real numbers;

$\rho_0, \tilde{\rho}, \rho$ are mass densities in initial, relaxed and actual configurations;

$\mathbf{Q}[\alpha] := \mathbf{Q}\alpha\mathbf{Q}^T$ for $\alpha \in Lin$, $\mathbf{Q}[\alpha] := \alpha$ for $\alpha \in R$.

2. Σ-models

We introduce now the constitutive framework of anisotropic elasto-plastic materials, $\Sigma-$models being included, see [8].

We fix a material point $\mathbf{X}$ in the body, considered in the reference configuration k. For an arbitrary given motion χ, defined in a certain neighborhood of $\mathbf{X}$, let consider the deformation gradient $\mathbf{F}(t)$, $\det \mathbf{F}(t) > 0$, $\mathbf{F}(0) = \mathbf{I}$. We assume the *multiplicative decomposition* of the deformation gradient into its *elastic* and *plastic* parts:

$$\mathbf{F}(t) = \mathbf{E}(t)\mathbf{P}(t) \quad \text{where} \quad \mathbf{E}(t) = \nabla\chi(\mathbf{X}, t)\mathbf{K}_t^{-1}, \ \mathbf{P}(t) = \mathbf{K}_t\mathbf{K}_0^{-1} \tag{1}$$

based on the local, current configuration $\mathbf{K}_t$.

We denote by $\mathbf{G} = \mathbf{E}^T\mathbf{E}$ the elastic strain, and by $\mathbf{Y} = (\mathbf{P}^{-1}, \alpha)$ the set of the irreversible variables, where α represent the set of internal variables, scalars and tensors, $\Pi-$ symmetric Piola-Kirchhoff stress tensor $\mathbf{K}_t$, $\mathbf{T}-$ Cauchy stress tensor, related by

$$\frac{\Pi}{\tilde{\rho}} = \mathbf{E}^{-1}\frac{\mathbf{T}}{\rho}\mathbf{E}^{-T}$$

The *elastic type constitutive* in term of Σ is written under the form

$$\begin{array}{l} \Sigma := \hat{\Sigma}(\mathbf{G}, \alpha), \quad \hat{\Sigma}(\mathbf{I}, \alpha) = 0, \\ \mathbf{G}^{-1}\hat{\Sigma}(\mathbf{G}, \alpha) = \hat{\Sigma}^T(\mathbf{G}, \alpha)\mathbf{G}^{-1}, \ \forall\, \mathbf{G} \in Sym^+. \end{array} \tag{2}$$

The value of the tensor function written in $(2)_2$ gives the current value of $\dfrac{\Pi}{\tilde{\rho}}$, taking into account the relation between symmetric Piola-Kirchhoff and Mandel's stress tensors

$$\Sigma = \mathbf{G}\frac{\Pi}{\tilde{\rho}}$$

The *rate independent evolution eqns.* for $\mathbf{P}, \alpha$ are expressed by

$$\begin{array}{l} \dot{\mathbf{P}}\mathbf{P}^{-1} = \mu\, \hat{\mathcal{B}}(\Sigma, \alpha), \quad \dot{\alpha} = \mu\, \hat{\mathbf{m}}(\Sigma, \alpha), \\ \hat{\mathcal{F}}(\cdot, \alpha) : \mathcal{D}_{\hat{\mathcal{F}}} \subset Lin \longrightarrow \mathbf{R}_{\leq 0}, \quad \text{and} \quad \hat{\mathcal{F}}(0, \alpha) < 0, \\ \mu \geq 0, \quad \mu\, \hat{\mathcal{F}} = 0, \quad \text{and} \quad \mu\, \dot{\hat{\mathcal{F}}} = 0. \end{array}$$

Material symmetry requirements (see [1, 3]). We assume that the *preexisting material symmetry* is characterized by *the symmetry group* $g_k \subset Ort^+$, that renders the material functions invariant

$$\hat{\Sigma}(\mathbf{Q}\mathbf{G}\mathbf{Q}^T, \mathbf{Q}[\alpha]) = \mathbf{Q}\hat{\Sigma}(\mathbf{G}, \alpha)\mathbf{Q}^T \quad , \quad \hat{\mathcal{F}}(\mathbf{Q}\Sigma\mathbf{Q}^T, \mathbf{Q}[\alpha]) = \hat{\mathcal{F}}(\Sigma, \alpha),$$

$$\hat{\mathcal{B}}(\mathbf{Q}\Sigma\mathbf{Q}^T, \mathbf{Q}[\alpha]) = \mathbf{Q}\hat{\mathcal{B}}(\Sigma, \alpha)(\mathbf{Q})^T, \quad \hat{\mathbf{m}}(\mathbf{Q}\Sigma\mathbf{Q}^T, \mathbf{Q}[\alpha]) = \mathbf{Q}[\hat{\mathbf{m}}(\mathbf{G}, \alpha)]$$

for every $\mathbf{Q} \in g_k$.

THEOREM 1. *Any $\Sigma-$ model leads to a strain formulation of the elasto- plastic behaviour of the material with respect to the relaxed configuration $\mathbf{K}_t$. Also the material functions are g_k- invariant.*

The appropriate material functions in strain formulations are related to the basic functions from $\Sigma-$models through relationships of the type:

$$\widetilde{\mathcal{F}}(\mathbf{G}, \alpha) = \hat{\mathcal{F}}(\hat{\Sigma}(\mathbf{G}, \alpha), \alpha), \quad \widetilde{\mathcal{B}}(\mathbf{G}, \alpha) = \hat{\mathcal{B}}(\hat{\Sigma}(\mathbf{G}, \alpha), \alpha), \quad \textit{etc.}$$

THEOREM 2 (STRAIN FORMULATION IN THE INITIAL CONFIGURATION).
1. Let $\mathbf{Y} := (\mathbf{P}^{-1}, \alpha)$ characterizes the irreversible behaviour of the body, at the fixed material point. The yield function in the reference configuration associated with the yield function in elastic strain is defined by

$$\mathcal{F}(\mathbf{C}, \mathbf{Y}) := \widetilde{\mathcal{F}}(\mathbf{P}^{-T}\mathbf{C}\mathbf{P}^{-1}, \alpha) \equiv \widetilde{\mathcal{F}}(\mathbf{G}, \alpha) \quad \textit{with}\ \mathbf{Y} \equiv (\mathbf{P}^{-1}, \alpha)$$

as a consequence of (1).

2. The evolution in time of $\mathbf{Y}$ *is governed by the solutions of Cauchy problem (see* [1]*)*

$$
\begin{aligned}
&\dot{\mathbf{Y}} = - < \beta(t, \mathbf{Y}) > \; \bar{\mathcal{Y}}(\mathbf{C}(t), \mathbf{Y}) H(\mathcal{F}(\mathbf{C}(t), \mathbf{Y})) \\
&\beta(t, \mathbf{C}) = \partial_{\mathbf{C}} \mathcal{F}(\mathbf{C}(t), \mathbf{Y}) \cdot \dot{\mathbf{C}}(t) \\
&\partial_{\mathbf{Y}} \bar{\mathcal{F}}(\mathbf{C}, \mathbf{Y}) \cdot \bar{\mathcal{Y}}(\mathbf{C}, \mathbf{Y}) = 1 \quad on \quad \mathcal{F}(\mathbf{C}, \mathbf{Y}) = 0 \\
&\mathbf{Y}(0) = \mathbf{Y}_0
\end{aligned}
\tag{3}
$$

for a given strain history, denoted $\hat{\mathbf{C}} \in \mathcal{G}_s$,

$$
t \in [0, d] \to \hat{\mathbf{C}}(t) \in Sym^+, \quad with \quad \hat{\mathbf{C}}(t) = \mathbf{C}(t) = \mathbf{F}^T(t)\mathbf{F}(t).
$$

Here H denotes the Heaviside function.

Basic assumptions:

I. There exists an unique solution of the Cauchy problem (3).

II. The smooth yield function $\widetilde{\mathcal{F}}$ is given in such way that

i) $\widetilde{\mathcal{F}} : \mathcal{D}_{\mathcal{F}} \subset Sym^+ \times R^n \longrightarrow R$ is of the class C^1, and $\widetilde{\mathcal{F}}(\mathbf{I}, \alpha) < 0$ for all α;

ii) for all fixed $\alpha \in pr_2\, \mathcal{D}_{\mathcal{F}}-$ the projection on the space of internal variables, the set

$$
\{\mathbf{G} \in Sym^+ \;\mid\; \widetilde{\mathcal{F}}(\mathbf{G}, \alpha) \le 0\}
$$

is the closure of a non-empty, connected open set, i.e. if necessary we restrict the yield function to the connected set that contains $\mathbf{I} \in pr_1\, \mathcal{D}_{\mathcal{F}} \subset Sym^+$;

iii) for all $\alpha \in pr_2\mathcal{D}_{\mathcal{F}}$ the set $\{\mathbf{G} \in Sym^+ \mid \widetilde{\mathcal{F}}(\mathbf{G}, \alpha) = 0\}$ defines a C^1 differential manifold, called the current yield surface. Hence $\partial_{\mathbf{G}} \widetilde{\mathcal{F}}(\mathbf{G}, \alpha) \neq 0$ on the yield surface.

THEOREM 3. *The dissipation postulate, introduced in* [7] *is equivalent to the existence of the stress potential* (I)*, together with the dissipation inequality* (II)*.*

I. For all $\hat{\mathbf{C}} \in \mathcal{G}_s$ *and for all* $t \in [0, 1)$ *there exist the smooth scalar valued functions,* $\varphi,\ \sigma$, *related by*

$$
\begin{aligned}
&\sigma(\mathbf{C}, \mathbf{Y}(t)) = \varphi(\mathbf{P}^{-T}(t)\mathbf{C}\mathbf{P}^{-1}(t), \alpha(t)) \quad \forall \mathbf{C} \in \mathcal{U}(\hat{\mathbf{C}}_t) \quad with \\
&\mathcal{U}(\hat{\mathbf{C}}_t) := \{\mathbf{B} \in Sym^+ \mid \mathcal{F}(\mathbf{B}, \mathbf{Y}(t)) \le 0\}
\end{aligned}
$$

the elastic range, at time t *corresponding to* $\hat{\mathbf{C}} \in \mathcal{G}_s$. *Here* $\hat{\mathbf{C}}_t$ *is the restriction on* $[0, t]$ *of the given history.*

The functions $\varphi,\ \sigma$, *are stress potentials*

$$
\begin{aligned}
&\frac{\Pi(t)}{\tilde{\rho}(t)} = 2\, \partial_{\mathbf{G}} \varphi(\mathbf{G}, \alpha(t)), \quad \frac{\mathbf{T}(t)}{\rho} = 2\, \mathbf{F} \partial_{\mathbf{C}} \sigma(\mathbf{C}(t), \mathbf{Y}(t)) \mathbf{F}^T, \\
&\mathbf{G} = \mathbf{P}^{-T}(t)\mathbf{C}(t)\mathbf{P}^{-1}(t).
\end{aligned}
\tag{4}
$$

II. The following equivalent dissipation inequalities

$$
\begin{aligned}
&[\partial_{\mathbf{Y}} \sigma(\mathbf{A}, \mathbf{Y}(t)) - \partial_{\mathbf{Y}} \sigma(\mathbf{C}(t), \mathbf{Y}(t))] \cdot \dot{\mathbf{Y}}(t) \ge 0 \quad and \\
&(\Sigma(t) - \Sigma^*) \cdot \dot{\mathbf{P}}(t)\mathbf{P}^{-1}(t) + (\mathbf{a}(t) - \mathbf{a}^*)\dot{\alpha}(t) \ge 0
\end{aligned}
\tag{5}
$$

hold for all $\mathbf{G}, \mathbf{G}^*$ *such that* $\widetilde{\mathcal{F}}(\mathbf{G}, \alpha) = 0$, $\widetilde{\mathcal{F}}(\mathbf{G}^*, \alpha) \leq 0$, *when the conjugated forces to internal variables (see [10]) are considered*

$$\mathbf{a}(t) := -\partial_\alpha \varphi(\mathbf{G}(t), \alpha(t)), \quad \mathbf{a}^* = -\partial_\alpha \varphi(\mathbf{G}^*, \alpha(t))$$

Here $\Sigma(t)$, Σ^* are calculated from (2) for the elastic strains $\mathbf{G}(t)$ and $\mathbf{G}^*$.

PROPOSITION 1. *When the dissipation inequality (5)$_2$ is satisfied then modified flow rule*

$$(\partial_{\mathbf{G}} \hat{\Sigma}(\mathbf{G}, \alpha))^T [\dot{\mathbf{P}}\mathbf{P}^{-1}] = \mu \partial_{\mathbf{G}} \widetilde{\mathcal{F}}(\mathbf{G}, \alpha) + \partial^2_{\alpha\, \mathbf{G}} \varphi(\mathbf{G}, \alpha)[\dot{\alpha}] \tag{6}$$

with $\mu \geq 0$, *holds. The dissipation inequality (5)$_1$ imposes that*

$$-\partial_{\mathbf{Y}}[\partial_{\mathbf{C}} \sigma(\mathbf{C}, \mathbf{Y})][\dot{\mathbf{Y}}] = \bar{\mu} \partial_{\mathbf{C}} \mathcal{F}(\mathbf{C}, \mathbf{Y}) \quad \bar{\mu} \geq 0, \tag{7}$$

for all $\mathbf{C} = \mathbf{C}(t)$ *on yield surface* $\mathcal{F}(\mathbf{C}, \mathbf{Y}) = 0$, *for the fixed* $\mathbf{Y} = \mathbf{Y}(t)$, *with* $\bar{\mu} \geq 0$.

To end the discussion about the consequences of the dissipation postulate we recall the basic result, similar to [13]:

THEOREM 4. *1. At any regular point* Σ *of the yield function in stress space* $\hat{\mathcal{F}}(\Sigma, \alpha) = 0$, *but with* $\Sigma = \hat{\Sigma}(\mathbf{G})$, *the appropriate flow rule, i.e. the modified flow rule, takes the form*

$$\begin{array}{l} \mathbf{L}^p \equiv \dot{\mathbf{P}}\mathbf{P}^{-1} = \mu\, \partial_\Sigma \hat{\mathcal{F}}(\Sigma, \alpha) + \mathbf{L}^{p*}; \\ \mathbf{L}^{p*} : \quad (d\, \hat{\Sigma}(\mathbf{G}))^T (\mathbf{L}^{p*}) = 0 \end{array} \tag{8}$$

3. Rate boundary value problem and variational inequalities

We derive the variational inequalities with respect to the actual and respectively initial configurations, related to the rate quasi-static boundary value problem and associated with a generic stage of the process, at the time t. We use an appropriate procedure as in [19, 4] and different motion descriptions that can be found in [25].

The *nominal stress* with respect to the actual configuration at time t, or the *non-symmetric relative* Piola- Kirchhoff, is defined by

$$\mathbf{S}_t(\mathbf{x}, \tau) = (\det \mathbf{F}_t(\mathbf{x}, \tau))\mathbf{T}(\mathbf{y}, \tau)(\mathbf{F}_t(\mathbf{x}, \tau))^{-T},$$

with

$$\mathbf{F}_t(\mathbf{x}, \tau) = \mathbf{F}(\mathbf{X}, \tau)(\mathbf{F}(\mathbf{X}, t))^{-1}$$

the relative deformation gradient.
Here $\mathbf{x} = \chi(\mathbf{X}, t)$, $\mathbf{y} = \chi(\mathbf{X}, \tau)$, or $\mathbf{y} = \chi_t(\mathbf{x}, \tau) \equiv \chi(\chi^{-1}(\mathbf{x}, t), \tau)-$ the motion in the relative description. At time t we have

$$\begin{array}{rcl} \mathbf{S}_t(\mathbf{x}, t) & = & \mathbf{T}(\mathbf{x}, t) \quad \text{and} \\ \dot{\mathbf{S}}_t(\mathbf{x}, t) & \equiv & \dfrac{\partial}{\partial \tau} \mathbf{S}_t(\mathbf{x}, \tau) \mid_{\tau = t} \\ & = & \rho(\mathbf{x}, t) \dfrac{\partial}{\partial \tau} (\dfrac{\mathbf{T}(\mathbf{y}, \tau)}{\rho(\mathbf{y}, \tau)}) \mid_{\tau = t} - \mathbf{T}(\mathbf{x}, t) \mathbf{L}^T(\mathbf{x}, t). \end{array} \tag{9}$$

Here $\mathbf{L}(\mathbf{x}, t) = \nabla \mathbf{v}(\mathbf{x}, t)$ represents the velocity gradient, in spatial representation.

Let us consider a body, identified with $\Omega \subset \mathbf{R}^3$ in the initial configuration, which undergoes the finite elasto-plastic deformation and occupies the domain $\Omega_\tau = \chi(\Omega, \tau) \subset R^3$, at time τ.

The *equilibrium equation* at time τ, in terms of Cauchy stress tensor $\mathbf{T}(\mathbf{y}, \tau) \in Sym$

$$\operatorname{div} \mathbf{T}(\mathbf{y}, \tau) + \rho(\mathbf{y}, \tau)\mathbf{b}(\mathbf{y}, \tau) = 0, \quad \text{in} \quad \Omega_\tau$$

where $\mathbf{b}$ are the body forces, can be equivalently expressed, with respect to the configuration at time $t-$ taken as the reference configuration

$$\text{(10)} \qquad \begin{aligned} &\operatorname{div} \mathbf{S}_t(\mathbf{x}, \tau) + \rho(\mathbf{x}, t)\mathbf{b}_t(\mathbf{x}, \tau) = 0\ , \quad \text{with} \quad \mathbf{b}_t(\mathbf{x}, \tau) = \mathbf{b}(\chi_t(\mathbf{x}, \tau), \tau) \\ &\mathbf{S}_t(\mathbf{x}, \tau)\mathbf{F}_t^T(\mathbf{x}, \tau) = \mathbf{F}_t(\mathbf{x}, \tau)\mathbf{S}_t^T(\mathbf{x}, \tau) \end{aligned}$$

When the reference configuration is considered to be a natural one, we add the initial conditions

$$\mathbf{S}_0(\mathbf{X}, 0) = 0, \quad \mathbf{F}(\mathbf{X}, 0) = \mathbf{I}, \quad \mathbf{P}(\mathbf{X}, 0) = \mathbf{I}, \quad \alpha(\mathbf{X}, 0) = 0,$$

for every $\mathbf{X} \in \Omega_0$ and the following boundary conditions on $\partial\Omega_t$:

$$\text{(11)} \qquad \mathbf{S}_t(\mathbf{x}, \tau)\mathbf{n}(t)\ |_{\Gamma_{1t}} = \hat{\mathbf{S}}_t(\mathbf{x}, \tau)\ , \quad (\chi_t(\mathbf{x}, \tau) - \mathbf{x})\ |_{\Gamma_{2t}} = \hat{\mathbf{U}}_t(\mathbf{x}, \tau)$$

Here $\partial\Omega_t \equiv \Gamma_{1t} \bigcup \Gamma_{2t}$ denotes the boundary of the thredimensional domain Ω_t, $\mathbf{n}(t)$ is the unit external normal at Γ_{1t}, while $\chi_t(\mathbf{x}, \tau) - \mathbf{x}$ is the displacement vector with respect to the configuration at time t. $\hat{\mathbf{S}}_t$ and $\hat{\mathbf{U}}_t$, the surface loading and the displacement vector are time dependent, τ, prescribed functions, with respect to the fixed at time t configuration.

The rate quasi-static boundary value problem at time t, involves the time differentiation, i.e. with respect to τ, of the equilibrium equations, (10), $\forall\, \mathbf{x} \in \Omega_t$, and of the boundary condition (11), when $\tau = t$

$$\text{(12)} \qquad \begin{aligned} &\operatorname{div} \dot{\mathbf{S}}_t(\mathbf{x}, t) + \rho(\mathbf{x}, t)\dot{\mathbf{b}}_t(\mathbf{x}, t) = 0\ , \\ &\dot{\mathbf{S}}_t(\mathbf{x}, t)\mathbf{n}(t)\ |_{\Gamma_{1t}} = \dot{\hat{\mathbf{S}}}_\mathbf{t}(\mathbf{x}, \mathbf{t}), \\ &\mathbf{v}(\mathbf{x}, t)\ |_{\Gamma_{2t}} = \hat{\mathbf{U}}_\mathbf{t}(\mathbf{x}, \mathbf{t}) \end{aligned}$$

using the notation $\dot{\mathbf{b}}_t(\mathbf{x}, t)$ for $\dfrac{\partial}{\partial\tau}\mathbf{b}_t(\mathbf{x}, \tau\ |_{\tau=t}$.

At a generic stage of the process the current values, i.e. at the time t, of $\mathbf{F}$, $\mathbf{T}$, $\mathbf{Y}$, and the set of all material particles, in which the stress reached the current yield surface

$$\Omega_t^p = \chi(\Omega^p, t), \quad \text{with} \quad \Omega^p \equiv \{\mathbf{X} \in \Omega \mid \overline{\mathcal{F}}(\mathbf{C}(\mathbf{X}, t), \mathbf{Y}(\mathbf{X}, t)) = 0\}$$

are known for all $\mathbf{x} \in \Omega_t$, with the current deformed domain Ω_t also determined.

The set of kinematically admissible (at time t) velocity fields is denoted by

$$\mathcal{V}_{ad}(t) \equiv \{\mathbf{v} : \Omega_t \longrightarrow \mathbf{R}^3 \mid\ \mathbf{v}\ |_{\Gamma_{2t}} = \dot{\hat{\mathbf{U}}}_\mathbf{t}\}.$$

and the set of all admissible plastic multiplier

$$\begin{aligned} \mathcal{M}(t) \equiv \{\delta : \Omega_t \longrightarrow \mathbf{R}_{\geq 0} \mid \quad &\delta(\mathbf{x}, t) = 0, \quad \text{if} \quad \mathbf{x} \in \Omega_t \backslash \Omega_t^p, \\ &\delta(\mathbf{x}, t) \geq 0, \quad \text{if} \quad \mathbf{x} \in \Omega_t^p\}. \end{aligned}$$

THEOREM 5. *At every time t the velocity field,* $\mathbf{v}$, *and the equivalent plastic factor* β *satisfy the following relationships*

$$\int_{\Omega_t} \rho\{\nabla\mathbf{v}\frac{\mathbf{T}}{\rho} \cdot (\nabla\mathbf{w} - \nabla\mathbf{v}) + 4\mathbf{F}\partial^2_{\mathbf{CC}}\sigma(\mathbf{C},\mathbf{Y})[\mathbf{F}^T\{\nabla\mathbf{v}\}^s\mathbf{F}]\mathbf{F}^T \cdot (\{\nabla\mathbf{w}\}^s - \{\nabla\mathbf{v}\}^s)\}dx - 2\int_{\Omega_t^p} \rho\frac{\beta}{h_r}\,\mathbf{F}\partial_{\mathbf{C}}\mathcal{F}(\mathbf{C},\mathbf{Y})\mathbf{F}^T \cdot (\{\nabla\mathbf{w}\}^s - \{\nabla\mathbf{v}\}^s)dx = \int_{\Omega_t} \rho\dot{\mathbf{b}} \cdot (\mathbf{w} - \mathbf{v})dx + \int_{\Gamma_{2t}} \dot{\hat{\mathbf{S}}}_{\mathbf{t}} \cdot (\mathbf{w} - \mathbf{v})\mathbf{da} \tag{13}$$

and

$$-2\int_{\Omega_t^p} \frac{\rho}{h_r}(\delta - \beta)\,\mathbf{F}\partial_{\mathbf{C}}\mathcal{F}(\mathbf{C},\mathbf{Y})\mathbf{F}^T \cdot (\{\nabla\mathbf{v}\}^s)dx + \int_{\Omega_t^p} \frac{\rho}{h_r}(\delta - \beta)\beta dx \geq 0, \tag{14}$$

which hold for every admissible vector field $\mathbf{w} \in \mathcal{V}_{ad}(t)$, *and for all* $\delta \in \mathcal{M}(t)$.

Proof. In the theorem of virtual power, derived from the rate quasi-static equilibrium equation (12):

$$\int_{\Omega_t} \dot{\mathbf{S}}_t \cdot \nabla\mathbf{w}dx = \int_{\partial\Omega_t} \dot{\mathbf{S}}_t\mathbf{n} \cdot \mathbf{w}da + \int_{\Omega_t} \rho\dot{\mathbf{b}}_t \cdot \mathbf{w}dx, \quad \forall\mathbf{w} \in \mathcal{V}_{ad}(t)$$

we substitute the rate of the nominal stress, at time t, calculated from (9), taking into account the potentiality condition $(4)_2$. First of all we calculate the differential with respect to τ of the right hand side in $(4)_2$, in which we replace $\dot{\mathbf{F}}\mathbf{F}^{-1} = \mathbf{L}$ and $\dot{\mathbf{C}} = 2\mathbf{FDF}^T$, with $\mathbf{D} = \mathbf{L}^s$. Thus

$$\frac{\partial}{\partial\tau}(\frac{\mathbf{T}}{\rho}) = 2\mathbf{LF}\partial_{\mathbf{C}}\sigma(\mathbf{C},\mathbf{Y})\mathbf{F}^T + 2\mathbf{F}\partial_{\mathbf{C}}\sigma(\mathbf{C},\mathbf{Y})\mathbf{F}^T\mathbf{L}^T + 2\mathbf{F}\partial^2_{\mathbf{CC}}\sigma(\mathbf{C},\mathbf{Y})[2\mathbf{FDF}^T]\mathbf{F}^T + 2\mathbf{F}(\partial^2_{\mathbf{YC}}\sigma(\mathbf{C},\mathbf{Y})[\dot{\mathbf{Y}}])\mathbf{F}^T \tag{15}$$

in which we introduce the modified flow rule, (7), written under the form (see Remark 2)

$$\partial^2_{\mathbf{YC}}\sigma(\mathbf{C},\mathbf{Y})[\dot{\mathbf{Y}}] = -\mu\partial_{\mathbf{C}}\mathcal{F}(\mathbf{C},\mathbf{Y}), \tag{16}$$

Hence the equality (13) follows at once from (9), (15)and (16).

In order to prove (14) we note that $\mu \geq 0$ can be express either by the inequality

$$(\tilde{\mu} - \mu)\,\dot{\hat{\mathcal{F}}} \leq 0,\ \forall\,\tilde{\mu} \geq 0, \quad \text{together with} \quad \mu\,\hat{\mathcal{F}} = 0, \tag{17}$$

or under its explicit dependence on the rate of strain:

$$\mu = \frac{\beta}{h_r}, \quad \text{with} \quad \beta = 2\partial_\Sigma\hat{\mathcal{F}}(\Sigma,\alpha) \cdot d\hat{\Sigma}(\mathbf{G},\alpha)[\mathbf{E}^T\mathbf{DE}],$$

$$h_r = 2\partial_\Sigma\hat{\mathcal{F}}(\Sigma,\alpha) \cdot d\hat{\Sigma}(\mathbf{G},\alpha)[\{\mathbf{G}\tilde{\mathcal{B}}\}^s] - \partial_\alpha\hat{\mathcal{F}}(\Sigma,\alpha) \cdot \tilde{\mathbf{m}},$$

where the hardening parameter $h_r > 0$. The time derivative of $\hat{\mathcal{F}}(\Sigma,\alpha)$ with (2) is introduced in (17). Consequently, for all $\mathbf{x} \in \Omega_t^p$ we get

$$(\tilde{\mu} - \mu)(-\mu h_r + 2\partial_\Sigma\hat{\mathcal{F}}(\Sigma,\alpha) \cdot d\hat{\Sigma}(\mathbf{G},\alpha)[\mathbf{E}^T\mathbf{DE}]) \leq 0. \tag{18}$$

$h_r > 0$. We can substitute μ and $\tilde{\mu}$ by β/h_r and δ/h_r. By integrating on Ω_t^p from (18) the inequality (14) holds, when the equality

$$\partial_{\mathbf{C}}\mathcal{F} \cdot \mathbf{A} = \partial_{\Sigma}\hat{\mathcal{F}}(\Sigma, \alpha) \cdot d\hat{\Sigma}(\mathbf{G}, \alpha)[\mathbf{P}^{-T}\mathbf{A}\mathbf{P}^{-1}]) \, , \forall\, \mathbf{A} \in Sym$$

is also used for $\mathbf{A} = \mathbf{F}^T\mathbf{D}\mathbf{F}$.

Let us define the convex set $\widetilde{\mathcal{K}}$ in the appropriate functional space of the solution $\mathbf{H}_{ad}$, by

$$\widetilde{\mathcal{K}} := \{(\mathbf{w}, \delta) \mid \mathbf{w} \in \mathcal{V}_{ad}(t), \quad \delta : \Omega \longrightarrow \mathbf{R}_{\geq 0}\},$$

and *the bilinear forms*, in the appropriate space $\mathcal{H}_{ab}$:

$$\begin{aligned} K[\mathbf{v}, \mathbf{w}] &= \int_{\Omega_t} \rho\big(\nabla \mathbf{v}\frac{\mathbf{T}}{\rho} \cdot \nabla \mathbf{w} + 4\mathbf{F}\partial^2_{\mathbf{CC}}\sigma(\mathbf{C}, \mathbf{Y})[\mathbf{F}^T\{\nabla \mathbf{v}\}^s\mathbf{F}]\mathbf{F}^T \cdot \{\nabla \mathbf{w}\}^s\big)dx \\ A[\beta, \delta] &= \int_{\Omega_t^p} \frac{\rho}{h_r}\,\beta\,\delta dx \\ B[\delta, \mathbf{v}] &= -2\int_{\Omega_t^p} \frac{\rho}{h_r}\delta\,\mathbf{F}\partial_{\mathbf{C}}\mathcal{F}(\mathbf{C}, \mathbf{Y})\mathbf{F}^T \cdot \{\nabla \mathbf{v}\}^s dx \end{aligned} \tag{19}$$

are defined $\forall\, \mathbf{v}, \mathbf{w} \in \mathcal{V}_{ad}(t)$, $\forall\, \delta,\ \beta : \Omega_t \longrightarrow \mathbf{R}_{\geq 0}$.

□

As a consequence of (19) , (13) and (14) the below statement holds:

THEOREM 6. *Find* $\mathbf{U} = (\mathbf{v}, \beta) \in \widetilde{\mathcal{K}}$, *solution of the variational inequality,* V.I.*:*

$$a[\mathbf{U}, \mathbf{V} - \mathbf{U}] \geq f[\mathbf{V} - \mathbf{U}] \quad \forall\, \mathbf{V} \in \widetilde{\mathcal{K}} \tag{20}$$

$a[\cdot, \cdot]$ is the bilinear and symmetric form *defined on* H_{ad}

$$a[\mathbf{V}, \mathbf{W}] := K[\mathbf{v}, \mathbf{w}] + B[\beta, \mathbf{w}] + B[\delta, \mathbf{v}] + A[\beta, \delta]$$

defined $\forall\, \mathbf{V} = (\mathbf{v}, \beta), \mathbf{W} = (\mathbf{w}, \delta)$ *and*

$$f[\mathbf{V}] := \int_{\Gamma_{1t}} \dot{\hat{\mathbf{S}}}_{\mathbf{t}} \cdot \mathbf{vda} + \int_{\Omega_t} \rho\dot{\mathbf{b}}_t \cdot \mathbf{vdx}, \quad \Gamma_{1t} \subset \partial\Omega_t. \tag{21}$$

REMARK 1. Under hypotheses: there exists $H_{ad}-$ a Hilbert space, with the scalar product denoted by $\cdot$, the continuity of the bilinear form on H_{ad}, $\mid a[\mathbf{V}, \mathbf{U}] \mid \leq c_o \mid\mid V \mid\mid_H \quad \mid\mid \mathbf{U} \mid\mid_H$, and of the linear functional from (21) then the existence of $Q-$ linear operator associated to the bilinear form:

$$a[\mathbf{U}, \mathbf{V}] = Q\mathbf{U} \cdot \mathbf{V} \quad \forall\, \mathbf{U}, \mathbf{V} \in H_{ad}.$$

The variational problem can be equivalently formulated (see for instance Glowinski, Lions, Trémolières [1976]): Find $\tilde{\mathbf{U}} \in H_{ad}$ such that

$$a[\tilde{\mathbf{U}}, \mathbf{U} - \tilde{\mathbf{U}}] - \mathbf{f} \cdot (\mathbf{U} - \tilde{\mathbf{U}}) + \Phi_{\tilde{K}}(\mathbf{U}) - \Phi_{\tilde{K}}(\tilde{\mathbf{U}}) \geq 0 \quad \forall\, \mathbf{U} \in H_{ad}.$$

Here $\Phi_{\tilde{K}}$ - the indicator function of $\tilde{K}$, is zero on $\tilde{K}$, and infinity outside.

By using the subdifferential $\partial\Phi_{\tilde{K}}$ of the function $\Phi_{\tilde{K}}$ the variational inequality becomes

$$-(Q\tilde{\mathbf{U}} - \mathbf{f}) \in \partial\Phi_{\tilde{K}}(\tilde{\mathbf{U}})$$

We recall that the *subdifferential* of $\Phi_{\tilde{K}}$ is defined as the mapping on H_{ad} such that

$$\partial\Phi_{\tilde{K}}(x) = \{\eta \in H \mid \Phi_{\tilde{K}}(y) - \Phi_{\tilde{K}}(x) \geq \eta \cdot (y - x) \quad \forall \quad y \in H\};$$

$\eta \in \partial\Phi_{\tilde{K}}(x)$ are called subgradients of $\Phi_{\tilde{K}}$ (see [18]). The domain of $\partial\Phi_{\tilde{K}}$ coincides with $\tilde{K}$, and $\partial\Phi_{\tilde{K}}(x) = \{0\}$ when x belongs to the interior of $\tilde{K}$.

PROPOSITION 2. *For linear elastic type constitutive equation, in the plastically deformed configuration, the following formula*

$$4\partial^2_{\mathbf{CC}}\sigma(\mathbf{C}, \mathbf{Y})[\mathbf{A}] = \mathbf{P}^{-1}\mathcal{E}[\mathbf{P}^{-T}\mathbf{A}\mathbf{P}^{-1}]\mathbf{P}^{-T}, \quad \forall\, \mathbf{A} \in Sym$$

follows.

In the case of small elastic strains

$$\Delta = \frac{1}{2}(\mathbf{G} - \mathbf{I}) \simeq \epsilon^e \quad \mathbf{E} = \mathbf{R}^e\mathbf{U}^e, \quad \text{where}$$

$$\mathbf{U}^e = \mathbf{I} + \epsilon^e, \quad \mathbf{G} = \mathbf{I} + 2\epsilon^e \quad \text{with} \quad |\, \epsilon^e \,| \leq 1,$$

$\mathbf{R}^e-$ elastic rotation, the following estimations

$$|\, \nabla\mathbf{w}\frac{\mathbf{T}}{\rho} \cdot \nabla\mathbf{w} \,| \leq |\, \nabla\mathbf{w} \,|^2 |\, \mathcal{E} \,|_4 |\, \epsilon^e \,|$$

$$4 \mid \mathbf{F}\partial^2_{\mathbf{CC}}\sigma(\mathbf{C}, \mathbf{Y})[\mathbf{F}^T\{\nabla\mathbf{w}\}^s\mathbf{F}]\mathbf{F}^T \cdot \{\nabla\mathbf{w}\}^s \mid \leq |\, \nabla\mathbf{w} \,|^2 |\, \mathcal{E} \,|_4$$

hold.

In conclusion: in the case of small elastic strains the first terms in the bilinear form $K[\cdot, \cdot]$ can be neglected in the presence of the second one. Moreover, if the behavior of the body, with small elastic strain only, is elastic, which means that $\beta = 0$ in the solution of the variational inequality, (20),then the bilinear form $a[\mathbf{V}, \mathbf{V}]$ for $\mathbf{V} = (\mathbf{v}, 0)$ is symmetric and positive definite.

In a similar manner, but starting from the *equilibrium equation* and the *balance equation of momentum* with respect to the initial configuration, expressed as

$$\mathrm{Div}\,\mathbf{S} + \mathbf{b}_0 = 0, \quad \text{and} \quad \mathbf{S}\mathbf{F}^T = \mathbf{F}\mathbf{S}^T, \quad \text{in} \quad \Omega \quad \text{with}$$

$$\mathbf{S} := (\det\mathbf{F})\mathbf{T}\mathbf{F}^{-T}, \quad \mathbf{S} := \rho_0\mathbf{F}\mathbf{P}^{-1}\frac{\Pi}{\tilde{\rho}}\mathbf{P}^{-T}$$

$\mathbf{S}-$ non-symmetric Piola- Kirchhoff stress tensor, where $\mathbf{b}_0$ are the body forces, we can prove:

THEOREM 7. *The formulation of the rate quasi- static boundary value problem, in the initial configuration leads to the variational inequality:*

Find $(\dot{\mathbf{u}}, \mu) \in \mathcal{V} \times \mathcal{M}$ *, such that* $\forall(\mathbf{v}, \nu) \in \mathcal{V} \times \mathcal{M}$

$$K_0[\dot{\mathbf{u}}, \mathbf{v} - \dot{\mathbf{u}}] + B_0[\mu, \mathbf{v} - \dot{\mathbf{u}}] = \mathcal{R}[\mathbf{v} - \dot{\mathbf{u}}],$$

(22)

$$B_0[\dot{\mathbf{u}}, \nu - \mu] + A_0[\mu, \nu - \mu] \geq 0$$

where K_0, B_0, A_0 *denote the bilinear forms:*

$$
\begin{aligned}
K_0[\mathbf{v},\mathbf{w}] &= \int_\Omega \rho_0\{\nabla\mathbf{v}\mathbf{P}^{-1}\frac{\Pi}{\tilde{\rho}}\mathbf{P}^{-T}\cdot\nabla\mathbf{w}+\overline{\mathcal{E}}^p[\{\mathbf{F}^T\nabla\mathbf{v}\}^s]\cdot\{\mathbf{F}^T\nabla\mathbf{w}\}^s\}d\mathbf{X}\\
B_0[\mu,\mathbf{w}] &= -2\int_{\Omega^p}\frac{\rho_0}{h_r}\mu\mathbf{P}^{-1}(d\,\hat{\Sigma})^T[\partial_\Sigma\hat{\mathcal{F}}]\mathbf{P}^{-T}\cdot\{\mathbf{F}^T\nabla\mathbf{w}\}^s d\mathbf{X}\\
A_0[\mu,\nu] &= \int_{\Omega^p}\frac{\rho_0}{h_r}\nu\mu d\mathbf{X}
\end{aligned}
$$

The linear functional

$$
\mathcal{R}[\mathbf{v}]=\int_{\Gamma_1}\dot{\mathbf{F}}_0\cdot\mathbf{v}da+\int_\Omega\rho_0\dot{\mathbf{b}}_0\cdot\mathbf{v}dx,
$$

represents the virtual power produced by the variation in time of the of the mass force $\mathbf{b}_0$ and of the forces acting on the part Γ_1 of the boundary domain $\partial\Omega$, i.e. $\mathbf{SN}\mid_{\Gamma_1}=\mathbf{F}_0$.

Here we have introduced the elastic tensor with respect to the reference configuration $\overline{\mathcal{E}}^p$

$$
\begin{aligned}
\overline{\mathcal{E}}^p[\mathbf{A}]: &= 4\,\mathbf{P}^{-1}\partial^2_{\mathbf{GG}}\varphi[\mathbf{P}^{-T}\mathbf{A}\mathbf{P}^{-1}]\mathbf{P}^{-1}\\
\varphi(\mathbf{G},\alpha) &= \sigma(\mathbf{C},\mathbf{Y}),\quad \mathbf{G}=\mathbf{P}^{-T}\mathbf{C}\mathbf{P}^{-1},\quad \mathbf{Y}=(\mathbf{P}^{-1},\alpha).
\end{aligned}
$$

Here we denoted by $\mathcal{V}\equiv\{\mathbf{v}\mid\mathbf{v}=\dot{\mathbf{U}}^0 \text{ on } \Gamma_2\subset\partial\Omega\}$, *the set of admissible displacement rate* (for a given function $\mathbf{U}^0$), and by $\mathcal{M}$, *the set of admissible plastic factors*.

REMARK 2. Note that $\mathbf{F}=\mathbf{I}+\nabla_{\mathbf{X}}\mathbf{u}$, where $\mathbf{u}(\mathbf{X},t)=\chi(\mathbf{X},t)-\mathbf{X}$ represents the displacement vector field and $\dot{\mathbf{F}}=\nabla_{\mathbf{X}}\dot{\mathbf{u}}$, and the spatial representations of the bilinear form (19) are just represented in (22).

The plastic factor $\mu=\dfrac{\beta}{h_r}$ which enter variational inequality is just the plastic factor which characterizes the evolution of plastic deformation, via the modified flow rule (7). In order to justify the above statement we recall the formula

$$
\partial_{\mathbf{C}}\mathcal{F}=\mathbf{P}^{-1}\partial_{\mathbf{G}}\tilde{\mathcal{F}}\mathbf{P}^{-T}=\mathbf{P}^{-1}d\hat{\Sigma}^T[\partial_\Sigma\hat{\mathcal{F}}(\Sigma,\alpha)]\mathbf{P}^{-T},
$$

and from the modified flow rule (6) we found

$$
d\hat{\Sigma}^T[\,\dot{\mathbf{P}}\mathbf{P}^{-1}-\mu\partial_\Sigma\hat{\mathcal{F}}(\Sigma,\alpha)]=0.
$$

On the other hand when we pass to the actual configuration we get

$$
B_0[\mu,\dot{\mathbf{u}}]=B[\mu,\mathbf{v}]
$$

for

$$
\dot{\mathbf{u}}=\frac{\partial\chi}{\partial t}(\mathbf{X},t)\quad\text{and}\quad\mathbf{v}=\frac{\partial\chi}{\partial t}(\mathbf{X},t)\mid_{\mathbf{x}=\chi^{-1}(\mathbf{X},t)}
$$

the rate of the displacement vector $\dot{\mathbf{u}}$ and $\mathbf{v}$ represent the velocity at the material point $\mathbf{X}$ in the material and the spatial representation.

4. Composite materials

We describe the composite materials within the framework of Σ-*models, with the potentiality condition and the modified flow rule*.

The macroscopic response will be orthotropic if there are two families reinforced fibres. In our model othotropic symmetry, characterized (see [12]) by the group $g_6 \in Ort$ defined by

$$g_6 := \{\mathbf{Q} \in Ort \mid \quad \mathbf{Q}\mathbf{n}_i = \mathbf{n}_i, \quad \text{or} \quad \mathbf{Q}\mathbf{n}_i = -\mathbf{n}_i, \quad i = 1, 2, 3.\}$$

where $\{\mathbf{n}_1, \mathbf{n}_2, \mathbf{n}_3\}$ is the orthonormal basis of the symmetry directions.

For transverse isotropy we distinguish the *subgroups* g_1, g_4, equivalently described in Liu [1983] by:

$$\begin{aligned} g_1 &\equiv \{\mathbf{Q} \in Ort \mid \quad \mathbf{Q}\mathbf{n}_1 = \mathbf{n}_1, \quad \mathbf{Q}\mathbf{N}_1\mathbf{Q}^T = \mathbf{N}_1\} \\ g_4 &\equiv \{\mathbf{Q} \in Ort \mid \quad \mathbf{Q}(\mathbf{n}_1 \otimes \mathbf{n}_1)\mathbf{Q}^T = \mathbf{n}_1 \otimes \mathbf{n}_1\} \end{aligned}$$

where $\mathbf{N}_1 = \mathbf{n}_2 \otimes \mathbf{n}_3 - \mathbf{n}_3 \otimes \mathbf{n}_2$, for $\{\mathbf{n}_1, \mathbf{n}_2, \mathbf{n}_3\}$ an orthonormal basis, with $\mathbf{n}_1-$ the *symmetry direction*. The general representation theorems of Liu [1983] and Wang [1970] for anisotropic and isotropic functions were consequently employed by [5], to describe the complete set of the constitutive equations under the hypotheses formulated above. Here we give such kind of the model.

The linear g_4-transversely isotropic elastic constitutive equation with five material parameters, in tensorial representation is written with respect to plastically deformed configuration, $\mathbf{K}_t$,

$$\begin{aligned} \frac{\Pi}{\tilde{\rho}} = \mathcal{E}(\Delta) \quad &\equiv \quad [a\Delta\mathbf{n}_1 \cdot \mathbf{n}_1 + c\mathrm{tr}\Delta](\mathbf{n}_1 \otimes \mathbf{n}_1) + (c\Delta\mathbf{n}_1 \cdot \mathbf{n}_1 + d\mathrm{tr}\Delta)\mathbf{I} + \\ &+ \quad e[(\mathbf{n}_1 \otimes \mathbf{n}_1)\Delta + \Delta(\mathbf{n}_1 \otimes \mathbf{n}_1)] + f\Delta \end{aligned}$$

The last representation is written in terms of the attached isotropic fourth order elastic tensor, $\widehat{\mathcal{E}}$, such that $\forall\, \mathbf{Q} \in Ort$. Here $\mathcal{E}$ is symmetric and positive definite.

The yield condition is generated via the formula (24) by the function f *orthotropic*, i.e. dependent on fourteen material constant (or scalar functions invariant relative to g_6), such that

$$\begin{aligned} f(\Sigma) \quad &:= \quad \hat{f}(\Sigma^s, \Sigma^a, (\mathbf{n}_1 \otimes \mathbf{n}_1), (\mathbf{n}_2 \otimes \mathbf{n}_2)) \equiv \\ &\equiv \quad \hat{\mathcal{M}}((\mathbf{n}_1 \otimes \mathbf{n}_1), (\mathbf{n}_2 \otimes \mathbf{n}_2))\Sigma \cdot \Sigma = \\ &= \quad C_1(\Sigma^s \cdot \mathbf{I})^2 + C_2\Sigma^s \cdot \Sigma^s + C_3(\Sigma^a)^2 \cdot \mathbf{I} + \\ &+ \quad C_4(\Sigma^s \cdot \mathbf{I})(\Sigma^s \cdot (\mathbf{n}_1 \otimes \mathbf{n}_1)) + C_5(\Sigma^s \cdot \mathbf{I})(\Sigma^s \cdot (\mathbf{n}_2 \otimes \mathbf{n}_2)) + \\ &+ \quad C_6\Sigma^s \cdot \{\Sigma^s(\mathbf{n}_1 \otimes \mathbf{n}_1)\}^s + C_7\Sigma^s \cdot \{\Sigma^s(\mathbf{n}_2 \otimes \mathbf{n}_2)\}^s + \\ &+ \quad C_8\Sigma^s \cdot \{(\mathbf{n}_1 \otimes \mathbf{n}_1)\Sigma^a\}^s + C_9\Sigma^s \cdot \{(\mathbf{n}_2 \otimes \mathbf{n}_2)\Sigma^a\}^s \\ &+ \quad C_{10}[\Sigma^s \cdot (\mathbf{n}_1 \otimes \mathbf{n}_1)]^2 + C_{11}[\Sigma^s \cdot (\mathbf{n}_2 \otimes \mathbf{n}_2)]^2 + \\ &+ \quad C_{12}[\Sigma^s \cdot (\mathbf{n}_1 \otimes \mathbf{n}_1)][\Sigma^s \cdot (\mathbf{n}_2 \otimes \mathbf{n}_2)] + C_{13}(\Sigma^a)^2 \cdot (\mathbf{n}_1 \otimes \mathbf{n}_1) + \\ &+ \quad C_{14}(\Sigma^a)^2 \cdot (\mathbf{n}_2 \otimes \mathbf{n}_2) \end{aligned} \tag{23}$$

REMARK 3. When we consider the symmetrical case, that corresponds to *small elastic strains*, i.e. when $\Sigma^s = \Pi$, $\Sigma^a = 0$ then the yield condition is given from (23) in which $C_3 = C_8 = C_9 = C_{13} = C_{14} = 0$.

The rate evolution equation for plastic deformation expressed by Mandel's nine- dimensional flow rule, i.e. there is a particular representation of the modified flow rule given in (8),

$$\dot{\mathbf{P}}\mathbf{P}^{-1} = \mu \partial_{\Sigma} \mathcal{F}(\Sigma, \alpha, \kappa)$$

is associated to the orthotropic yield function, generated by (23), which describe the proportional and kinematic hardening given by

$$\begin{aligned} &\mathcal{F}(\Sigma, \alpha, \kappa) \equiv f(\overline{\Sigma}, \kappa) - 1 \equiv \\ &\hat{\mathcal{M}}((\mathbf{n}_1 \otimes \mathbf{n}_1), (\mathbf{n}_2 \otimes \mathbf{n}_2), \kappa)\overline{\Sigma} \cdot \overline{\Sigma} - 1 = 0, \quad \overline{\Sigma} = \Sigma - \alpha. \end{aligned} \tag{24}$$

Here we put into evidence the possible dependence on κ of the yield function through the fourth order tensor $\mathcal{M}$.

We provide the constitutive relations for the plastic strain rate, $\mathbf{D}^p$, as well as for the plastic spin $\mathbf{W}^p$, defined by

$$\mathbf{D}^p = 1/2(\mathbf{L}^p + \mathbf{L}^{pT}), \quad \mathbf{W}^p = 1/2(\mathbf{L}^p - \mathbf{L}^{pT}), \quad \text{where} \quad \mathbf{L}^p = \dot{\mathbf{P}}\mathbf{P}^{-1}$$

For orthotropic material the plastic strain rate is given by

$$\mathbf{D}^p = \mu\, \hat{\mathbf{N}}^p(\Sigma, \alpha, \kappa, (\mathbf{n}_1 \otimes \mathbf{n}_1), (\mathbf{n}_2 \otimes \mathbf{n}_2))$$

with

$$\begin{aligned} \hat{\mathbf{N}}^p \;=\;& 2C_1(\overline{\Sigma}^s \cdot \mathbf{I})\mathbf{I} + 2C_2\overline{\Sigma}^s + C_4[(\overline{\Sigma}^s \cdot \mathbf{I})(\mathbf{n}_1 \otimes \mathbf{n}_1) + \\ +\;& (\overline{\Sigma}^s \cdot \mathbf{n}_1 \otimes \mathbf{n}_1)\mathbf{I}] + C_5[(\overline{\Sigma}^s \cdot \mathbf{I})(\mathbf{n}_2 \otimes \mathbf{n}_2) + (\overline{\Sigma}^s \cdot \mathbf{n}_2 \otimes \mathbf{n}_2)\mathbf{I}] + \\ +\;& 2C_6\{\overline{\Sigma}^s(\mathbf{n}_1 \otimes \mathbf{n}_1)\}^s + 2C_7\{\overline{\Sigma}^s(\mathbf{n}_2 \otimes \mathbf{n}_2)\}^s + \\ +\;& C_8\{(\mathbf{n}_1 \otimes \mathbf{n}_1)\overline{\Sigma}^a\}^s + C_9\{(\mathbf{n}_2 \otimes \mathbf{n}_2)\overline{\Sigma}^a\}^s + \\ +\;& 2C_{10}(\overline{\Sigma}^s \cdot (\mathbf{n}_1 \otimes \mathbf{n}_1))(\mathbf{n}_1 \otimes \mathbf{n}_1) + \\ +\;& 2C_{11}(\overline{\Sigma}^s \cdot (\mathbf{n}_2 \otimes \mathbf{n}_2))(\mathbf{n}_2 \otimes \mathbf{n}_2) + \\ +\;& 2C_{12}[(\overline{\Sigma} \cdot (\mathbf{n}_1 \otimes \mathbf{n}_1))(\mathbf{n}_2 \otimes \mathbf{n}_2) + (\overline{\Sigma} \cdot (\mathbf{n}_2 \otimes \mathbf{n}_2))(\mathbf{n}_1 \otimes \mathbf{n}_1)] \end{aligned} \tag{25}$$

and the plastic spin is expressed under the form

$$\begin{aligned} \mathbf{W}^p \;&= \mu\, \hat{\Omega}^p(\Sigma, \alpha, \kappa, \mathbf{n}_1 \otimes \mathbf{n}_1, \mathbf{n}_2 \otimes \mathbf{n}_2) \quad \text{with} \\ \hat{\Omega}^p \;&= -2C_3\overline{\Sigma}^a + C_8\{(\mathbf{n}_1 \otimes \mathbf{n}_1)\overline{\Sigma}^s\}^a + C_9\{(\mathbf{n}_2 \otimes \mathbf{n}_2)\overline{\Sigma}^s\}^a - \\ &-2C_{13}\{\overline{\Sigma}^a(\mathbf{n}_1 \otimes \mathbf{n}_1)\}^a - 2C_{14}\{\overline{\Sigma}^a(\mathbf{n}_2 \otimes \mathbf{n}_2)\}^a \end{aligned} \tag{26}$$

REMARK 4. $\mathbf{W}^p$ involves the terms generated by the symmetric part of $\overline{\Sigma}$, while $\mathbf{D}^p$ contains terms generated by the skew- symmetric part of $\overline{\Sigma}$, with two coupling coefficients C_8, C_9.

REMARK 5. In the case of $\overline{\Sigma} \in Sym$, i.e. for *small elastic strains* and $\alpha \in Sym$, directly from (26) we derive the following expression for *orthotropic plastic spin*

$$\mathbf{W}^p = \mu\, \Omega^p = \mu\, \{C_8\{(\mathbf{n}_1 \otimes \mathbf{n}_1)\overline{\Sigma}^s\}^a + C_9\{(\mathbf{n}_2 \otimes \mathbf{n}_2)\overline{\Sigma}^s\}^a\} \tag{27}$$

But in this case, the yield condition (23) does not depend on the parameters which enter the expression (27) of the plastic spin.

PROPOSITION 3. *From the orthotropic Mandel's flow rule (26) the flow rule characterizing the g_4- transversely isotropic material is derived when $C_5 = C_7 = C_9 = C_{11} = C_{12} = 0$, i.e. dependent on six material constants. The plastic spin is given by (25), in which $C_9 = C_{14} = 0$, i.e. dependent on three constant only.*

Evolution equation for internal variable can be described, see [6], by some new generalization to finite deformation of Armstrong- Frederick hardening rule.

From the orthotrop representation g_4- transversely isotropic case only can be obtained. Thus for plastically *incompressible* material, i.e. $\tilde{\rho} = \rho_0$, the representatio from [21] can be obtained by taking into account small deformation theory. The fibre-inextensible case given in [22] can be also derived from our general representation, when the appropriate yield constant is much grater then the others.

References

[1] CLEJA-ŢIGOIU S. AND SOÓS E., *Elastoplastic models with relaxed configurations and internal state variables*, Appl. Mech. Rev. **43** (1990), 131–151.

[2] CLEJA-ŢIGOIU S., *Large elasto-plastic deformations of materials with relaxed configura tions. I. Constitutive assumptions. II. Role of the complementary plastic factor*, Int. J. Eng. Sci. **28** (1990), 171–180, 273–284.

[3] CLEJA-ŢIGOIU S., *Material symmetry of elastoplastic materials with relaxed configurations*, Rev. Roum. Math. Pures Appl. **34** (1989), 513–521.

[4] CLEJA-ŢIGOIU S., *Bifurcations of homogeneous deformations of the bar in finite elastoplasticity*, Eur. J. Mech. A, Solids **34** (1986),761–786.

[5] CLEJA-ŢIGOIU S., *Nonlinear elasto-plastic deformations of transversely isotropic materials and plastic spin*, Int. J. Engng. Sci. **38** (2000), 737–763.

[6] CLEJA-ŢIGOIU S., *Orthotropic $\Sigma-$ models in finite elasto-plasticy*, Rev. Roumaine Math. Pures Appl. **45** (2000), 219–227.

[7] CLEJA-ŢIGOIU S., *Some remarks on dissipation postulate in anisotropic finite elastoplasticity*, Technische Mechanik **20** (2000), 183–193.

[8] CLEJA-ŢIGOIU S. AND MAUGIN G.A., *Eshelby's stress tensors in finite elastoplasticity*, Acta Mech. **139** (2000), 231–249.

[9] CLEJA-ŢIGOIU S., *Consequences of the dissipative restrictions in finite anisotropic elastoplasticity*, Int. J. Plasticity, submitted.

[10] HALPHEN B. AND NGUYEN Q.S., *Sur les matériaux standards généralisés*, J. de Mécanique **14** (1975), 39–63.

[11] HILL R., *A general theory of uniqueness and stability in elastic- plastic solids*, J. Mech. Phys. Solids **6** (1958), 236–248.

[12] I-SHIH LIU, *On the representations of anisotropic invariants*, Int. J. Engng. Sci. **40** (1982), 1099–1109.

[13] LUBLINER J., *Normality rules in large-deformation plasticity* Mech. Mat. **5** (1986), 29–34.

[14] LUCCHESI M. AND PODIO-GUIDUGLI P., *Materials with elastic range. A theory with a view toward applications, Part II*, Arch. Rat. Mech. Anal. **110** (1990), 9–42.

[15] MANDEL J., *Plasticité classique et viscoplasticité*, CISM- Udine, Springer-Verlag, New-York 1972.

[16] MARIGO J.J., *Constitutive relations in plasticity, damage and fracture mechanics based on a work property*, Nuclear Eng.and Design **114** (1989), 249–272.

[17] MAUGIN G.A., *Eshelby stress in elastoplasticity and fracture*, Int. J. Plasticity **10** (1994), 393–408.

[18] MOREAU J.J., *Fonctionnelle convexes*, Séminaire J. Lerray, Collége de France, Paris 1966.

[19] NGUYEN Q.S:, *Some Remarks on Plastic Bifurcation*, Eur. J. Mech. A, Solids **13** (1994), 485–500.

[20] NIGAM H., DVORAK G.J. AND BAHEI-EL-DIN,*An experimental investigation of elastic-plastic behavior of a fibrous boron- aluminium composite: I. Matrix- dominant mode; II. Fiber-dominant mode*, Int. J. Plasticity **10** (1994), 23–48, 49–62.

[21] ROGERS T.G., *Plasticity of fibre-reinforced materials*, in: "Continuum model in discret system" (Ed. G.A. Maugin), Vol.1, Longman 1990, 87–102.

[22] SPENCER A.J.M., *Kinematic constraints, constitutive equations and failure rules for anisotropic materials*, in: "Applications of tensor functions in solid mechanics" (Ed. J.P. Boehler), CISM Courses and Lecture Notes **292**, Springer 1987, 187–201.

[23] SPENCER A.J.M., *Plasticity theory for fibre-reinforced composites*, J. Eng. Math. **29** (1992), 107–118.

[24] SRINIVASA A.R., *On the nature of the response functions in rate-independent plasticity*, Int. J. Non-Linear Mech. **32** (1997), 103–119.

[25] TRUESDELL C. AND NOLL W., *The non-linear field theory of mechanics*, in: "Handbuch der Phys., III/3", (Ed. Flüge), Springer, Berlin - Göttingen - Heidelgerg 1965.

[26] VOGLER T.J., HSU S.Y. AND KYRIAKIDES S., *Composite failure under combined compression and shear*. Int. J. Solids Struct. **37** (2000), 1765–1791.

AMS Subject Classification: 74C15.

Sanda CLEJA-ŢIGOIU
Faculty of Mathematics
University of Bucharest
Str. Academiei 14
70109 Bucharest, ROMANIA
e-mail: `tigoiu@math.math.unibuc.ro`

Rend. Sem. Mat. Univ. Pol. Torino
Vol. 58, 1 (2000)
Geom., Cont. and Micros., I

J. Engelbrecht - M. Vendelin*

MICROSTRUCTURE DESCRIBED BY HIERARCHICAL INTERNAL VARIABLES

Abstract. In this paper a clear distinction is made between the different scales and the different processes in the microstructure which influence the dynamics at the macrolevel. In the first case the governing equation for wave propagation is represented by a hierarchy of waves. In the second case it has been shown, how useful the concept of internal variables is. The different processes can be best described by a hierarchy of internal variables. An example of cardiac muscle contraction is briefly described, demonstrating the dependence of the active stress on sliding the molecules and ion concentration involving the corresponding internal variables.

1. Introduction

Continuum mechanics is usually based on macroscopic concepts and quantities, such as energy density, stress, strain, etc. However, materials (whatever their origin is) have usually a microstructure because of inhomogeneities, pores, embedded layers, reinforcements, etc.. This list can be prolonged but one is clear - the description of the behaviour of many materials should take into account both the macroscopic and microscopic properties, occuring at different length scales and involving different physical effects. Within the framework of continuum mechanics, such a behaviour is best described by distinguishing macro stresses and microstresses with interactive microforces ([1], [2]). We feel however, that for materials with complicated properties indicated above, one should start distinguishing clearly the observable and internal variables ([10], [13]). Although the formalism of internal variables is well known ([10], [13]), for the clarity sake we repeat here some basic concepts.

The observable variables are the usual macroscopic field quantities such as elastic strain, for example. These variables are governed by conservation laws and possess inertia. The internal structure of the material (body, tissue, composite, etc.) is supposed to be described by internal variables which are not observable and do not possess inertia. They should compensate our lack of knowledge of the precise description of the microstructure. The formalism of internal variables involves constructing of a dissipation potential $\mathcal{D}$ in parallel to the Lagrangian $\mathcal{L}$ for the observable variable. However, the governing equations of internal variables are kinetic equations (not hyperbolic) – see [10], [13].

The idea of using internal variables for describing dynamical processes in microstructured materials has earlier been presented in [12], [4]. The problems become more complicated when either the scales or possible processes in materials are different and form a certain hierarchy. This brings us directly to the idea of hierarchical internal variables that certainly need generalization

*This study is supported by the Estonian Science Foundation. J.E. would like to thank Department of Mathematics, University of Turin, for the financial support to attend the 4 th International seminar "Geometry, Continua & Microstructure" where the ideas of this paper were discussed.

of the existing formalism. An example and main concepts of hierarchical internal variables are given in [6], here a certain systematic approach is presented following by an example.

In Section 2 basic ideas of modelling are briefly described. The description involves continuum mechanics, internal variables and evolution equations - all needed for further presentation. More detailed description can, for example, be found in [3]. Section 3 presents the central ideology of this paper. It makes clear distinction between different scales and different processes in the microstructure. In the first case the result is a wave hierarchy, in the second case - a hierarchy of internal variables. In Section 4 an example is presented, illustrating the hierarchical internal variables. The case study is based on the contraction of the cardiac muscle depending on the cell energetics. Last Section 5 includes conclusions and open problems.

2. Basic modelling

2.1. Continuum mechanics

To be brief, we refer to [1], [2] for basic concepts for microstructured solids. For a body $\mathcal{B} \subset \Re^3$ with microstructure, an added field δ describes the mechanical characteristics of the microstructure. The stress fields can be introduced after the definition of the expended power in arbitrary processes [9], including a macroscopic (gross structure) stress and force, a microscopic (fine structure) stress and force, and an interaction force between the macro- and microstructures. In [2], this approach has been extended to include different microstructures at their characteristic scales. Then for arbitrary region $\mathcal{W}$ in $\Re^3$ with outward unit normal $\mathbf{m}$ we have for the actual power $\Pi_0(\mathcal{W})$:

$$\Pi_0(\mathcal{W}) = \int_{\partial\mathcal{W}} \mathbf{T}_g\mathbf{m}\cdot\mathbf{v}da + \int_{\mathcal{W}} \mathbf{f}_g\cdot\mathbf{v}dv + \Pi_{micro,1}(\mathcal{W}).$$

Here $\mathbf{v}$ is the velocity, $\mathbf{T}_g$ is the macroscopic stress, and $\mathbf{f}_g$ is the macroscopic body force. Note that indexing has here and below been changed compared with [2]. The field $\Pi_{micro,1}(\mathcal{W})$ is the power expended by the microstructure. Further, the difference from the general theory [9] involves a sequence of microscopic processes $\mathbf{d}_k, k = 2, 3, ...$ Now, we can magnify a small region of $\mathcal{W}$ iteratively by magnifications λ^k. At the first stage

$$\Pi_{micro,1}(\mathcal{W}) = \int_{\partial\mathcal{W}_1} \mathbf{T}_1\mathbf{m}\cdot\mathbf{v_1}da + \int_{\mathcal{W}_1} \mathbf{f}_1\cdot\mathbf{v}_1dv + \Pi_{micro,2}(\mathcal{W}).$$

where $\mathbf{v_1} = \lambda\mathbf{v} + \dot{\mathbf{d}}_1$ and $\mathbf{T}_1$ is the microscopic stress at this level. Further on,

$$\Pi_{micro,2}(\mathcal{W}) = \int_{\partial\mathcal{W}_2} \mathbf{T}_2\mathbf{m}\cdot\mathbf{v_2}da + \int_{\mathcal{W}_2} \mathbf{f}_2\cdot\mathbf{v}_2dv + \Pi_{micro,3}(\mathcal{W}),$$

etc. (for details, see [2]. The general balance laws can now easily be rewritten in the referential form.

2.2. Internal variables

The formalism of internal variables is presented in [10], [13]. Here we need point out just essentials for further analysis in Section 3. The behaviour of a system, i.e. dynamic state of a body involves description of observable state variables χ (e.g. elastic strain and particle velocity) and a certain number of internal variables α. The dependent variable(s) (e.g. the stress) must be simultaneously a function of both

$$\sigma = \sigma(\chi, \alpha)$$

which must be complemented by a governing equation for α:

$$\dot{\alpha} = f(\chi, \alpha) + g(\chi, \alpha)\dot{\chi}. \tag{1}$$

It is assumed that the strain ϵ is split up in an elastic part ϵ^e and an "anelastic" part ϵ^p:

$$\epsilon = \epsilon^e + \epsilon^p.$$

The free energy function ψ is assumed to be

$$\psi = \psi(\epsilon^e, T; \alpha, \nabla\alpha)$$

where T is temperature. The equations of motion are then easily derived. In addition, we need to concretize Eq (1). For that, a dissipation potential $\mathcal{D}$ is postulated

$$\mathcal{D} = \mathcal{D}(\sigma, \dot{\alpha}, \epsilon^e, T, \alpha, \nabla\alpha) > 0$$

possessing certain properties [10]. Then the governing Eq (1) for α is derived as

$$\frac{\delta\psi}{\delta\alpha} + \frac{\partial\mathcal{D}}{\partial\dot{\alpha}} = 0.$$

As a rule, this equation is not hyperbolic.

2.3. Mathematical models

It is clear that mathematical models involving both observable and internal variables are of the mixed (e.g. inertial-diffusive [10]) type. The general ideas for asymptotic analysis of such systems are presented in [4], [5]. To get an idea, the simplest 1D case could be described. Let an n-vector $\mathbf{U}$ be the vector of the observable variables, a scalar w – the internal variable and $X_1 = X$. Then the governing system is of the following form

$$I\frac{\partial\mathbf{U}}{\partial t} + A_1\frac{\partial\mathbf{U}}{\partial X} + \epsilon B_{11}\frac{\partial^2\mathbf{U}}{\partial t\partial X} + h.o.t = \mathbf{H}(\mathbf{U}, w) \tag{2}$$

$$\frac{\partial w}{\partial t} + d_{11}\frac{\partial^2 w}{\partial X^2} + h.o.t = p(\mathbf{U}, w) \tag{3}$$

where I is a unit matrix, $A_1(\mathbf{U}, X)$, $B_{11}(\mathbf{U}, X)$ are the matrices of parameters, $\mathbf{H}(\mathbf{U}, w)$ and $p(\mathbf{U}, w)$ are the coupling vector and function, respectively, d_{11} is a constant and ϵ a small parameter while h.o.t stands for higher order terms (derivatives).

It is proposed [4], [5] to use conventional asymptotic approach for deriving the evolution equation(s) for system (2), (3) (see [3]).

3. Types of models

Depending on the different length and time scales, the asymptotic governing equations derived along the ideas of Section 2, may have different character. Nevertheless, it is possible to distinguish between the two types of governing equations.

The *first type* is based on structural hierarchy of a material (body) and strong dependence on length scales within the material and of the excitation which are the leading factors. The simplest example is just a material where macro- and microstructure are described by their own balance laws [1], [9]. It means that the dynamic behaviour of the constituents is basically similar and differs in parameters.

The *second type* is based on process hierarchy in a material (body) where at various levels various dynamical processes are of importance, all influencing the macrobehaviour. This is an example of the cardiac muscle [6] and characterized best by internal variables that form a hierarchy.

Below both types are briefly characterized.

3.1. Structural hierarchy and hierarchy of waves.

Many materials possess microstructure at various scales. On the other hand, it is widely known that dissipation and dispersion is different for various frequency scales. Hence, given the initial excitation with a fixed frequency (wavelength), the response of the material depends actually on a certain underlying microstructure which is responsible for the governing physical effects. Actually, this could be just a case of macro- and microstructure, or then a case of several microstructures. The outcome, i.e. the governing equation should certainly reflect this possible choice emphasized by certain input-dependent parameters. One could intuitively address the problem asking a question, which material properties are more important: those characteristic to the macrostructure or those characteristic to the microstructure of a certain level. It is clear that a single governing equation should have a certain hierarchy embedded into it.

Wave hierarchies are analysed by Whitham [15], showing the hierarchy of just two orders. A case, demonstrating the wave hierarchy in dissipative solids, is analysed in [4]. For a dissipative microstructured solids where dissipation rates are different for macro- and microstructure, the final linearized governing equation in the dimensionless form is the following:

$$\frac{\partial}{\partial \xi}\left(\frac{\partial u}{\partial \tau} - K_1 \frac{\partial^2 u}{\partial \xi^2}\right) + \lambda^2 \left(L\frac{\partial u}{\partial \tau} + M\frac{\partial u}{\partial \xi} - K_2 \frac{\partial^2 u}{\partial \xi^2}\right) = 0. \tag{4}$$

where u stands for the displacement gradient, τ and ξ are the moving coordinates, K_1, K_2, L, N are the constants and λ is the input-depending scale parameter. Equation (4) is derived from the conventional equations of motion in the reference form by using the asymptotic (reductive perturbative) method (see, for example [3]). For λ small, the influence of the microstructure may be neglected and dissipation is governed by the constant K_1, for λ large, the dissipation is governed by microstructural properties, i.e. by K_2, while $K_1 \neq K_2$.

Waves in dispersive solids (granular materials) where dissipation is neglected are analysed in [7]. In this case for scaled density fluctuation w the governing equation is

$$\frac{\partial^2}{\partial \xi^2}\left(\frac{\partial w}{\partial \tau} + w\frac{\partial w}{\partial \xi} + N_1 \frac{\partial^3 w}{\partial \xi^3}\right) + \mu \left(\frac{\partial w}{\partial \tau} + w\frac{\partial w}{\partial \xi} + N_2 \frac{\partial^3 w}{\partial \xi^3}\right) = 0. \tag{5}$$

where N_1, N_2, μ are the coefficients. Contrary to the case (3.1), here dispersion is important and (5) represents actually a hierarchy of the Korteweg-de Vries equations. Intuitively, denoting by π an operator for the Burger's-type (dissipative) materials, Korteweg-de Vries-type (dispersive) materials, or both, the hierarchy of waves could be represented by

$$\sum_m \epsilon_m \frac{\partial^n}{\partial \xi^n} \pi_m = 0$$

where π_m denotes the operator for m-th scale and ϵ_m – a corresponding small parameter, if any. Hence, π_0 denotes the wave operator in the highest, i.e. in the macrolevel (c.f. Section 2.1). The order of derivatives $n(m)$ represents the order of coupling between various effects. As a conjecture, one could propose that dispersive effects are characterized by n = 2,4,... and dissipative effects – by n = 1,3,... (c.f. Eqs (4) and (5)).

3.2. Process hierarchy and hierarchical internal variables.

Beside the different scales, the embedded microstructures are sometimes characterized by completely different physical processes going on simultaneously. As said before, such processes are internal and governed by internal variables [10], [13]. If now these processes are linked to the macrobehaviour by a certain hierarchy then the corresponding internal variables form also a hierarchy. We use then notion of hierarchical internal variables [6].

In general terms, the idea of building up the mathematical model is the following [6]:
1) a constitutive equation for a dependent variable, say σ (i.e. stress, for example), depends on observable variable χ and the *first-level* internal variable α

$$\sigma = \sigma(\chi, \alpha);$$

2) the evolution law for α is

$$\dot{\alpha} = f(\chi, \alpha, \beta), \tag{6}$$

where β is the next, *second-level* internal variable influencing σ only through dynamics of the first-level internal variable α;
3) the evolution law for β is

$$\dot{\beta} = g(\chi, \alpha, \beta, \gamma), \tag{7}$$

where γ is again the next, now the *third-level* internal variable, influencing σ only through dynamics of the second level internal variable β;
4) the evolution law for γ is

$$\dot{\gamma} = h(\chi, \alpha, \beta, \gamma, ...), \tag{8}$$

etc.

Internal variables $\alpha, \beta, \gamma, ...$ form a hierarchy reflecting the hierarchical processes in the material.

Consequently, the mathematical model of the macrobehaviour is governed by a system including several equations that can be of the various types. Note, however, that Eqs. (6), (7), (8) could also include gradients and then at least the governing system is composed by partial differential equation.

4. Example: cardiac muscle contraction

Here we refer to the fundamental treatises on cardiac performance [8], [16]. In terms of continuum mechanics, ventricles are thick-walled shells made of anisotropic fibres. These fibres have complicated microstructure and act as following. The muscle fibres are made up by the bunches of smaller elements called myofibrils with a surrounding sarcotubular system. The main task of myofibrils is to convert metabolic energy into mechanical energy while the surrounding sarcotubular system governs the behaviour of Ca^{2+} ions needed for activation. In sense of continuum mechanics, these processes include the internal variables compared to the observable macrovariables like strain. The stress in the muscle is the dependent variable and its constitutive law is linked to the observable variable and then the hierarchy of internal variables. Leaving aside the details of this extremely fascinating mechanism (the reader is referred to [6], [14]), we concentrate here on the description of the mathematical model.

We assume, that the total (Cauchy) stress in the muscle can be split up into two parts

$$\boldsymbol{\sigma} = \boldsymbol{\sigma}_p + \boldsymbol{\sigma}_a,$$

where $\boldsymbol{\sigma}_p$ and $\boldsymbol{\sigma}_a$ denote passive and active stress, respectively. The passive stress results from the elastic deformation of the tissue and can be calculated traditionally like

$$\boldsymbol{\sigma}_p = \frac{\partial \psi}{\partial \boldsymbol{\epsilon}^e},$$

where ψ is the free energy and $\boldsymbol{\epsilon}^e$ is the strain. Given ψ, the passive stress is easily calculated. The active stress σ_a is generated in myofibrils by activation and is directed parallel to the fibre orientation. Hence

$$\boldsymbol{\sigma}_a = \sigma_a \boldsymbol{\epsilon}_1 \boldsymbol{\epsilon}_1,$$

where ϵ_1 is the unit vector showing the orientation. Now the complicated mechanism producing active stress needs the more detailed description of the sequence of internal variables, which are the main actors. At this structural level, myofibrils are the starting point. A myofibril is composed of repeating units of myosin and actin filaments, called sarcomeres. The actin filament is made of a double helix of actin molecules with troponin molecules localized in certain intervals. The myosin filament consists of myosin proteins with certain spatially localized meromyosin molecules with heads resembling "golf-clubs". These heads are called cross-bridges. The excitation of a muscle is triggered by an action potential from the conducting system. This potential in its turn releases Ca^{2+} ions in the sarcotubular system which then activate the troponin molecules so that they will be able to attach the heads of myosin molecules. This attaching means swivelling of myosin molecules that cause sliding the actin and myosin filaments against each other. As a result, active stress is created.

The mechanism briefly described above (for details see [6], [14] and the references therein) needs to be cast into a mathematical model.

We start here from the macrolevel down. The force on actin molecules (along the actin filament) depends on the distance z between an attached cross-bridge and the nearest actin site. There are two states through the cycle, producing force. Denoting them by A and B, we may calculate the corresponding forces by

$$F_A = K_A\, z, \qquad F_B = K_B\, z$$

where $K_A,\ K_B$ are elastic constants. Further we take $K_A = K_B = K$. The total force over a sarcomere of the length l_s depends on the number of crossbridges between z and $z - dz$ in both states. We take the uniform distribution of crossbridges in z over an internal d. The active stress is then found by

$$\sigma_a = \frac{ml_s K}{2d}\left(\int_{-d/2}^{d/2} n_A(z)dz + \int_{-d/2}^{d/2} n_B(z)dz\right)$$

where m is the number of cross-bridges per unit volume and $n_A(z), n_B(z)$ are relative amounts of cross-bridges producing force (i.e. being in states A and B). These variables, n_A and n_B are nothing else than the *first-level internal variables*. They (c.f. Section 3.2) are governed by the following kinetic equations

$$\frac{\partial n_A}{\partial t} + w\frac{\partial n_A}{\partial z} = f_1 n_C + g_2 n_B - (g_1 + f_2)n_A,$$

$$\frac{\partial n_B}{\partial t} + w\frac{\partial n_B}{\partial z} = f_1 n_A - (g_2 + f_3)n_B,$$

where w is the velocity of lengthening, f_1, f_2, f_3, g_1, g_2 are kinetic constants between the states and n_C is the amount of cross-bridges that does not produce force. Clearly, the summation of all activated cross-bridges gives

$$A = n_A + n_B + n_C.$$

Now, A is the next, i.e. the *second-level internal variable*, the changes of which affects the variable σ_a only over n_A, n_B. The internal variable A (the activation parameter) has its own kinetic equation

$$\frac{dA}{dt} = c_1(l_s)[Ca^{2+}](1 - A) - c_2(l_s)A, \tag{9}$$

with $c_1(l_s), c_2(l_s)$ as certain parameters. Equation (9) involves the *third-level internal variable* $[Ca^{2+}]$ which must be governed by its own kinetic equation

$$\frac{d[Ca^{2+}]}{dt} = f([Ca^{2+}]).$$

In practice, the last equation is usually replaced by the approximation of experimental curves.

So, in this case the variable σ_a is influenced by three levels of internal variables that form a hierarchy.

The calculations of contraction are performed by using this model and FEM for the idealized spheroidal left ventricle and will be published elsewhere.

5. Discussion

As explained in Section 3 and demonstrated in Section 4, hierarchies of the internal structure of a material (body, tissue) lead to certain hierarchies in mathematical models. These hierarchies can be either the hierarchy of waves in the Whitham's sense [15] or the hierarchy of internal variables. Both cases need actually more detailed analysis. The models are complicated that is why in order to get practical results, numerical simulation must be used. However, there are many open questions also from the theoretical viewpoint.

For example, the question on dispersive properties embedded into the hierarchy of waves must be analysed. It is known that higher-order dispersion terms are the same in the wave hierarchy ((3.2) in [7]) and in the governing equation obtained by a direct asymptotic derivation [11].

This certainly shows the correctness in leading terms but the properties of the wave hierarchy are not clear.

For hierarchical internal variables the line of questions seems to be longer. The extra entropy flux **k** in the formalism of internal variables [10], [13] depends then also on internal variables in a certain sequence that must be analysed. Open is the question, how to construct dissipative potentials $\mathcal{D}_\alpha, \mathcal{D}_\beta, \mathcal{D}_\gamma, \ldots$ corresponding to the each level of internal variables. It seems, that a more detailed formalism of internal variables might cast light over the formation of dissipative structures.

References

[1] CAPRIZ G., *Continua with microstructure*, Springer, New York 1989.

[2] CERMELLI P. AND PASTRONE F., *Influence of a dissipative microstructure on wave propagation*, in: "Nonlinear waves in solids", (Eds. J.L. Wegner and F.R. Norwood), ASME Book **137** 1995, 279–284.

[3] ENGELBRECHT J., *Nonlinear wave dynamics: complexity and simplicity*, 1997.

[4] ENGELBRECHT J., CERMELLI P. AND PASTRONE F., *Wave hierarchy in microstructured solids*, in: "Geometry, continua and microstructure" (Ed. G.A. Maugin), Hermann Publ., Paris 1999, 99–111.

[5] ENGELBRECHT J. AND MAUGIN G.A., *Deformation waves in thermoelastic media and the concept of internal variables*, Arch. Appl. Mech. **66** (1996), 200–207.

[6] ENGELBRECHT J., VENDELIN M. AND MAUGIN G.A., *Hierarchical internal variables reflecting microstructural properties: application to cardiac muscle contraction*, J. Non-Equilib. Thermodyn. **25** (2000), 119–130.

[7] GIOVINE P. AND OLIVERI F., *Dynamics and wave propagation in dilatant granular materials*, Meccanica **30** (1995), 341–357.

[8] GLASS L., HUNTER .P, AND MCCULLOCH A., *Theory of heart. Biomechanics, biophysics, and nonlinear dynamics of cardiac function*, Springer, New York 1991.

[9] GURTIN M.E. AND PODIO-GUIDUGLI P., *On the formulation of mechanical balance laws for structured continua*, ZAMP **43** (1992), 181–190.

[10] MAUGIN G.A., *Internal variables and dissipative structures*, J. Non-Equilib. Thermodyn. **15** (1990), 173–192.

[11] MAUGIN G.A., *On some generalizations of Boussinesq and KdV systems*, Proc. Estonian Acad. Sci. Phys. Math. **44** (1995), 40–55.

[12] MAUGIN G.A. AND ENGELBRECHT J., *A thermodynamical viewpoint on nerve pulse dynamics*, Proc. Estonian Acad. Sci. Phys. Math. **19** (1994), 9–23.

[13] MAUGIN G.A. AND MUSCHIK W., *Thermodynamics with internal variables*, Ibid **19** (1994), 217–249 (part I), 250–289 (part II).

[14] VENDELIN M., BOVENDEERD P.H.M., ARTS T., ENGELBRECHT J. AND VAN CAMPEN D.H., *Cardiac mechanoenergetics replicated by cross-bridge model*, Annals Biomed. Eng. **28** 6 (2000), 629–640.

[15] WHITHAM G.B., *Linear and nonlinear waves*, J. Wiley, New York 1974.

[16] ZIPES D.P. AND JALIFE J., *Cardiac electrophysiology: from cell to bedside*, Saunders, Philadelphia 1995.

AMS Subject Classification: 35Q53, 74J30, 92C05.

Jüri ENGELBRECHT, Marko VENDELIN
Centre for Nonlinear Studies, Institute of Cybernetics
Tallinn Technical University
Akadeemia tee 21
12618 Tallinn, ESTONIA
e-mail: `je@ioc.ee`

Rend. Sem. Mat. Univ. Pol. Torino
Vol. 58, 1 (2000)
Geom., Cont. and Micros., I

M. Epstein*

ARE CONTINUOUS DISTRIBUTIONS OF INHOMOGENEITIES IN LIQUID CRYSTALS POSSIBLE?

Abstract. Within a theory of liquid-crystals-like materials based on a generalized Cosserat-type formulation, it is shown that continuous distributions of inhomogeneities may exist at the microstructural level.

1. Introduction

In the conventional theories of liquid crystals, the free-energy density is assumed to be a function of a *spatial* vector field and its spatial gradient. Starting from the pioneering work of Frank [6], various improvements were proposed by Leslie [9] and by Ericksen [4] [5]. A different point of view was advocated by Lee and Eringen [7] [8], as early as 1972, when considering a liquid criystal within the framework of the theory of materials with internal structure. The main difference between these points of view is that the second approach emphasizes the dependence of the constitutive equations on the *mappings* between vectors or tensor fields, rather than on their values alone. This mapping-dependence is essential not only for sustaining continuous distributions of inhomogeneities, but also, as shown by Maugin and Trimarco [10], for the proper setting of a definition of Eshelby stresses. The general connection between these two aspects of material behaviour is described in [3].

2. The generalized Cosserat medium

A *generalized Cosserat body* (GCB) consists of the frame bundle of an ordinary body $\mathcal{B}$. In other words, a GCB is a body plus the collection of all its local frames at each point. Denoting by X^I $(I = 1, 2, 3)$ and x^i $(i = 1, 2, 3)$ Cartesian coordinate systems for the body $\mathcal{B}$ and for physical space, respectively, a configuration of a GCB consists of the twelve independent functions:

$$x^i = x^i(X^J)$$
$$H^i{}_I = H^i{}_I(X^J)$$

where H^i_I represents the mapping of the frames attached at point X^J. It is important to stress that the ordinary deformation gradient $F^i_I = \frac{\partial x^i}{\partial X^I}$ and the mapping H^i_I are of the same nature, but represent two independent vector-dragging mechanisms.

A GCB is *hyperelastic* of the first grade if its material response can be completely characterized by a single scalar ("strain-energy") function:

$$W = W(F^i{}_I, H^i{}_I, H^i{}_{I,J}; X^K)$$

*Partially supported by the Natural Sciences and Engineering Research Council of Canada, and DGI-CYT (Spain) (Project PB97-1257).

where comma subscripts denote partial derivatives. Under a change of reference configuration of the form

$$Y^A = Y^A(X^J)$$
$$H^A{}_I = H^A{}_I(X^J)$$

where the indices A, B, C are used for the new reference, the energy function changes to:

$$\begin{aligned} W &= W'(F^i{}_A, H^i{}_A, H^i{}_{A,B}; Y^C) \\ &= W(F^i{}_A F^A{}_I, H^i{}_A H^A{}_I, H^i{}_{A,B} F^B{}_J H^A{}_I + H^i{}_A H^A{}_{I,J}; X^K(Y^C)) \end{aligned} \tag{1}$$

Notice the special form of the composition law for the derivatives of H^i_I.

Generalizing Noll's idea of uniformity [11], by taking into account the composition laws in Equation (1), one can show [1] [2] that in terms of an archetypal energy function

$$W_c = W_c(F^i{}_\alpha, H^i{}_\alpha, H^i{}_{\alpha\beta})$$

where Greek indices are used for the archetype, a GCB is *uniform* (namely, it is made of "the same material" at all points) if there exist three uniformity fields of tensors $P^I{}_\alpha(X^J)$, $Q^I{}_\alpha(X^J)$ and $R^I{}_{\alpha\beta}(X^J)$ such that the equation

$$W(F^i{}_I, H^i{}_I, H^i{}_{I,J}; X^K) = W_c(F^i{}_I P^I{}_\alpha, H^i{}_I Q^I{}_\alpha, H^i{}_{I,J} P^J{}_\beta Q^I{}_\alpha + H^i{}_I R^I{}_{\alpha\beta})$$

is satisfied identically for all non-singular $F^i{}_I$ and $H^i{}_I$ and for all $H^i{}_{I,J}$. *Homogeneity* (global or local) follows if, and only if, there exists a (global or local) reference configuration such that these fields become trivial.

3. The liquid-crystal-like model

We call a *liquid-crystal-like model* (LCM) a material whose internal structure can be represented by the deformation of one or more vector or tensor fields. More specifically, we say that a GCB is of the LCM type if a nowhere-zero material vector field $\mathbf{D} = D^I \mathbf{E}_I$ and a material tensor field $\mathbf{A} = A^I{}_J \mathbf{E}_I \otimes \mathbf{E}^J$ exist such that the energy density function depends on its arguments in the following way:

$$W = W(F^i{}_I, H^i{}_I, H^i{}_{I,J}; X^K) = f(F^i{}_I, H^i{}_I D^I, H^i{}_{I,J} D^I + H^i{}_I A^I{}_J; X^K) \tag{2}$$

where we have used the letter f to denote the new functional dependence.

To clarify the rationale behind this definition, we consider first the particular case of a reference configuration in which $\mathbf{D}(\mathbf{X})$ constitutes a parallel unit vector field and $\mathbf{A}(\mathbf{X})$ vanishes identically. We can then write (for that particular reference configuration, if it exists) that

$$W = f(F^i{}_I, H^i{}_I D^I, (H^i{}_I D^I)_{,J}; X^K)$$

This constitutive equation is unable to detect any difference between different deformations of triads that happen to map the director into the same vector in space. In other words, all that matters is the resulting vector and its gradient, just as in the "conventional" theory of liquid crystals, and it is in this sense that Equation (2) constitutes a generalization. More importantly, when seen under this light, the tensor $\mathbf{A}$ no longer appears as an artificial construct, but as the natural outcome of describing the manner in which the conventional archetype has been inserted in the body in a pointwise fashion.

It is apparent that the particular form of the constitutive law adopted for an LCM must entail certain *minimal symmetries*, namely, certain local changes of reference configuration that are indistinguishable as far as the material response is concerned. In addition, an LCM may have other non-generic symmetries, but here we are interested in deriving those symmetries that are already inherent in the definition. Now, any symmetry of a GCB consists of a triple $\{G, K, L\}$ satisfying:

$$f(F^i{}_J, H^i{}_J D^J, H^i{}_{M,N} D^M + H^i{}_M A^M{}_N; X^K) =$$
$$f(F^i{}_I G^I{}_J, H^i{}_I K^I{}_J D^J, (H^i{}_{I,J} G^J{}_N K^I{}_M + H^i{}_I L^I{}_{MN}) D^M + H^i{}_I K^I{}_M A^M{}_N; X^K)$$

for all non-singular $F^i{}_I$ and $H^i{}_I$ and for all $H^i{}_{I,J}$. Since we are looking for minimal symmetries, namely, those stemming from the particular dependence assumed on H and its gradient, we set G equal to the identity. It then follows that the energy function will have the same values for all K and L satisfying the following identities:

$$H^i{}_J D^J = H^i{}_I K^I{}_J D^J$$

and

$$H^i{}_{M,N} D^M + H^i{}_M A^M{}_N = H^i{}_{I,N} K^I{}_M D^M + H^i{}_I L^I{}_{MN} D^M + H^i{}_I K^I{}_M A^M{}_N$$

for all non-singular $F^i{}_I$ and $H^i{}_I$ and for all $H^i{}_{I,J}$. It follows immediately that the minimal symmetries are those satisfying the following conditions:

$$K^I{}_J D^J = D^I \tag{3}$$

and

$$L^I{}_{MN} D^M = (\delta^I{}_M - K^I{}_M) A^M{}_N \tag{4}$$

The first condition is the obvious one: the energy function at a point remains invariant under any change of reference configuration which leaves the director at that point unchanged. In other words, the matrix K has the director as an eigenvector corresponding to a unit eigenvalue. The second condition, on the other hand, is far from obvious and could not have been predicted except by means of the kinematically based method we have used. Note that in the particular case in which the tensor field $\mathbf{A}$ is zero, the right-hand side of the second condition vanishes. It is not difficult to show by a direct calculation that the collection of all the symmetries satisfying the above two conditions forms a group $\mathcal{G}_{min}$, which we will call the *minimal symmetry group* of any LCM, under the multiplication law given by Equation (1).

Although not strictly necessary, we will adopt as the *LCM archetype* a point whose constitutive law is of the form

$$W_c = W_c(F^i{}_\alpha, H^i{}_\alpha, H^i{}_{\alpha\beta}) = f_c(F^i{}_\alpha, H^i{}_\alpha D^\alpha, H^i{}_{\alpha\beta})$$

namely, we adopt $A^\alpha{}_{\beta\gamma} = 0$ at the archetype. According to the general prescription for uniformity, then, fields $P^I{}_\alpha(X^K)$, $Q^I{}_\alpha(X^K)$ and $R^I{}_{\alpha\beta}(X^K)$ must exist such that:

$$\begin{aligned}
&W(F^i{}_I, H^i{}_I, H^i{}_{I,J}; X^K)\\
&= W_c(F^i{}_I P^I{}_\alpha, H^i{}_I Q^I{}_\alpha, H^i{}_{I,J} P^J{}_\beta Q^I{}_\alpha + H^i{}_I R^I{}_{\alpha\beta})\\
&= f_c(F^i{}_I P^I{}_\alpha, H^i{}_I Q^I{}_\alpha D^\alpha, (H^i{}_{I,J} P^J{}_\beta Q^I{}_\alpha + H^i{}_I R^I{}_{\alpha\beta}) D^\alpha)
\end{aligned}$$

It is a straightforward matter to verify that the resulting function W has the requisite form:

$$W(F^i{}_I, H^i{}_I, H^i{}_{I,J}; X^K) = f(F^i{}_I, H^i{}_I D^I, (H^i{}_{I,J} D^I + H^i{}_I A^I{}_J))$$

where

$$D^I = Q^I{}_\alpha D^\alpha$$

and

$$A^I{}_J = R^I{}_{\alpha\beta}(P^{-1})^\beta{}_J D^\alpha$$

Indeed

$$\begin{aligned}
&f_c(F^i{}_I P^I{}_\alpha, H^i{}_I Q^I{}_\alpha D^\alpha, (H^i{}_{I,J} P^J{}_\beta Q^I{}_\alpha + H^i{}_I R^I{}_{\alpha\beta}) D^\alpha)\\
&= f_c(F^i{}_I P^I{}_\alpha, H^i{}_I D^I, P^J{}_\beta (H^i{}_{I,J} D^I + H^i{}_I A^I{}_J))\\
&= f(F^i{}_I, H^i{}_I D^I, H^i{}_{I,J} D^I + H^i{}_I A^I{}_J; X^K)
\end{aligned}$$

Under a change of reference configuration we know that the tensor field $A^I{}_J$ transforms to

$$A^A{}_B = (H^A{}_{I,J} D^I + H^A{}_I A^I{}_J)(F^{-1})^J{}_B$$

and we ask the question: does there exist a change of reference configuration leading to an identically vanishing $A^A{}_B$ in an open neighbourhood of a point? It is not difficult to show that a sufficient condition for this local homogeneity requirement to take place is that:

$$A^I{}_J = D^I{}_{,J}$$

identically in that neighbourhood. Indeed, if that is the case, we can write:

$$A^A{}_B = (H^A{}_I D^I)_{,J}(F^{-1})^J{}_B$$

Therefore, any change of reference configuration of the form

$$Y^A = Y^A(X^K)$$

$$H^A{}_I = (Q^{-1})^\alpha{}_I \delta^A{}_\alpha$$

will do the job. We conclude then that the local homogeneity of an LCM body is guaranteed, in addition to the ordinary condition of homogeneity of the macromedium, by the equation

$$A^I{}_J = D^I{}_{,J} \tag{5}$$

describing the compatibility of the liquid crystal superstructure. If, however, the underlying macromedium is homogeneous but condition (5) is violated, we have a genuine distribution of inhomogeneities at the microstructural level. On the other hand, it can be shown that the two conditions taken together are not only sufficient, but also necessary, for local homogeneity of an LCM uniform body whose symmetry group is minimal. This fact holds true even though the minimal symmetry group is continuous. More surprisingly, perhaps, the same conclusion holds even when the macromedium is a genuine liquid, namely, when its symmetry group is the whole unimodular group.

Assume that we have a reference configuration that is homogeneous as far as the underlying macromedium is concerned and in which the director field is unit and parallel. The only source of inhomogeneity left is, therefore, a smooth second-order tensor field $\mathbf{A}(\mathbf{X})$. By the polar decomposition theorem, this field can be seen geometrically as a field of ellipsoids, whose axes and eccentricities vary smoothly from point to point. In principle, then, we have a situation equivalent to that of a standard liquid crystal, except that the standard ellipsoids of orientational distribution are now replaced by the ellipsoids arising form the inhomogeneity of the microstructure. These last ellipsoids are manifest, as already noted, even if the director field is perfectly unitary and parallel! The typical optical patterns, whose beautiful curvy shapes have become associated in popular imagination with liquid crystals, and usually explained as a manifestation of the variation of the mean orientational order of the molecules, could therefore be explained equivalently by the presence of continuous distributions of inhomogeneities.

4. Concluding remarks

We have shown that, at least in principle, it is possible to formulate a theory of liquid-crystal-like uniform bodies that admit continuous distributions of inhomogeneities. The main ingredient of this theory is the inclusion of maps, and derivatives thereof, between whole fibres of the principal frame bundle of the underlying body. This stands in contrast with the conventional theory, which recognizes only the transformation of a single vector field and its derivative. Although the treatment of a liquid crystal as some kind of generalized Cosserat body is not new, the way in which a particular director field is made to enter the formulation is different from previous formulations. Instead of imposing a constitutive symmetry upon a standard Cosserat medium, we emphasize a kinematic motivation as a rationale for constraining the constitutive functional to a particular form, and only then derive a-posteriori results for the minimal symmetry group. These results differ form the a-priori counterparts in [7] and [8] in the rather complicated symmetry requirement for the microstructural component, a requirement that is absent in the a-priori statement. But it is precisely this condition that allows for the existence of legitimate microstructural inhomogeneities. Further mathematical details of the theory are now under investigation, including differential-geometric implications.

References

[1] EPSTEIN M. AND DE LEÓN M., *Homogeneity conditions for generalized Cosserat media*, J. Elasticity **43** (1996), 189–201.

[2] EPSTEIN M. AND DE LEÓN M., *Geometrical theory of uniform Cosserat media*, J. Geom. Phys. **26** (1998), 127–170.

[3] EPSTEIN M. AND MAUGIN, G. A., *The energy-momentum tensor and material uniformity in finite elasticity*, Acta Mech. **83** (1990), 127–133.

[4] ERICKSEN J. L., *Anisotropic fluids*, Arch. Rational Mech. Anal **4** (1960), 231–237.

[5] ERICKSEN J. L., *Liquid crystals with variable degree of orientation*, Arch. Rational Mech. Anal. **113** (1991), 97–120.

[6] FRANK F. C. *On the theory of liquid crystals*, Discuss. Faraday Soc. **25** (1958), 19–28.

[7] LEE J. D. AND ERINGEN A. C. *Wave propagation in nematic liquid crystals*, J. Chem. Phys. **54** (1971), 5027–5034.

[8] LEE J. D. AND ERINGEN A. C. *Continuum theory of smectic liquid crystals*, J. Chem. Phys. **58** (1973), 4203–4211.

[9] LESLIE F. M. *Some constitutive equations for liquid crystals*, Arch. Rational Mech. Anal. **28** (1968), 265–283.

[10] MAUGIN G. A. AND TRIMARCO C. *On material and physical forces in liquid crystals*, Int. J. Engng. Sci. **33** (1995), 1663–1678.

[11] NOLL W. *Materially uniform simple bodies with inhomogeneities*, Arch. Rational Mech. Anal. **27** (1967), 1–32.

AMS Subject Classification: 73B25, 53C10.

Marcelo EPSTEIN
Department of Mechanical and Manufacturing Engineering
University of Calgary
Calgary, Alberta T2N 1N4, CANADA
e-mail: `epstein@enme.ucalgary.ca`

Rend. Sem. Mat. Univ. Pol. Torino
Vol. 58, 1 (2000)
Geom., Cont. and Micros., I

S. Forest - R. Parisot*

MATERIAL CRYSTAL PLASTICITY AND DEFORMATION TWINNING

Abstract. In classical crystal plasticity, the lattice orientation is unchanged from the reference configuration to the local to the local intermediate is plastically deformed configuration. Material plasticity corresponds to a different irreversible process by which the lattice rotates together with material lines between reference and intermediate configurations. Deformation twinning is an example of material plasticity. A continuum model for mechanical twinning of single crystals is presented in this work. Twin formation is regarded as an unstable localization phenomenon, followed by twin front propagation. Finite element simulations are provided showing the twinning and untwinning of a single crystal under cyclic loading, the development of twins at a crack tip, and lastly the formation of twin networks in a coating on an elastic substrate.

1. Material vs. dislocation-based crystal plasticity

The constitutive framework of anisotropic elastoplasticity has been settled by Mandel in [11]: it requires the definition of a tryad of directors attached to each material point. In the case of single crystal plasticity, the relative rotation rate of lattice directors with respect to material lines is derived in a unique way from the kinematics of plastic glide according to N slip systems. A unique intermediate configuration can be defined for which the lattice orientation is the same as the initial one. This results in a multiplicative decomposition of the deformation gradient $\underset{\sim}{\mathbf{F}}$ into elastic and plastic parts, as shown on figure 1a:

$$\underset{\sim}{\mathbf{F}} = \underset{\sim}{\mathbf{E}}\underset{\sim}{\mathbf{P}}, \qquad \dot{\underset{\sim}{\mathbf{P}}}\underset{\sim}{\mathbf{P}}^{-1} = \sum_{s=1}^{N} \dot{\gamma}^s \underline{\mathbf{m}}^s \otimes \underline{\mathbf{n}}^s$$

where slip system s is described by the slip direction $\underline{\mathbf{m}}^s$ and the normal to the slip plane $\underline{\mathbf{n}}^s$, and γ^s denotes the amount of associated slip. It follows that from the reference configuration to the intermediate one, the lattice directions are left unchanged whereas the material lines rotate according to the rotation part in the polar decomposition of $\underset{\sim}{\mathbf{P}}$.

One can also imagine an irreversible deformation process by which the lattice directions of the crystal would simply follow the material lines. This is what we call *material crystal plasticity*. It leads to the picture of figure 1b where the individual atoms undergo a uniform simple glide in a cooperative way. However this process is not so simple as it may look since during the shearing the lattice structure is changed usually going from a highly symmetric class to a less symmetric one. Some critical shear amount γ_0 may exist for which the crystal structure is retrieved with possibly an orientation different from the initial one ([14]). Such a deformation process exists

*The authors want to thank Prof. André Pineau for many discussions on twinning phenomena in zinc.

in some crystals. It is referred to as *deformation twinning* ([2, 16]). The sequel of the paper is devoted to the continuum modelling of this particular mode material crystal plasticity.

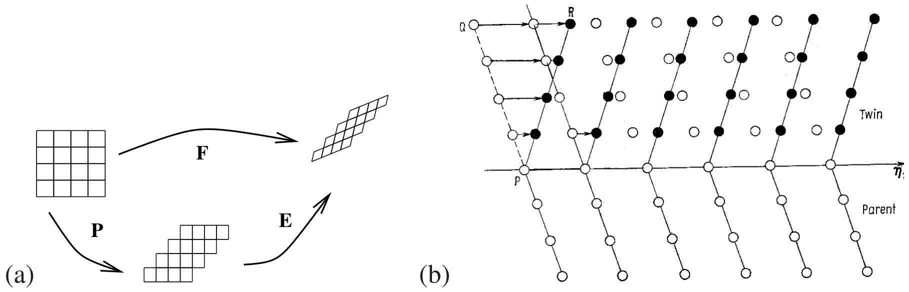

Figure 1: Kinematics of crystal plasticity based on dislocation glide (a); homogeneous shearing of a lattice as an example of material crystal plasticity (b).

Figure 2: Twin network and four cleavage cracks in a large flat zinc grain coated on a steel sheet (grain size : 500μm).

2. Continuum modelling of deformation twinning

2.1. Elements of deformation twinning

Deformation twinning now is a well–known deformation mechanism in cubic and hexagonal crystals. A modern and exhaustive account of the current knowledge from the crystallographic, metallurgical and mechanical point of view can be found in [3]. We will simply retain the following features:

• the deformation of the twinned part of the crystal can be described by a homogeneous shearing γ_0 in direction η_1 and in the plane S;

• the crystal structure of the twin usually is the mirror image of the parent crystal in the crystallographic twin plane K_1; K_1 very often coincides with the plane of contact between the two crystals called composition plane which is neither rotated nor distorted; the direction in S undergoing only a rotation is called η_2 and K_2 denotes the plane containing η_2 and normal to S;

• in fact, a simple shear applied to atom positions, as distinct from lattice points, is not always capable of producing all the atom movements which are needed to form a twin: additional *reshuffle* of some atoms of the unit cell is necessary, in particular in multiple lattices.

For simplicity, the present work is actually restricted to compound twins for which all elements K_i, η_i are rational ([10]). More specifically, the provided examples deal with pure zinc having hexagonal closed–packed symmetry. Using classical index notations for this type of symmetry ([2]), the twinning system of pure zinc is given by:

$$\eta_1 = < 10\overline{1}\overline{1} >,\ K_1 = \{10\overline{1}2\},\ \eta_2 = < \overline{1}01\overline{1} >,\ K_2 = \{\overline{1}012\},\ \gamma_0 = 0.139$$

The lattice orientation relationship between the parent crystal and the twin in zinc are: a mirror symmetry in K_1, or equivalently a rotation of angle π around η_1, a mirror symmetry in the plane normal to η_1 or a rotation of angle π around the normal to K_1.

2.2. Elastoplastic model of twinning

Mechanical models for twinning are available from both microscopic and macroscopic points of view. At the level of the cooperative behaviour of atoms, non–linear elasticity with a non–convex potential has proved to be an efficient method to describe such a phase transition–like process ([4, 19]). Indeed *elastic twinning* exists if there are no lattice friction forces opposing the motion of the dislocations at irregular interfaces. In this case, twins will run back when the applied stress is removed. In calcite for instance, small twins nucleate by indentation and disappear when the load is removed ([10]). However, more generally twinning is *not reversible* and twins remain in a crystal after it has been unloaded. The reason often is that accommodation has occurred by slip, relieving the stresses at the edge of the twin. Under these conditions, blunt twin plates with quite irregular interfaces are possible (figure 2). That is why deformation twinning is modelled here as an elastoplastic process associated with dissipation. Such an approach has already been proposed to model at the macroscopic level the volume fraction of twins appearing in a polycrystalline volume element of metal deforming by both slip and twinning ([9, 18]). We tackle here a different problem since the aim is to simulate the nucleation and propagation of twins at the grain level.

The classical framework of crystal plasticity is now extended to incorporate the following features of twinning (figure 3):

• twin formation is modelled as an unstable plastic slip process according to classical dislocation–based crystal plasticity;

• as soon as a critical amount of shear $\gamma = \gamma_0$ has been reached for the activated twin system, the orientation of the isoclinic intermediate configuration is changed switching from the initial parent one to that of the associated twin.

The driving force for twinning is the resolved shear stress τ on the twin plane in the twinning direction and the slip rate is computed using:

$$\dot{\gamma} = < \frac{\tau - \tau_c}{K} >^n, \quad \tau_c = \tau_0 + Q(1 - e^{-b(\gamma - E(\gamma/\gamma_0))})$$

where the viscosity parameters K and n are chosen so that the resulting behaviour is as rate–independent as necessary. τ_0 denotes the initial threshold for twinning and the hardening parameter Q is taken negative. Such a softening behaviour makes twin nucleation an unstable deformation mode associated with strain localization. The function floor $E(.)$ taking the integer part of . is introduced so that the initial threshold is recovered once the local twinning process is finished. Contrary to the classical Schmid law in dislocation - based plasticity, the sign of τ plays a role since twinning is possible only in one specific direction : compression in direction $\underline{\mathbf{c}}$ in zinc triggers deformation twinning, but not tension. The choice of $\underline{\mathbf{m}}$ and $\underline{\mathbf{n}}$ is such that τ, γ and $\dot{\gamma}$ are positive when twinning occurs.

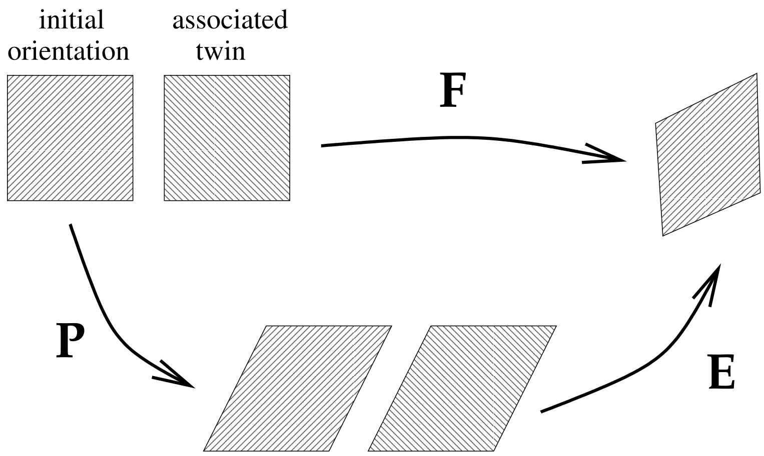

Figure 3: Kinematics of twinning plasticity

2.3. Thermodynamic setting

The state variables of the system can be taken as the Green–Lagrange strain tensor with respect to the intermediate configuration $\sharp$:

$$^{\sharp}\underset{\sim}{\Delta} = \frac{1}{2}(\underset{\sim}{\mathbf{E}}^T \underset{\sim}{\mathbf{E}} - \underset{\sim}{\mathbf{1}})$$

and temperature. The free energy $\psi(^{\sharp}\underset{\sim}{\Delta}, \alpha)$ may also be a function of an internal variable α to be specified. In the sequel, it is referred to the pure isothermal case. Only one twinning system is considered for simplicity. The local form of the energy balance equations then reads:

$$\rho\dot{\epsilon} = \underset{\sim}{\mathbf{T}} : \underset{\sim}{\dot{\mathbf{F}}}\underset{\sim}{\mathbf{F}}^{-1}$$

where $\underset{\sim}{\mathbf{T}}$ is the Cauchy stress tensor and ϵ the internal energy. The free energy takes the form:

$$\rho_\sharp \psi({}^\sharp\underset{\sim}{\Delta}, \alpha) = \frac{1}{2}\,{}^\sharp\underset{\sim}{\Delta} : \underset{\approx}{\mathbf{C}} : {}^\sharp\underset{\sim}{\Delta} + g(\alpha)$$

The Clausius–Duhem inequality reads:

$$-\rho_\sharp\dot{\psi} + \underset{\sim}{\mathbf{T}} : \underset{\sim}{\dot{\mathbf{F}}}\underset{\sim}{\mathbf{F}}^{-1} \geq 0$$

Noting that

$$\underset{\sim}{\mathbf{T}} : \underset{\sim}{\dot{\mathbf{F}}}\underset{\sim}{\mathbf{F}}^{-1} = (\underset{\sim}{\mathbf{E}}\underset{\sim}{\mathbf{T}}\underset{\sim}{\mathbf{E}}^{-T}) : \underset{\sim}{\dot{\mathbf{P}}}\underset{\sim}{\mathbf{P}}^{-1} + (\underset{\sim}{\mathbf{E}}^{-1}\underset{\sim}{\mathbf{T}}\underset{\sim}{\mathbf{E}}^{-T}) : {}^\sharp\dot{\underset{\sim}{\Delta}}$$

it follows that

$$-(\rho\frac{\partial\psi}{\partial\,{}^\sharp\underset{\sim}{\Delta}} - \underset{\sim}{\mathbf{E}}^{-1}\underset{\sim}{\mathbf{T}}\underset{\sim}{\mathbf{E}}^{-T}) : {}^\sharp\dot{\underset{\sim}{\Delta}} + (\underset{\sim}{\mathbf{E}}\underset{\sim}{\mathbf{T}}\underset{\sim}{\mathbf{E}}^{-T}) : \underset{\sim}{\dot{\mathbf{P}}}\underset{\sim}{\mathbf{P}}^{-1} - \rho\frac{\partial\psi}{\partial\alpha}\dot{\alpha} \geq 0$$

from which the state laws are deduced:

$${}^\sharp\underset{\sim}{\mathbf{T}} = \rho_\sharp\frac{\partial\psi}{\partial\,{}^\sharp\underset{\sim}{\Delta}} = \frac{\rho_\sharp}{\rho}\underset{\sim}{\mathbf{E}}^{-1}\underset{\sim}{\mathbf{T}}\underset{\sim}{\mathbf{E}}^{-T}$$

The thermodynamic force associated with the internal variable is:

$$A = -\rho_\sharp\frac{\partial\psi}{\partial\alpha} = -g'$$

The intrinsic dissipation rate then becomes:

$$D = {}^\sharp\underset{\sim}{\mathbf{S}} : \underset{\sim}{\dot{\mathbf{P}}}\underset{\sim}{\mathbf{P}}^{-1} + A\dot{\alpha}, \quad \text{with} \quad {}^\sharp\underset{\sim}{\mathbf{S}} = \frac{\rho_\sharp}{\rho}\underset{\sim}{\mathbf{E}}^{T}\underset{\sim}{\mathbf{T}}\underset{\sim}{\mathbf{E}}^{-T} = \underset{\sim}{\mathbf{E}}^{T}\underset{\sim}{\mathbf{E}}\,{}^\sharp\underset{\sim}{\mathbf{T}}$$

The positiveness of the intrinsic dissipation is then ensured by the choice of a convex dissipation potential $\Omega({}^\sharp\underset{\sim}{\mathbf{S}}, A)$:

$$\Omega({}^\sharp\underset{\sim}{\mathbf{S}}, A) = \frac{1}{n+1} < \frac{\tau - \tau_c}{K} >^{n+1}, \quad \text{with} \quad \tau = {}^\sharp\underset{\sim}{\mathbf{S}} : (\underline{\mathbf{m}} \otimes \underline{\mathbf{n}})$$

such that

$$\underset{\sim}{\dot{\mathbf{P}}}\underset{\sim}{\mathbf{P}}^{-1} = \frac{\partial\Omega}{\partial\,{}^\sharp\underset{\sim}{\mathbf{S}}} =< \frac{\tau - \tau_c}{K} >^{n} \ \underline{\mathbf{m}} \otimes \underline{\mathbf{n}}$$

$$\dot{\alpha} = \frac{\partial\Omega}{\partial A} = -\dot{\gamma}\frac{\partial\tau_c}{\partial A}$$

(1) $$D = \tau\dot{\gamma} + A\dot{\alpha}$$

Only calorimetric measurements can lead to an estimation of the dissipation associated with twinning in a single crystal. It appears from (1) that the amount of dissipated power is determined by the proper choice of the internal variable α and this will be dictated by the experimental measurements. Let us distinguish three cases:

• if no internal variable is introduced, $D = \tau\dot{\gamma}$ so that the entire plastic power is dissipated into heat; it is positive for a proper choice of $\underline{\mathbf{m}}$ and $\underline{\mathbf{n}}$ (such that $\tau > 0$ when $\dot{\gamma} > 0$), even if a softening behaviour is introduced;

• if we take $g' = \tau_c = -A$, then $\alpha = \gamma$ and $D = (\tau - \tau_c)\dot{\gamma}$ which vanishes in the rate-independent case; accordingly, the entire plastic power is considered as irreversibly stored, like dislocation forest hardening in dislocation–glide plasticity;

• if we take $\tau_c = \tau_0 - A$, i.e. $g' = -A = Q(1 - e^{-b\gamma})$, then $\alpha = \gamma$ and $D = (\tau - (\tau_c - \tau_0))\dot{\gamma} \simeq \tau_0\dot{\gamma}$ in the quasi–rate–independent case; it is again positive since the twinning system orientation convention is such that $\dot{\gamma} \geq 0$. This choice is classical in conventional elastoviscoplasticity ([1]).

A much more fine tuning of the internal variable will be necessary in the case of twinning ([17]) and is not undertaken here.

3. Finite element simulations of twinning in single crystals

The ability of the model to reproduce several experimental features of deformation twinning in single crystals is illustrated for three different situations. For that purpose, finite element simulations are provided based on classical nonlinear algorithms for the resolution of global equilibrium and the local integration of the evolution equations.

3.1. Twinning and untwinning under cyclic loading

The main justification for choosing a softening stress-strain constitutive equation in the model stems from the experimental results obtained by Price ([15]) on zinc whiskers deformed in tension under a transmission electron microscope. He was able to observe and control the nucleation of a single twin and its propagation in the sample cross–section. The twin then thickens and invades the entire specimen. The load–displacement curve displays a sharp softening stage associated with twin nucleation. The parameters of the model have been adjusted according to this curve.

The simulation of a single crystal zinc plate oriented for plane single twinning in tension is now considered. A geometrical defect is introduced to trigger strain localization that is interpreted here as twin nucleation. Indeed a deformation band appears and its orientation corresponds to that of a twin. Once the critical amount of shear γ_0 is reached, the twin starts growing. Twin growths is the result of the motion of the localization front on one or both sides of the twin in the spirit of ([12]). The twin thickens and spreads over the entire specimen (figure 5a). When the whole sample has twinned, the crystal behaves elastically in tension. The crystal can then be entirely untwinned if it is subsequently subjected to compression (figure 5b). It must be noted that at the last deformation stage, a virgin crystal is obtained that can again twin in tension. This results in the hysteresis loop shown in figure 4.

3.2. Twinning modes at a crack tip

Let us now consider a single crystalline Compact Tension specimen classically used in fracture mechanics. The $\underline{\mathbf{c}}$–axis of the zinc crystal is normal to the crack plane and the initial crack growth direction coincides with $[01\bar{1}0]$. It is recalled that twinning occurs in a specific direction η_1 and not in the opposite direction. A positive resolved shear stress in this direction is necessary for twinning to become possible. The distribution of resolved shear stresses for the single considered

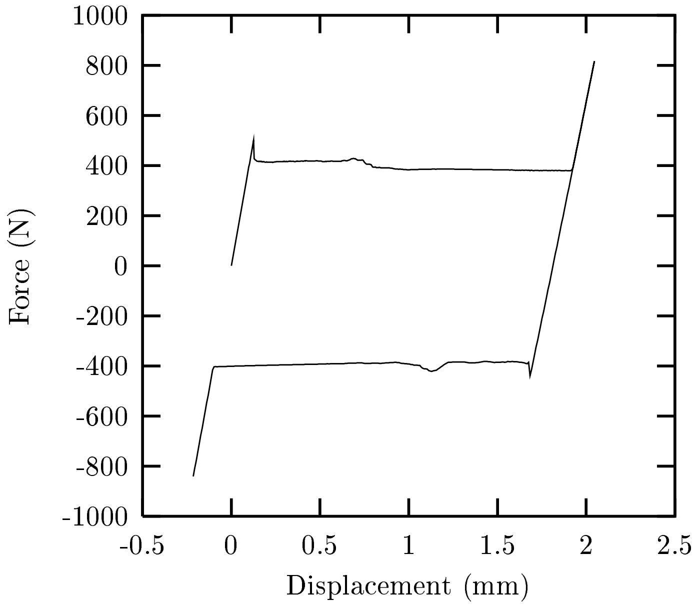

Figure 4: Load-displacement curve of the twinning and untwinning of a single crystal in tension-compression

twin system is shown on figure 6a. It appears that for the chosen orientation the resolved shear stress is negative ahead of the crack tip. Accordingly, a twin can form only behind the crack tip where the stresses are compressive. This is indeed possible as shown on figure 6b. This situation has been observed very often in the deformation of zinc coatings and is therefore justified by the present computation ([13]).

3.3. Multiple twinning in a zinc coating

The last example deals with the simulation of the formation of twin networks in a single crystal coating on an isotropic hyperelastic substrate subjected to tension. Two twinning systems are taken into account here: $[0\bar{1}1\bar{1}]$, $(0\bar{1}12)$ and $[01\bar{1}\bar{1}]$, $(01\bar{1}2)$. The $\underline{\mathbf{c}}$–axis of the crystal is normal to the coating and the tensile vertical direction is $[01\bar{1}0]$, parallel to the interface. The twinning directions of the considered systems are contained in the plane of the two–dimensional simulation. A displacement is prescribed at the top of the sample and the specimen is fixed at the bottom. Figure 7 shows that a first twin forms and is repelled at the interface, which corresponds to the formation of a second twin. A second pair of twins forms then independently at the lower part of the sample. Two of the twins intersect. The growth of the twins is limited by the fact that the interface cannot accommodate the deformation since the substrate remains elastic. Instead many twins form to build an actual network. This type of network is similar to that of figure 2. Sections of the coating are presented on figure 8 showing the twin development in the thickness of the coating. No direct experimental evidence of twin reflexion at the interface has been detected but this may be due to the specific crystal orientations.

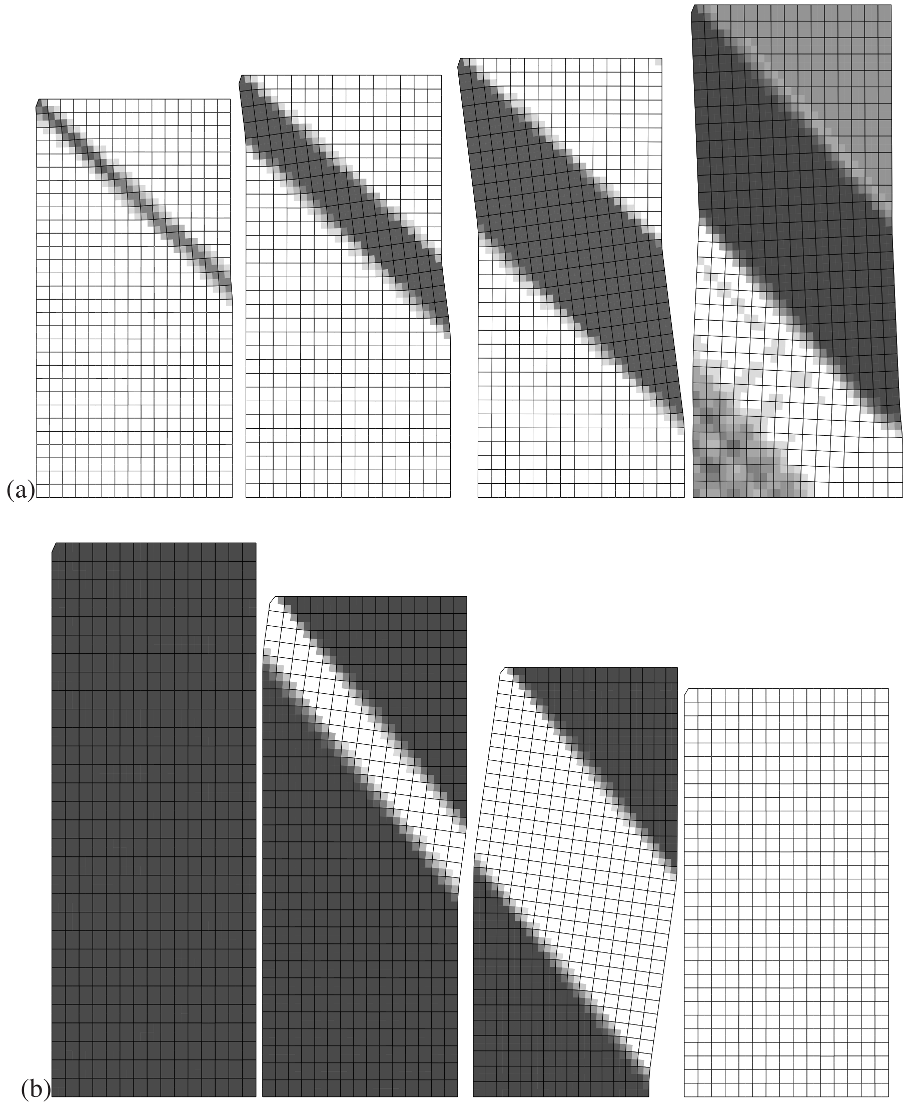

Figure 5: Twin formation and propagation in a single crystal in tension (a) followed by compression (b).

The twin systems activated in each strain localization band are given on figure 9. In the computation, the orientation of the sample is sligthly tilted with respect to the previously given orientation so that twin system 1 is significantly more activated than twin system 2. It is however quite surprising to see that the pair of almost perpendicular bands at the top of the sample belongs to the same twin system. This should in principle be impossible since two twins having the

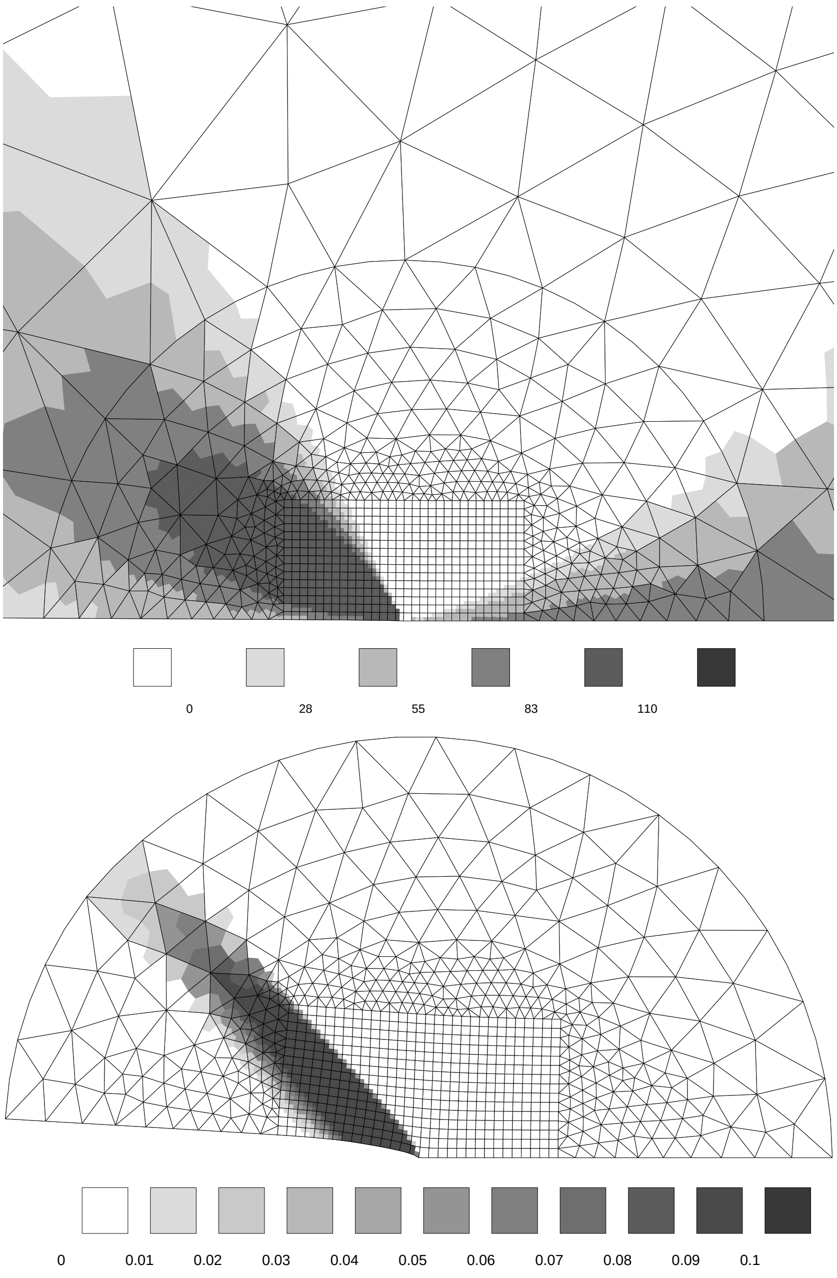

Figure 6: Twin formation at a cleavage crack tip : resolved shear stress distribution ((a), in MPa) and equivalent plastic deformation field (b).

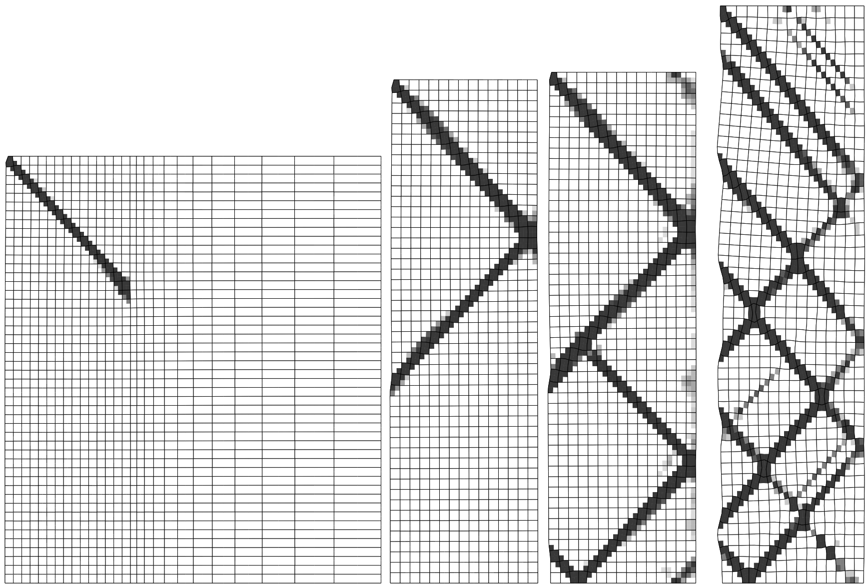

Figure 7: Multiple twinning in a zinc coating: the first twin is repelled at the interface coating/substrate (left), multiple reflexion and formation lead to a network of twins in the coating (right, only the coating is represented).

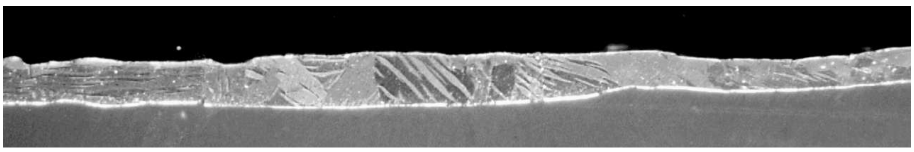

Figure 8: Section of the coating in the thickness showing the shape and orientation of the twins; the thickness of the coating is 10μm.

same twin plane should be parallel. These bands must be interpreted in fact as shear bands in a single crystal undergoing single slip. Simple glide in the twinning direction has been artificially introduced in the modelling to simulate twin formation. Twin formation has been interpreted as a strain localization phenomenon. In single slip, it is known that two localization planes are possible : slip bands lying in the slip plane but also kink bands that are normal to the slip direction ([5]). The last picture gives the distribution of lattice rotation with respect to the initial orientation before the twinned lattice has been reindexed. This information enables us in fact to distinguish the different types of bands : slip bands are usually associated with no lattice rotation whereas kink banding induces lattice curvature. It appears that the first twin at the top is a *kink twin* and the second one a “slip twin”. A “kink twin” can be seen as a stacking of many parallel twin lamellae. A severe limitation of the model is that such kink twins are usually not observed experimentally.

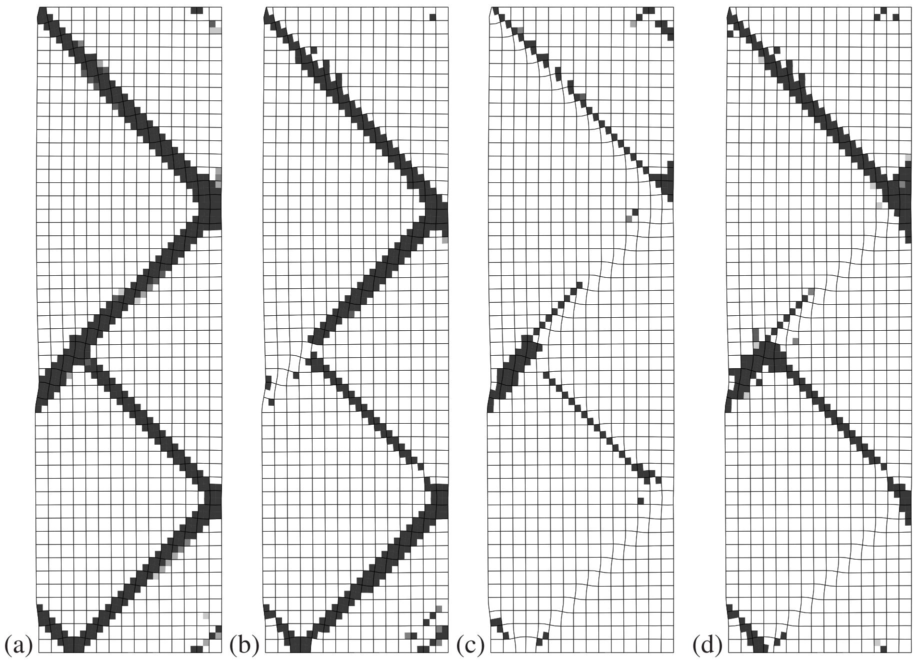

Figure 9: Structure of the twins in the coating : (a) equivalent plastic deformation, (b) twinning system 1, (c) twinning system 2, (d) lattice rotation before reindexing.

4. Discussion: The pros and the cons of the model

The proposed finite strain elastoplastic model of deformation twinning is able to account for several experimental features : twin formation and propagation in a single crystal, hysteresis loop associated with a twinning–untwinning process, arrow shape of twins at a cleavage crack tip and build–up of twin networks in a coating on a substrate.

Several important limitations remain however. One may for instance discuss the fact that a twinning criterion based on a critical resolved shear stress has been chosen. It is often recalled that twin initiation is a nucleation (in contrast to propagation) controlled process. It can therefore be affected for instance by prior dislocation glide so that it may be difficult to assign a critical value τ_0 to the twinning mechanism. Let us then admit that τ_0 is the critical resolved shear stress for twinning in a dislocation–free crystal like Price's zinc whiskers. The effective twin nucleation stress can then decrease if dislocation glide has already taken place, according to a softening law like:

$$\tau = \tau_0 + Q_2(1 - e^{-b_2\gamma_{slip}})$$

where Q_2 is negative and γ_{slip} denotes the cumulative amount of prior dislocation glide.

Furthermore, deformation twinning is systematically associated with dislocation glide because of the high local stresses arising for instance at the twin tip. This interaction has not been taken into account yet, which leads to unrealistic local high stresses. Plastic slip can take place before twinning and the question to be solved is then : what happens to the obtained dislocation structure when it twins? How can prior slip activity affect further dislocation glide within the newly formed twin? Mechanical metallurgy has already provided some answers that must be incorporated into continuum modelling.

Special attention should also be paid to the intersection of twins that has occured in some simulations.

A strong limitation has already been pointed out, namely the prediction of kink twins that are not observed in practise. The elimination of such deformation modes is however possible using for instance Cosserat crystal plasticity ([6, 7]).

An alternative approach to deformation twinning is proposed in ([8]) based on minimization principles. This global approach enables one to predict self–equilibrating structures that are frequently observed. The difficulty then is the numerical exploration of all possible regions and shapes where twinning can occur in order to finger out the most favourable configuration. The authors themselves plead for a Landau–Ginzburg or Cahn–Hilliard–type of modelling of displacives phase transitions and deformation twinning. That is why an improvement of the present model could be the introduction of an order parameter, aiming at forbiding "interrupted twins", i.e. regions where crystal glide has begun but where the value γ_0 has not been reached yet.

References

[1] CHABOCHE J. L., *Thermodynamic formulation of constitutive equations and application to the viscoplasticity and viscoelasticity of metals and polymers*, Int. J. Solids Structures **34** (1997), 2239–2254.

[2] CHRISTIAN J. W., *The theory of transformations in metals and alloys*, Pergamon Press 1965.

[3] CHRISTIAN J. W. AND MAHAJAN S., *Deformation twinning*, Progress in Materials Science **39** (1995), 1-157.

[4] ERICKSEN J. L., *Some phase transitions in crystals*, Arch. Rat. Mech. Anal. **73** (1980), 99–124.

[5] FOREST S. AND CAILLETAUD G., *Strain localization in single crystals: effect of boundaries and interfaces*, European Journal of Mechanics A-Solids **14** (1995), 747–771.

[6] FOREST S., BARBE F. AND CAILLETAUD G., *Cosserat modelling of size effects in the mechanical behaviour of polycrystals and multiphase materials*, Int. J. Solids Structures **37** (2000), 7105–7126.

[7] FOREST S., *Modeling slip, kink and shear banding in classical and generalized single crystal plasticity* Acta Materialia **46** (1998), 3265–3281.

[8] IDESMAN A. V., LEVITAS V. I. AND STEIN E., *Structural changes in elastoplastic material: a unified finite-element approach to phase transformation, twinning and fracture*, Int. J. Plasticity **16** (2000), 893–949.

[9] KALIDINDI S. R., *Incorporation of deformation twinning in crystal plasticity models*, J. Mech. Phys. Solids **46** (1998), 267–290.

[10] KELLY A. AND GROVES G. W., *Crystallography and crystal defects*, Longman, London 1970.

[11] MANDEL J., *Equations constitutives et directeurs dans les milieux plastiques et viscoplastiques*, Int. J. Solids Structures **9** (1973), 725–740.

[12] MAUGIN G. A., *On shock waves and phase-transition fronts in continua*, ARI **50** (1998), 141–150.

[13] PARISOT R., FOREST S., GOURGURES A. F. AND PINEAU A., *Modelling the mechanical behaviour of a multicrystalline zinc coating on a galvanized steel sheet*, Computational Materials Science **19** (2000), 189–204.

[14] PITTERI M., *On the kinematics of mechanical twinning in crystals*, Arch. Rat. Mech. Anal. **58** (1985), 25–57.

[15] PRICE P. B., *Nucleation and growth of twins in dislocation-free zinc*, Proc. Roy. Soc. London **260** A (1961), 251–262.

[16] REED-HILL R. E., HIRTH J. P. AND ROGERS H. C., *Deformation twinning*, Metallurgical Society Conferences **25**, Gordon and Breach Science Publishers 1964.

[17] SRINIVASA A. R., RAJAGOPAL K. R. AND AMSTRONG R. W., *A phenomenological model of twinning based on dual reference structures*, Acta Mater. **46** (1998), 1235–1254.

[18] STAROSELSKY A. AND ANAND L., *Inelastic deformation of polycrystalline f.c.c. materials by slip and twinning*, J. Mech. Phys. Solids **46** (1998), 671–696.

[19] TRUSKINOVSKY L. AND ZANZOTTO G., *Ericksen's bar revisited: energy wiggles*, J. Mech. Phys. Solids **44** (1996), 1371–1408.

AMS Subject Classification: 74C15, 74E10, 74Nxx.

Samuel FOREST, Rodolphe PARISOT
Ecole des Mines de Paris / CNRS
Centre des Matériaux / UMR 7633, BP 87
91003 Evry, FRANCE
e-mail: `Samuel.Forest@mat.ensmp.fr`

Rend. Sem. Mat. Univ. Pol. Torino
Vol. 58, 1 (2000)
Geom., Cont. and Micros., I

J. F. Ganghoffer

NEW CONCEPTS IN NONLOCAL CONTINUUM MECHANICS

Abstract. A new theoretical framework in nonlocal mechanics is defined, based on the concept of influence functions between material points within the continuum. The traditional idea of a fixed and isotropic representative volume is abandoned and the non-locality is introduced via an influence function, which defines a nonlocal interaction between material points. The general framework developed is exemplified by the description of damage as a scalar internal variable : the local damage rate at a given point can be expressed as a path integral involving the influence functions and the values of the local rate of damage transported along each path. The properties satisfied by the influence function are first evidenced and the influence function is given an explicit expression, using a path integration technique. The concept of a representative volume is further defined as an outcome of the stationarity of the internal entropy production with respect to the path. An implicit equation which defines the representative volume is formulated. The strength of the nonlocal interaction is further incorporated into the space geometry, so that a metric characteristic of a Riemanian space is coupled to the internal variable distribution. It appears that the curvature characterises the strength of the nonlocal interaction.

1. Introduction

Traditional continuum models in nonlocal mechanics usually rely on the assumption that the nonlocal variables are simply volume averages of the corresponding local variables over a fixed and isotropic representative volume element around the considered material point, see e.g. [1, 2, 3, 4, 5]. Considerations based on micromechanical arguments however show that the size of the representative volume, i.e. the extension of the interaction shall depend on the local variable distribution itself : in the work by Mühlhaus et al. ([6]), a Cosserat theory for granular materials is elaborated, starting from a particulate model. The model predicts that the shear band thickness evolves with the shear strain. A micromechanical argument for nonlocal damage has been advanced in [2]: the strain-softening damage due to distributed cracking is modelled by a periodic array of cracks. The results of the model show that the elastic part of the response shall be local, whereas the damage recovered at the macro scale shall be nonlocal. Furthermore, the size of the averaging region is determined by the crack spacing.

During loading of the cracked body, the increment of the stress along one crack is the sum of the average stress increment over the crack length and the contributions of all other cracks :

$$\Delta S^i(x) = \left\langle \Delta S^i(x) \right\rangle + \int_V \Lambda_{ij}(x,\xi)\Delta S^j(\xi) dV(\xi). \tag{1}$$

The interactions of a set of microcracks cancel out over a short distance, and this in turn determines the size of the representative volume. The kernel $\Lambda(x,\xi)$ that determines the influence between two cracks located at points x and ξ depends on both the radial and angular variables, and evolves with the current crack distribution pattern. Thus, the form of the influence function shall depend upon the distribution of the internal variables at each time / loading – step. The last integral is in fact a path integral, depending on the spatial distribution of the cracks. The path that do effectively contribute to the local stress increment on the left-hand side of (1) change according to the evolution of the spatial pattern of cracks.

In Ganghoffer et al., a path integral formulation of the nonlocal interactions has been formulated, with damage as a focus. The scalar damage variable there represents the internal variable. The new concepts advanced therein can be considered as an attempt to model in a phenomenological manner the nonlocal interactions between defects in a solid material. In this contribution, we only give the main thrust of the ideas developed in [7].

2. Path integral formulation of nonlocal mechanics

The formulation of nonlocal damage relies upon the thermodynamics of irreversi-ble processes; accordingly, a damage potential function is set up, with arguments the internal variables, namely the local and the nonlocal damage. The consistency condition for the damage potential function and its dependence upon the local and nonlocal damage imply an integro-differential equation for the rate of the local damage, that can be recast into the general form

$$\dot{d}(x) = \frac{1}{\int\limits_{\Omega} G_1(x, y)dy} \int\limits_{\Omega} G_1(x, y)\dot{d}(y)dy, \tag{2}$$

with $G_1(x, y)$ an influence function. Equality (2) is rewritten into the more compact form

$$\dot{d}(x) = G(x, y) \circ \dot{d}(y), \tag{3}$$

whereby the kernel G and the composition operator $\circ$ are identified from the integral form in (2), i.e. (3) defines an integral operator having the kernel

$$G(x, y) = \frac{1}{\int\limits_{\Omega} G_1(x, y)dy} G_1(x, y).$$

When the kernel $G(x, y)$ only depends on the difference $(x - y)$ (e.g. in the form of the gaussian (3)), equality (2) gives the rate of damage as the convolution product of the kernel with the rate of damage. From now on, the starting point shall be the relation (2), in which *we do not a priori know the kernel* $G(x, y)$. A path integration technique will then be used to determine the expression of this kernel.

Since the kernel G determines the evolution of the internal variable, it shall be called the *propagator* as well. Properties satisfied by the kernel G are first evidenced. First note that relation (3) embodies an implicit definition of G : elaborating (3) yields

$$\dot{d}(x) = G(x, y) \circ G(y, z) \circ \dot{d}(z) = G(x, z) \circ \dot{d}(z) \tag{4}$$

and therefore, one has formally

$$G(x, z) = G(x, y) \circ G(y, z) \tag{5}$$

in which the composition operator means that one first propagates the influence from x to y, and then from y to z. Relation (5) is called the *inclusion relation* of an intermediate point. In its present form (4), G appears as a linear operator - acting on functions $f : \mathbb{R}^3 \to \mathbb{R}^+$ - and not depending on time (it only depends on the space variables). This is consistent with the fact that we shall only treat instantaneous quasi-static dissipative processes in this contribution (consideration of time-dependent or dynamic phenomena would involve a dependence of the kernel G on time as well). As a consequence, the inversion property for G reads as

$$G(x, x) = Id = G(y, x) \circ G(x, y) \Rightarrow G(x, y) = G(y, x)^{-1}. \tag{6}$$

According to the elementary property satisfied by G :

$$G(x, x) = Id, \tag{7}$$

we define the infinitesimal operator B, such that

$$G(x, x + dx) = Id + dxB(x). \tag{8}$$

Note that (8) has been set up as an exact relation, which means that $B(x)$ includes virtually all powers of dx in the series expansion of $G(x, x+dx)$. Since $G(x, x+dx)$ connects two material points x and $y = x + dx$ which are in the same infinitesimal neighbourhood, $G(x, x + dx)$ is in fact the infinitesimal propagator and it is seen that the knowledge of the operator B completely determines $G(x, x + dx)$. In the sequel, we shall formally evaluate the propagator between two points located at a finite distance from each other. This is done in a two steps procedure : first, the infinitesimal propagator is evaluated, and then a path integration technique shall be used to reconstruct the propagator for finitely distant points.

The operator B is involved to derive a partial differential equation - p.d.e. - for $G(. , .)$. Since $G(x + dx, y) = G(x + dx, x) \circ G(x, y) = (Id + B(x)dx) \circ G(x, y)$, one has the limit

$$\lim_{dx \to 0} \frac{G(x + dx, y) - G(x, y)}{dx} = B(x) \circ G(x, y),$$

which implies

$$\frac{\partial G}{\partial x}(x, y) = B(x) \circ G(x, y). \tag{9}$$

From (3), one then obtains the p.d.e. for the local damage

$$\frac{\partial \dot{d}}{\partial x}(x) = \frac{\partial G}{\partial x}(x, y) \circ \dot{d}(y) = B(x).\dot{d}(x)$$

with $B(x) = G'(0)$. Equations (7) and (9) imply that the influence function is given by the integral

$$G(x, y) = Id + \int_{S(y,x)} B(z) \circ G(z, y) dz$$

with $S(x, y)$ a continuous path from y to x, while the inversion rule (6) can be rewritten as

$$dG(x, y) \circ G^{-1}(x, y) = B(x).dx \tag{10}$$

and one cannot integrate directly the left-hand side of this equation.

An iterative solution of equation (10) is constructed, which renders the limit function $G(x, y) := \lim_{n\to\infty} G_n(x, y)$:

$$G(x, y) = M\left[\exp\left\{\int_{S(y,x)} B(z)dz\right\}\right] \tag{11}$$

with M an operator, that orders the material points in space. Invariance by space translation - which can be easily deduced from (11) - results in the more specific form $G(x, y) = G(x - y)$.

Assuming further that angular variations of the rate of damage are much smaller compared to the radial variations, at least infinitesimally, we get

$$
\begin{aligned}
G(x, y = x + dx) &= exp \int_y^x a_2(x)(z - x)dz = \\
&= exp \left[a_2(x) \frac{(z - x)^2}{2} \right]_{x+dx}^x = \\
&= exp - k \left[\frac{(y - x)}{l(x)} \right]^2
\end{aligned}
\tag{12}
$$

introducing a quantity $l(x)$ as a function of x, (such that $a_2(x) = -k/l(x)^2$), which can be thought of as an internal length (it has the dimension of a length); k is a constant which depends on the dimension of space. Note that since expression (2.1312) is only valid for points x and y such that $y - x = dx$, the internal length depends on the distance (not on the orientation of the vector $y - x$ if the isotropy assumption is kept) between x and y as well, thus we use the notation $l(x, dist(x, y))$ in the sequel.

In the second step of the procedure, the form (12) of the infinitesimal propagator is used to evaluate the propagator for arbitrary points x and y, now separated by a finite distance. Iterating the integral equation in (2) yields :

$$
\dot{d}(x) = \frac{1}{C(x)} \int_\Omega \frac{G(x, y)}{C(y)} dy \int_\Omega G(y, z)\dot{d}(z)dz = \frac{1}{C(x)} \int_\Omega G(x, z)\dot{d}(z)dz
\tag{13}
$$

with the coefficients

$$
C(x) := \int_\Omega G(x, y)dy.
$$

We next define the concept of path integral, and rewrite (13) as

$$
\dot{d}(x) = \int_\Omega dy \left\{ \sum_{S[x,y]} \int_{z \in S[x,y]} K(y, z)\dot{d}(z)ds(z) \right\}
\tag{14}
$$

in which the function $K(y, z)$ is identified from (13) :

$$
K(y, z) := \frac{G(x, y).G(y, z)}{C(x)C(y)}
$$

which means that one propagates the intermediate point z over all possible paths $S[x, y]$ joining the points x and y, fig.1. The summation done over all possible paths that join the points x and y means that the variable z covers the whole space. A final summation is done so that the influence is evaluated at all points y. Since a given path is in fact a line in space, the infinitesimal distance element ds in (14) is given by the expression

$$
ds^2 = g_{ij} dx^i dx^j
\tag{15}
$$

which involves the metric tensor (g_{ij}) of the space. The co-ordinates of the generic point are $x^1 = x$; $x^2 = y$; $x^3 = z$, when the space is sustained by a set of basis vectors $(e_i)_i$. The coefficients of the metric in (15) are simply the inner products $g_{ij} = e_i.e_j$.

Next, the concept of sum over all paths is given a more precise meaning, since we must first characterise and label the paths in some systematic way. For that purpose, we make a space slicing, so that a continuous path from the end points x and z shall be decomposed in n discrete parts $(z, z_1, z_2, ..., z_{n-1}, x)$ of straight lines, having all the same size $\epsilon := \left\| z_i - z_{i-1} \right\| / n$, fig.2. Iterating the inclusion rule so as to include the influence of all intermediate points, we get

$$\begin{aligned} G(x,z) &= \int\limits_{\Omega} \frac{G(x, z_{n-1})}{C(z_{n-1})} ds(z_{n-1}) \int\limits_{\Omega} \frac{G(z_{n-1}, z_{n-2})}{C(z_{n-2})} ds(z_{n-2}) ... \\ & ... \int\limits_{\Omega} \frac{G(z_2, z_1)}{C(z_1)} \int\limits_{\Omega} G(z_1, z) ds(z_1) dy \end{aligned}$$

which means that the effect of z on x is propagated through the discrete path defined by the set of intermediate points $(z_1, z_2, ..., z_{n-1})$, fig.2. In that way, a discretization of the propagator $G(x, y)$ is performed. Recall then the expression of the influence coefficient

$$G(z_i, z_{i-1}) = \exp -k \left\{ \frac{(z_i - z_{i-1})}{l(z_{i-1}, dist(z_i, z_{i-1}))} \right\}^2 .$$

We further assume that the length can be written $l(z_{i-1}, dist(z_i, z_{i-1})) = l(\epsilon.N)$, with N the unit vector that joins z_{i-1}, z_i, and ϵ the length of the segment $\left[z_{i-1}, z_i\right]$, supposed to be identical for all segments. Restricting further to the isotropic assumption, the length l does not depend on the vector N, which justifies the notation $l(\epsilon)$. Furthermore, we suppose that we can locally find a system of co-ordinates such that the Riemannian space can be locally considered as Euclidean; as a consequence, since the infinitesimal length ds is an invariant, the infinitesimal segments $ds(z_p)$ are all equal to the Euclidean distance, i.e. $ds(z_p) = ds = dz$, $\forall p \in [0, n]$. Since now all the segments have the same length, the internal length $l(\epsilon)$ remains constant. With these assumptions, we evaluate the propagator from z to z_2, which is the nearest point after z_1:

$$\begin{aligned} G(z_2, z) &= \int_{\Omega} \frac{G(z_2, z_1).G(z_1, z)}{C(z_1)} dz_1 \\ &= \int\limits_{\Omega} \frac{\exp -k \left[(z_2 - z_1)^2 + (z_1 - z)^2 \right] / l(2\epsilon)^2}{\int\limits_{\Omega} \exp -k(z - z_1)^2 / l(\epsilon)^2 dz} dz_1 \end{aligned}$$

in which the two lengths $l(\epsilon)$ and $l(2\epsilon)$ are involved. We then use the following general equality, valid for any non zero real numbers a and b

$$\int \exp \left[a(x - x_1)^2 + b(x - x_2)^2 \right] dx = \left(\frac{-\pi}{a + b} \right)^{1/2} \exp \left[\frac{ab}{a + b} (x_1 - x_2)^2 \right]$$

to derive the expression

$$\int\limits_{\Omega} \exp - \frac{k(z - z_1)^2}{l(\epsilon)^2} dz_1 \cong \int\limits_{]-\infty, +\infty[^3} \exp - \frac{kx^2}{l(\epsilon)^2} dx = \sqrt{\pi} \frac{l(\epsilon)}{\sqrt{k}},$$

replacing the volume occupied by the solid Ω by the infinite space $]-\infty, +\infty[$. We thus obtain

$$G(z_2, z) = \liminf_{\epsilon \to 0} \frac{1}{\sqrt{2}} \frac{l(2\epsilon)}{l(2\epsilon - \epsilon)} \exp \left[- \frac{k}{2l(2\epsilon)^2} (z - z_2)^2 \right]$$

which is nothing else than the influence coefficient $G(z_1, z)$ when z_1 is replaced by z_2 and ϵ by 2ϵ (defining $l(0) := 1$). The integration over z_1 has been performed over the whole space of reels, i.e. over $]-\infty, +\infty[$, whereas the solid occupies a finite volume in space : it is thought however that this is a valid approximation when the length of the interactions is much smaller than the global dimension of the body. Repeating this process then leads to

$$G(x, z) = \frac{1}{\sqrt{2}} \liminf_{\epsilon \to 0} \frac{l(n\epsilon)}{l((n-1)\epsilon)} \exp\left[-\frac{k}{2l(n\epsilon)^2}(x-z)^2\right]. \tag{16}$$

The continuous case in (16) is recovered when taking the limit of the discrete influence coefficient in the following way : the length of the segments tends to zero, thus $n \to \infty$, $\epsilon \to 0$, $n\epsilon \to dist(x, z)$, and the internal length becomes $l(n\epsilon) \to l(d(x, z))$: we obtain the final expression

$$G(x, z) = \frac{1}{\sqrt{2}} \exp\left[-\frac{k}{2l(dist(x, z))^2}(x-z)^2\right]. \tag{17}$$

When a more complete expansion of the function $B(x, z)$ is retained, we believe that a closed form of the kernel $G(x, y)$ is much more difficult to derive. The nonlocal damage is further defined as

$$\overline{d}(x) := \frac{1}{\int\limits_{\Omega} G(x, y)dy} \int\limits_{\Omega} G(x, y)d(y)dy$$

using the kernel determined in (12).

The differences with the more traditional approaches, e.g. the nonlocal damage model in [2] are: the internal length is a function of both the material point considered, and on the distance between the points x and y, whereas the traditional models assume it is a fixed, uniform quantity. In (17), $l(x, y)$ is not defined, thus a complementary rule is still needed; this rule will be elaborated in the next section. Note furthermore that in (13), the normalisation condition

$$\forall y \in \Omega, d(y) = 1 \quad \Rightarrow \quad \forall x \in \Omega, \overline{d}(x) = 1$$

is satisfied.

The path integral formulation can further be interpreted in the following way : consider a path S joining x and z, and make a partition of the space Ω in all sets of possible such paths. Then, for a fixed point y, the integral (14) can be formally expressed as a sum over all possible paths of the damage rate convected along each path with an amplitude equal to the influence coefficient $K(x, z)$. The set of paths that effectively contribute to the damage rate at a given point shall be selected from a thermodynamic criterion elaborated in the next section.

3. Selection rule for the path

We first rewrite formally the dissipation as an integral involving a product of - local - thermodynamic forces F_i and associated fluxes V_i in the more condensed form

$$\phi = \frac{1}{\int\limits_{\Omega} G_i(x, y)dy} \int\limits_{\Omega} F_i(y).V_i(y)G_i(x, y)dy \tag{18}$$

in which the summation is intended over the index i. A specific kernel $G_i(x, y)$ is associated to each dissipative mechanism, and it has the form established in the previous section. Considering nonlocal damage coupled to elasticity, the fluxes are the rate of irreversible strain and the rate of damage (with a minus sign), and the associated thermodynamic forces are the local stress and the damage driving force, respectively : according to (17), we can identify the force and the kernel associated to the irreversible strain as

$$F_\sigma(y) := \sigma(y); \qquad G_\sigma(x, y) := \delta(x - y)$$

and the force conjugated to the damage rate splits into a local contribution

$$F_d^l(y) := W^e(y); \qquad G_{F_d^l} := \delta(x - y),$$

and a nonlocal contribution

$$F_d(y) := \beta(1 - d(y)),$$

in which the kernel $G(x, y)$ has the form defined in the previous section. We then perform the variation of the integral in (18), considering that x is a fixed point in space :

$$\delta\phi = \frac{1}{\int\limits_\Omega G_i(x, y)dy} \int\limits_\Omega \delta\left\{F_i(y)V_i(y)G_i(x, y)\right\}dy - \tag{19}$$

$$- \frac{\delta\left\{\int\limits_\Omega G_i(x, y)dy\right\}}{\left[\int\limits_\Omega G_i(x, y)dy\right]^2} \int\limits_\Omega \left\{F_i(y)V_i(y)G_i(x, y)\right\}dy.$$

We first work out the term $\int\limits_\Omega \delta\left\{F_i(y)V_i(y)G_i(x, y)\right\}dy$, which is rewritten as the path integral

$$\int\limits_\Omega \delta\left\{F_i(y)V_i(y)G_i(x, y)\right\}dy =$$

$$\int\limits_\Omega F_i(y)V_i(y)\delta \sum_{z \in S[x,y]} \left\{ \int\limits_{S[x,y]} G_i(x - z)\frac{G_i(z, y)}{C_i(z)}ds(z) \right\} dy$$

where the summation (defined by the symbol $\sum$) is performed over all paths $S[x, y]$ that connect points x and y. The variation in (18), (19) is performed with the quantities at the extremal points x and y considered as fixed. Furthermore, in a first step, we consider the metric of space as a given quantity, at each point along any path.

As a matter of simplification, we set up $S(z) := S[x, y]$; the stationarity condition of the internal entropy condition, $\delta(\frac{dS_i}{dt}) = 0$, is finally expressed into the condensed form [7]

$$\int\limits_\Omega G_i(x, y)dy \int\limits_{y \in \partial\Omega} F_i(y)V_i(y)dy \sum_{S(z)} \int\limits_{\gamma \in \partial S(z)} G_i(x, \gamma)\frac{G_i(\gamma, y)}{C_i(\gamma)}d\gamma$$

$$- \int\limits_{y \in \partial\Omega} G_i(x, y)dy \int\limits_\Omega \left\{F_i(y)V_i(y)G_i(x, y)\right\}dy = 0 \tag{20}$$

which appears as a mixture of boundary and volume terms. Expression (20) is compacted as

$$\frac{\phi\left[\partial V_r(x)\right]}{\int\limits_{\partial\Omega} G(x,y)dy} = \frac{\phi\left[\Omega\right]}{\int\limits_{\Omega} G(x,y)dy} \tag{21}$$

with self-explanatory notations. The left-hand side represents the average flux of internal entropy through the boundary of Ω (due to the normalisation coefficient $1/\int\limits_{\partial\Omega} G_i(x,y)dy$), and the right-hand side is the average internal entropy produced in the volume Ω (according to the normalisation coefficient $1/\int\limits_{\Omega} G_i(x,y)dy$).

The concept of representative volume at the material point x, $V_r(x)$, arises from the set of all points z enclosed within the volume delimited by the boundary $\partial S(z)$ in (4.9): equality (21) then defines implicitly the representative volume as the set of points interacting with the point x, such that the internal entropy produced within $V_r(x)$ is equilibrated by an equal and opposite flux of internal entropy across the boundary $\partial V_r(x)$. Thus, we further rewrite (21) a

$$\frac{\phi\left[\partial V_r(x)\right]}{\int\limits_{\gamma\in\partial V_r(x)} G(x,\gamma)d\gamma} = \frac{\phi\left[V_r(x)\right]}{\int\limits_{y\in V_r(x)} G(x,y)dy}. \tag{22}$$

Since only the contribution to the dissipation due to non-local variables intervene in (21), equality (22) can be rewritten :

$$\frac{\int_{\gamma\in\partial V_r(x)}\{F_d(\gamma)V_d\}\exp\left\{-\frac{1}{2}\left[\frac{k(x-\gamma)}{l(x,\gamma)}\right]^2\right\}d\gamma}{\int\limits_{\gamma\in\partial V_r(x)}\exp\left\{-\frac{1}{2}\left[\frac{k(x-\gamma)}{l(x,\gamma)}\right]^2\right\}d\gamma} = \frac{\int_{y\in V_r(x)}\{F_d(y)V_d\}\exp\left\{-\frac{1}{2}\left[\frac{k(x-y)}{l(x,y)}\right]^2\right\}dy}{\int\limits_{y\in V_r(x)}\exp\left\{-\frac{1}{2}\left[\frac{k(x-\gamma)}{l(x,\gamma)}\right]^2\right\}dy} \tag{23}$$

with the non-local damage driving force $F_d(y)$ defined at the beginning of previous section.

The concept of a *representative volume* is then defined via the internal length $l(x, dist(x,y))$ which connects the point x - centre of the representative volume - and the point y on its boundary, as the following set of points :

$$V_r(x) := \{y \in \Omega/dist(x,y) \le l(x,y)\}$$

which is not necessarily a sphere. The internal length is an unknown that is determined from equation (23).

The evaluation of the internal length at each time step is then done in a two-step uncoupled procedure : in the first step, equation (23) is solved, using the value of the damage and rate of damage at previous time step. In the second step, the local and nonlocal damage variables are updated, according to the return mapping algorithm described in [6].

4. Geometrisation of the interaction

The path selection rule has been obtained under the assumption that the metric (g_{ij}) of this space is given; in fact, the influence function $G(x,y)$ is a function of the metric, via the internal length.

We want to reflect the fact that the forces responsible for the nonlocal interaction can be included into the geometry of the interaction, thus we envisage a situation in which the metric is coupled to the internal variable distribution.

As a matter of simplification, define the coefficients

$$A_{xy}(z) := \frac{G(x,z)G(z,y)}{C(z)},$$

that intervene in equation (20). The coefficient A_{xy} depends on the metric, and possibly on the first order spatial gradient of the metric, thus we use the notation $A_{xy}(g_{ij}(z), g_{ij,l}(z))$; the differential element of length $ds(z)$ involves the metric tensor according to the relation (15). Latin indices take their values in the set $\{1, 2, 3\}$. We now perform the variation in the path integral (18) with respect to the metric, which gives the variation of the term

$$\delta\left\{\int\limits_{S[x,y]} A_{xy}(g_{ij}(z), g_{ij,l}(z))ds(z)\right\} =$$

$$\int\limits_{S[x,y]} \left[\delta A_{xy}(g_{ij}(z), g_{ij,l}(z)) + A_{xy}\delta ds(z)\right] ds(z).$$

We introduce the energy-momentum tensor T_{ij}, see [8], defined as

$$T_{ij} := \frac{\partial A_{xy}}{\partial g^{ij}} - \partial l\left(\frac{\partial A_{xy}}{\partial(\partial l g_{ij})}\right)$$

and the Christoffel symbols

$$\Gamma^k_{ij} := \frac{1}{2}g^{km}(g_{jm,l} + g_{im,j} - g_{ij,m})$$

such that the covariant derivative Du^j of the contravariant vector $u := \frac{dx^j}{ds}e_j$, locally tangent to the path, expresses as

$$Du^j := du^j + \Gamma^j_{rt}u^r u^t ds.$$

A set of elementary calculation [7] renders the variation

(24)
$$\delta\left\{\int_{S[x,y]} A_{xy}(g_{ij}(z), g_{ij,l}(z))ds(z)\right\} =$$

$$-\int_{S[x,y]}\left[T_{ik,l} + \delta_{il}\frac{Du^k}{ds}A_{xy}\right]g_{ik}\delta x^l(z)ds(z).$$

Since the variations $\delta x^l(z)$ in (24) are arbitrary, we get the following condition, valid at each point $z \in S[x,y]$:

(25)
$$\left(T_{ik,l} + \delta_{il}\frac{Du^k}{Ds}A_{xy}\right)g_{ij} = 0, \qquad \forall l.$$

Equation (25) is the sum of one term that contains the energy content of the nonlocal interaction (due to the energy-momentum tensor) and of a second term that accounts for the geometric part of the interaction (via the metric tensor and the covariant derivative of the vector tangent to the path).

The energy-momentum tensor reflects the strength of the nonlocal interaction, and we see from the structure of (25) that the induced curvature also has the meaning of a field strength. The Christoffel symbols Γ_{ij}^{k} that intervene in the covariant derivative Du^{j} are indeed directly related to the - contracted twice - curvature tensor (Ricci tensor), defined as

$$R_{ik} := \Gamma_{ik,l}^{l} - \Gamma_{il,k}^{l} + \Gamma_{ik}^{l}\Gamma_{lm}^{m} - \Gamma_{il}^{m}\Gamma_{km}^{l}.$$

The scalar obtained by the contraction $g_{ik}R^{ik}$ represents the scalar measure of the curvature of space. The higher the strength of the nonlocal interaction, the higher the curvature; this idea is supported by the well-known case of plasticity within solid materials, where a high density of dislocations at a place curves the space around. Therefore, the physical meaning of relation (25) is that the strength of the interaction is incorporated into the geometry of the space. We follow thereby a trend which is nowadays classical in physics, which started with general relativity (the metric tensor plays there the role of the gravitation potential).

The fact that the nonlocal interaction shall follow certain paths in space can be understood from qualitative micromechanical arguments : when these defects are not isotropically distributed in space, but along certain lines instead, their mutual interaction will follow these lines. As a perspective of development of the present work, we can mention the involvement of such a formalism to treat the more general case of a tensorial-like internal variable, having plasticity in mind.

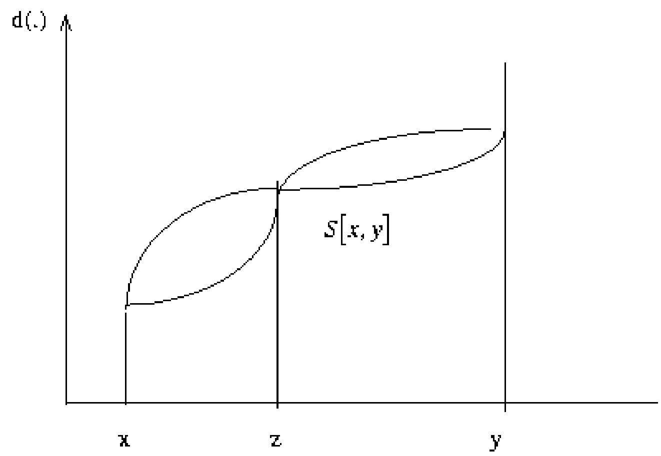

Figure 1: Splitting up of all spatial paths from x to y.

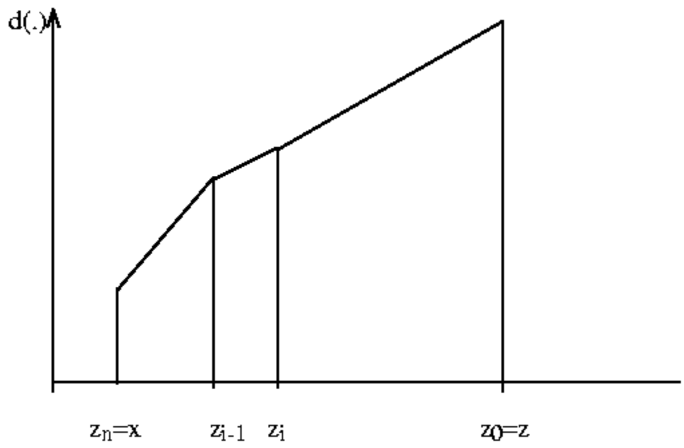

Figure 2: Space slicing. A continuous path from $d(x)$ to $d(z)$ can be approximated by a sequence of values $d(z_1), d(z_2), \ldots, d(z_n)$. This approximation becomes exact if $d(z_{i-1}, z_i) \to 0$.

References

[1] DE BORST R., SLUYS L. J., MÜLHAUS H. B. AND PAMIN J., *Fundamental issues in finite element analyses of localisation of deformation*, Eng. Comp. **10** (1993), 99–121.

[2] BAZANT Z. P. AND PIJAUDIER-CABOT G., *Nonlocal damage theory*, J. Eng Mech. **113** n. 10 (1987), 1512.

[3] BAZANT Z. P. AND PIJAUDIER-CABOT G., *Dynamic stability analysis with nonlocal damage*, Computers and Structures **29** 3 (1988), 503.

[4] PIJAUDIER-CABOT G. AND BODE L., *Localisation of damage in a nonlocal continuum*, Mech. Res. Commun. **19** 2 (1992), 145.

[5] PIJAUDIER-CABOT G. AND BENALLAL A., *Strain localisation and bifurcation in a nonlocal continuum*, Int. J. Solids Struc. **30** 13 (1993), 1761.

[6] MÜHLHAUS H. B., VARDOULAKIS I., Géotechnique **37** 3 (1987), 271.

[7] GANGHOFFER J. F. AND DE BORST R., *A new framework in nonlocal mechanics*, Int. J. Engng Sci. **38** (2000), 453–486.

AMS Subject Classification: 74A60, 74M25.

Jean-Francois GANGHOFFER
Lemta–Ensem
2, Avenue de la Forêt de Haye
B.P. 160-54504
Vandoeuvre Cedex, FRANCE
e-mail: `Jean-francois.Ganghoffer@ensem.inpl-nancy.fr`

Rend. Sem. Mat. Univ. Pol. Torino
Vol. 58, 1 (2000)
Geom., Cont. and Micros., I

S. Gümbel - W. Muschik[†]

GENERIC*, AN ALTERNATIVE FORMULATION OF NONEQUILIBRIUM CONTINUUM MECHANICS?

Abstract.

During the last 15 years a bracket formalism of dissipative continuum physics has been developed which resulted in a formulation which is shortly denoted as GENERIC. GENERIC has been applied to different problems of continuum thermodynamics, often in this way, that a well-known problem was reformulated in GENERIC formalism. So in 1997 the GENERIC form of the equations of motion of a Navier-Stokes fluid was formulated. To learn some more about the GENERIC procedure we consider here a general 5-field theory of fluids. Usually GENERIC is formulated for an isolated system, but here we will discuss the facility to formulate GENERIC for an open system.

1. Introduction

The phenomenological theories of thermodynamics are divided into continuumtheoretical ones and into those of discrete systems. There is a variety of phenomenological non-equilibrium continuum theories which are similar, but differ in basic concepts [10]. These are the Linear Irreversible Thermodynamics [2], Rational and Extended Thermodynamics ([14] to [7]), Non-Classical Thermodynamics [9], and theories using evolution criteria [11] and variational principles [6]. These well-known thermodynamical theories are now added by a special dissipative continuum procedure which was developped during the last 15 years starting out with a bracket formalism originated by an extension of Hamiltonian mechanics [3]. One result of this bracket approach is the GENERIC formalism [4, 5] which is totally different from the theories mentioned above, but is claimed by its investigators to be generally valid for all discrete systemsall theories in field formulation. In GENERIC the balance equations are generated by total energy and total entropy both acting as potentials and being only dependent on the wanted fields and not on the state space. The GENERIC balances are splitted additively into a reversible and an irreversible part. Beyond the balance equations there are so-called degeneracy conditions which are unknown in conventional, rational, and extended thermodynamics. Jacobi identities stemming from the antisymmetric bracket of the reversible part of the balance equations and calling to mind the Hamiltonian mechanics background of the GENERIC formalism are also unknown in the other approaches [1].

The distinctions between GENERIC and the usual approach demand for a possibility to compare them in a way as general as possible. Here a general 5-field formulation for fluids is considered in GENERIC treatment. First of all we report on general the GENERIC setting which is independent of special constitutive assumptions. Then we will extend the GENERIC

*General Equation for the NonEquilibrium Reversible-Irreversible Coupling

†Finacial support by the VISMAI Company, D-95085 Selb, Germany.

formalism to open systems. The structure of GENERIC can be motivated by a microscopic foundation [12],[13].

2. GENERIC setting

The fundamental structure of GENERIC is determined by six building blocks [3] to [12].

1. The set of the basic or wanted fields $\mathbf{Z}$ of the system which is presupposed to be open,
2. the total energy $E^{tot}(\mathbf{Z})$ of the open system and
3. its total entropy $S(\mathbf{Z})$, as two global potentials which depend only of the basic fields
4. two, in general operator-valued matrices $\mathcal{L}(\mathbf{Z})$ and
5. the dissipation operator $\mathcal{M}(\mathcal{Z})$ which depend on the state space $\mathcal{Z}$ which is not identical to the basic fields $\mathbf{Z}$,
6. the supply of the wanted fields $\mathbf{f}_e$ wich is vanishing for an isolated system.

The *equations of motion* of the basic fields $\mathbf{Z}$ have the special GENERIC form

$$\partial_t \mathbf{Z} = \mathcal{L} \cdot \frac{\delta E^{tot}}{\delta \mathbf{Z}} + \mathcal{M} \cdot \frac{\delta S}{\delta \mathbf{Z}} + \mathbf{f}_e, \tag{1}$$

which always can be split into its reversible, its irreversible and its supply part

$$\partial_t \mathbf{Z}^{rev} := \mathcal{L} \cdot \frac{\delta E^{tot}}{\delta \mathbf{Z}}, \qquad \partial_t \mathbf{Z}^{irr} := \mathcal{M} \cdot \frac{\delta S}{\delta \mathbf{Z}}, \qquad \partial_t \mathbf{Z}^{sup} := \mathbf{f}_e. \tag{2}$$

Here δ/δ is the functional derivative which maps global quantities to local ones, as we will see in the GENERIC treatment.

Beyond the equations of motion (1) the complementary degeneracy conditions

$$\mathcal{L} \cdot \frac{\delta S(\mathbf{Z})}{\delta \mathbf{Z}} = \mathbf{0}, \qquad \mathcal{M} \cdot \frac{\delta E^{tot}(\mathbf{Z})}{\delta \mathbf{Z}} = \mathbf{0} \tag{3}$$

are satisfied by $\mathcal{L}$ and $\mathcal{M}$. Therefore the degeneracy conditions (3) describe the reversible-irreversible coupling which is meant in the name of GENERIC. The two contributions (3) to the time evolution of $\mathbf{Z}$ generated by the total energy E^{tot} and by the total entropy S are called the reversible and irreversible contributions to dynamics, respectively.

General properties of $\mathcal{L}$ and $\mathcal{M}$ are discussed easily in terms of two brackets, one is anti-symmetric, the other one symmetric

$$\begin{aligned} &[A, B] := \left\langle \frac{\delta A}{\delta \mathbf{Z}}, \mathcal{L} \cdot \frac{\delta B}{\delta \mathbf{Z}} \right\rangle \doteq -[B, A] + \frac{1}{2}(\mathcal{O}^{rev}(A, B) + \mathcal{O}^{rev}(B, A)), \\ &[A, A] = \mathcal{O}^{rev}(A, A), \end{aligned} \tag{4}$$

$$\{A, B\} := \left\langle \frac{\delta A}{\delta \mathbf{Z}}, \mathcal{M} \cdot \frac{\delta B}{\delta \mathbf{Z}} \right\rangle \doteq \{B, A\} + \frac{1}{2}(\mathcal{O}^{irr}(B, A) - \mathcal{O}^{irr}(A, B)), \tag{5}$$

$$\{A, A\} + \mathcal{O}^{irr}(A, A) \stackrel{.}{\geq} 0. \tag{6}$$

Here $\langle\ ,\ \rangle$ denotes a scalar product, especially

$$\left\langle \frac{\delta A}{\delta \mathbf{Z}}, \mathcal{L} \cdot \frac{\delta B}{\delta \mathbf{Z}} \right\rangle := \int_{\mathcal{G}} \left[\frac{\delta A}{\delta \mathbf{Z}} \cdot \mathcal{L} \cdot \frac{\delta B}{\delta \mathbf{Z}} \right] d^3x, \tag{7}$$

A and B are sufficiently regular and real-valued functionals on $\mathbf{Z}$, $\mathcal{O}^{rev}$ is the reversible part, and $\mathcal{O}^{irr}$ is the irreversible part of the flux through the surface of the Volume $\mathcal{G}$. From the setting (4) follows, that $\mathcal{L}$ is antisymmetric, whereas we have to demand the symmetry of $\mathcal{M}$ which cannot be concluded from (5). Now we can express the degeneracy conditions (3) with the brackets, we find

$$[S, E^{tot}] - \mathcal{O}^{rev}(E^{tot}, S) = 0, \qquad \{E^{tot}, S\} + \mathcal{O}^{irr}(E^{tot}, S) = 0 \tag{8}$$

The antisymmetric bracket is presupposed to satisfy the Jacobi identity for closed systems, i.e all the surface terms vanish

$$[A, [B, C]] + [B, [C, A]] + [C, [A, B]] \doteq 0. \tag{9}$$

According to (1), (4) and (5) we can write the time evolution of A as

$$A = \int a(\mathbf{Z})\, d^3x, \ \longrightarrow\ \frac{\delta A}{\delta \mathbf{Z}} = \frac{\partial a}{\partial \mathbf{Z}}, \tag{10}$$

and because the system is an open one, we obtain

$$\frac{d}{dt} A = \int \partial_t a(\mathbf{Z})\, d^3x = [A, E^{tot}] + \{A, S\} + \int \frac{\partial a}{\partial \mathbf{Z}} \cdot \mathbf{f_e}\, d^3x. \tag{11}$$

According to (11), (8), (4) and (5) we obtain the time rate of the total energy and that of the total entropy of the isolated system

$$\begin{aligned} \frac{d}{dt} E^{tot} &= [E^{tot}, E^{tot}] + \{E^{tot}, S\} + \int \frac{\partial e^{tot}}{\partial \mathbf{Z}} \cdot \mathbf{f_e}\, d^3x \\ &= \mathcal{O}^{rev}(E^{tot}, E^{tot}) - \mathcal{O}^{irr}(E^{tot}, S) + \int \frac{\partial e^{tot}}{\partial \mathbf{Z}} \cdot \mathbf{f_e}\, d^3x, \end{aligned} \tag{12}$$

$$\begin{aligned} \frac{d}{dt} S &= [S, E^{tot}] + \{S, S\} + \int \frac{\partial \varrho s}{\partial \mathbf{Z}} \cdot \mathbf{f_e}\, d^3x \\ &= \mathcal{O}^{rev}(E^{tot}, S) + \{S, S\} + \int \frac{\partial \varrho s}{\partial \mathbf{Z}} \cdot \mathbf{f_e}\, d^3x. \end{aligned} \tag{13}$$

with the entropy production

$$\sigma = \{S, S\} + \mathcal{O}^{irr}(S, S) \geq 0.$$

This inequality represents the second law of thermodynamics of an open system in global formulation, where the surface term represents the flux of the entropy through the surface of the system. It is also clear, that all the surface terms have to vanish, if we want to describe an isolated system.

To go on with the GENERIC treatment we now have to introduce constitutive assumptions, that means, we have to proceed beyond the general setting of GENERIC.

3. GENERIC treatment

We consider an one-component simple fluid which is decribed by five basic fields: Mass density ϱ, material velocity $\mathbf{v}$, and specific internal energy ε. Therefore is the set of the wanted field given by

$$\mathbf{Z}(\mathbf{x},t) = (\varrho,\ \mathbf{p} := \varrho\mathbf{v},\ \eta := \varrho\varepsilon)(\mathbf{x},t). \tag{14}$$

Then we can introduce the global potentials, as the total energy of the system

$$E^{tot}(\mathbf{Z}) = \int \left[\frac{\mathbf{p}^2(\mathbf{x},t)}{2\varrho(\mathbf{x},t)} + \eta(\mathbf{x},t)\right] d^3x, \tag{15}$$

and the global entropy of the system is by setting a functional on $\mathbf{Z}$

$$S(\mathbf{Z}) = \int \varrho s(\varrho, \mathbf{p}, \eta)\, d^3x. \tag{16}$$

More over, we know about a five field theorie, that the fields have to satisfy the following balance equation for the wanted fields

$$\begin{array}{llll} & \text{reversible part} & \text{irreversible part} & \text{supply} \\ \partial_t\rho = & -\nabla\cdot\rho\mathbf{v} & +0 & +0 \\ \partial_t\mathbf{p} = & -\nabla\cdot\mathbf{pv} - \nabla P & +\nabla\cdot\mathbf{V} & +\mathbf{f} \\ \partial_t\eta = & -\nabla\cdot\eta\mathbf{v} - P\nabla\cdot\mathbf{v} & +\nabla\mathbf{v}:\mathbf{V} - \nabla\cdot\mathbf{q} & +r \end{array} \tag{17}$$

where P is the pressure, $\mathbf{V}$ is the traceless viscous pressure tensor, $\mathbf{q}$ is the heat flux density, $\mathbf{f}$ is the supply of the momentum and r is the supply of the internal energy. We have also performed a split into a reversible and an irreversible part, respectively. But this is an unsolved problem in GENERIC, how to do the right split. Until now it is only possible to see that the split has been found correct, if the resulting entropy production is the right one. But for knowing the entropy production you have to treat the five field theory by another theory, for example by Rational Thermodynamics and by exploiting the Liu-procedure [9].

3.1. State space

In 5-field theory the wanted basic fields (14) are those of a fluid and because we consider dissipative fluids, we choose as a state space one includes the gradients of the basic fields

$$\mathcal{Z}^+ := (\varrho, \eta, \mathbf{v}, \nabla\varrho, \nabla\eta, \nabla\mathbf{v}). \tag{18}$$

Taking into account, that state spaces are spanned by objective quantities we have to change (18) into

$$\mathcal{Z} := (\varrho, \eta, \nabla\varrho, \nabla\eta, (\nabla\mathbf{v})^s). \tag{19}$$

Here $()^s$ is the symmetric part of a tensor. Because of (14) the constitutive quantities in the balances (17) are

$$\mathbf{V} = \mathcal{V}(\mathcal{Z}(\mathbf{x},t)), \qquad \mathbf{q}(\mathbf{x},t) = \mathcal{Q}(\mathcal{Z}(\mathbf{x},t)). \tag{20}$$

(21)

The viscous pressure tensor is symmetric

$$\mathbf{V}(\mathbf{x},t) = \mathbf{V}^\top(\mathbf{x},t), \tag{22}$$

because we only consider fluids without internal spin.

3.2. Reversible part

Because in GENERIC the equations of motions for the basic fields (1) can be split into their reversible and irreversible part (2), we start out with the reversible part of (1) which is as represented in the first column in (17). The first step is that we have to calculate the functional derivative from the global total energy (15). According to (14) the functional derivative in $(2)_1$ generates from (15) the local fields

$$\left(\frac{\delta E^{tot}}{\delta \mathbf{Z}}\right)^T = \left(-\frac{1}{2}\mathbf{v}^2(\mathbf{x},t),\ \mathbf{v}(\mathbf{x},t),\ 1\right), \tag{23}$$

which inserted in $(2)_1$ result in the reversible part of the equations of motion

$$\begin{pmatrix} \partial_t \varrho \\ \partial_t \mathbf{p} \\ \partial_t \eta \end{pmatrix}_{rev} = \mathcal{L}\cdot \begin{pmatrix} -\frac{1}{2}\mathbf{v}^2 \\ \mathbf{v} \\ 1 \end{pmatrix} = \begin{pmatrix} -\nabla\cdot(\mathbf{v}\varrho) \\ -\nabla\cdot(\mathbf{v}\mathbf{p}) - \nabla P \\ -\nabla\cdot(\mathbf{v}\eta) - P\nabla\cdot\mathbf{v} \end{pmatrix}. \tag{24}$$

These five equations are not sufficient to determine the 13 components of the antisymmetric $\mathcal{L}$. Concerning the balances (17) this undetermination is not important, because all the different $\mathcal{L}$ result in the same balances. Concerning the degeneracy conditions $(3)_1$ it is not evident that all these different $\mathcal{L}$ have the same kernel. On the other hand $\mathcal{L}$ is also not determined by the kernel $\delta S/\delta\mathbf{Z}$. The consequences of this undetermination of $\mathcal{L}$ are not fully discussed up to now.

Now we can show, that one operator-valued matrix satisfying (24) is the following one

$$\mathcal{L} = -\begin{pmatrix} 0 & \nabla\varrho\cdot & 0 \\ \varrho\nabla & [\nabla\mathbf{p}+\mathbf{p}\nabla]^\top\cdot & \nabla P + \eta\nabla \\ 0 & (P\nabla+\nabla\eta)\cdot & 0 \end{pmatrix}. \tag{25}$$

The degeneracy conditions $(3)_1$ are now used to determine the kernel $\delta S/\delta\mathbf{Z}$ of $\mathcal{L}$. As already remarked, it is not evident, that this kernel is unique. The global entropy of the system depending only on $\mathbf{Z}$ is given by (16) and the functional derivative of S generates local quantities

$$\left(\frac{\delta S}{\delta \mathbf{Z}}\right)^T = \left(\frac{\partial(\varrho s)}{\partial\varrho} =: -\frac{g}{T}(\mathbf{x},t),\ \frac{\partial(\varrho s)}{\partial\mathbf{p}}(\mathbf{x},t),\ \frac{\partial(\varrho s)}{\partial\eta} =: \frac{1}{T}(\mathbf{x},t)\right). \tag{26}$$

Here the usual abbreviations *specific free enthalpy* g and *absolute equilibrium temperature* T for the derivatives of the entropy are introduced. The degeneracy condition $(3)_1$ results in the following equations

$$\frac{\partial\varrho s}{\partial\mathbf{p}} = \mathbf{0}, \tag{27}$$

$$-\varrho\nabla\frac{g}{T} + \nabla\frac{P}{T} + \eta\nabla\frac{1}{T} = 0. \tag{28}$$

As (27) shows, the GENERIC setting allows to derive that the entropy density does not depend on the velocity $\mathbf{v}$. From (28) follows immediately by use of (26) and (27) that the following equation yields

$$-\varrho s = \frac{1}{T}(\varrho g - P - \eta) + const \longrightarrow \tag{29}$$

$$\longrightarrow g = \varepsilon + \frac{P}{\varrho} - Ts\,, \quad const = 0, \tag{30}$$

because (30) is the definition of the specific free enthalpy g.

The exploitation of the reversible part of the GENERIC equations of motion (1) results in (25), (27), and (28). Now we investigate its irreversible part in the next section.

3.3. Irreversible part

We now have to generate one $\mathcal{M}$ by use of the irreversible part of the equations of motion $(2)_2$ and by the degeneracy condition $(3)_2$

$$\mathcal{M}\cdot\frac{\delta S(\mathbf{Z})}{\delta \mathbf{Z}} = \mathcal{M}\cdot\begin{pmatrix} -\frac{g}{T} \\ \mathbf{0} \\ \frac{1}{T}\end{pmatrix} = \begin{pmatrix} 0 \\ \nabla\cdot\mathbf{V} \\ \nabla\mathbf{v}:\mathbf{V}-\nabla\cdot\mathbf{q}\end{pmatrix}, \tag{31}$$

$$\mathcal{M}\cdot\frac{\delta E^{tot}(\mathbf{Z})}{\delta \mathbf{Z}} = \mathcal{M}\cdot\begin{pmatrix} -(1/2)\mathbf{v}^2 \\ \mathbf{v} \\ 1\end{pmatrix} = \begin{pmatrix} 0 \\ \mathbf{0} \\ 0\end{pmatrix}. \tag{32}$$

From (6) and (31) we can immediately read off the entropy production without any knowledge of $\mathcal{M}$

$$\begin{aligned}\sigma &= \left\langle\frac{\delta S(\mathbf{Z})}{\delta \mathbf{Z}}, \mathcal{M}\cdot\frac{\delta S(\mathbf{Z})}{\delta \mathbf{Z}}\right\rangle + \int\nabla\cdot\frac{\mathbf{q}}{T}d^3x \\ &= \int\left(\frac{1}{T}[\nabla\mathbf{v}:\mathbf{V}-\nabla\cdot\mathbf{q}]+\nabla\cdot\frac{\mathbf{q}}{T}\right)d^3x \\ &= \int[\frac{1}{T}\nabla\mathbf{v}:\mathbf{V}+\mathbf{q}\cdot\nabla\frac{1}{T}]\,d^3x = \int\pi^s\,d^3x \geq 0 \end{aligned}\tag{33}$$

Because the last equal sign is valid for all domains of integration, we obtain for the local entropy production density

$$\pi^s = \frac{1}{T}\nabla\mathbf{v}:\mathbf{V}+\mathbf{q}\cdot\nabla\frac{1}{T}. \tag{34}$$

This is the same result as in the conventional procedure like in rational thermodynamics [9] and has the usual form of a product between fluxes and forces.

For the sake of simplicity, we set here the first column and row equal to zero. Consequently we are looking for a symmetric matrix of the form

$$\mathcal{M} = \begin{pmatrix} 0 & \mathbf{0} & 0 \\ \mathbf{0} & \mathbf{M}^{22} & \mathbf{M}^{23} \\ 0 & \mathbf{M}^{32} & M^{33}\end{pmatrix}. \tag{35}$$

Now we can show, that one of the possible choice of the operator-valued matrix elements of the dissipation operator $\mathcal{M}$ have the following form due to the conditions (31) and (32)

$$M^{22}[*] = -\nabla\cdot\mathbf{V}T\frac{1}{(\nabla\cdot\mathbf{v})}\nabla * \tag{36}$$

$$M_k^{23}[*] = \nabla\cdot\mathbf{V}T * \tag{37}$$

$$M_k^{32}[*] = -(\mathbf{V}T\cdot\nabla)^T\cdot * \tag{38}$$

$$M^{33}[*] = \nabla\cdot\lambda\cdot\nabla+(\nabla\mathbf{v}:\mathbf{V})T*$$

with

$$\lambda_{ij} := \frac{q_i(\partial_j T)}{(\nabla T)^2}T^2.$$

The exploitation of the irrversible part results in (34) and (36) - (39).More over, we see that the generalized transport coefficients in (36) - (39) are not independent of each other. This is a result what is analogue to the Casimir Onsager recriprocal relations in TIP.

3.4. Balance equation for the global potentials

The last point, we have to discuss are the dynamic equations for both global potentials. The supply vector of the wanted fields is according to the last column in (15) is

$$\mathbf{f}_e^T = (0, \mathbf{f}, r), \tag{39}$$

and thus we get immediately from (13) using (29) and (33)

$$\frac{d}{dt} S(\mathbf{Z}) \quad = \quad [S, E^{tot}] + \{S, S\} + \int \frac{\partial \varrho s}{\partial \mathbf{Z}} \cdot \mathbf{f_e}\, d^3x \tag{40}$$

$$= \int \Big[-\nabla \cdot \mathbf{v} \varrho s(\mathbf{Z}) + \pi^s - \nabla \cdot \frac{\mathbf{q}}{T} + \frac{r}{T} \Big] d^3 x. \tag{41}$$

Similiar we get from (12) using (4), (5) and $(3)_2$ the balance equation of the total energy

$$\begin{aligned} \frac{d}{dt} E^{tot}(\mathbf{Z}) &= [E^{tot}, E^{tot}] + \{E^{tot}, S\} + \int \frac{\partial e^{tot}}{\partial \mathbf{Z}} \cdot \mathbf{f_e}\, d^3x \\ &= \int \Big\{ -\nabla \cdot [(\mathbf{v} e^{tot}(\mathbf{Z}) + \mathbf{v} P) + (\mathbf{V}^T \cdot \mathbf{v} - \mathbf{q})] + \mathbf{v} \cdot \mathbf{f^e} + r \Big\} d^3x \\ &= \dot{W} + \dot{Q} \end{aligned} \tag{42}$$

with the work

$$\dot{W} := \int \Big[-\nabla \cdot (\mathbf{v} e^{tot}(\mathbf{Z}) + \mathbf{v} P) + \nabla \cdot (\mathbf{V}^T \cdot \mathbf{v}) + \mathbf{v} \cdot \mathbf{f^e} + r \Big] d^3x \tag{43}$$

and the heat exchange

$$\dot{Q} := \int \nabla \cdot \mathbf{q} d^3 x. \tag{44}$$

4. Conclusion

An important statement of GENERIC is the fact, that the generalized transport coefficients of the dissipation operator are not independent. In GENERIC one derive a generalisation of Casimir-Onsager recriprocal relations. The structure of GENERIC provides, that the dissipation operator is positive definit and thus that a closed system decays to equilibrium.

It is also possible to give a microscopic foundation of the GENERIC formalism [12], [13] which gives us a powerfull argument for the validity of this structure. But nevertheless, we have the unsolved problem in GENERIC, that is a correct split into a reversible and an irreversible part is not achieved up to now. Although it seems to be possible to transform the whole GENERIC structure to open systems which was demonstrated here. Another important statement of GENERIC is, that we have to preassume local equilibrium, i.e the global potentials depend only on the wanted fields.

References

[1] Edwards B. J. and Öttinger H. C., *Time-structure invariance criteria for closure approximation*, Phys. Rev. E **56** (1997), 4097.

[2] DE GROOT S. R. AND MAZUR P., *Non-equilibrium thermodynamics*, North-Holland, Amsterdam 1963.

[3] GRMELA M., *Bracket formulation of dissipative fluid mechanics equations*, Phys. Lett. A **102** (1984), 335–358.

[4] GRMELA M. AND ÖTTINGER H. C., *Dynamics and thermodynamics of complex fluids. Development of a general formalism*, Phys. Rev. E **56** (1997), 6620.

[5] GRMELA M. AND ÖTTINGER H. C., *Dynamics and thermodynamics of complex fluids. Development of a general formalism*, Phys. Rev. E **56** (1997), 6633.

[6] GYARMATI I., *Nonequilibrium thermodynamics (field theory and variational principles)*, Springer Verlag, Berlin 1970.

[7] JOU D., CASAS-VÁZQUEZ V. AND LEBON G., *Extended irreversible thermodynamics*, Springer, Berlin 1996.

[8] MÜLLER I. AND RUGGERI T., *Extended Thermodynamics*, Springer Tracts in Natural Philosophy **37**, Springer, Berlin 1993.

[9] MUSCHIK W., *Aspects of non-equilibrium thermodynamics*, World Scientific, Singapore 1990.

[10] MUSCHIK W., *Fundamentals of nonequilibrium thermodynamics*, in: "Non-equilibrium thermodynamics with applications to solids", CISM Courses and Lectures **336** (sect. 1) Springer, Wien 1993.

[11] MUSCHIK W. AND PAPENFUSS C., *An evolution criterion of nonequilibrium thermodynamics and its application to liquid crystals*, Physica A **201** (1993), 515.

[12] ÖTTINGER H. C., *General projection operator formalism for the dynamics and thermodynamics of complex fluids*, Phys. Rev. E **57** (1998), 1416.

[13] ÖTTINGER H. C., *Derivation of a two-generator framework of nonequilibrium thermodynamics for quantum systems*, Phys. Rev. E **62** (2000), 4720.

[14] TRUESDELL C. AND TOUPIN R., *The classical field theories*, in: "Handbook of Physics, III/1", Springer, Berlin 1960.

[15] WILMAŃSKI K., *Thermomechanics of continua*, Springer, Berlin 1998.

AMS Subject Classification: 74A15.

Sebastian GÜMBEL, Wolfgang MUSCHIK
Institut für Theoretische Physik
Technische Universität Berlin
Sekretariat PN7-1 Hardenbergstrasse 36
D-10623 Berlin, GERMANY
e-mail: `guembel@physik.tu-berlin.de`
e-mail: `muschik@physik.tu-berlin.de`